UNIVERSITAT DE BARCELONA

Study of pro-apoptotic protein RTP801 homeostasis and its regulation by NEDD4 in Parkinson's disease

Mercè Canal de la Iglesia

Barcelona, 2016

Programa de Doctorat en Biomedicina

UNIVERSITAT DE BARCELONA

STUDY OF PRO-APOPTOTIC PROTEIN RTP801 HOMEOSTASIS AND ITS REGULATION BY NEDD4 IN PARKINSON'S DISEASE

Dissertation submitted by

MERCÈ CANAL DE LA IGLESIA

To opt for a doctoral degree in biomedicine for Universitat de Barcelona

This work was performed at Departament de Biomedicina de la Universitat de Barcelona, under the supervision of Dr. Cristina Malagelada Grau and the tutoring of Dr. Esther Pérez Navarro

Doctoral student	Supervisor	Tutor
Mercè Canal de la Iglesia	Cristina Malagelada Grau	Esther Pérez Navarro

La nostra glòria més gran no rau a no haver caigut mai,
sinó a aixecar-nos cada vegada que caiem

Oliver Goldsmith

A la meva família

Als meus amics

AGRAÏMENTS

Sembla mentida, però ha arribat el dia de presentar la tesi, moment desitjat i temut a parts iguals. Han sigut quatre anys i mig intensos, en els que hi ha hagut de tot, moments bons i dolents, però ha valgut la pena, ja que ha sigut una experiència molt enriquidora. Si he arribat fins aquí ha estat gràcies al recolzament de molta gent, i us volia donar les gràcies.

Primer de tot, vull agrair a la Cris, per donar-me la oportunitat de fer la tesi al seu laboratori. El dia que ens vam conèixer, a la primera entrevista, ja vaig tenir la sensació que series una bona directora de tesi, i no m'equivocava. La teva passió per la ciència i motivació m'han servit de guia, i espero haver-me'n "empapat" al màxim. Gràcies per tot el que m'has ensenyat, per les teves bones paraules (que mai estan de més) i pel teu suport en tot moment, fins i tot quan els resultats no acompanyaven.

Als meus companys, amb els quals he compartit incomptables hores al laboratori! Sort n'he tingut de vosaltres, que m'heu fet la rutina més amena i els moments d'estrès més suportables. Tot i ser poquets, hem fet molt bon equip. A en Joan, per ensenyar-m'ho tot les primeres setmanes, per escoltar-me i animar-me sempre que ho he necessitat, i per seguir-me en els moments puntuals de bogeria, en els quals hem acabat rient com nens de qualsevol "xorrada". A la Núria, per estar sempre, sempre, i sempre disposada a donar-me un cop de mà, i per no queixar-se mai! Encara estic esperant que deixis anar algun renec! La veritat és que no es pot tenir més bona companya de feina, fas que tot sigui molt fàcil. I als dos per les bones estones compartides fora del laboratori, fent birres a l'Ascot, mirant partits del Barça, la sortida estiuenca a la platja... A en Víctor, per la feina feta i per ser tan tranquil, a vegades massa i tot! A la Clara, perquè tot i que no vam coincidir gaire temps, va ser agradable treballar amb tu. I a la Leti, per la teva bona predisposició, per ser tan alegre i per transmetre bon rotllo des del primer dia.

També vull agrair a la Clara i la Cris, heu sigut les millors veïnes de laboratori! Quants cops dec haver picat a la vostra porta per preguntar-vos o explicar-vos alguna cosa? La vostra arribada va donar molta vida al departament. Gràcies per tots els dinars de "tupper" al claustre, ja que han suposat agradables parèntesis de desconnexió. A l'Anna, per tenir sempre una rialla i un "xupito" de vodka apunt, i a en Carles, pels teus bons consells i per la companyia els caps de setmana que m'ha tocat anar al laboratori.

I per suposat, als companys del nou departament, la unitat de Bioquímica, per la vostra extraordinària rebuda i per deixar-nos un laboratori amb llum natural i finestres grans, lo nunca visto! Ens heu fet sentir com a casa des del primer dia. A la Marga, en Jose, en Manolo, en Jou, la Roser i la Carmen, per l'ajuda logística, el suport i les xerrades a la sala d'ordinadors. A la Marta, l'Eva i l'Arnau, per les estones a la sala de cultius, per estar sempre disposats a donar-me un cop de mà, i per fer més tonteries que jo! A la Rosario, per el suport durant el trasllat i perquè sempre aconsegueixes fer-me riure amb les teves històries, i a en Mario, per les converses entretingudes a l'entrada del departament.

També vull donar les gràcies a l'Esther, la meva tutora de tesi, pel teu assessorament científic i per haver-me rebut sempre de bon grat al despatx, ja fos per demanar-te algun dubte o alguna signatura. A la Sílvia, pels teus comentaris constructius durant els seminaris i per aconsellar-me sobre Boston. A en Jordi Alberch, pel teu recolzament en els moments més

difícils i delicats del grup, i a en Pep i en Xavi pel vostre suport. A en Rafa, pel teu tracte immillorable quan he vingut a la cinquena, sempre que pujava et buscava a tu! A l'Ana Saavedra, per les teves valuoses correccions, no sé com t'ho fas, però no se te n'escapa ni una. A en Jordi Creus, per les classes de dissecció, a en Marco, per divertir-me amb les teves bromes quan ens hem trobat revelant o pels passadissos, i a l'Inés, per la teva alegria i positivisme. A la Mònica, la Mar, la Marta, la Marta Cherubini, l'Elena.... i a tota la resta dels de dalt per la vostra simpatia i recolzament.

Una menció especial als companys de laboratori de Boston, ja que tot i que va ser breu, l'estada va ser molt positiva. Thanks Heng-Ye for giving me the opportunity to be a member of your lab and for your valuable scientific comments and ideas. To Natasha, I will always be grateful for your support and for your helpful emails before coming to Boston. We have shared a lot of awesome moments there and during your visit to Barcelona. Good luck for your graduation! To J.P, for your help with the electrophysiology experiments and for inviting me to a real American barbecue! To Yuda, I will never forget your naps on the table, I hope you find your future wife soon!

No em vull oblidar dels "biofrikis", els primers companys de laboratori que vaig tenir. A l'Albert, per les seves continues bromes i "burxades", pels consells musicals, per les nits a l'Apolo i per les escapades a Blanes. Et prometo que algun dia (quan deixi de ser becària precària) em compraré una entrada per anar al Sónar de dia! A la Neus Mora, per la teva senzillesa i sinceritat, i per ser del reialme de Moià! A la Núria, per ser com una mami i perquè al teu costat vaig aprendre moltes coses. A la Pili per ser autèntica i regalar-nos moments inoblidables tipus "voy a callarme porque es sábado.." A la Rosa i a l'Anto, perquè tot i que no vam coincidir molt a l'IQS, guardo molt bon record de les escapades rurals i dels sopars compartits.

També als meus companys del PRBB, on vaig fer les pràctiques de màster. Al Xavi Mayol, per ensenyar-me de primera mà i per la teva inesgotable paciència. Al Jorjako, per fer tants disbarats i per fer-m'ho passar tan bé durant el temps que vam treballar junts. A la Konsti, la Vaso, la Tania, la Mireia, la Sílvia, la Laura i la Conchi, i en Josu, tots em vau ajudar durant aquells mesos, i en guardo molt bon record.

I ja deixant de banda els laboratoris.. vull agrair als amics que vaig conèixer durant l'etapa universitària. A la Maria, pels brunchs i les IPES a Barcelona, i per presentar-me tota la colla catalana de Boston! I per suposat al Biel, que tot i no ser IQS, n'estàs rodejat i ja ets com un més! Gràcies pels cafès matiners a l'Starbucks i per ensenyar-me els racons més macos de Jamaica Plain. A la Xufi, pels bons moments compartits, espero que segueixis disfrutant al màxim per Austràlia! A en Jonny, perquè encara recordo la nostra etapa compartint pis, i ves tu per on, ara ja ets pare! A en Bruno i l'Axel, perquè tot i que no ens veiem gaire sovint, quan coincidim sembla que el temps no hagi passat.

Als biomeds, sou molt grans!! Què seria dels estius sense la nostra escapada a Menorca? Els quatre dies a la casa de Cala Morell han sigut cada any una glopada d'aire fresc! A l'Anna Palau, per la teva simpatia i dolçor. A la Laura, per ajudar-me amb els "dibuixets" i per despendre sempre bones vibracions. A la Cate, per la nostra bona sintonia, i per totes les

estones compartides als bancs del PRBB. A en Lorenzo, pel teu punt de bogeria sana i a en Marc, per la teva vitalitat i motivació. I al Carlos, pels teus comentaris espontanis tan graciosos i per tancar amb mi totes les festes, encara que sigui dormint de peu!

I especialment a l'Aran, perquè també hem viscut juntes l'etapa del doctorat al Clínic i molts bons moments fora! Gràcies per ser tan "happy flower", tan oberta de ment, i per escoltar-me les neures. Et trobo a faltar, espero que quan acabis el teu viatge per Amèrica del Sud tornis a Barcelona. I a la Leti, la Núria i l'Albert, pels dijous de trivial, i per amenitzar amb cafès pel raval l'etapa d'escriptura.

A les "iaies", per la bonica etapa al pis d'Entença i perquè sou com la meva família barcelonina. A la Maria, perquè des de que ens vam conèixer has estat sempre allà, a les bones i a les dolentes, i sempre disposada a anar algun "concertillo" de música catalana. A l'Anna, pel teu entusiasme, bon humor i optimisme. I per tots els moments compartits, els 13 anys vivint a Barcelona no haguessin set el mateix sense tu! A la Clàudia, et conec des de que tinc ús de raó i encara som amigues! Moltes gràcies pel teu suport incondicional i per les nostres xerrades vespertines al sofà. També vull agrair a l'Ander, per ser el millor guia turístic durant el meu viatge a L.A, i a en Pere, pels carnets del Barça.

A la colla de Vic, perquè anar a la plana i fer coses amb vosaltres sempre és un plaer. I no puc estar-me de mencionar el trentenni, quin any 2015 més intens i ple d'activitats! Hem fet de tot i ens ho hem passat "teta"! A l'Eli, perquè tot i estar al Brasil compartim experiències científiques per Skype i ens entenem perfectament. A la Farrés, per ser la millor organitzadora "d'eventos", i per ser tan "pel·liculera". A la Raquel, per la teva empatia i senzillesa, i per les teves ganes de passar-ho bé. A l'Olga, pels vespres de noies fent vinets pel barri, i a l'Esther, per mostrar tanta serenor i fortalesa. I també a en Pep, en Mateu i en Pablo! I a les peques de la colla, la Bruna i la Carlota, perquè veure-us créixer és un regal. En especial a la Bosch, per la teva ajuda amb la portada. Gràcies per acompanyar-me durant l'inici de l'aventura americana, per les nostres caminades i vermuts, i per la teva energia positiva encomanadora! També vull agrair a la Sílvia i l'Aïda, per estar al meu costat durant tants anys. I al grup "tracatá" per les nits de "bailoteo"!

Finalment, vull donar les gràcies a la meva família. A la meva àvia, i a tots els meus tiets i cosins per interessar-se per la meva tesi al llarg d'aquests anys. Als meus pares, perquè m'ho han donat tot i m'han recolzat en totes les decisions que he pres. I també, perquè han valorat més que ningú que estigués fent el doctorat. A la Laia, perquè hem crescut juntes, hem jugat, ens hem barallat, ens hem divertit...i sempre m'has fet de germana gran, aconsellant-me davant dels meus dubtes i inquietuds. A en Joan, pel teu sentit de l'humor "made in Coma", que sempre m'arranca alguna rialla. I perquè, tot i estar rodejats de metges, segurament serem els únics doctors de la família! I als meus nebots, en Lluc i la Joana, perquè no hi ha res més alliberador que veure com se us dibuixa un somriure a la cara.

Gràcies a tots!!

Barcelona, maig 2016

The work presented in this dissertation has been developed with the financial support given by the following grants:

• Grants from the Spanish Ministry of Science and Innovation (SAF2010-21058, SAF2013-45888R and SAF-2014-57160R).

• PEOPLE Programme - Marie Curie Actions, European Community (PIRG08-GA-2010-276957).

Supported also by the crowd funding campaign “SOS recerca en Parkinson” via Goteo.org, Portal d’Avall, S.L. and “Mememtum: early detection of neurological disorders”.

We are indebted to the Neurological Tissue Bank (Biobank-Hospital Clínic-IDIBAPS) and to Dr. Ellen Gelpi, for the human postmortem brain samples and data procurement. We also thank Dr. Hiroshi Kawabe (Max Planck Institute of Experimental Medicine) for the NEDD4$^{f/f}$; EmxCre mice and Dr. Enrique Santamaria and the proteomics unit (Navarrabiomed) for the proteomic analyses.

ABBREVIATIONS

4E-BP1	Eukaryotic translation initiation factor 4E binding protein 1
6-OHDA	6-hydroxydopamine
Aβ	Amyloid beta peptide
AD	Alzheimer's disease
ALP	Autophagy-lysosomal pathway
AMPARs	Alpha-amino-3-hydroxy-5-methyl-isoxazole-4-propionic acid receptors
AMPK	Adenosine monophosphate-activated protein kinase
AR-JP	Autosomal Recessive Juvenile Parkinsonism
ATF4	Activating transcription factor 4
ATP	Adenosine triphosphate
Bcl-2	B-cell lymphoma 2
BSA	Bovine serum albumin
C	Amino acid cysteine
Cbl	Casitas B-lineage lymphoma
CHX	Cycloheximide
CKI	Casein kinase 1
CMA	Chaperone-mediated autophagy
CMV	Citomegalovirus
c-Src	Proto-oncogene tyrosine-protein kinase Src
CUL4A	Cullin 4a
DA	Dopamine
DBS	Deep brain stimulation
DDIT4	DNA-damage-inducible transcript 4
DEPTOR	DEP domain containing mTOR-interacting protein
Dig2	Dexamethasone-induced gene 2
DIV	Day in vitro
DMEM	Dulbecco's Modified Eagle Medium
DMSO	Dimethyl sulfoxide
DSP	Dithiobis (succinimidyl proprionate)
DTT	Dithiothreitol
E6-AP	E6-associated protein
EDTA	Ethylenediaminetetraacetic acid
EGFR	Epidermal growth factor receptor

EGTA	Ethylene glycol tetraacetic acid
ENaC	Epithelial sodium channel
ER	Endoplasmic reticulum
ERK1/2	Extracellular-signal-regulated kinase 1/2
ESCRT	Endosomal sorting complexes required for transport
FGFR1	Fibroblast growth factor receptor 1
GABA	Gamma-amminobutyric acid
GAP	GTPase activating protein
GAPDH	Glyceraldehyde 3-phosphate dehydrogenase
GDP	Guanosine diphosphate
GFP	Green fluorescent protein
GPCRs	G protein-coupled receptors
GPe	External globus pallidus
GPi	Internal globus pallidus
Grb10	Growth factor receptor-bound protein 10
GTP	Guanosine triphosphate
GSK3β	Glycogen synthase kinase 3 β
GST	Glutathione S-transferase
GWAS	Genome-wide association study
HA	Hemagglutinin
HD	Huntington's disease
HECT	Homologous to the E6-AP Carboxyl Terminus
HIF-1	Hypoxia inducible factor 1
His_6	Hexa histidine
HSF1	Heat shock transcription factor 1
IB	Immunoblot
IGF-1	Insulin-like growth factor 1
IGF-1R	Insulin-like growth factor 1 receptor
IGF-1Rβ	Insulin-like growth factor 1 receptor β
IP	Immunoprecipitation
IRES	Internal Ribosome Entry Site
IRS1	Insulin receptor substrate 1
JNK	c-Jun N-terminal kinase

K	Amino acid lysine
LAMP2	Lysosome-associated membrane protein 2
LAR	Leukocyte common antigen-related
LB	Lysogeny broth
LBs	Lewy bodies
LC	Locus Coeruleus
LC-MS/MS	Liquid chromatography-tandem mass spectrometry
LRRK2	Leucine-rich repeat kinase 2
LTP	Long-term potentiation
MAO	Monoamine oxidase enzyme
MAP	Mitogen-activated protein
MEFs	Mouse embryo fibroblasts
MEM	Minimum essential media
miRNA	Micro RNA
mLST8	Mammalian lethal with sec13 protein 8
MOI	Multiplicity of infection
MPP^+	1-methyl-4-phenylpyridinium
MPTP	1-methyl-4-phenyl-1,2,3,6-tetrahydropyridine
mSIN1	Mammalian stress-activated MAP kinase-interacting protein 1
MS/MS	Tandem mass spectrometry
mTOR	Mechanistic target of rapamycin
Ndfip1	NEDD4 family interacting protein 1
Ndfip 2	NEDD4 family interacting protein 2
NEDD4	Neural precursor cell-expressed developmentally down-regulated gene 4
NEDL	NEDD4-like ubiquitin-protein ligase
NGF	Nerve growth factor
NM	Neuromelanin
NPC12	Neuronal PC12 cells
ORF	Open reading frame
PaKO	Parkin knockout
PBS	Phosphate buffered saline
PCR	Polymerase chain reaction
PD	Parkinson’s disease

PDK1	Pyruvate dehydrogenase lipoamide kinase isozyme 1
PI3K	Phosphoinositide 3-kinase
PINK1	PTEN-induced putative kinase 1
PIP2	Phosphatidylinositol 4,5-bisphosphate
PIP3	Phosphatidylinositol 3,4,5-triphosphate
PKA	Protein kinase A
PKC	Protein kinase C
PKC-α	Protein kinase C-α
PKG	Protein kinase G
PP1	Protein phosphatase 1
PP2A	Protein phosphatase 2
PRAS40	Proline-rich Akt substrate 40 KDa
PROTOR	Protein observed with rictor
PTEN	Phosphatase and tensin homolog
R	Amino acid arginine
REM	Rapid eye movement
Raptor	Regulatory-associated protein of mTOR
REDD1	Regulated in DNA damage response 1
REDD2	Regulated in DNA damage response 2
Rheb	Ras homolog enriched in brain
Rictor	Rapamycin-insensitive companion of mTOR
RING	Really interesting new gene
RIPA	Radioimmunoprecipitation assay
ROS	Reactive oxygen species
RT-qPCR	Quantitative reverse transcription PCR
S	Amino acid serine
S6K1	p70-S6 kinase 1
SAGE	Serial analysis of gene expression
SBDP120	Spectrin breakdown product 120
SBDP145	Spectrin breakdown product 145
$SCF^{\beta\text{-}TRCP}$	Skp, Cullin, F-box containing complex, E3 ubiquitin-ligase
SEM	Standard error of the mean
SGK1	Serum and glucocorticoid-induced protein kinase 1

ShRNA	Short hairpin RNA
SiRNA	Small interfering RNA
SMURF	Smad ubiquitin regulatory factor
SN	Substantia nigra
SNP	Single nucleotide polymorphism
SNpc	Substantia nigra pars compacta
SNpr	Substantia nigra pars reticulata
STN	Subthalamic nucleus
SV40	Simian Virus 40
T	Amino acid threonine
TBS	Tris buffered saline
TOF	Time of flight
TSC1/2	Tuberous sclerosis ½
TSG1	Tumor susceptibility gene 101
Ub	Ubiquitin
UPR	Unfolded protein response
UPS	Ubiquitin-proteasome system
WB	Western Blot
WT	Wild-type

FIGURES AND TABLES INDEX

INDEX

INTRODUCTION

1. PARKINSON'S DISEASE OVERVIEW

Parkinson's disease (PD) was first described in 1817 by the neurologist James Parkinson, who reported the main clinical features in his "Essay on the shaking palsy"[1]. PD is the second most common neurodegenerative disease after Alzheimer's disease. It has a prevalence of 0,5-1% in 65-69 years old people, rising to 1-3% in 80 years old and beyond[2,3]. It is estimated to affect 6 million people worldwide, with the prediction of increase two-fold within 25 years[4].

The majority of the cases are sporadic, because they do not affect other family members, and are also referred as idiopathic PD. However, a subset of PD cases are inheritable, since they are caused by mutations in specific genes; they are known as familial PD[2].

1.1 Neuropathology

The two main pathological hallmarks of PD are the progressive demise of nigrostriatal dopaminergic neurons and the presence of cytoplasmic protein inclusions named Lewy Bodies (LBs)[5].

The cell bodies of nigral dopaminergic neurons are localized in the Substantia Nigra pars compacta (SNpc), and innervate principally the putamen, a substructure of the striatum. A remarkable feature of nigral neurons is that they usually contain cytoplasmic neuromelanin, a conspicuous dark pigment[6]. Therefore, the loss of these type of neurons in PD patients results in a classical neuropathological observation; SNpc depigmentation (Figure 1)[5]. The degree of depigmentation correlates well with neuronal loss, increasing proportionally with the severity and the duration of the disease[7].

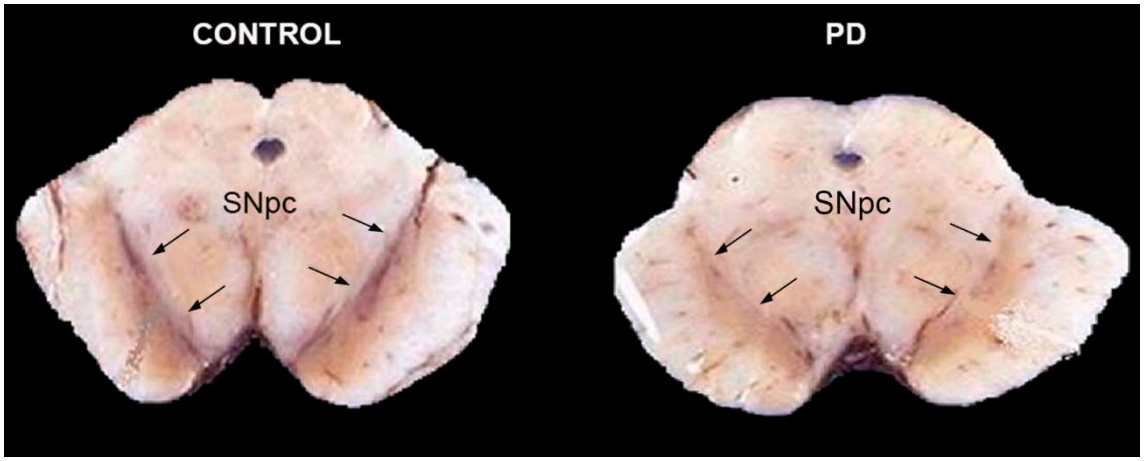

Figure 1. Horizontal midbrain sections from a control and a PD patient. Loss of pigmentation (neuromelanin) in the SNpc of PD brain is clearly appreciated. Image adapted from the web: https://i.ytimg.com/vi/fdyoJma-35g/maxresdefault.jpg

Since nigrostriatal dopaminergic neurons project mainly to the dorsolateral putamen, dopamine (DA) levels are considerably reduced in this brain area[8]. This DA deficiency both at the SNpc and striatum is responsible for the main motor symptoms of PD, also known as parkinsonism. Generally, at the onset of parkinsonism symptoms, approximately 60% of SNpc dopaminergic neurons have already been lost and 80% of dopamine has been depleted in the putamen[5,9].

The other principal pathological hallmark of PD is the presence of LBs in neurons of the SNpc and other affected brain areas[10–12]. These aggregates can be composed of different proteins, such as, α-synuclein, parkin, ubiquitin and neurofilaments[13]. LBs are usually more than 15 μm in diameter and present an organized structure characterized by a spherical dense hyaline core surrounded by a clearer halo (Figure 2)[3,10,14]. However, their role in the pathology is not well established, being still debated whether they have a protective or a pathological function[15].

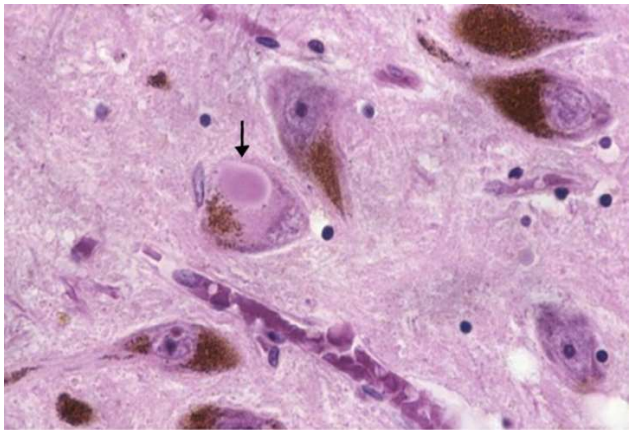

Figure 2. Lewy body present in a SNpc dopaminergic neuron. Note the presence of neuromelanin (in brown) in dopaminergic neurons. The Lewy body is localized (indicated with an arrow) at the cytoplasm of one of these neurons. Image adapted from the web: https://quizlet.com/10453505/neurodegenerative-diseases-flash-cards/

Despite PD neuropathology is primarily defined by the loss of dopaminergic neurons, other brain regions deteriorate and show the presence of LBs. For instance, noradrenergic neurons loss in the Locus Coeruleus (LC) can be very pronounced at late stages of the disease. Other affected areas include the serotonergic neurons of the raphe nucleus, the cholinergic neurons of the basal nucleus of Meynert and the dorsal motor nucleus of the vagus. Moreover, cerebral cortex, olfactory bulb and autonomic nervous system can also present neurodegeneration. These deficits in other regions generally account for the non-motor symptoms of the disease (see section 1.3 clinical features)[5,16].

1.2 Basal ganglia pathophysiology

The basal ganglia network receives signaling inputs from the cortex to produce an output signal to the thalamus/cortex that regulates movement execution. In PD, the loss of SNpc dopaminergic neurons markedly affects basal ganglia circuitry activity, leading to the inability of controlling voluntary movements[17].

The basal ganglia are composed of several subcortical nuclei located at the base of the forebrain. These structures are the nuclei caudate and putamen, which form the striatum, the external and internal segments of the globus pallidus (GPe and GPi), the subthalamic nucleus (STN), and the pars compacta and pars reticulata of the substantia nigra (SNpc and SNpr). These basal nuclei are interconnected themselves and with the cortex, the thalamus and the brainstem to accomplish different functions[16]. Regarding the intrinsic circuitry of the basal ganglia, two major projection systems have been reported: a direct pathway between striatum and GPi/SNpr and an indirect pathway involving GPe and STN. The SNpc dopaminergic innervation to the striatum is responsible for the balance maintenance between these direct and indirect pathways of motor control[16].

Different subpopulations of striatal GABAergic neurons control the direct and indirect pathways, differing in terms of associated co-transmitters. While the direct pathway carries substance P, the indirect pathway has enkephalin as a co-transmitter. Activation of the direct pathway leads to inhibition of the GPi and SNpr nuclei, and thereby disinhibits thalamocortical signaling. On the other hand, stimulation of striatal neurons that give rise to the indirect pathway leads to inhibition of the GPe, disinhibition of the STN, activation of the GPi/SNpr, and thereby inhibits thalamocortical signaling. Since the activation of these pathways induce contrary effects, a balance between them may be fundamental to regulate basal ganglia output[2,16].

Another relevant difference between the two pathways is that they are distinctly modulated by dopamine (DA). Neurons from direct pathway express preferentially dopamine D1 receptors, while neurons from indirect pathway express preferentially D2 receptors[18]. Activation of D1 receptors by DA at spines of direct pathway neurons enhances corticostriatal transmission. On the other hand, activation of D2 receptors by DA prevents from synaptic activation of indirect pathway neurons[19]. According to this model, DA deficiency associated to PD leads to a decreased activation of the direct pathway and to a hyperactivation of the indirect pathway. This imbalance inhibits the thalamocortical motor circuitry leading to parkinsonian motor signs (Figure 3).

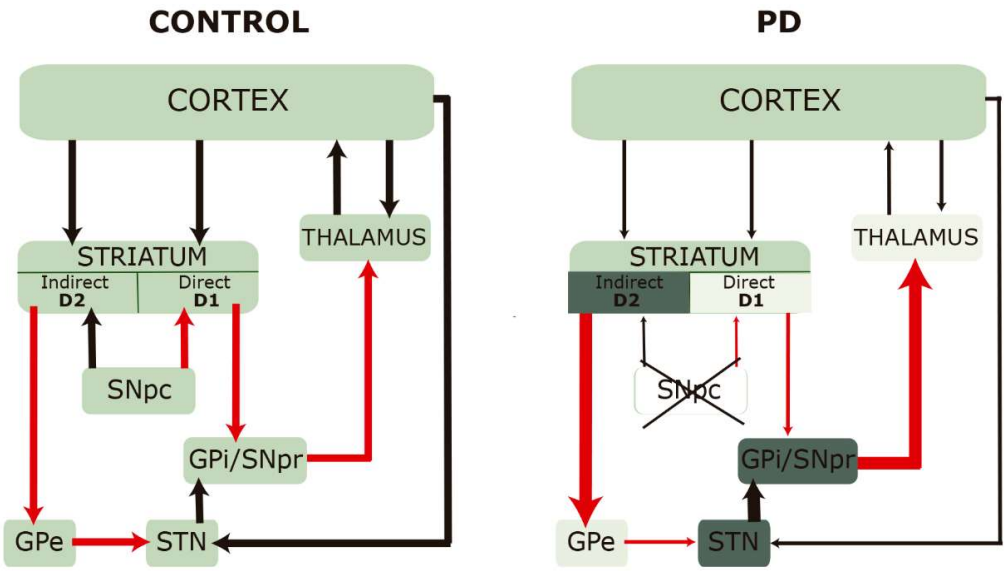

Figure 3. Basal ganglia pathophysiology in PD. Representation of basal ganglia nuclei activity in physiological conditions (left panel), and activity changes associated with PD SNpc neuronal loss (right panel). Black arrows show excitatory connections, whereas red arrows show inhibitory connections. Changes in the thickness of arrows indicate modifications in firing rates. In the right panel, over activated nuclei are displayed in a darker color, while the more inhibited nuclei are displayed in a lighter color. Abbreviations: SNpc, substantia nigra pars compacta; SNpr, substantia nigra pars reticulata; GPe, external pallidal segment; GPi, internal pallidal segment; STN, subthalamic nucleus. Figure adapted from Wicham T and DeLong MR (2008)[16].

1.3 Clinical features

PD is characterized by a broad range of motor and non-motor symptoms.

Parkinsonism is defined by any combination of these six cardinal motor deficits: tremor at rest, rigidity, bradykinesia (slowness of movement), postural instability, flexed posture and freezing (feet are transiently “glued” to the ground)[20]. Two of these motor features need to be present before the diagnosis is made, being at least one of them tremor at rest or bradykinesia. PD is the type of parkinsonism most frequently encountered by clinicians[4,9].

Symptoms start insidiously and become worse over time. Appearance of asymmetrical symptoms, affecting only one side of the body, is typical at disease onset, before they eventually spread to the other side[3,4,9]. Then, with disease evolution, motor symptoms are more generalized, and can result in a tendency of the trunk to bend forward, a balance impairment and walking difficulties[21].

Although motor symptoms are considered capital, PD is also associated with some non-motor symptoms that markedly impair the quality of life of patients. These include autonomic system dysfunction, cognitive and behavioral abnormalities, sleep disorders and sensory impairment (summarized in Figure 4)[9,22,23]. Dementia occurs frequently in advanced stages of PD, since 75-80% of patients suffer it after 20 years of disease onset[3]. Other frequent non-motor PD symptoms are depression, it is estimated that the 40% of patients experience it[24], and sleep disorders, since the majority of patients suffer some kind of sleep disorder[25].

INTRODUCTION

Autonomic system dysfunction	Sleep disoders
Hypotension	Sleep fragmentation
Constipation	REM sleep behavior disorder
Sexual dysfunction	Excessive daytime sleepiness
Seborrhea	
Sweating	
Cognitive and behavioral abnormalities	**Sensory impairment**
Dementia	Olfactory dysfunction
Depression	Pain
Anxiety	Paresthesia (sensation of skin tickling, pricking or burning)
Aphaty	Akathisia (”inability to sit”)

Figure 4. Non-motor symptoms of Parkinson’s disease. Common non-motor PD symptoms classified in four groups according to the type of affectation.

While the dopamine-dependent motor abnormalities dominate in early stages of the disease, the non-dopaminergic or non-motor symptoms, are frequently more disabling in advanced stages of PD[16,26].

1.4 Etiology

Even though the neuropathological features are well defined, the etiology of sporadic PD, which represents the 90-95 % of cases, is still not clear. Nowadays, is widely accepted to be multifactorial, combining environmental factors, genetics and aging, which is the factor that most strongly correlates to the illness onset[27–29].

Environmental factors known to influence PD condition range from general factors, including rural environment, well water, exposure to plant-derived toxins or pesticides, to more specific factors, such as exposure to organic solvents, carbon monoxide and carbon disulfide[28,30]. Regarding the genetic factors, some susceptibility genes have been implicated in the disease, but need to be further confirmed[31].

The other 5-10% of PD cases are known to be monogenic forms of the disease. At least, seven genes have been identified as causative genes for PD. Mutations in SNCA (α-synuclein) and LRKK2 genes are associated with autosomal dominant PD, and mutations in parkin, PINK1, DJ-1 and ATP13A2 genes are associated with autosomal recessive PD (Table 1)[31,32]. The functional characterization of these PD-associated genes has importantly contributed to obtain new insights into the molecular pathogenesis of idiopathic PD[33].

INTRODUCTION

Locus name	Gene	Protein	Mode of inheritance	Types of mutations	Onset age	Ref.
PARK1 /4	SNCA	α-synuclein	Dominant	A53T, E46K, A30P, H50Q, G51N and gene multiplications	24-65	34,35
PARK2	PARK2/ parkin	parkin	Recessive	>100 mutations (point mutations, exonic rearrangements)	<45	36
PARK6	PINK1	PTEN-induced putative kinase 1	Recessive	>40 point mutations, rare large deletions	20-40	37
PARK7	DJ-1	DJ-1	Recessive	>10 point mutations and large deletions	20-40	38
PARK8	LRRK2	Leucine-rich repeat 2	Dominant	>5 point mutations	50-70	39,40
PARK9	ATP13A2	ATP13A2	Recessive	Point mutations, insertions and deletions	12-18	41

Table 1. Gene mutations that cause Parkinson's disease. Ref.= References

1.5 Treatment

So far, no therapy has demonstrated to be effective in preventing dopaminergic neuron death. Hence, PD treatment is focused on counteract the symptoms, and current therapies can be grouped in three categories: medication, surgery and physical therapy (addressed to improve gait and balance)[4].

Within the medication group, dopamine replacement is the principal approach to treat PD. Although several dopaminergic agents are available, the most effective drug to treat PD symptoms is levodopa, which is the immediate precursor of dopamine. Levodopa is commonly administered with a peripheral decarboxylase inhibitor in order to avoid formation of dopamine in the peripheral tissues. However, after five years of treatment, 60% of patients develop troublesome complications, such as the "wearing-off" effect (the improvement gained from a dose of levodopa does not last until the next dose) and dyskinesia (abnormal involuntary movements)[4,9].

Stereotaxic deep brain stimulation (DBS) is a surgical procedure used in PD treatment when medication cannot adequately control the symptoms. This technique is based on electrical stimulation, and adjustments of the parameters, such as voltage and frequency, are regularly needed. The location of the stereotaxic target is an aspect that needs to be studied for each patient, since depending on the brain region targeted different symptoms can be controlled[4,9].

2. MOLECULAR MECHANISMS AND MODELS IN PARKINSON'S DISEASE

Although many potential mechanisms have been implicated in PD pathogenesis, causes underlying neuronal death remain poorly understood. In this sense, the use of cellular and animal PD models represents a valuable tool to investigate specific molecular events promoting neurodegeneration. A better understanding of these mechanisms would be crucial to attain new strategies to halt neuron death[5].

2.1 Pathogenic molecular mechanisms implicated in PD

To date, defects in many cellular processes have been proposed as early triggers of neuronal death in PD, including protein misfolding and aggregation, impaired protein degradation, mitochondrial dysfunction and oxidative stress. An increasing dysfunction of these systems can recruit pathways directly involved in cell death, such as JNK (c-Jun N-terminal kinase) signaling, p53 activation, cell cycle re-activation and Bcl-2 signaling, eventually leading to neurodegeneration (reviewed in [42]).

2.1.1 Protein misfolding and aggregation

Protein misfolding and aggregation have been involved in PD pathogenesis since LBs were found in affected brain regions[43]. Interestingly, α-synuclein, a pre-synaptic protein encoded by a PD-linked gene (Table 1), is the major component of LBs[33,44]. Apart from its presence in PD, α-synuclein aggregates have been observed in other neurodegenerative diseases, which have been named synucleinopathies[45]. Protein aggregates that cannot be cleared by the cell can hamper normal cellular topography and physiology, eventually leading to cell death[46–48]. Moreover, evidence suggest a general increment in protein aggregation in PD substantia nigra[49].

2.1.2 Impaired protein degradation

Eukaryotic cells possess two major pathways that mediate protein degradation and deal with abnormal proteins: the ubiquitin-proteasome system (UPS) and the lysosomal system. Deficits in these pathways can lead to accumulation of toxic proteins compromising cellular function and survival[50]. Prior to their breakdown, proteins are generally tagged with ubiquitin as a degrading signal[51].

Ubiquitination is an energy-dependent multistep process that requires three enzymes: an ubiquitin-activating enzyme (E1), an ubiquitin-conjugating enzyme (E2) and an ubiquitin-ligase enzyme (E3). In the first step, which is ATP-dependent, the carboxyl terminus of ubiquitin is conjugated to a cysteine residue of the E1 enzyme, generating a thiol ester linkage. Then, ubiquitin is transferred to a cysteine residue of the E2, and finally, in the last

step, E3 enzyme catalyzes the transfer of ubiquitin to a lysine ε-amino group of the substrate protein forming an isopeptide bond (Figure 5)[52–54].

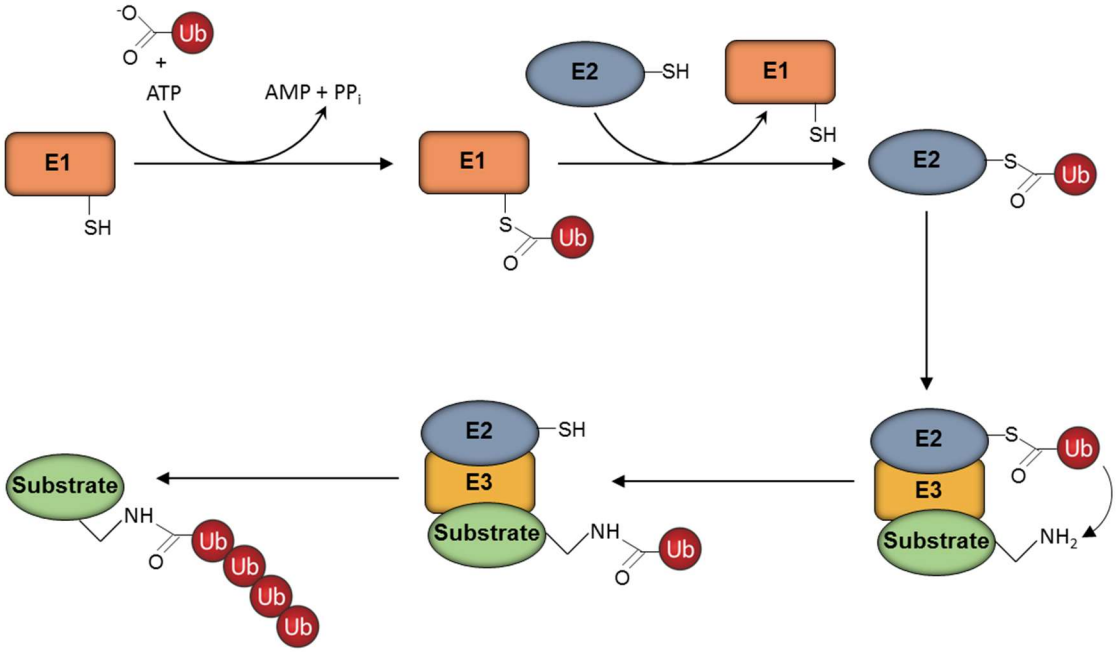

Figure 5. Ubiquitination process. Ubiquitination is a three-step process that results in the transfer of ubiquitin to protein substrates. .

This post-translational modification results in conjugation of ubiquitin to protein substrates. As final outcome, an ubiquitin molecule can be attached to a lysine residue in the substrate protein (monoubiquitination), single ubiquitin molecules can be conjugated to different lysines in the substrate (multi-monoubiquitination) or multiple ubiquitin molecules can be attached to the same lysine residue forming a polyubiquitin chain (polyubiquitination) (Figure 6)[55].

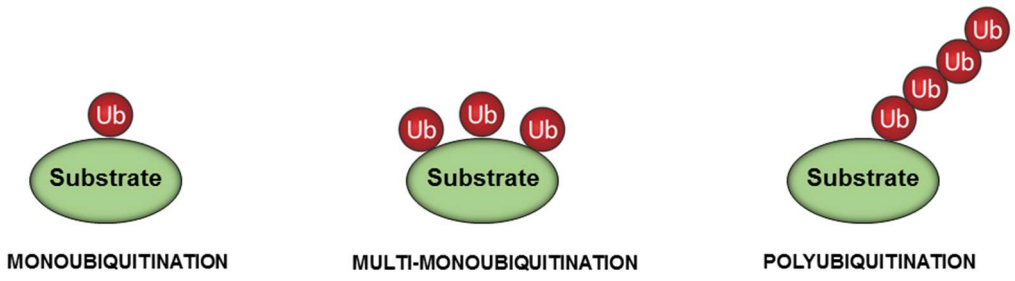

Figure 6. Types of ubiquitination. The ubiquitination process has three general outcomes: monoubiquitination, multi-monoubiquitination and polyubiquitination of substrate proteins.

Since ubiquitin has seven lysines (K6, K11, K27, K29, K33, K48 and K63), different type of polyubiquitin chains can be formed[56,57]. Importantly, the type of ubiquitination/polyubiquitination will determine the protein fate, which can vary from degradation to function regulation in non-proteolytic processes[53].

For instance, polyubiquitin chains formed by the successive linkage of ubiquitin molecules through lysine K48 target proteins for degradation via UPS[58,59], while polyubiquitin chains formed by the successive linkage of ubiquitin through lysine K63 target proteins to lysosomal degradation[60–62] or regulate processes such as receptor endocytosis[63] and DNA repair[64]. Other type of polyubiquitin chains can be formed, but their function is not as well characterized[61].

2.1.2.1 Ubiquitin-proteasome system (UPS)

The UPS is the primary pathway mediating normal and abnormal protein degradation, and its failure triggers protein accumulation and cell death[65,66]. Briefly, proteins tagged with K48-linked polyubiquitin chains are recognized and degraded by the 26S proteasome in an ATP-dependent process[67]. The 26S proteasome is a large cylinder composed of three parts: one 20S catalytic subunit and two 19S regulatory subunits that recognize and facilitate entrance of the substrates. After degradation of the substrate, ubiquitin monomers are released and can be reused[68].

Increasing evidence point out to a dysfunction of this system in PD. In line with this, many UPS components have been found in LBs[69]. Proteasome structure and activity is selectively altered in several brain areas of PD patients, including the SNpc[69,70]. Furthermore, pharmacologic UPS inhibition promotes the formation of α-synuclein inclusions and induces apoptotic cell death in dopaminergic cells[71–73].

2.1.2.2 Lysosomal degradation

Lysosomal degradation is the common final step at which two different pathways converge: the endosomal-lysosomal pathway and the autophagy-lysosomal pathway (ALP) (Figure 7). Hence, the vast majority of membrane proteins are endocytosed and degraded via lysosomes. However, lysosomes are also involved in the degradation of cytosolic proteins via autophagy[51].

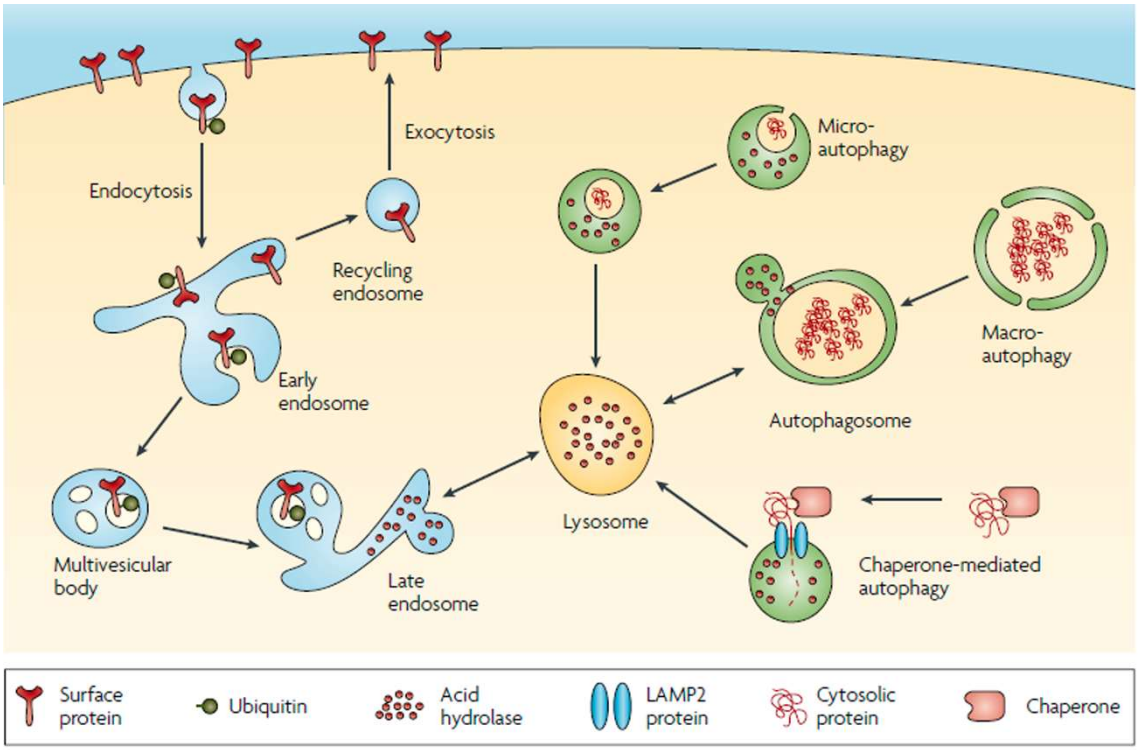

Figure 7. Protein degradation through lysosomal pathways. Lysosomes are the common degradative end-point of the endosomal-lysosomal and the autophagy-lysosomal pathways. In the endosomal-lysosomal pathway monoubiquitinated or K63-polyubiquitinated membrane proteins are endocytosed to early endosomes. Next, they can be sorted to recycling endosomes (for going back to the membrane via exocytosis) or to multivesicular bodies (for transport to late endosomes and lysosomes). In the autophagy-lysosomal pathway cytosolic proteins can enter lysosomes via different mechanisms[63]. In macroautophagy, a large amount of cytoplasm is surrounded by a membrane to form an autophagosome that will fuse with lysosomes. In microautophagy, a small quantity of cytosolic material is internalized to lysosomes via invagination. In chaperone-mediated autophagy, cargo is recognized by chaperones and directly translocates to lysosomes through interactions with LAMP2 (lysosome-associated membrane protein 2)[74]. Lysosomes are organelles that contain acid hydrolases capable of breaking down several biomolecules[75]. Image obtained from Tai H and Schuman E (2008)[51].

-Endosomal/lysosomal pathway

The endosomal pathway is crucial for the degradation or recycling of membrane proteins and for the trafficking of Golgi-associated proteins. Besides, it is also implicated in the extracellular release of proteins within exosomes, a type of microvesicles that mediate cell-to-cell communication[76].

Regarding membrane proteins sorting, monoubiquitination or K63-linked polyubiquitination functions as a signal for trafficking to the endosome via ESCRT (endosomal sorting complexes required for transport). Internalized proteins are delivered to early endosomes, a point where they can be returned to the membrane by exocytosis or they can continue the degrading process through multivesicular bodies, late endosomes and lysosomes (Figure 7)[63].

Importantly, neurons are highly reliant on this pathway, since neurotransmission requires a fine-tuned regulation of synaptic vesicles recycling and degradation[76]. Of note, changes in the activity of endo-lysosomal enzymes are found in the cerebrospinal fluid of sporadic PD patients[77]. Moreover, α-synuclein can hinder cellular function by altering membrane fusion events in the endosomal pathway[78].

-Autophagy-lysosomal pathway (ALP)

Autophagy is a lysosomal degradation pathway involved in the clearance of misfolded proteins, large debris and damaged organelles. Depending on the delivery mode of the substrates to lysosomes, three types of autophagy have been reported: macroautophagy, microautophagy and chaperone-mediated autophagy (CMA) (reviewed in [79,80]). Macroautophagy is the best characterized type of autophagy, and it is generally referred as autophagy (Figure 7).

Although this pathway is commonly considered a bulk degradation system, increasing evidence reveal that different cellular structures can be selectively cleared[81]. In these cases, cargo needs to be tagged for further recognition and degradation. In particular, K63-linked polyubiquitination has been reported as a signaling strategy for autophagy-mediated clearance of protein inclusions[82].

Autophagy is induced in response to nutrient deprivation, but is constitutively active in neurons, becoming crucial for survival[83]. Autophagy impairment produces accumulation of abnormal proteins and damaged organelles, a feature usually observed in PD and other neurodegenerative diseases[84,85]. Of note, accumulation of autophagic vacuoles has been observed in the SN of PD patients[86]. In additional, compounds that function as autophagy enhancers mitigate dopaminergic neurodegeneration *in vitro* and *in vivo*, supporting a protective role of autophagy in PD pathogenesis[87–89]. Besides, autophagy is important for the degradation of α-synuclein[90,91], and conversely, mutant forms of α-synuclein can hamper ALP function[90].

In addition to UPS and lysosomes, cells can deal with accumulation of proteins through an alternative pathway, the unfolded protein response (UPR). This system may also be involved in PD pathogenesis since it is activated by several PD neurotoxins and by mutant α-synuclein[46,92,93].

2.1.3 Mitochondrial dysfunction

Abnormal function of the mitochondria has been proposed as a pathogenic mechanism in PD[94]. Mitochondrial defects can result in insufficient ATP production and reactive oxygen species (ROS) generation. Evidence reveal a decrease of the mitochondrial complex I activity

in the SNpc of PD patients[95]. Mutations in PINK1 and parkin genes, have also been related to mitochondrial dysfunction[96,97]. Additionally, exposure to neurotoxins reported to affect mitochondria, such as MPTP (1-methyl-4-phenyl-1,2,5,6-tetrahydropyridine), mimic several PD features[98].

2.1.4 Oxidative stress

Oxidative stress is known to play an important role in dopaminergic neurons degeneration. Many biological markers linked to oxidative damage are upregulated in the SNpc of PD patients, while the levels of the antioxidant glutathione are reduced[99,100]. Furthermore, dopamine metabolism and autoxidation can generate different ROS, creating a state of oxidative stress that may particularly affect dopaminergic neurons[101,102]. Additionally, nitrosative stress also contributes to neurodegeneration[103,104].

Apart from the aforementioned mechanisms, neuroinflammation, impaired kinase signaling and calcium deregulation have also been involved in PD pathogenesis[42]. However, it is important to highlight that the exact mechanism triggering final cell death in PD is still unknown.

2.2 Models of PD

The use of cellular and animal models is crucial to better comprehend molecular mechanisms underlying neurodegeneration and to test new potential therapeutic targets. Unfortunately, none of the existing PD models exactly phenocopy the disease, but two main types of models have contributed to gain knowledge: genetic and neurotoxin models[105].

2.2.1 Neurotoxin-based models

Neurotoxin-based models have been widely used, since they specifically affect catecholaminergic neurons and induce degeneration. Among these toxins, 6-OHDA (6-hydroxydopamine), MPTP, rotenone and paraquat have obtained the most attention (reviewed in [106]). In this thesis, 6-OHDA has been used as a neurotoxin in cellular PD models.

6-OHDA was the first catecholaminergic neurotoxin discovered 45 years ago and nowadays, is one of the best characterized PD toxins[107]. Since it structurally resembles DA and norepinephrine, 6-OHDA is efficiently uptaken and accumulated by neurons that have catecholaminergic transporters for these neurotransmitters, causing a selective toxicity to monoaminergic neurons[108]. Furthermore, 6-OHDA has been found in patients as the result of endogenous dopamine oxidation[109–111].

Inside cells, 6-OHDA is metabolized by monoamine oxidase enzyme (MAO) generating hydrogen peroxide[112], but it is also rapidly autoxidized producing ROS and metabolites that

INTRODUCTION

can damage cells[113–117]. These events mimic one of the main pathogenic mechanisms of PD, oxidative stress[118–120]. Moreover, it has been described that 6-OHDA can directly inhibit complex I of the mitochondrial respiratory chain, causing a harmful depletion of intracellular ATP that can eventually lead to cell death[121–124] (Figure 8). This two 6-OHDA toxic actions are biochemically independent, although they may act in a synergistic way *in vivo*[123].

Extracellular ROS generation caused by 6-OHDA autoxidation is also a toxic process that leads to cell death (Figure 8). In this case, the selectivity of the toxin for dopaminergic neurons is explained for their extraordinary sensitivity to oxidative stress[125–127]. However, this toxic mechanism can also promote the non-specific death of other cell types devoid of catecholamine transporters[128], such as cortical neurons[129].

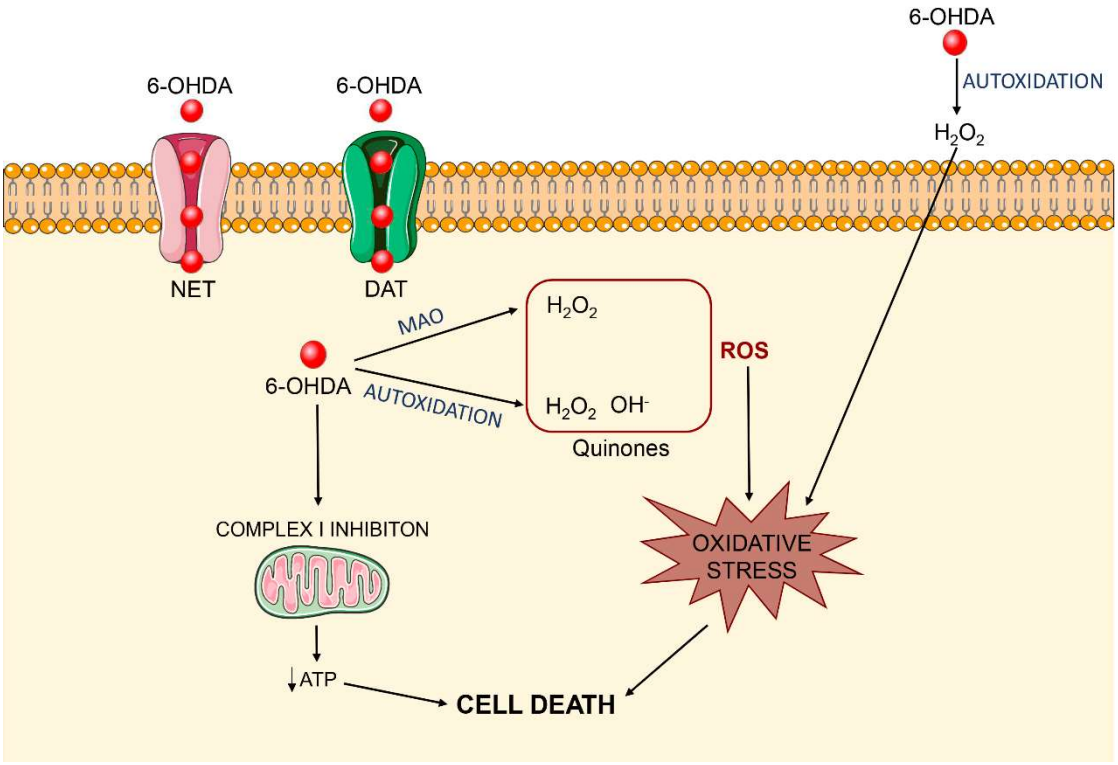

Figure 8. Mechanisms of 6-OHDA toxicity. PD toxin 6-OHDA can selectively enter catecholaminergic neurons through dopamine (DAT) and norepinephrine transporters (NET). Inside the cell, 6-OHDA can promote toxicity by two main mechanisms: oxidative stress caused by ROS generation that result from 6-OHDA autoxidation or monoamine oxidase enzyme (MAO) activity, or ATP depletion caused by inhibition of the mitochondrial respiratory chain complex I. Moreover, extracellular 6-OHDA autoxidation also generates ROS, contributing to oxidative stress and consequent cell death. Abbreviations: ROS, reactive oxygen species. Figure adapted from Brum, et al. 2001[130], some images were obtained from http://servier.co.uk/content/servier-medical-art.

The first animal PD model associated with dopamine neuron death in the SNpc was developed using 6-OHDA[131]. Since then, this PD-mimetic toxin has been widely used not only for *in vivo* studies, but also for *in vitro* assays. *In vitro* studies are particularly useful to study the consequences of toxin exposure in a cellular environment. A cell type that has been extensively used with 6-OHDA are NPC12 cells (PC12 cells differentiated with nerve growth factor, NGF)[125,127,132–137], since they present a catecholaminergic phenotype that resemble

INTRODUCTION

sympathetic neurons[138,139], a subpopulation also affected in PD[140–142]. The use of cellular PD models is instrumental to simplify such a complex disease, since individual pathogenic molecular mechanisms and the proteins involved can be explored separately. Moreover, they have the advantage of a controlled microenvironment and of being fast and reproducible methods[143].

2.2.2 The use of human samples from PD patients

However, since neither of the available models are able to replicate all major characteristics of human PD, it is convenient to employ human samples to corroborate hypothesis tested *in vitro* and *in vivo* [144]. In this study we have worked with two different types of human samples: postmortem SNpc sections and skin fibroblasts from PD patients.

Postmortem brain tissue and sections have been widely used in PD investigations[136,137,145–148]. However, when working with these samples is important to consider the age, clinical information and postmortem collection time of each patient, since these parameters may affect the results. Furthermore, control patients with similar age and postmortem time are needed for proper comparison. Despite these limitations, biochemical studies of postmortem brains have largely contributed to confirm molecular mechanisms implicated in PD pathogenesis[149].

On the other hand, cultures of skin fibroblasts derived from genetic and sporadic PD patients have the advantage of their easy availability and robustness. Moreover, they are being studied as a potential helpful tool to identify PD biomarkers, since they are primary human cells that retain the harmful biological effects of aging, even in culture[150].

3. mTOR SIGNALING PATHWAY DEREGULATION IN PARKINSON'S DISEASE

The aforementioned alterations in various cellular processes can trigger deregulation of important signaling pathways in PD. In this thesis, we have focused on mTOR pathway and its implication in neuronal death. This signaling pathway integrates internal and external cues to regulate major cellular processes involved in the maintenance of cellular homeostasis. For this reason, deregulation of mTOR has been implicated in many diseases, including neurodegenerative disorders (reviewed in [151]).

3.1 Mechanistic target of rapamycin (mTOR)

As deduced from its name, mTOR is the kinase target of rapamycin, a macrolide produced by *Streptomyces hygroscopicus* bacteria that was initially discovered in a soil sample from the Eastern Island[152]. mTOR is an atypical serine/threonine kinase that belongs to the family of phosphoinositide 3-kinase (PI3K)-related kinases. It is an extremely large protein of 289 KDa ubiquitously expressed in the majority of tissues and cell types, including neurons[153].

mTOR interacts with distinct proteins forming two different complexes, named mTOR complex 1 (mTORC1) and mTOR complex 2 (mTORC2), which have different composition and function. Both complexes share some proteins, but also present unique components that distinguish them (Figure 9). They respond to various upstream inputs to regulate different cellular processes; mTORC1 senses oxygen, amino acids, stress, energy and growth factors to modulate macromolecular biosynthesis, cell cycle progression, growth, metabolism and autophagy, while mTORC2 responds to growth factors to regulate metabolism, cytoskeletal organization and cell survival[151,154].

Furthermore, mTORC1 and mTORC2 complexes display different sensitivities to rapamycin inhibitor; the first was initially considered sensitive, while the second was considered insensitive to rapamycin[155,156]. Rapamycin, as an allosteric inhibitor, interacts with FK506-binding protein (FKBP12)[157,158]. This complex only binds raptor-bound mTOR[155,156,159,160], inhibiting mTORC1 kinase activity, probably by disrupting complex assembly[161,162]. Nonetheless, prolonged rapamycin exposure has been described to inhibit mTORC2 complex in several cell types[163].

INTRODUCTION

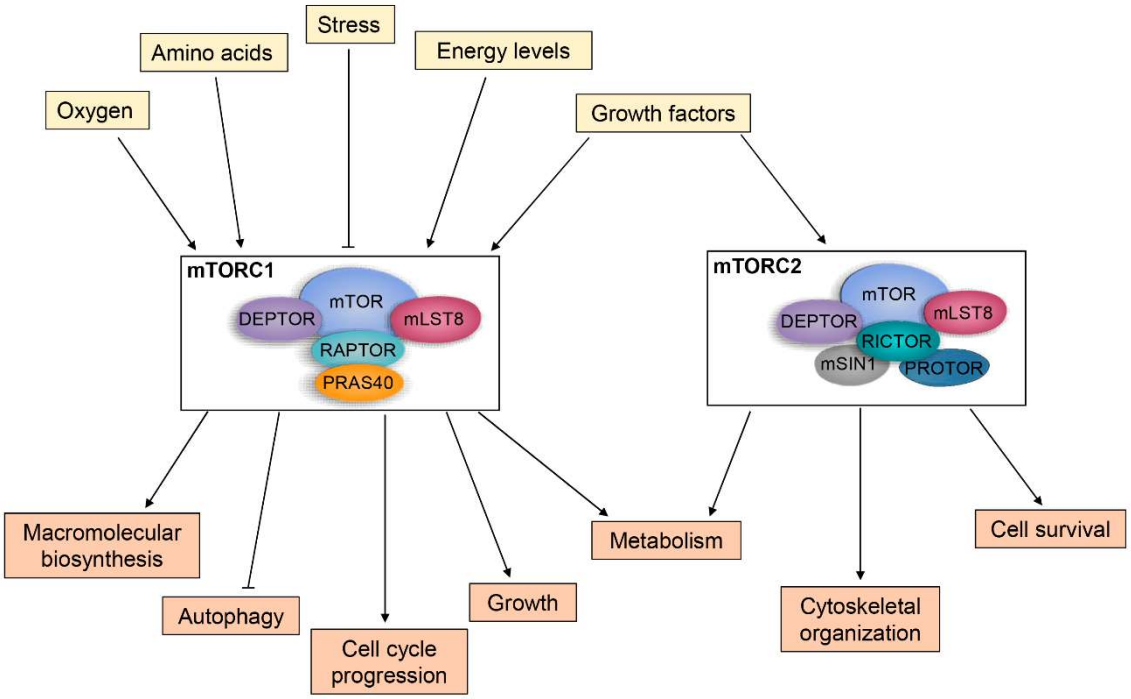

Figure 9. Composition and regulation of mTORC1 and mTORC2 complexes. Both complexes share the catalytic subunit mTOR, mammalian lethal with sec13 protein 8 (mLST8; also known as GbL) and DEP domain containing mTOR-interacting protein (DEPTOR). mTORC1 is distinguished by the presence of regulatory-associated protein of mammalian target of rapamycin (raptor) and proline-rich Akt substrate 40 KDa (PRAS40); whereas mTORC2 is distinguished by the presence of rapamycin-insensitive companion of mTOR (rictor), mammalian stress-activated MAP kinase-interacting protein 1 (mSin1) and protein observed with rictor (protor)[151]. They are sensitive to various upstream signals to regulate different cellular processes. Image adapted from Zoncu, et al. (2011) [164] and Laplante, et al. (2012)[151].

3.2 mTOR signaling pathway

Several growth factors, such as insulin, can activate the PI3K and Ras pathways through its effector kinases Akt and ERK1/2 (extracellular-signal-regulated kinase 1/2), respectively[165–167]. Both pathways converge into TSC2 phosphorylation, leading to heterodimeric TSC1/2 (tuberous sclerosis 1/2) complex inactivation[168–172]. This complex functions as a GTPase activating protein (GAP) towards Rheb (Ras homolog enriched in brain), promoting its conversion to the inactive guanosine diphosphate-bound state (Rheb-GDP)[173]. Hence, growth factors, by inactivating TSC1/2 complex, stimulate the formation of the active Rheb-GTP form. This active form of Rheb is able to activate mTORC1 kinase activity[174–176], and it also seems to induce mTORC2 kinase activity[136,137,177] (Figure 10).

INTRODUCTION

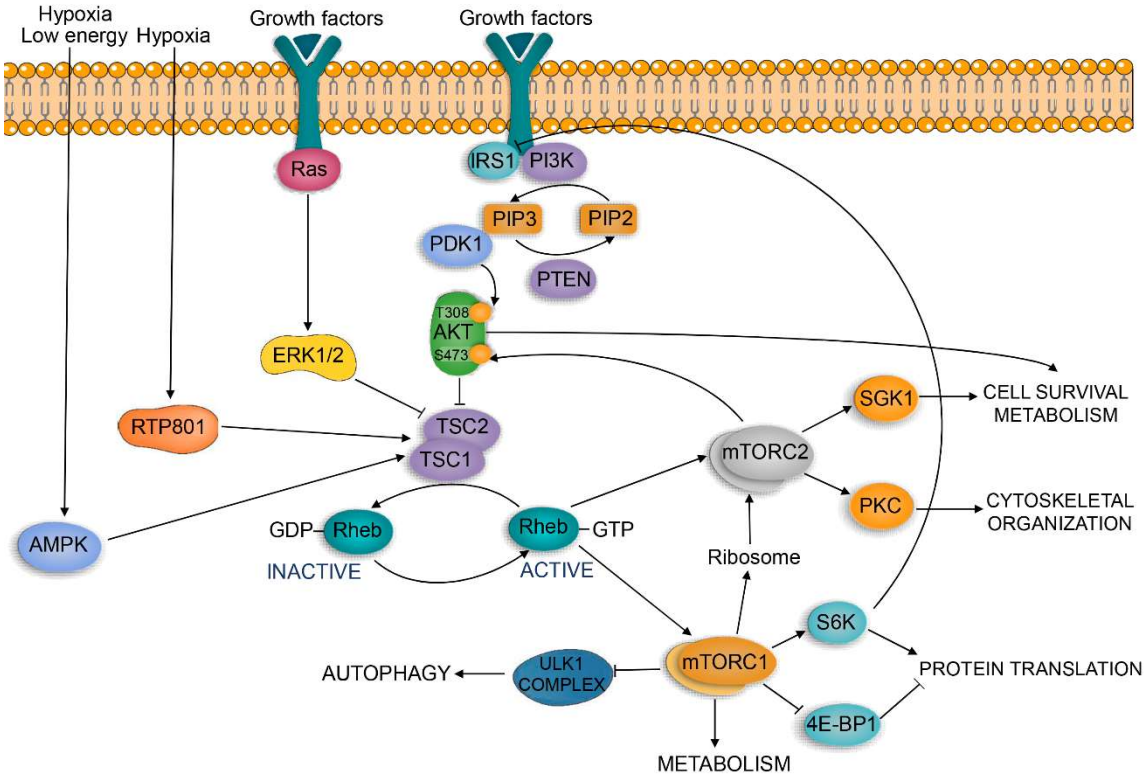

Figure 10. mTOR signaling pathway. Schematic representation of the key upstream regulators and downstream effectors of mTORC1 and mTORC2 and their signaling interrelation. Figure adapted from Laplante and Sabatini (2012)[151] and Wullschleger et al. (2006)[177].

Some cellular stresses regulate mTOR activity through TSC1/2 complex. For instance, hypoxia or low energy levels induce AMPK (adenosine monophosphate-activated protein kinase), which in turn phosphorylates TSC2, promoting its GAP activity[178]. RTP801/REDD1 also responds to hypoxia and enhances TSC2 activity through a not well established mechanism, leading to mTOR signaling repression[179–181].

mTORC1 controls protein translation via 4E-BP1 (eukaryotic translation initiation factor 4E binding protein 1) and S6K1 (p70-S6 kinase 1) phosphorylation (reviewed in [182,183]), autophagy via ULK1 complex inhibition[184–186], cellular metabolism via HIF-1 (Hypoxia inducible factor 1)[187,188], lipid synthesis[189] and ribosome biogenesis[190].

mTORC2 responds to growth factors via PIP3 (phosphatidylinositol 3,4,5-triphosphate) activation/PI3 kinase, although the mechanism is poorly understood[191]. Recently, it has been proposed that ribosomes induce mTORC2 signaling by directly binding it in a PI3K-dependent manner[192]. Taking into account that mTORC1 regulates ribosome biogenesis, the activity of both complexes would be interrelated.

mTORC2 downstream targets include some AGC family kinases (named after the protein kinase A, G, and C families, PKA, PKC and PKG); it phosphorylates SGK1 (serum and glucocorticoid-induced protein kinase 1)[193] and Akt at serine residue 473 (S473)[194],

controlling cell survival and metabolism. mTORC2 also phosphorylates PKC-α (protein kinase C-α), a protein that regulates cytoskeletal organization[155,156].

Akt, also known as PKB, is a critical signaling protein that regulates a range of processes, including survival, proliferation, metabolism, and apoptosis[195,196]. It can be phosphorylated by PDK1 at threonine residue 308 (T308)[197] and by mTORC2 at serine residue 473 (S473)[194], requiring phosphorylation at both sites to be fully active. Furthermore, Akt is upstream of mTORC1, and activates it via TSC1/2 phosphorylation[168,170,171], but also via inactivation of PRAS40, which is a mTORC1 component (see figure 9)[198–201].

Importantly, the PI3K-Akt axis has been reported to be critical for survival maintenance in several neuronal systems[137,202–207]. Akt pro-survival kinase exerts its protective function by inactivating several pro-apoptotic downstream targets, such as Bad[208], Bax[209], Bim[210,211] and JNK[212].

3.3 mTOR/Akt signaling alterations in PD

In the nervous system, mTOR pathway has emerged as a central signaling hub, since it controls autophagy, survival via Akt (reviewed in [204,213]), and protein translation, a process considered crucial for the formation and consolidation of synaptic contacts[214–216].

In the case of PD, deregulation of mTOR pathway has been observed at different levels. Defects in autophagy-mediated protein clearance, a process mainly regulated by mTORC1, have been implicated in PD pathogenesis (as previously mentioned in section 2.1.2). Importantly, rapamycin, an allosteric mTORC1 inhibitor, promoted autophagy and reduced the accumulation of ubiquitinated α-synuclein in neuronal cells[86,91].

On the other hand, alterations in Akt pro-survival kinase activity have been involved in PD-related cell death[139]. Indeed, Akt phosphorylation levels at S473 and T308 were significantly reduced in nigral neurons from postmortem PD brains[137]. Supporting this notion, constitutively active Akt was protective in front of 6-OHDA toxicity[137] and in the soma and axons of dopaminergic neurons in PD mouse models[217,218]. Moreover, in cells exposed to PD toxins, inhibition of the downstream mTORC1 effectors S6K1 and 4E-BP1 also contributed to neuronal death[219,220].

4. NEDD4

NEDD4 (Neural precursor cell-expressed developmentally down-regulated gene 4) was originally discovered in 1992 as a highly expressed gene in the central nervous system from mouse embryos[221,222]. This protein is a member of the evolutionarily conserved NEDD4 family, which in mammals is composed of nine members: NEDD4, NEDD4-2 (NEDD4L), ITCH, SMURF1, SMURF2, WWP1, WWP2, NEDL1 and NEDL2. In fact, NEDD4 and NEDD4-2 are the most closely related[223–225]. Conversely, NEDD4 family consists of only a member in yeast *Saccharomyces cerevisiae*, termed Rsp5[226].

NEDD4 gene encodes a protein of approximately 120 KDa that is expressed in most tissues[222]. It localizes at the cytoplasm, predominantly at the perinuclear and periphery regions[227] and at the cell membrane[228]. NEDD4 is also present in neurites of differentiated neuronal cells[227] and can be recruited to be released within exosomes by Ndfip1 (NEDD4 family interacting protein 1)[229].

4.1 NEDD4 as an E3 ubiquitin ligase

NEDD4 is an E3 ubiquitin-protein ligase, an enzyme that catalyzes the transfer of ubiquitin (Ub) to protein substrates (see figure 5). Depending on how ubiquitin is transferred to the substrate, there are two main types of E3 ligases: RING-type (Really Interesting New Gene) and HECT-type (Homologous to the E6-AP Carboxyl Terminus). RING E3 ligases facilitate the direct transfer of ubiquitin from the E2 to the substrate, whereas HECT E3 ligases accept ubiquitin before transferring it to the substrate (Figure 11)[230].

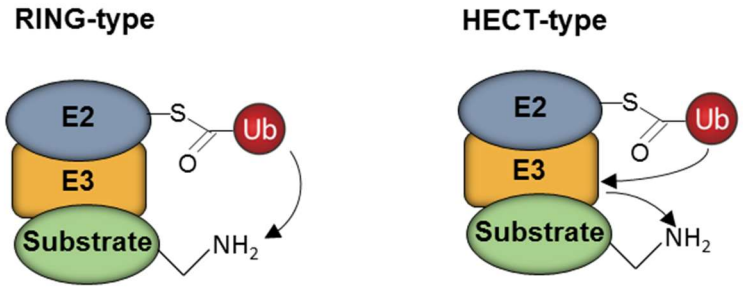

Figure 11. Ubiquitination mechanism of RING and HECT E3 ligases. RING E3 ligases function as scaffolding proteins that facilitate ubiquitin transfer from the E2 to the substrates, while HECT E3 ligases accept ubiquitin prior transferring it to the substrate.

NEDD4 belongs to the group of HECT E3 ubiquitin ligases (reviewed in [231]). In humans, there are few E1, dozens of E2 and hundreds of E3 enzymes. The last ones are the most diverse class and confer specificity for the substrates[232]. An E3 ligase can function with several E2 enzymes. For instance, NEDD4 is able to accept ubiquitin from Ubc4, UbcH5a, UbcH5b, UbcH5c, UbcH6, UbcH7 and AtUBC8 E2 enzymes[227,233].

4.2 NEDD4 protein structure

NEDD4 is a modular protein composed of an N-terminal (amino-terminus) calcium/lipid-binding domain (C2 domain), three (in mouse and rat) or four (in human) WW protein-protein interaction domains and a C-terminal (carboxyl-terminus) catalytic HECT domain responsible for ubiquitin ligation. This general protein domain architecture is shared by all NEDD4 family members (Figure 12)[226].

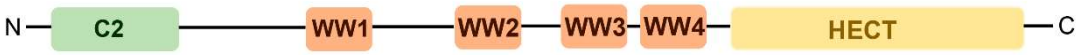

Figure 12. NEDD4 modular structure. Schematic representation of the human NEDD4 protein domains.

The C2 domain targets proteins to membranes[234] but it can also interact with other proteins[235,236]. The WW domains are characterized by the presence of two conserved tryptophan (W) residues and are implicated in protein binding through recognition of proline-rich PY motifs (PPXY or PPLP) or phospho-serine/threonine residues in substrate proteins[237–239]. The HECT domain contains a conserved catalytic cysteine that accepts ubiquitin from the E2 enzyme before transferring it to the substrate[240]. This catalytic residue corresponds to the cysteine 867 (C867) in human NEDD4 protein[241,242].

4.3 NEDD4 function

Several proteins have been identified as NEDD4 substrates, revealing its implication in a wide range of cellular processes. For instance, NEDD4 has been reported to reduce the activity of some ion channels, such as the epithelial sodium channel (ENaC), by regulating their turnover and localization[243]. Moreover, NEDD4 also plays a role in the regulation of some growth factor signaling receptors, including IGF-1R (Insulin-like growth factor 1 receptor)[228,244,245], FGFR1 (Fibroblast growth factor receptor 1)[246] and EGFR (epidermal growth factor receptor)[247].

Besides, NEDD4 might facilitate tumorigenesis by degrading some tumor suppressor genes, such as Beclin 1 and PTEN (phosphatase and tensin homolog)[86,248,249]. However, PTEN/Akt axis regulation by NEDD4 is nowadays controversial, since PTEN levels or stability were not modified in NEDD4$^{-/-}$ MEFs (Mouse embryo fibroblasts)[250]. Many other potential NEDD4 substrates have been described, involving this E3 ligase in much more functions and signaling pathways[231].

In order to examine its physiological role *in vivo*, a NEDD4 knockout mouse model was generated. The resulting animals presented a neonatal lethal phenotype, revealing that NEDD4 regulates critical cellular functions during development. They also showed embryonic retardation, reduced body weight and defects in the structure and function of the neuromuscular junction[251,252]. This growth retardation was attributed to a reduced IGF-1

INTRODUCTION

(Insulin-like growth factor 1) signaling, since NEDD4 positively regulates it through adaptor Grb10[251].

A second NEDD4 knockout mouse was independently created and also displayed embryonic lethality, along with heart defects, vasculature anomalies, and impaired dendrite development[253,254]. Considering NEDD4 conventional knockout mice mortality, further studies have been performed with heterozygous mice or with conditional knockout mice[254,255].

4.4 NEDD4 regulation

NEDD4 E3 ligase activity is controlled through an autoinhibitory conformation that is characterized by the intramolecular interaction between the N-terminal C2 domain and the catalytic C-terminal HECT domain (Figure 13). This catalytically inactive state can be released by abrogation of the C2 domain or by elevation of intracellular calcium, which is proposed to bind the C2 domain, targeting NEDD4 to the membrane and thereby disrupting the intramolecular autoinhibitory interaction[256].

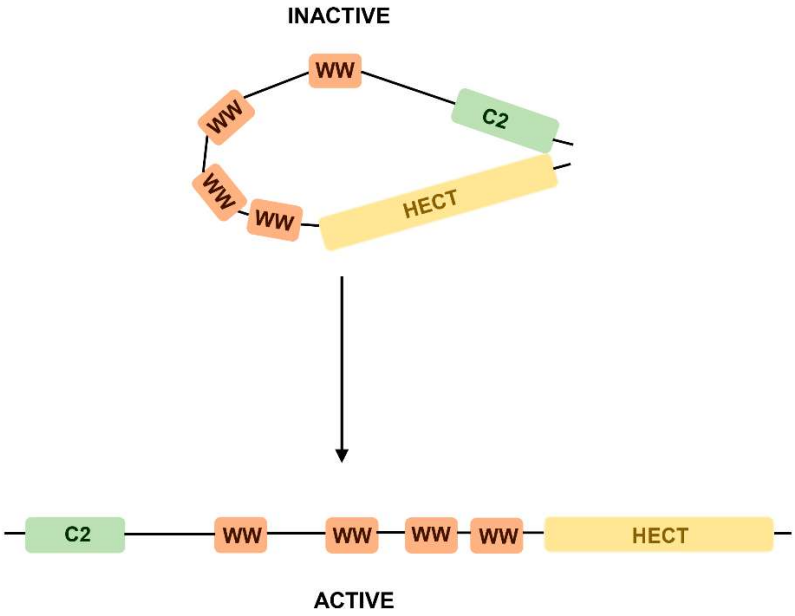

Figure 13. Schematic representation of the C2-mediated regulation of NEDD4 activity. In basal conditions NEDD4 exhibits an intramolecular autoinhibitory interaction (upper part) that can be shifted to an active conformation (lower part) by different signaling stimuli. Image adapted from Persaud et al. (2014)[257].

Other proteins known as NEDD4 activators can counteract this inhibitory conformation. NDFIP1 and NDIFP2 (NEDD4 family-interacting proteins) proteins induce NEDD4 E3 ligase activity by directly binding to NEDD4 WW domains[258]. Beyond that, these proteins can function as NEDD4 adaptors by facilitating binding of substrate proteins lacking PY motifs[259,260]. Moreover, c-Src-mediated phosphorylation also stimulate NEDD4 activity by shifting its conformation to an active state[257].

In regard to NEDD4 protein stability regulation, only a mechanism have been described; NEDD4 can be phosphorylated by CKI (Casein Kinase-I) leading to $SCF^{\beta\text{-}TRCP}$-mediated (Skp, Cullin, F-box containing complex, E3 ubiquitin-ligase) ubiquitination and subsequent degradation[249].

Interestingly, some neurotoxins that trigger oxidative stress, such as hydrogen peroxide, zinc or camptothecin, upregulated NEDD4 transcription in cortical neurons, leading to enhanced IGF-1Rβ (Insulin-like growth factor 1 receptor β) protein degradation via UPS[245].

4.5 NEDD4 in neurons

NEDD4 is a protein highly expressed in mammalian neurons that plays an important role in neuronal development and function[254,261,262].

NEDD4 has been involved in the development of neuronal circuits by regulating branching of dendrites and axons. By using conventional and conditional NEDD4 knockout mice it was demonstrated that the lack of NEDD4 decreased dendrite growth and arborization[254]. Importantly, Rap2a was identified as the NEDD4 substrate responsible for this phenotype[254]. On the other hand, NEDD4 E3 ligase controlled axon branching in *Xenopus* retinal ganglion cells and in mammalian peripheral neurons[263,264]. In this case, PTEN was described as the key NEDD4 substrate regulating these events[263,264]. However, others support that PTEN acts upstream of NEDD4 through mTORC1-dependent regulation of its translation[265,266].

Beyond neuronal development, NEDD4 has also been involved in synaptic transmission through regulation of AMPARs (Alpha-amino-3-hydroxy-5-methyl-isoxazole-4-propionic acid receptors), the principal mediators of excitatory currents. NEDD4 was enriched in the synaptosomal fraction and was reported to ubiquitinate AMPARs, altering their localization. Thus, NEDD4 promoted AMPAR endocytosis, leading to receptor reduction at the cell surface and the consequent depression of excitatory synaptic transmission[267]. Moreover, AMPAR activation promoted a rapid NEDD4 redistribution to dendritic spines[268]. Recently, this regulatory mechanism has also been implicated in the synaptic defects caused by the pathogenic peptide amyloid-β (Aβ)[269].

Furthermore, NEDD4 has been confirmed as an important physiological regulator of synaptic plasticity *in vivo*. Heterozygous mice, which present a 50% reduction in NEDD4 expression, showed long-term spatial learning and memory and long-term potentiation (LTP) impairment[270].

4.6 NEDD4 in PD

NEDD4 has been directly linked to PD pathogenesis since it was reported to target α-synuclein for degradation. NEDD4 ubiquitinated α-synuclein preferentially with K63 polyubiquitin chains, targeting it to endosomal-lysosomal degradation. Moreover, NEDD4 staining was higher in nigral neurons containing LBs in the human SN and LC from patients with LB pathologies (includes PD, incidental Lewy body disease and diffuse Lewy body dementia)[271].

Moreover, NEDD4 was protective against α-synuclein toxicity in Drosophila brain and in rat dopaminergic neurons, suggesting that NEDD4 could be a potential therapeutic target to halt neurodegeneration[272]. In line with this, NAB2, a compound that activates NEDD4 pathway, was identified in a yeast screen as a neuroprotective agent in various α-synuclein toxicity models. This N-arylbenzimidazole promoted NEDD4-dependent trafficking events, reducing endoplasmic reticulum (ER) and nitrosative stress[273,274].

Furthermore, NEDD4 presents a single nucleotide polymorphism (SNP) that has been associated with a major risk factor for sporadic PD in a whole genome association study (GWAS)[14].

INTRODUCTION

5. RTP801

RTP801, also known as REDD1 (regulated in development and DNA damage responses 1) or Dig2 (dexamethasone-induced gene 2) is a protein encoded by the stress responsive gene DDIT4 (DNA-damage-inducible transcript 4). This gene was identified and cloned in 2002 simultaneously by two different groups[275 276].

5.1 DDIT4: a stress responsive gene

DDIT4 is rapidly induced in response to cellular stressors under the control of different transcription factors. For instance, DDIT4 transcription is activated by hypoxia through HIF-1 transcription factor[179,275], by DNA damage under the control of p53[180], by oxidative and ER stress, via ATF4 (Activating transcription factor 4)[277–279], and by energy depletion[280] (Figure 14).

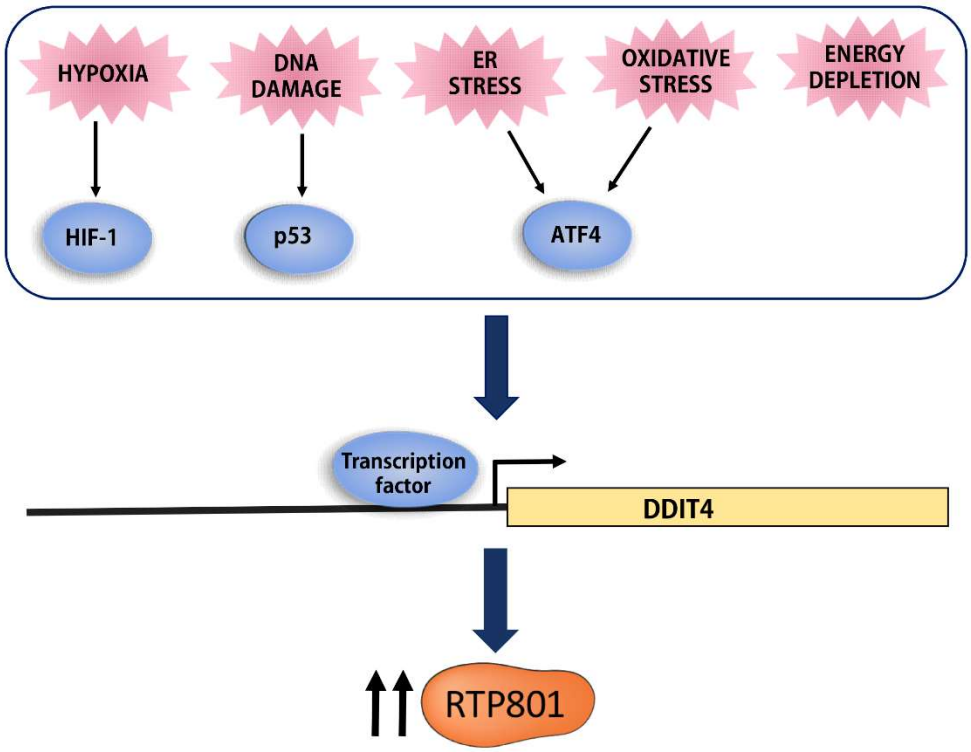

Figure 14. DDIT4 induction by cellular stress. Multiple types of cellular stress upregulate DDIT4 gene under the control of different transcription factors. This gene upregulation is translated to an increase of RTP801 protein. ER= endoplasmic reticulum, HIF-1= Hypoxia-inducible factor 1, ATF4= Activating transcription factor 4.

INTRODUCTION

5.2 RTP801 protein

RTP801 open reading frame (ORF) codes for a 232 amino acid protein in humans, with orthologs in rat, mouse, Xenopus and Drosophila. Based on its amino acid sequence, an acidic, serine-rich protein is predicted, displaying evolutionarily sequence conservation at the carboxyl terminus (C-terminus)[276]. Rat RTP801 ORF encodes for a 229 amino acid protein that is highly homologous to human RTP801, showing 85% identity (Figure 15)[275]. There is a related transcript named RTP801L (RTP801- like) or REDD2 that presents 50% sequence identity and similar functions compared to RTP801[276,281].

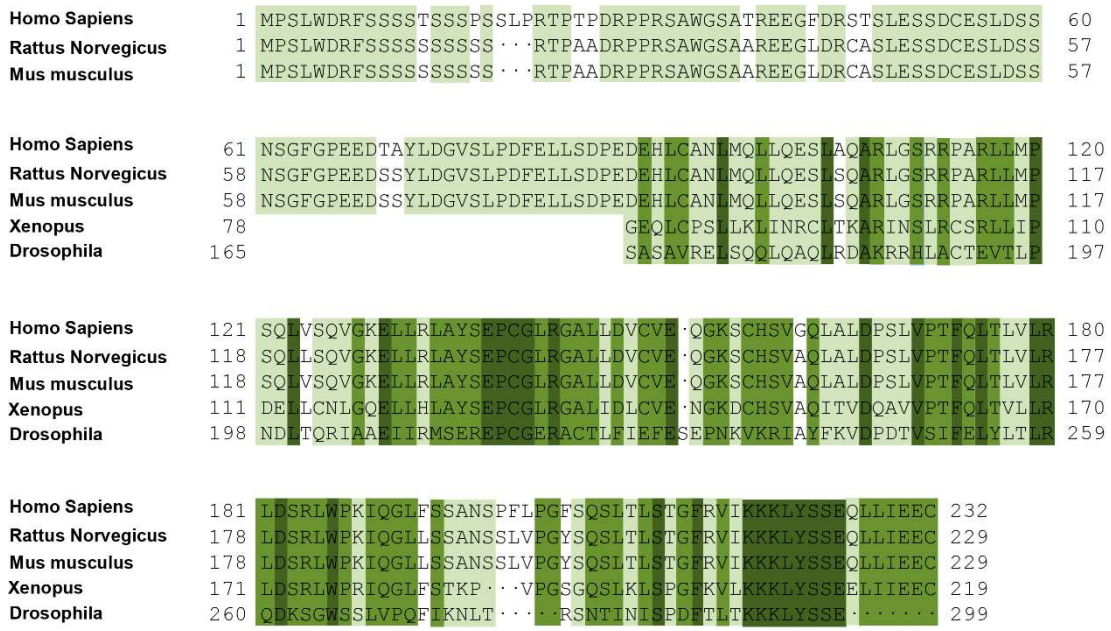

Figure 15. RTP801 sequence alignment from different species. Amino acid sequence alignment of RTP801 protein from human (Homo sapiens), rat (Rattus Norvegicus), mouse (Mus Musculus), frog (Xenopus Laevis) and fly (Drosophila Melanogaster). The non-well conserved N-terminal part of Xenopus and Drosophila are not included. The degree of conservation is represented in green, using increasing darkness to indicate increasing conservation. Image adapted from Vega-Rubin-de-Celis, et al. 2010[282].

RTP801 is ubiquitously expressed at low levels in multiple human adult tissues[275]. Despite it has a predicted molecular weight of 25 KDa, it usually migrates at 34 KDa. This aberrant migration is presumably caused by the presence of multiple lysine residues at the C-terminus[276]. The protein can be localized at the cytoplasm[276,283,284], the nucleus[283,284] and the plasma membrane[180,284]. In addition, a small fraction of RTP801 was also found at mitochondria in HEK293T cells[285] and in *RGC-5* retinal ganglion cells[286].

5.2.1 RTP801 protein structure

By analyzing RTP801 amino acid sequence, no functional motifs or structural domains could be identified. RTP801 presents a poorly preserved N-terminus and a highly conserved C-terminus. In agreement with that, the N-terminus 84 amino acids of human RTP801 were not necessary to maintain its inhibitory function towards mTOR, while, only few residues could be deleted from the C-terminus without altering function. Further studies were performed with several RTP801 truncated forms to conclude that there are two RTP801 segments required for function: RTP801$^{85\text{-}193}$ and RTP801$^{207\text{-}225}$ [282].

Moreover, a segment of human RTP801 protein containing amino acids 89-226 with a deletion of the hydrophobic region ^{200}FLPGF^{204} was crystallized (RTP801$^{89\text{-}226\Delta\Phi}$). This RTP801 mutant form maintained activity and was more soluble, making it easier to crystallize. The resulting structure exhibited a novel topology characterized by a two-layered α-helix/β-sheet sandwich with a psi-loop motif (Figure 16)[282].

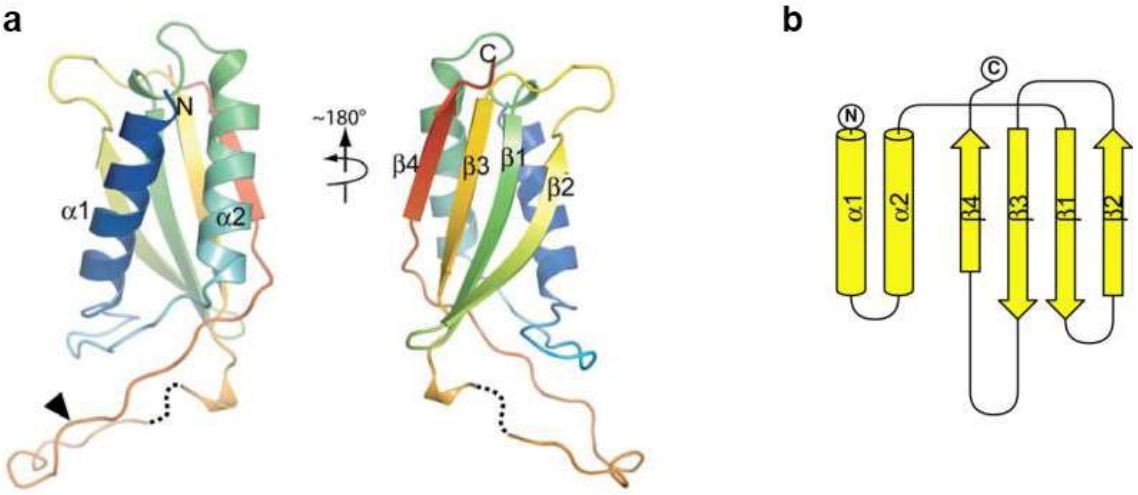

Figure 16. RTP801 presents a unique topology. a) Representation of the RTP801$^{89\text{-}226\Delta\Phi}$ structure obtained by crystallization. The protein is composed by a layer made of two antiparallel α-helices and another layer made of a mixed β-sheet. The cartoon is colored in rainbow mode from the N-terminus to the C-terminus. Dots represent a disordered region, and the black arrowhead shows the location of the deleted hydrophobic region. b) Diagram of RTP801$^{89\text{-}226\Delta\Phi}$ topology. The β-sheet is formed for four strands ordered 2134. Images obtained from Vega-Rubin-de-Celis, et al. (2010)[282].

Besides, a surface patch composed of highly conserved residues was suggested to be critical for RTP801 function. It is formed by two separated segments, ^{138}EPCG^{141} and ^{218}KKKLYSSE^{225}, that are adjacent in the three-dimensional structure[282]. Importantly, the stretch ^{218}KKK^{220} has been reported necessary for targeting RTP801 to mitochondria[285] and plasma membrane[284].

5.3 RTP801 function

The main known function of RTP801 is its ability to repress mTOR activity[179,281], a master kinase involved in the regulation of basic cell processes, such as, growth, proliferation, protein synthesis and cell survival (reviewed in[151]). The fact that DDIT4 gene is rapidly induced by several stressors points out that its mTOR inhibitory function may be crucial for coping stress and maintaining cellular homeostasis[287].

To date, the RTP801 inhibitory mechanism towards mTOR has not been completely elucidated. RTP801 activates TSC1/2 complex[136,179,280], although both proteins do not appear to interact to each other[282]. It has been proposed that RTP801 binds and sequesters 14-3-3, thus disrupting the inhibitory function of this protein towards TSC2[180]. RTP801 also promotes protein phosphatase 2 (PP2A) dependent dephosphorylation of Akt at T308 residue, preventing TSC2 phosphorylation, attenuating Rheb-GTP loading and leading to the subsequent mTORC1 signaling repression[288].

Interestingly, RTP801 has a dual role depending on the cellular context. In proliferating cells, RTP801 exerts a protective anti-apoptotic role in front of several noxious stimuli, such as H_2O_2-induced oxidative stress[275], dexamethasone treatment[278,289], serum deprivation[290] and DNA damage. Conversely, in non-proliferating differentiated cells, RTP801 exerts a pro-apoptotic role, since it results toxic in neuronal PC12 cells[136] and increases their sensitivity to oxidative stress[275].

This peculiar feature was also observed in a corticogenesis study in which RTP801 was identified as a regulator of neuronal differentiation and migration. RTP801 levels were high in embryonic cortical neuroprogenitors without being toxic, decreased in newborn neurons, and low in mature neurons. This gradual decline of RTP801 levels was reported to contribute to the progression of neuronal migration and maturation[291].

5.4 RTP801 in PD

RTP801 has been linked to PD, since in 2004 was described as the most induced transcript in a Serial Analysis of Gene Expression (SAGE) performed in a cellular model of this disease. In the study, NGF-differentiated PC12 cells were exposed to the neurotoxin 6-OHDA for 8 hours. RTP801 transcript expression resulted in a 98-fold increase. This finding first identified RTP801 as a candidate to be considered in neuron death associated to PD[135].

RTP801 transcriptional elevation induced by 6-ODHA was later confirmed and extended to protein level. Moreover, exposure to PD neurotoxins MPP+ and rotenone also resulted in RTP801 elevation. Importantly, RTP801 was also elevated in SNpc dopaminergic neurons of the mouse MPTP model and in human substantia nigra postmortem sections from sporadic PD patients[136].

RTP801 upregulation mediates death in cellular models of PD, since its knockdown was protective in neuronal PC12 cells and in sympathetic neurons exposed to 6-OHDA. Furthermore, RTP801 overexpression in neuronal PC12 cells promoted around 50% of cell death[136].

Interestingly, 6-OHDA exposure and RTP801 overexpression promoted mTOR/Akt repression, as judged by the loss of mTOR phosphorylation at serine 2448 (S2448) and the loss of Akt phosphorylation at residues threonine 308 (T308) and serine 473 (S473)[136,137]. This mTOR pathway blockade has been implicated in the mechanism underlying neuron death, since either TSC2 knockdown[136], mTOR overexpression[292] or constitutively active Akt[137] prevented from 6-OHDA and RTP801-induced cell death. Of note, the loss of mTOR and Akt phosphorylation was also observed in human substantia nigra postmortem sections from sporadic PD patients[137,292].

Finally, it was reported that rapamycin, an inhibitor of certain mTOR actions, was protective in *in vitro* and *in vivo* toxin models of PD by blocking RTP801 translation and by preserving Akt phosphorylation at T308 residue[292]. This protective effect is explained by the capacity of rapamycin to suppress the mTOR-dependent translation of a subset of transcripts without altering others[293,294].

To sum up, RTP801 is induced in cellular and animal models of PD, and is elevated in nigral neurons of PD patients. In a variety of neuronal systems, RTP801 upregulation is sufficient and necessary to mediate death by a mechanism involving sequential repression of mTOR and Akt kinases (Figure 17).

INTRODUCTION

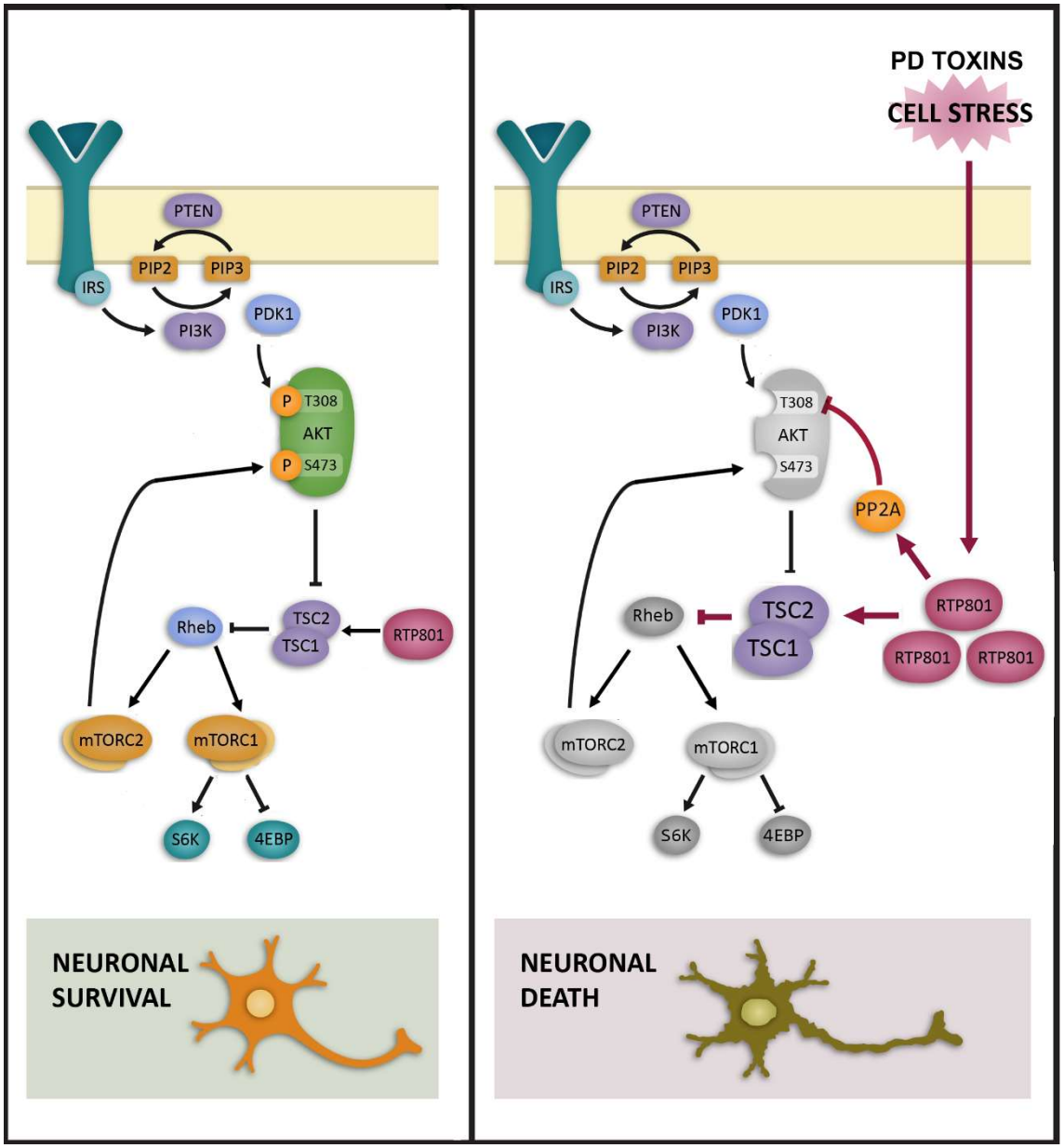

Figure 17. Schematic representation of the mTOR/Akt pathway regulation by RTP801 in neuronal cells. In physiological conditions RTP801 levels are low, contributing to maintain mTOR/Akt activity and subsequently cell survival (left panel). However, when neurons are exposed to PD toxins or suffer stress, RTP801 is rapidly induced promoting mTORC1 and mTORC2 repression through TSC1/2 complex and Rheb protein. Akt pro-survival kinase is dephosphorylated at both residues; at S473 due to mTORC2 blockade, and at T308 probably due to PP2A overactivation. This sequential mTOR/Akt repression contributes to abrogate survival signaling, and if this situation is sustained over time, neuron function is impaired and leads to neuron death (right panel). Image adapted from Canal, et al. 2014[287].

INTRODUCTION

5.5 RTP801 protein degradation

RTP801 is a very unstable protein, with an extremely short half-life (2-7 minutes)[292,295]. Therefore, its synthesis and degradation is subjected to a very fine-tuned regulation to precisely modulate mTOR pathway, promoting neuronal survival. Although RTP801 gene is rapidly induced by several stressors, little is known about the post-translational modifications that govern its protein stability. Hence, elucidating which proteins regulate RTP801 proteostasis and degradation would be a stepping-stone to design new therapies to block neurodegeneration in PD.

To date, only two E3 ligases have been described to mediate RTP801 protein ubiquitination and degradation: CUL4A-DDB1-ROC1-β-TRCP E3 ligase complex and parkin. CUL4A-DDB polyubiquitinated RTP801 and mediated its proteasomal degradation in a GSK3β (glycogen synthase kinase 3 β)-dependent phosphorylation manner[295]. In our group, we recently found that parkin, a RING E3 ligase, polyubiquitinated RTP801 mediating its proteasomal degradation[296].

Interestingly, parkin dysfunction due to mutations (parkin is a PD causative gene, see Table 1) or oxidative/nitrosative stress has been consistently linked to PD[36,297–300]. Indeed, elevated RTP801 levels were observed in parkin knockout mice brains, and in postmortem brains and fibroblasts from PD patients bearing parkin mutations. Furthermore, ectopic WT parkin, but not its inactive mutants, protected neuronal cells from RTP801 and 6-OHDA-induced death by mediating RTP801 protein degradation. Similarly, parkin knockdown elevated RTP801 levels and increased sensitivity of neuronal cells to 6-OHDA. Thus, parkin loss of function may contribute to toxic accumulation of pro-apoptotic protein RTP801 and subsequent neurodegeneration in PD[296].

AIMS

RTP801 elevation can promote death in differentiated cells via mTOR/Akt pathway inactivation, so elucidating mechanisms that regulate its levels will help to design new therapeutic strategies to halt neurodegeneration in PD[136,137]. Considering that RTP801 protein half-life is extremely short (2-7 minutes)[292,295], its synthesis and degradation must be strictly and dynamically controlled.

Thus, it would be valuable to identify E3 ligases mediating RTP801 ubiquitination and protein degradation and to study its possible implication in the disease pathogenesis. Interestingly, NEDD4 has been described to play an important role in PD by mediating α-synuclein degradation[271,272], so our goal is to investigate whether this E3 ligase regulates RTP801/mTOR/Akt axis in neurodegeneration.

Another goal is to examine the role of ubiquitination in RTP801 protein homeostasis and function, and to perform proteomic analysis to identify potential new RTP801 interactors and to elucidate significant protein changes induced by its overexpression.

Hence, the specific aims are:

- Determine whether RTP801 is ubiquitinated and regulated by NEDD4 E3 ligase.
- Investigate whether NEDD4 is neuroprotective in cells exposed to PD toxins, such as 6-OHDA, and if so, whether it is by promoting RTP801 degradation.
- Assess whether NEDD4 knockdown triggers cell death, and if this is the case, elucidate whether NEDD4 deregulation is responsible for mTOR and Akt inactivation, via RTP801 elevation.
- Explore whether NEDD4 protein levels are altered in sporadic PD human postmortem SNpc sections.
- Study how ubiquitination affects RTP801 homeostasis and function by generating different mutant forms.
- Screen for new RTP801 potential interacting partners.
- Study proteome modulation by RTP801.

METHODOLOGY

1. CELL CULTURE

1.1 HEK293 cells

Human Embryonic Kidney 293 cells (HEK293) is a cell line originally derived from human embryonic kidney cells that shows an epithelial phenotype[301]. HEK293 cells were cultured in DMEM medium supplemented with 10% fetal bovine serum and penicillin/streptomycin (all from Thermo Fisher Scientific) in a 5% CO_2 atmosphere at 37ºC. Medium was replenished every other day and cells were reseeded when confluent.

1.2 PC12 cells

PC12 cells were established as a clonal cell line from a transplantable rat pheochromocytoma[302]. They are tumoral cells from adrenal medulla that can synthesize, store and release catecholamines. A remarkable feature of PC12 cells is that they have the capacity to respond to NGF by exiting the cell cycle and undergoing differentiation. NGF-differentiated PC12 cells (NPC12 cells) present a phenotype that resembles sympathetic neurons. They show branched axons, they are electrically excitable and respond to neurotransmitters. They also express diverse neuronal markers and retain their capacity for dopamine synthesis, storage, uptake and release[302,303]. NPC12 cells have been widely used as a cellular PD model, for example in studies using dopaminergic neurotoxins, in investigations about oxidative stress or in α-synuclein overexpression experiments (reviewed in [138,139]).

Naïve PC12 cells were maintained in RPMI 1640 medium (Thermo Fisher Scientific) supplemented with 10% heat-inactivated horse serum (Sigma-Aldrich), 1% fetal bovine serum and penicillin/streptomycin in a 7.5% CO_2 atmosphere at 37ºC. Plates were previously coated with collagen type I rat tail (Corning) and cells were reseeded when confluence was reached. To obtain neuronal PC12 (NPC12) cells, standard medium was replaced for differentiation medium, which consists of RPMI 1640 supplemented with 1% heat-inactivated horse serum, penicillin/streptomycin and 50 ng/ml recombinant human β-NGF (Alomone Labs). Cells were differentiated during 6-7 days prior performing experiments. Medium was changed every other day and before transfection or neurotoxin treatment.

1.3 Rat primary cortical neurons

Rat primary cortical cultures were prepared starting from embryonic (E18) Sprague-Dawley rats. Cortices were dissected out, dissociated and plated at a density of 250 cells/mm^2 on poly-L-lysine-coated (Sigma-Aldrich) glass coverslips for imaging experiments, or at a density of 750 cells/mm^2 on poly-L-lysine-coated plates for biochemistry experiments. Neurons were maintained in Neurobasal medium supplemented with B27 and 2mM GlutaMAX™ (all from Thermo Fisher Scientific) in a 5% CO_2 atmosphere at 37ºC. Medium was partially replenished every 5 days. However, coverslip-plated neurons were initially

seeded with MEM medium (Thermo Fisher Scientific) supplemented with 100 mM pyruvic acid (Thermo Fisher Scientific), 20% glucose (Sigma-Aldrich) and 10% heat-inactivated horse serum during 1 hour.

1.4 Human fibroblasts

Fibroblasts cultures were established from skin punches collected from six diagnosed AR-JP (Autosomal Recessive Juvenile Parkinsonism) patients bearing *PARK2* dysfunctional mutations and six control individuals. They were obtained from the Neurology Service-Movement Disorders Biorepository (IDIBAPS, Hospital Clinic, University of Barcelona, Barcelona) thanks to Dr. Eduardo Tolosa. Fibroblasts were cultured in DMEM medium supplemented with 10% fetal bovine serum and penicillin/streptomycin in a 5% CO_2 atmosphere at 37ºC. Medium was changed every other day. In order to obtain pure cultures, fibroblasts were reseeded between five or six times before analysis.

2. CELLULAR TREATMENTS

Cell cultures were exposed to the following compounds as indicated (Table 2):

Compound	Function	Concentration	Exposure time	Company
Epoxomicin	Proteasome inhibitor	1 μM	2-4 h	Calbiochem
MG132	Proteasome inhibitor	10 μM	3-4 h	Calbiochem
Chloroquine	Lysosomal inhibitor	50 μM	4 h	Sigma-Aldrich
Cobalt (II) chloride	Hypoxia-mimetic agent	200 μM	16 h	Sigma-Aldrich
Cycloheximide	Protein synthesis inhibitor	10 μg/ml	10’ or 60’	Calbiochem
Z-VAD-FMK	Pan-caspase inhibitor	100 μM	17 h	Calbiochem
ALLN	Calpain inhibitor	1 μM	17 h	Calbiochem
NAB2	NEDD4 signaling inducer	20 μM	48 h	EMD Millipore
6-OHDA	PD neurotoxin	100 μM (NPC12 cells) 25-50 μM (neurons)	16 h	Tocris Bioscience

Table 2. Compounds used for cellular treatments

In the case of PD neurotoxin 6-OHDA, NPC12 cells were treated at day 6-7 of differentiation, while cortical neurons were exposed between DIV 10 and DIV 14 depending on the experiment. Before treatment, medium was totally replaced in NPC12 cells and partially replaced in neurons.

3. DNA MANIPULATION

3.1 Subcloning

In this work, a ShRNA (short hairpin RNA) sequence against RTP801 and a scrambled ShRNA control were subcloned into the lentiviral vector pLL3.7 (Addgene). For that purpose, the following steps were carried out:

3.1.1 ShRNA sequence design

Previously, a ShRNA sequence against RTP801 was designed by Dr. Cristina Malagelada and validated in two different constructs (ShRTP801 A[136], and ShRTP801 1[137]). Hence, we designed new oligonucleotides flanked with the HpaI and XhoI restriction sites to obtain the same ShRTP801 sequence and a scrambled control ShRNA sequence:

•ShCt: 5'-GTGCGTTGCTAGTACCAAC-3'

•ShRTP801: 5'-AAG ACT CCT CAT ACC TGG ATG-3' (specific for human, rat and mouse RTP801 transcript)

The corresponding oligonucleotides were 5' phosphorylated and annealed prior to ligation.

3.1.2 Vector linearization

The pLL3.7 vector was linearized with the restriction enzymes HpaI and XhoI (New England Biolabs) at 37ºC during 2 hours. Then, calf-intestinal alkaline phosphatase (New England Biolabs) was added to the digestion products and incubated at 37ºC for 1 hour, in order to dephosphorylate the linearized vector and avoid its recircularization.

3.1.3 DNA extraction from agarose gel

Digested DNA was separated by electrophoresis in a 1% agarose gel containing 0.5 µg/ml of ethidium bromide. DNA Gel Loading Dye (Thermo Fisher Scientific) was added to DNA samples before running. A lane with the molecular weight marker GeneRuler 1kb DNA Ladder (Thermo Fisher Scientific) was loaded along with experimental samples. Gels were run in TAE buffer (Thermo Fisher Scientific) and the DNA bands were visualized under ultraviolet light due to ethidium bromide fluorescence. DNA bands corresponding to linearized vector were cut from the gel and purified using the kit QIAquick Gel Extraction Kit (Qiagen).

3.1.4 Ligation

The linearized vector purified from the gel and the annealed oligonucleotides were ligated using a molar ratio of 1:3. The reaction was performed with T4 DNA Ligase enzyme and with Quick ligation buffer (all from New England Biolabs) during 3 hours at room temperature. Escherichia coli DH5α bacteria were transformed with the ligation products (see section 4.1) and the resulting colonies were grown in Terrific Broth medium (Thermo Fisher Scientific).

3.2 Site-directed mutagenesis

Several constructs expressing mutant forms of a protein were obtained by site-directed mutagenesis using the kit QuickChange Lightning II Multi Site-Directed Mutagenesis Kit (Agilent Technologies). The primers used were designed with the software offered by the company (www.agilent.com/genomics/qcpd) and are summarized below (Table 3).

Mutant construct	Initial construct	Mutant primers
pCI-HA-NEDD4-C867S	pCI-HA-NEDD4	5'-GTCCAGGCGATTAAAACTGGTATGAGCTCTTGGCA-3'
pHAGE-NEDD4-C867S	pHAGE-NEDD4	5'-GTCCAGGCGATTAAAACTGGTATGAGCTCTTGGCA-3'
pCMS-eGFP-RTP801-K126R	pCMS-eGFP-RTP801	5'-GCAGGAGTTCCCTGCCCACCTGGCTC-3'
pCMS-eGFP-RTP801-K152R	pCMS-eGFP-RTP801	5'-ACACTATGGCAGCTCCTGCCTTGCTCCACAC-3'
pCMS-eGFP-RTP801-K185R	pCMS-eGFP-RTP801	5'-AGGCCCTGGATCCTGGGCCAGAGGC-3'
pCMS-eGFP-RTP801-K215R	pCMS-eGFP-RTP801	5'-CCGGCTTCAGAGTCATCAGAAAGAAACTCTACAGCTC-3'
pCMS-eGFP-RTP801-K216R	pCMS-eGFP-RTP801	5'-GGAGCTGTAGAGTTTCCTTTTGATGACTCTGAAGCC-3'
pCMS-eGFP-RTP801-K217R	pCMS-eGFP-RTP801	5'-CGGCTTCAGAGTCATCAAAAAGAGACTCTACAGCTC-3'
pCMS-eGFP-RTP801-KR	pCMS-eGFP-RTP801	5'-CTCGGAGCTGTAGAGTCTCCTTCTGATGACTCTGAAGCCGGTG-3' 5'-GCAGGAGTTCCCTGCCCACCTGGCTC-3' 5'-ACACTATGGCAGCTCCTGCCTTGCTCCACAC-3' 5'-AGGCCCTGGATCCTGGGCCAGAGGC-3'

Table 3. Constructs obtained by site-directed mutagenesis. Detail of the starting constructs, the mutant primers employed and the mutant constructs obtained.

First, an accelerated thermal cycling procedure was performed to synthesize multiple copies of the mutant strand. The reaction was performed by mixing 100 ng of DNA template, 100 ng of mutagenic primer (or mix of mutagenic primers) and all other reaction components from the kit. The obtained products were treated with the restriction endonuclease DpnI to digest the parental DNA template. The resulting DNA was transformed (see section 4.1) and some colonies were grown in Terrific Broth medium. Finally, DNA was purified using the QIAprep Spin Miniprep Kit (Qiagen) and verified by sequencing.

4. DNA PLASMID AMPLIFICATION AND PURIFICATION

All DNA plasmids used in this work were amplified by bacterial transformation and then purified.

4.1 Bacterial transformation

Escherichia coli DH5α competent cells (Thermo Fisher Scientific) were used to transform and amplify the DNA content of plasmids and ligation products. DNA of interest was added to bacterial competent cells, mixed and incubated for 15 minutes on ice. To induce transformation, the mixture was placed at 42 ºC for 2 minutes (heat shock) and placed back on ice for 5 minutes. Next, S.O.C medium (Thermo Fisher Scientific) was added and incubated at 37ºC for 1 hour to grow transformed bacteria. Finally, bacteria were seeded on LB (Lysogeny broth)-agar (Panreac) plates supplemented with the corresponding antibiotic and incubated overnight (O/N) at 37ºC. The antibiotic used was selected depending on which resistance gene is expressed by the transformed plasmid. In this work, ampicillin (Thermo Fisher Scientific) at concentration of 100 µg/ml was used.

4.2 Plasmid DNA purification

A single colony was selected and inoculated in Terrific Broth medium containing 100 µg/ml ampicillin. The bacterial culture was grown at 37ºC and 200 rpm until saturation was reached. The commercial kit HiPure Plasmid Filter Maxiprep Kit (Thermo Fisher Scientific) was used to isolate plasmid DNA. All new constructs and the plasmids were verified by sequencing.

4.3 Description of plasmids

All constructs used in this work to overexpress or knockdown proteins are listed below. The main features of the corresponding backbones or empty vectors are also specified (Table 4). All of them are mammalian expression vectors with ampicillin resistance.

Backbone / empty vector	Construct	Obtention
pCMS-eGFP Provided by Dr. Lloyd Greene • Express eGFP (enhanced green fluorescent protein) under the control of the SV40 promoter • Express the inserted protein under the control of the CMV promoter	pCMS-eGFP-RTP801	Rat RTP801 cDNA was subcloned by Dr. Cristina Malagelada
	pMCS-eGFP-RTP801-KR	Site-directed mutagenesis (see section 3.2)
	pCMS-eGFP-RTP801-K126R	Site-directed mutagenesis (see section 3.2)
	pCMS-eGFP-RTP801-K152R	Site-directed mutagenesis (see section 3.2)
	pCMS-eGFP-RTP801-K185R	Site-directed mutagenesis (see section 3.2)
	pCMS-eGFP-RTP801-K215R	Site-directed mutagenesis (see section 3.2)
	pCMS-eGFP-RTP801-K216R	Site-directed mutagenesis (see section 3.2)
	pCMS-eGFP-RTP801-K217R	Site-directed mutagenesis (see section 3.2)
pCI-HA Provided by Dr. Joan Massagué • Express N-terminal HA-tagged protein under the control of CMV promoter	pCI-HA-NEDD4	Addgene
	pCI-HA-NEDD4-C867S	Site-directed mutagenesis (see section 3.2)
pHAGE Provided by Dr. Heng-Ye Man • Lentiviral vector • Express the inserted protein under the control of the CMV promoter • Express Zsgreen protein under the control of IRES	pHAGE-NEDD4	Provided by Dr. Heng-Ye Man
	pHAGE-NEDD4-C867S	Site-directed mutagenesis (see section 3.2)
pCDNA3-HA Obained from Addgene • Express N-terminal HA-tagged protein under the control of CMV promoter	pCDNA3-HA-Ubiquitin	Addgene
pRK5-HA Provided by Dr. Bernat Crosas • Express N-terminal HA-tagged protein under the control of CMV promoter	pRK5-HA-Ubiquitin-K48	Provided by Dr. Bernat Crosas
	pRK5-HA-Ubiquitin-K63	Provided by Dr. Bernat Crosas
pLL3.7 Obtained from Addgene • Lentiviral vector • Express eGFP under the control of CMV promoter and the inserted ShRNA under the control of U6 promoter	pLL3.7-ShCt / ShCt	Subcloning (see section 3.1)
	pLL3.7-ShRTP801 / ShRTP801	Subcloning (see section 3.1)
pRK5-myc Provided by Dr. Serge Przedborsky • Express N-terminal myc-tagged protein under the control of CMV promoter	pRK5-myc-parkin	Provided by Dr. Serge Przedborsky
	pRK5-myc-parkin-ΔUBL	Provided by Dr. Leonidas Stefanis
	pRK5-myc-parkin-ΔR2	Provided by Dr. Leonidas Stefanis

Table 4. List of the constructs used. The main features of the backbone / empty vector of each construct and how they have been obtained are specified. SV40= Simian Virus 40, CMV=Citomegalovirus, HA= hemagglutinin, IRES= Internal Ribosome Entry Site.

5. PROTEIN EXPRESSION

5.1 Liposome-mediated transfection

Transient transfections were performed in different cell types using the lipid reagent Lipofectamine® 2000 (Thermo Fisher Scientific).

5.1.1 Transfection of HEK293 and NPC12 cells

Shortly, cell cultures were grown up to 50-70% confluence, and 30 minutes before transfection, medium was replaced for transfection medium (medium without serum and antibiotics). Plasmidic DNA and Lipofectamine 2000 mixtures were prepared and added to cells as instructed by the manufacturer. Four hours later, medium was replaced by fresh complete medium (supplemented with serum and antibiotics) or by differentiation medium in the case of NPC12 cells.

5.1.2 Transfection of cortical neurons

Coverslip-plated cortical neurons were transfected for imaging experiments. Plasmid DNA and Lipofectamine 2000 mixtures were prepared and added to neurons according to manufacturer's instructions. Four hours later, coverslips were transferred to a new plate containing conditioned medium (medium in which cells have been cultivated previously).

5.2 Lentiviral infection

Primary rat cortical neurons were infected with the following lentiviruses under the specified experimental conditions (Table 5):

Lentiviruses	Lentiviral particles obtention	DIV of infection	MOI	Infection time
pHAGE pHAGE-NEDD4 pHAGE-NEDD4-C867S	Produced in HEK293 cells	DIV 8	1	4 days
ShCt ShNEDD4	Commercial (Santa Cruz Biotechnology)	DIV4 or DIV7	1	6 or 4 days
ShCt ShRTP801	Produced in HEK293 cells	DIV 5	1	6 days

Table 5. Description of the lentiviral infections performed. Cortical neurons were infected with different lentiviral particles. DIV (day in vitro) of infection, MOI (multiplicity of infection) and the time of infection are detailed for each case. Lentiviruses were produced in HEK293, with the exception of ShCt/ShNEDD4 that were commercial.

5.2.1 Lentiviral particles production

To produce lentiviral particles, 10 cm plates containing HEK293 cells at 70-80% confluency were transfected using Lipofectamine 2000. To overexpress NEDD4 and NEDD4-C867S, cells were transfected with 3 µg pHDM-Tat 1b (tat accessory protein), 3 µg pRC/CMV-Rev 1b (rev accessory protein), 3 µg pHDM-Hgpm2 (HIV gag-pol expression plasmid), 6 µg

pHDM.G (envelope, VSV pseudotype) and 12 µg of the target vector (pHAGE, pHAGE-NEDD4 or pHAGE-NEDD4-C867S). All constructs were kindly provided by Dr. Heng-Ye Man. To knockdown RTP801, cells were transfected with 5 µg of pMDLg/pRRE (HIV gag-pol expression plasmid), 5 µg of pRSV-Rev (rev accessory protein), 5 µg pMD2.G (envelope, VSV pseudotype) and 10 µg of the target vector (pLL3.7-ShCt or pLL3.7-ShRTP801). All constructs were obtained from Addgene. After 4 hours, medium was replaced with fresh complete DMEM.

Approximately 72 hours post-transfection, cell medium was collected, centrifuged to remove debris and filtered through 0.45 µm-pore filters (Thermo Fisher Scientific). Lentiviruses were concentrated by ultracentrifugation and resuspended in sterile PBS (phosphate buffered saline) Ca^{2+}/Mg^{2+} (Thermo Fisher Scientific). Viral titer was assessed by transduction of several viral dilutions.

6. GENE EXPRESSION ANALYSIS

The expression of different genes was quantified by quantitative reverse transcription-PCR (RT-qPCR). Total RNA was isolated from NPC12 cells or cortical neurons using the High Pure RNA Isolation Kit (Roche) following manufacturer's instructions. cDNA was synthesized from 1 µg of total RNA by using the Transcriptor First Strand cDNA synthesis Kit (Roche). Equal amounts of cDNA were amplified by quantitative PCR (qPCR) using the following primers: RTP801 forward primer, 5'-GCTCTGGACCCCAGTCTAGT-3'; RTP801 reverse primer, 5'-GGGACAGTCCTTCAGTCCTT-3'; NEDD4 forward primer, 5'-GGACGAGGTATGGGAGTTCT-3' ; NEDD4 reverse primer, 5'-CTCCACTCATCGGGTCATAC-3' ; α-actin forward primer, 5'-GGGTATGGGTCAGAAGGACT-3'; α-actin reverse primer, 5'-GAGGCATACAGGGACAACAC-3'. qPCR was performed with SYBR® master mix (Thermo Fisher Scientific) in a 7500 Real Time PCR system (Applied Biosystems). RTP801 and NEDD4 expression results were normalized by α-actin and analysed using the comparative quantification.

7. WESTERN BLOT (WB)

This technique was used to quantify proteins from cellular extracts or tissue homogenates. Whole cell extracts were collected in cell lysis buffer (20 mM Tris-HCl pH=7.5, 150 mM NaCl, 1 mM Na_2EDTA, 1 mM EGTA, 1% Triton, 2.5 mM sodium pyrophosphate, 1 mM beta-glicerophosphate, 1 mM Na_3VO_4, 1 µg/ml leupeptin) (Cell Signaling Technology) containing 1 mM phenylmethanesulfonyl fluoride (Sigma-Aldrich). Cortical lysates from four $NEDD4^{f/f}$;Emx1Cre mice and four WT littermates were obtained thanks to Dr. Hiroshi Kawabe (Max-Planck-Institut für Experimentelle Medizin, Gottingen, Germany) collaboration.

Homogenized samples were next sonicated and centrifuged at 14000 g to remove debris. Protein concentration was determined using Bradford reagent (Bio-Rad). Before loading, cell extracts were prepared with Pierce™ Lane Marker Reducing Sample Buffer (Thermo Fisher Scientific) and heated at 97ºC during 5 minutes. Samples were usually resolved in 4-12% polyacrylamide gels (NuPAGE™ Novex™ 4-12% Bis-Tris, Thermo Fisher Scientific), except for high molecular weight proteins analysis, when 3-8% polyacrylamide gels were used (NuPAGE™ Novex™ 3-8% Bis-Tris, Thermo Fisher Scientific). The molecular weight marker used was the PageRuler™ Prestained Protein Ladder (Thermo Fisher Scientific). Gels were run in the XCell SureLock™ Mini-Cell system containing NuPAGE® MOPS SDS Running buffer (4-12% gels) or NuPAGE® Tris-Acetate SDS Running buffer (3-8% gels) (all from Thermo Fisher Scientific).

Proteins were transferred to nitrocellulose membranes with the iBlot® system using iBlot® Transfer Stack supports (all from Thermo Fisher Scientific). Membranes were washed with TBS-T (Tris-buffered Saline (Thermo Fisher Scientific) containing 0.1% Tween® 20 (Sigma-Aldrich)) and blocked with TBS-T 5% milk (Bio-Rad) for 1 hour at room temperature. Then, membranes were incubated with the corresponding primary antibody (Table 6) diluted in TBS-T 5% BSA (Bovine Serum Albumin) (Sigma-Aldrich). Usually, membranes were incubated during 16 hours at 4ºC, except for anti-α-actin antibody that was incubated during 30 minutes at room temperature.

Antibody	Host specie	Dilution	Company
RTP801	Rabbit polyclonal	1:500	Proteintech
NEDD4	Rabbit polyclonal	1:1000	Santa Cruz Biotechnology
HA	Rabbit monoclonal	1:1000	Cell Signaling
P-Akt (S473)	Rabbit monoclonal	1:1000	Cell Signaling
P-Akt (T308)	Rabbit polyclonal	1:500	Cell Signaling
Akt	Rabbit polyclonal	1:1000	Cell Signaling
P-S6 (S235/236)	Rabbit monoclonal	1:500	Cell Signaling
P-mTOR (S2448)	Rabbit polyclonal	1:1000	Cell Signaling
αII-spectrin	Rabbit polyclonal	1:1000	Merck Millipore
Ubiquitin (FK2)	Mouse monoclonal	1:500	Enzo Life Sciences
GFP	Rabbit polyclonal	1:1000	Santa Cruz Biotechnology
TSG101	Mouse monoclonal	1:1000	Abcam
Flotillin-1	Mouse monoclonal	1:1000	BD Biosciences
Parkin	Mouse monoclonal	1:500	Cell Signaling
Myc	Rabbit monoclonal	1:1000	Cell Signaling
Clathrin	Mouse monoclonal	1:500	Abcam
β-adaptin	Mouse monoclonal	1:1000	BD Biosciences
GAPDH	Mouse monoclonal	1:1000	Merck Millipore
β-tubulin	Mouse monoclonal	1:15000	Santa Cruz Biotechnology
α-actin	Mouse monoclonal	1:20000	BD Biosciences

Table 6. Primary antibodies used in WB analysis.

After primary antibody incubation, membranes were washed with TBS-T three times during 5 minutes. Then, membranes were incubated with the appropriated secondary antibody diluted 1:10000-1:20000 in TBS-T 5% milk during 1 hour at room temperature. The secondary antibodies used were goat anti-mouse IgG (H+L) and goat anti-rabbit IgG (H+L) conjugated to horseradish peroxidase (Thermo Fisher Scientific).

Next, membranes were washed with TBS-T three times during 10 minutes to remove the excess of secondary antibody. Proteins were detected with Clarity Western ECL Substrate (Bio-Rad). Chemiluminescent images were acquired using LAS-3000 imager (Fujifilm) and quantified by densitometric analysis using ImageJ software (NIH). In case of reincubation with another antibody, membranes were washed for 5-20 minutes with Restore™ PLUS Western Blot Stripping Buffer (Thermo Scientific) to remove previous signal.

8. IMMUNOPRECIPITATION (IP)

8.1 Immunoprecipitation to study ubiquitination levels

Cells were lysed with RIPA buffer (50 mM Tris-HCl pH=7.4, 150 mM NaCl, 1% NP-40, 1% sodium deoxycholate and 0.1% sodium dodecyl sulfate), containing mini complete protease inhibitor (Roche Diagnostics Corporation). Lysates were further sonicated and centrifuged at 13000 g for 10 minutes to remove debris, and protein concentration was determined using Bradford reagent. Equal amounts of total protein were incubated O/N at 4ºC on rotation with protein A-agarose beads (Santa Cruz Biotechnology) and with NEDD4 or RTP801 primary antibody (Table 7). Negative control was obtained by adding rabbit normal immunoglobulins (IgG) (Santa Cruz Biotechnology) instead of the appropriated antibody. After that, beads were centrifuged and washed four times with RIPA buffer. Immunocomplexes were eluted by adding sample buffer to beads and by heating the mix to 97 ºC during 5 minutes. The resulting samples were analysed by WB as previously described.

Antibody	Host specie	Concentration	Company
RTP801	Rabbit polyclonal	5 µg/mg lysate	Proteintech
NEDD4	Rabbit monoclonal	1:50	Cell Signaling
Clathrin	Mouse monoclonal	1:50	Abcam

Table 7. Primary antibodies used to immunoprecipitate target proteins

8.2 Co-immunoprecipitation

When indicated, cell cultures were exposed to 1mM DSP (dithiobis (succinimidyl proprionate)) (Thermo Fisher Scientific), a crosslinker agent, for 2 hours at 4ºC. Next, cell extracts were collected with cell lysis buffer (Cell Signaling Technology) and protein concentration was determined. Equal amounts of total protein were incubated O/N at 4ºC on rotation with protein A-agarose beads and with RTP801 or clathrin primary antibody (Table 7). As negative control, rabbit or mouse normal immunoglobulins (IgG) were added. Then, beads were centrifuged and washed four times with CHAPS buffer (Tris 50 mM pH=7.4, NaCl 150 mM, $MgCl_2$ 10 mM, CHAPS 0.4%). Finally, immunocomplexes were eluted with sample buffer (5 minutes at 97ºC) and resolved by WB.

9. CELL-FREE UBIQUITINATION ASSAY

This assay was performed using the Ubiquitinylation Kit (Enzo Life Sciences). In brief, the reaction buffer was composed of 1 mM dithiothreitol (DTT) (Sigma-Aldrich), 20 mM Tris-HCl pH=7.5, 20 U/ml inorganic pyrophosphatase (Sigma-Aldrich) and 5 mM Mg-ATP. The following recombinant proteins were added to the reaction buffer, as specified in each condition: 2.5 μM biotinylated ubiquitin, 0.1 μM His_6-tagged human ubiquitin-activating enzyme E1, 2.5 μM His_6-tagged human ubiquitin-conjugating enzyme UbcH5b E2 (Enzo Life Sciences), 100 nM human NEDD4 protein (Sigma-Aldrich) and 1 μM N-terminal GST-tagged (glutathione S-transferase) human RTP801 full-length protein (Novus Biologicals). Mixtures were incubated for 90 minutes at 37ºC to allow the reaction to take place. Next, RTP801 was immunoprecipitated (see section 8.1), and immunocomplexes were analysed by WB. Membranes were probed for biotinylated ubiquitin using Avidin/Biotin-Horseradish Peroxidase (Ultra-sensitive ABC staining kit; Thermo Fisher Scientific) and for RTP801 to verify correct immunoprecipitation.

10. IMMUNOFLUORESCENCE

10.1 Immunocytofluorescence

Neuronal PC12 cells and cortical neurons were both fixed with 4% paraformaldehyde (Electron Microscopy Sciences) in PBS for 15 minutes at room temperature. After that, NPC12 cells were blocked and permeabilized for one hour with Superblock-PBS (Thermo Fisher Scientific) containing 0.3% Triton X-100 (Sigma-Aldrich). In contrast, cortical neurons were permeabilized with PBS containing 0.25% Triton X-100 during 5 minutes, and blocked with superblock-PBS for 30 minutes. Primary antibodies were diluted in superblock-PBS and incubated O/N at 4ºC (Table 8):

Antibody	Host specie	Dilution	Company
HA	Mouse monoclonal	1:750	Sigma-Aldrich
RTP801	Rabbit polyclonal	1:150	Proteintech
GFP	Mouse monoclonal	1:500	Santa Cruz Biotechnology

Table 8. Primary antibodies used for immunofluorescence of cultured cells

Then, cells were incubated for 2 hours at room temperature with the corresponding secondary antibodies diluted 1:500-1:1000 in PBS. The secondary antibodies used were goat anti-mouse or goat anti-rabbit IgG (H+L) conjugated to Alexa Fluor® 488 or Alexa Fluor 568® (Thermo Fisher Scientific). For nuclear staining, sections were incubated for 10 minutes with Hoechst 33342 (Thermo Fisher Scientific) 1:5000 in PBS. Cells were washed with PBS between different steps, and after secondary antibody incubation. Coverslips were finally mounted onto a slide with the mountant liquid ProLong® Gold Antifade (Thermo Fisher Scientific). Cells were observed with an epifluorescent microscope (Leica) using the software

AF6000 E. In cell survival assays, transfected eGFP+ viable cells or surviving nucleus were scored by strip counting directly onto plastic plates (without using mounting medium).

10.2 Immunohistofluorescence of mouse sections

Fixed cryopreserved brains from Nedd4$^{f/f}$;Emx1Cre and their WT littermates were kindly provided by Dr. Hiroshi Kawabe (Max-Planck-Institut für Experimentelle Medizin, Gottingen, Germany). Coronal 30 µm-thick sections were collected in PBS as free-floating sections and were incubated with NH_4Cl 50 mM for 30 minutes to block autofluorescence caused by free aldehydes. Tissue was blocked during 2 hours with superblock-PBS containing 0.3% Triton X-100 (blocking solution), and incubated O/N at 4ºC with the corresponding primary antibodies diluted in blocking solution (Table 9).

Antibody	Host specie	Dilution	Company
RTP801	Rabbit polyclonal	1:50	Proteintech
NEDD4	Rabbit polyclonal	1:50	Abcam

Table 9. Primary antibodies used for immunofluorescence of mouse brain sections

Slices were then washed with PBS and incubated for 2 hours at room temperature with secondary antibody Alexa Fluor® 488-conjugated goat anti-rabbit IgG (H+L) diluted 1:500 in blocking solution. For nuclear staining, sections were incubated for 10 minutes with Hoechst 33342 1:5000 in PBS. Sections were washed three times with PBS before being mounted with ProLong® Gold Antifade Mountant on SuperFrost™ Plus Adhesion Slides (Thermo Fisher Scientific). Finally, stained sections were examined by confocal microscopy using the Leica LCS SL system. RTP801 fluorescence was quantified using ImageJ software.

11. IMMUNOHISTOCHEMISTRY OF HUMAN SECTIONS

Postmortem human SNpc paraffin-embedded sections from sporadic PD patients and control individuals were obtained from the Neurological Tissue Bank (Biobank-HC-IDIBAPS) thanks to Dr. Ellen Gelpi collaboration.

Shortly, sections were dewaxed with xylene and rehydrated by incubation in ethanol series (100%, 95%, 70% and 50%). Antigen retrieval was performed with Tris-EDTA buffer (10 mM Tris-base pH=9, 1 mM EDTA, 0.05% Tween 20) in a vegetable steamer at 100 ºC for 20 minutes. Next, slides were washed with TBS-0.025% Triton X-100 and blocked in superblock-PBS for 2 hours at room temperature. They were then incubated with avidin D solution (Vector Laboratories) for 15 minutes, washed with TBS and incubated with biotin solution (Vector Laboratories) for 15 minutes. Sections were incubated O/N at 4ºC with a 1/50 dilution of anti-NEDD4 antibody (Abcam) in TBS. Then, slides were washed with TBS-0.025% Triton X-100 and they were incubated for 15 minutes with 0.3% H_2O_2 in TBS to block

nonspecific peroxidase activity. Biotinylated goat anti-rabbit IgG (H+L) secondary antibody (Vector Laboratories) diluted 1:500 in TBS was added and incubated for 2 hours at room temperature. Finally, sections were incubated with ABC Peroxidase Standard Staining Kit (Thermo Fisher Scientific) for 30 minutes and with ImmPACT SG Peroxidase Substrate (Vector Laboratories) for 20 minutes. Sections were washed, dehydrated by incubation in ethanol series (50%, 70%, 95% and 100%) and xylene, mounted with DPX mountant (Sigma-Aldrich) and analysed under Olympus BX5 (Olympus) bright-field microscope.

12. ISOLATION OF EXTRACELLULAR MICROVESICLES FROM CULTURE MEDIA

Extracellular microvesicles (exosomes) were isolated from culture media of DIV 14 cortical neurons by sequential ultracentrifugation. Briefly, culture media was centrifuged at 300 g for 5 minutes to remove death cells or dirtiness. Then, supernatant was further centrifuged at 2500 g for 20 minutes, at 10000 g for 30 minutes and ultracentrifuged at 100000 g for 2 hours with a fixed rotor. Then, the resultant pellet was washed in PBS and ultracentrifuged again at 100000g for 1 hour. Finally, the pellet was resuspended in sample buffer.

13. PROTEOMIC STUDIES

The proteomic studies were performed in collaboration with Dr. Enrique Santamaría (Proteomics Unit, Navarrabiomed, Pamplona, Spain).

13.1 Protein identification from gel bands (In-gel tryptic digestion)

RTP801 was immunoprecipitated (see section 8.2) and the resulting immunocomplexes were separated by polyacrylamide gel electrophoresis. Gels were incubated 30 minutes with fix solution (50% methanol, 7% acetic acid) two consecutive times and stained with Sypro® Ruby Protein Gel Stain (Thermo Fisher Scientific) O/N at 4ºC. Then, gels were washed 30 minutes with wash solution (10% methanol, 7% acetic acid) and 10 minutes with water. Proteins were viewed with a blue-light transilluminator and the bands of interest were excised and picked up. Gel bands were destained with 50 mM ammonium bicarbonate in 50% acetonitrile. Then, proteins were reduced with 10 mM DTT in 100 mM ammonium bicarbonate and alkylated with 55 mM iodoacetamide in 100 mM ammonium bicarbonate. In-gel protein digestion was carried out with 10 ng trypsin (Promega) in 50 mM ammonium bicarbonate for 12h at 37°C as previously described[304]. The resulting peptides were extracted with 2% formic acid in 2% acetonitrile and were analysed by LC-MS/MS (liquid chromatography-tandem mass spectrometry).

Concretely, peptides were separated by reverse phase chromatography using an Eksigent nanoLC ultra 2D pump fitted with a 75 µm ID column (Eksigent 0.075 x 250). Previously, samples were loaded into a 0.5 cm length 100 µm ID precolumn for desalting and

concentration. Mobile phases consisted of 0.1% formic acid in water (buffer A) and 0.1% formic acid in acetonitrile (buffer B). Column was equilibrated in 95% buffer B during 10 minutes and in 5% buffer B for 10 minutes more. Elution was carried out with a two-step gradient of 60 minutes: from 5% buffer B to 25% buffer B in 50 minutes and from 25% buffer B to 40% buffer B in 10 minutes. During all process, precolumn and column were in line and the flow was maintained at 300 nl/min. Eluting peptides were analysed using an AB Sciex 5600 Triple-TOF system. Data was acquired upon a survey scan performed in a mass range between 350 m/z and 1250 m/z during 250 ms. Top 30 peaks were selected for further fragmentation. Minimum accumulation time for MS/MS was set up at 100 ms giving a total cycle time of 3.8 s. Product ions were scanned in a mass range from 230 m/z up to 1500 m/z and were excluded for further fragmentation for 15 s.

13.2 Proteome modulation

Whole cell extracts were collected in the following lysis buffer: 7 M urea, 2 M thiourea, 4% CHAPS and 50 mM DTT. Homogenates were further sonicated and centrifuged at 14000 g for 40 minutes at 4ºC to remove debris. Proteins were precipitated with methanol/chloroform, and the resulting pellets were dissolved in 6 M urea, 100 mM Tris pH=7.8. Protein concentration was determined using Bradford reagent and enzymatic cleavage was performed with trypsin at 37ºC for 16 hours as previously described[304]. Peptides were separated and analysed by label free LC-MS/MS (as described in section 13.1).

MS/MS data acquisition was performed using Analyst 1.5.2 (AB Sciex) and spectra files were processed through Protein Pilot TM Software (v.4.0.8085-ABSciex) using ParagonTM Algorithm (v.4.0.0.0)[305] for database search, Progroup™ for data grouping, and searched against the concatenated target-decoy UniProt Rat database (Database: 10116 - Rattus norvegicus, Nov 2015). False discovery rate was performed using a non-lineal fitting method and displayed results were those presenting a Global false discovery rate of at least 1%[306]. Peptide quantification was done using the Progenesis LC−MS software (ver. 2.0.5556.29015, Nonlinear Dynamics). Accurate mass measurements from full survey scans in the TOF detector and monitored retention times were aligned to compensate for between-run variations in the nanoLC separation system. All runs were aligned to a reference run automatically chosen by the software generating a master list of features considering m/z values and retention times. The quality of these alignments was manually supervised using the quality scores provided by the software. Peptide identifications were exported from Protein Pilot and imported in Progenesis LC− MS where they were matched to the respective features. Output data files were managed using R scripts for subsequent statistical analyses and representation. Proteins identified by site (identification based only on a modification), reverse proteins (identified by decoy database) and potential contaminants were excluded. Proteins quantified with at least one unique peptide, an ANOVA p-value lower than 0.05, and

an absolute fold changes of <0.77 (down-regulation) or >1.3 (up-regulation) in linear scale were considered to be significantly differentially expressed.

14. STATISTICAL ANALYSIS

All experiments were performed at least in triplicate and the results are expressed as mean ± SEM (standard error of the mean). Statistical analyses were performed using Student's *t* test or when comparing multiple groups using one-way ANOVA with Bonferroni or Newman-Keuls multiple comparison test, as indicated in figure legends. Values of $P<0.05$ were considered as statistically significant.

RESULTS

1. RTP801 PROTEIN DEGRADATION

RTP801, an mTOR pathway inhibitor, is rapidly induced under many stress situations in an attempt to maintain cellular function and viability[287]. However, a sustained and chronic RTP801 elevation can be detrimental and lead to neuronal death by a sequential inhibition of mTOR and Akt survival kinases[136,137]. Hence, RTP801 protein levels regulation will be pivotal to determine the cellular response to different environmental contexts.

Apart from its rapid gene induction, RTP801 post-translational modifications and proteostasis will determine its stability, cellular localization and function, and therefore will be important to precisely modulate mTOR pathway. The fact that RTP801 presents an extremely short protein half-life (2-7 minutes)[292,295], points out that a proper RTP801 degradation should be crucial for neuronal survival.

Therefore, a sustained RTP801 elevation can be the end point of several processes, including stress-induced gene expression and defective protein degradation. In neurodegenerative disorders, the idea of an impaired RTP801 degradation becomes more relevant, since malfunction of protein degradation pathways have been reported[70,76,307,308].

1.1 RTP801 is degraded by the UPS and by the lysosomal pathway

Thus, protein levels in cells are determined by the rate of synthesis and degradation. There are two major pathways that mediate protein degradation: the ubiquitin-proteasome system (UPS) and the lysosomal pathway.

First, the mechanisms that underlie RTP801 protein degradation were studied in different cell types. For that purpose, NGF-differentiated PC12 cells (NPC12) or rat primary cortical neurons were exposed during 4 hours to epoxomicin or MG132, both selective proteasome inhibitors[309,310], or chloroquine, an inhibitor of intralysosomal catabolism[311]. Western Blot (WB) analysis of cell lysates showed a significant RTP801 accumulation after proteasome inhibition in both cell types (Figure 18a-b), indicating that is mainly degraded by the UPS. However, there was also a moderate RTP801 accumulation after chloroquine exposure. These data reveal unexpectedly that a pool of total RTP801 is degraded through the lysosomal pathway. Interestingly, the amount of RTP801 degraded by lysosomes in cortical neurons is slightly higher if compared to neuronal PC12 cells.

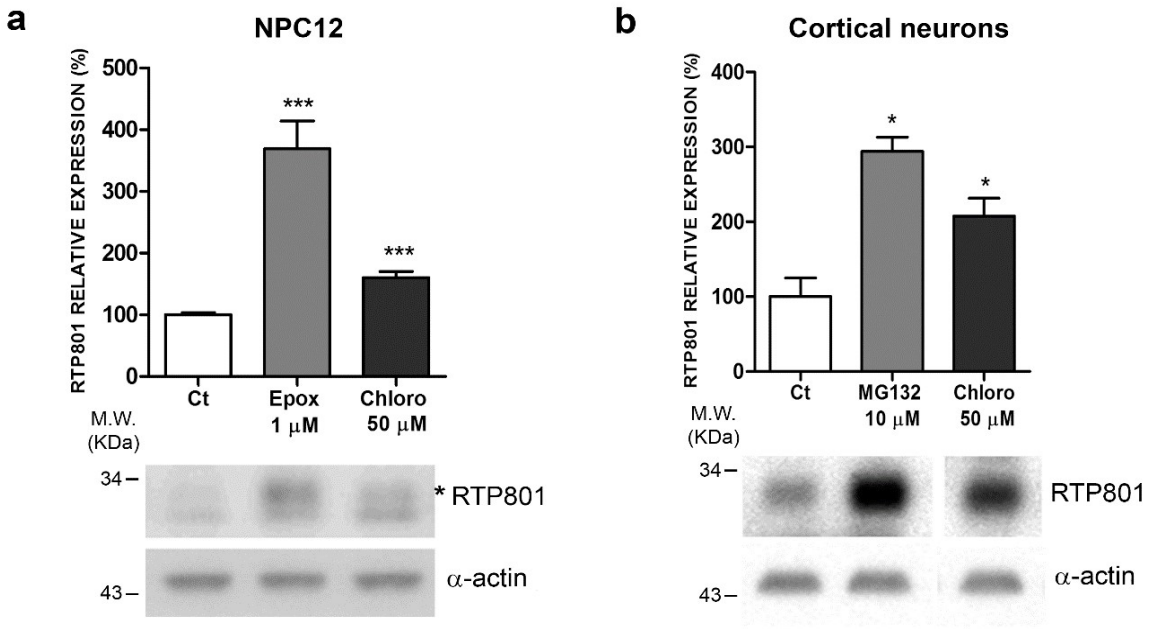

Figure 18. RTP801 can be degraded by both the ubiquitin-proteasome system (UPS) and by the lysosomal pathway. NGF-differentiated PC12 cells **(a)** or cortical neurons at DIV 16 **(b)** were exposed for 4 hours to 1 μM epoxomicin/10 μM MG132 or 50 μM chloroquine, and cell lysates were subjected to WB. Membranes were probed with anti-RTP801 antibody and then with anti-α-actin antibody as a loading control (*: specific band for RTP801). All samples were immunoblotted in the same membrane, but some irrelevant bands were deleted. Graphs represent densitometries (mean ± SEM) normalized to α-actin of three independent experiments in triplicates. Student's t-test, ***P<0.001 and *P<0.05 *versus* control.

2. RTP801 AS A NOVEL SUBSTRATE FOR NEDD4 E3 LIGASE

Selective protein degradation through UPS or lysosomal pathway requires a previous signal: conjugation of ubiquitin. Ubiquitination is a post-translational modification, which involves the attachment of ubiquitin molecules to lysine residues (K) on the substrate protein, being a multistep process that requires three enzymes: E1 or ubiquitin-activating enzyme, E2 or ubiquitin-conjugating enzyme, and E3 or ubiquitin ligase enzyme, being the E3 enzyme the one that gives specificity for the substrate[52,53].

So, we next wondered which E3 ligase could be responsible for RTP801 ubiquitination. In our group we have already described parkin as a RING E3 ligase that ubiquinates RTP801 targeting it to proteasomal degradation[296]. Based on the rapid turnover of RTP801 and its crucial functions over key kinases that mediate cell survival, we suspected that other E3 ligases than parkin could be regulating RTP801.

NEDD4 is one of the most abundant E3 ubiquitin ligases in mammalian neurons[254]. Interestingly, NEDD4 has been recently linked to PD pathogenesis since it has been reported that ubiquitinates α-synuclein targeting it to endosomal-lysosomal degradation[271]. A role for NEDD4 in PD is further supported by the identification of a coding SNP as a risk factor for idiopathic PD[14]. Based on these background, we asked whether NEDD4 ubiquitinates RTP801 and therefore modulates its proteostasis.

2.1 NEDD4 E3 ligase ubiquitinates RTP801

First, we investigated whether NEDD4 polyubiquitinates RTP801 and which type of polyubiquitin chains NEDD4 preferentially attaches to RTP801.

2.1.1 NEDD4 is capable to ubiquitinate RTP801 in a cell-free in vitro system

To investigate whether NEDD4 is able to directly polyubiquitinate RTP801 a cell-free ubiquitination assay was performed. Recombinant NEDD4 as the E3 ligase, recombinant GST-RTP801 as putative substrate, biotinylated ubiquitin, E1 human activating enzyme and E2 conjugating enzyme UbcH5b were mixed and incubated at 37ºC to allow the reaction to take place. E2 UbcH5b enzyme was used because it has been reported to work efficiently with NEDD4 E3 ligase[233]. Negative controls were performed in the absence of either E2 enzyme, or GST-RTP801 or NEDD4. RTP801 was then immunoprecipitated in order to discern between ubiquitinated RTP801 and auto-ubiquitinated NEDD4. The resulting immunocomplexes were assessed by WB. High molecular weight species corresponding to poly-ubiquitinated RTP801 (HMW Ub-RTP801) appeared only when NEDD4 along with the other reaction components were present (Figure 19). Hence, NEDD4 is capable to direct polyubiquitinate RTP801 in a cell free system.

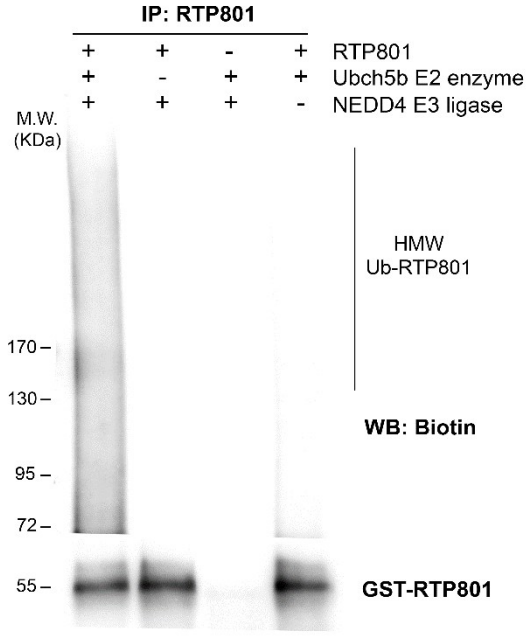

Figure 19. NEDD4 polyubiquitinates RTP801 in a cell free assay. Recombinant NEDD4 E3 ligase, recombinant GST-RTP801, UbcH5b E2 enzyme, E1 enzyme, biotinylated ubiquitin and ATP were mixed and incubated at 37ºC for 90 minutes. Then, RTP801 was immunoprecipitated and immunocomplexes were analysed by WB. The membrane was incubated with Avidin/Biotin and with chemiluminescent peroxidase substrate solution to detect ubiquitinated species (upper panel) and reprobed for anti-RTP801 antibody (lower panel) to confirm a proper immunoprecipitation. A representative image of three independent experiments is shown. HMW Ub-RTP801=High molecular weight ubiquitinated RTP801; IP= immunoprecipitation.

2.1.2 NEDD4 enhances RTP801 polyubiquitination in cells

Next, we assessed whether ectopic NEDD4 enhances RTP801 polyubiquitination in cells. HEK293 cells were co-transfected with a plasmid to overexpress ubiquitin tagged with hemagglutinin epitope (HA) along with the empty vector (pHAGE) or a vector that overexpresses NEDD4 (pHAGE-NEDD4). Forty-eight hours later, cells were exposed to 10 μM MG132 for 3 hours in order to inhibit the degradation of ubiquitinated proteins by the proteasome. Afterwards, RTP801 was immunoprecipitated and immunocomplexes along with whole cell lysates analysed by WB. Indeed, the presence of ectopic NEDD4 increased

the appearance of high molecular weight species smear of ubiquitinated RTP801 (HMW Ub-RTP801) (Figure 20a). Thus, NEDD4 enhances endogenous RTP801 polyubiquitination.

Then, HEK293 cells were co-transfected with RTP801, HA-Ubiquitin along with pHAGE-NEDD4 or the empty vector pHAGE. Forty-eight hours later, RTP801 was immunoprecipitated and the resulting samples resolved in a WB. By overexpressing RTP801 we did not need to treat the cultures with proteasome inhibitor MG132 to visualize ubiquitinated species. Again, ectopic NEDD4 increased significantly the intensity of polyubiquitinated RTP801 smear (HMW Ub-RTP801) (Figure 20b). Therefore, NEDD4 enhances both endogenous and ectopic RTP801 polyubiquitination.

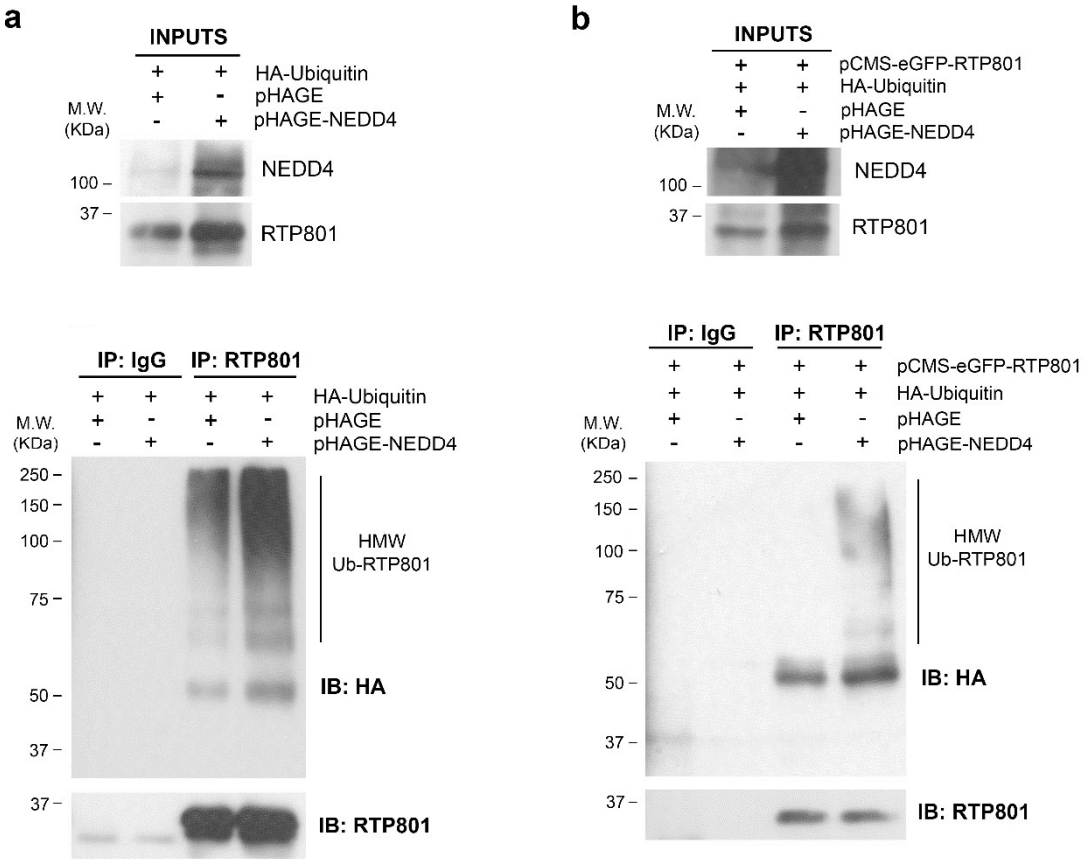

Figure 20. NEDD4 enhances endogenous (a) and ectopic (b) RTP801 polyubiquitination. a) HEK293 cells were transfected with empty vector pHAGE or pHAGE-NEDD4 along with HA-ubiquitin. Forty-eight hours post-transfection, cultures were exposed to 10 μM MG132 for 3 hours prior to RTP801 immunoprecipitation. Non-specific rabbit immunoglobulins (IgG) were used as a negative control. Whole cell lysates (inputs) and the resulting immunocomplexes were analysed by WB. The membrane was probed for HA to assess RTP801 ubiquitination levels, for RTP801 to check immunoprecipitation efficiency, and for NEDD4 to demonstrate proper transfection. A representative image of two independent experiments is shown. **b)** HEK293 cells were transfected with pHAGE or pHAGE-NEDD4 along with HA-ubiquitin and pCMS-eGFP-RTP801 constructs. Forty-eight hours post-transfection, either RTP801 was immunoprecipitated or non-specific rabbit immunoglobulins (IgG) were added. Whole cell lysates (inputs) and the resulting immunocomplexes were analysed by WB with anti-HA, anti-RTP801 and anti-NEDD4 antibodies. A representative image of two independent experiments is shown. HMW Ub-RTP801=High molecular weight ubiquitinated RTP801; IP= immunoprecipitation; IB= immunoblot.

2.1.3 NEDD4 attaches K63-ubiquitin chains to RTP801

One important point in ubiquitination studies is to investigate which type of polyubiquitin chains are used preferentially by the E3 ligase of the study, since the nature of the isopeptide linkages in the polyubiquitin chain determines the degradation pathway in cells[53]. NEDD4 typically attaches K48 or K63 polyubiquitin chains to their protein substrates[271,312–314]. Hence, to explore which ubiquitin chains are attached to RTP801 by NEDD4, HEK293 cells were co-transfected with RTP801 and NEDD4 along with HA-Ubiquitin-K48 (all ubiquitin lysines are mutated to arginine except K48) or HA-Ubiquitin-K63 (all ubiquitin lysines are mutated to arginine except K63). RTP801 was then immunoprecipitated and the resulting samples were analysed by WB. Interestingly, NEDD4 enhanced RTP801 polyubiquitination in the presence of HA-Ubiquitin-K63 but not in the presence of HA-Ubiquitin-K48 (Figure 21). These results suggest that NEDD4 links K63-polyubiquitin chains to RTP801, probably targeting it to lysosomal degradation.

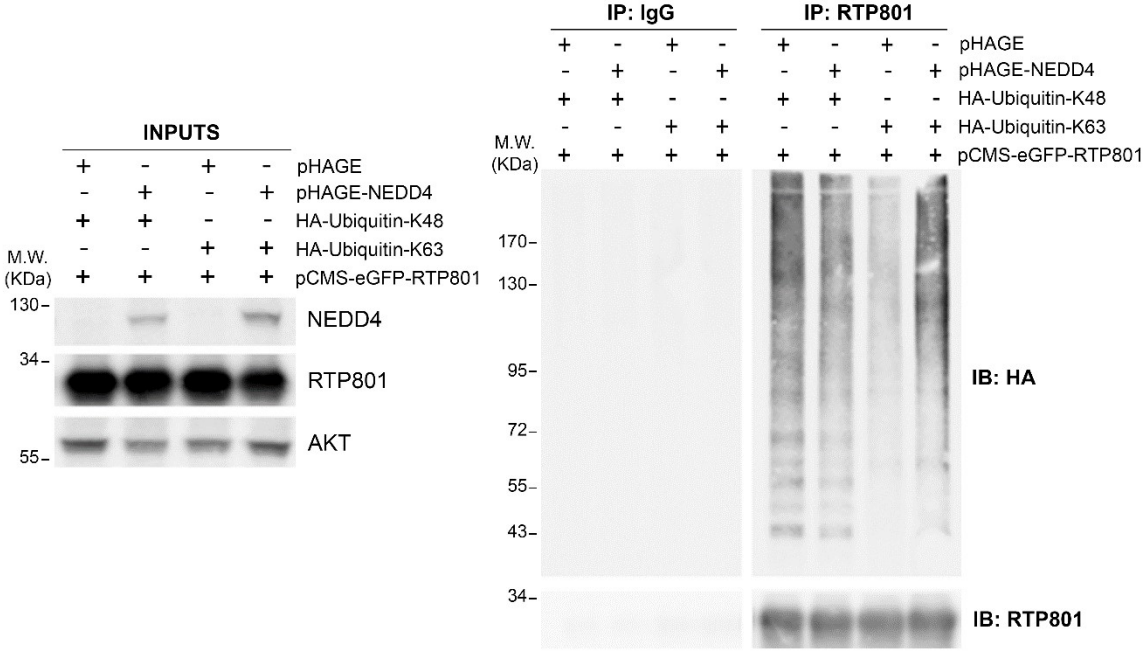

Figure 21. NEDD4 polyubiquitinates RTP801 with Ub-K63 chains. HEK293 cells were transfected with pCMS-eGFP-RTP801, along with pRK5-HA-Ub-K48 or pRK5-HA-Ub-K63 and pHAGE or pHAGE-NEDD4, as indicated. Forty-eight hours later, cultures were harvested and RTP801 was immunoprecipitated. Non-specific rabbit immunoglobulins (IgG) were used as negative control. Whole cell lysates (inputs) and RTP801 immunocomplexes were resolved in a WB. Membrane was probed for HA, and reprobed for RTP801 to confirm proper immunoprecipitation, for NEDD4 to check transfection levels and for Akt as loading control. All samples were immunoblotted in the same membrane, but some irrelevant bands were deleted. Note the high molecular weight smears corresponding to polyubiquitinated RTP801. A representative image of two independent experiments is shown. IP= immunoprecipitation; IB= immunoblot.

2.2 NEDD4 and RTP801 interact in cells

So far, we showed that NEDD4 polyubiquitinates RTP801 *in vitro* and in living cells, pointing out RTP801 as a putative substrate for NEDD4. Since direct interaction enzyme-substrate is a common step in a reaction, we next assessed whether NEDD4 and RTP801 co-immunoprecipitate in a cellular model. NEDD4 and RTP801, or the corresponding empty vectors were overexpressed in HEK293 cells prior to RTP801 immunoprecipitation. We performed a parallel immunoprecipitation with DSP, which is a chemical crosslinker of intracellular proteins. This compound helps to identify weak or transient interactions between proteins that otherwise could not be observed. In the resulting WB, NEDD4 and RTP801 co-immunoprecipitation was observed when crosslinker DSP was present (Figure 22b), but not without DSP (Figure 22a). This result suggests a weak or transient interaction between the two proteins, which is in fact, the typical nature of an E3-substrate interaction[315].

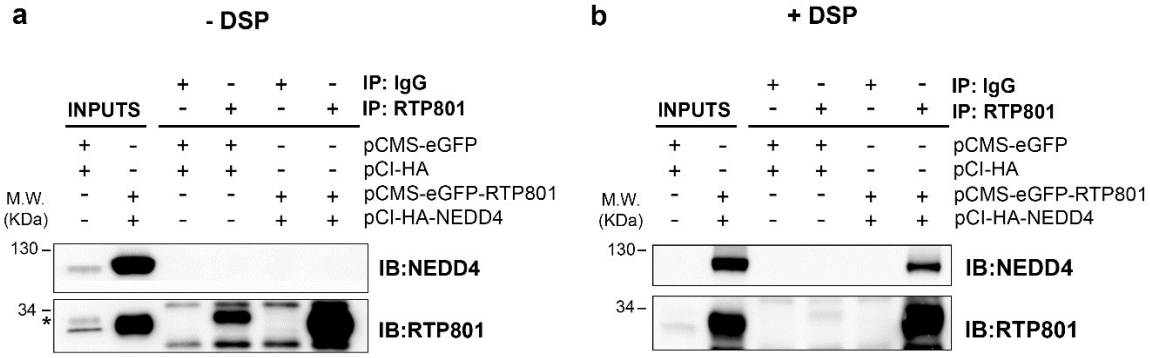

Figure 22. NEDD4 and RTP801 interact in cells exposed to crosslinker DSP. a) NEDD4 does not co-immunoprecipitate with RTP801 in cells that were not exposed to crosslinker DSP. HEK293 cells were co-transfected with empty vectors pCMS-eGFP and pCI-HA or with pCMS-eGFP-RTP801 and pCI-HA-NEDD4. Twenty-four hours post-transfection, cells were harvested and RTP801 was immunoprecipitated. The resulting samples were analysed by WB with anti-NEDD4 and anti-RTP801 antibodies (*: specific band for RTP801). **a) NEDD4 co-immunoprecipitates with RTP801 in cells exposed to DSP.** HEK293 cells were co-transfected with empty vectors pCMS-eGFP and pCI-HA or with pCMS-eGFP-RTP801 and pCI-HA-NEDD4. Twenty-four hours post-transfection, cells were exposed to cross-linker DSP for 2 hours at 4 ºC prior harvesting. RTP801 was immunoprecipitated and the samples were analysed by WB. Membranes were probed with anti-NEDD4 and anti-RTP801 antibodies. Representative images are shown of at least two independent experiments. IP= immunoprecipitation; IB=immunoblot.

Since protein overexpression approaches are prone to deliver false positives, subsequently, we wanted to corroborate this interaction between endogenous RTP801 and NEDD4. For that, NGF-differentiated PC12 were exposed to 1 μM epoxomicin for 2 hours. Then, cells were treated with DSP prior to RTP801 immunoprecipitation. Once more, NEDD4 and RTP801 co-immunoprecipitation was observed in the presence of the chemical crosslinker DSP (Figure 23). Thus, interaction between both proteins is confirmed.

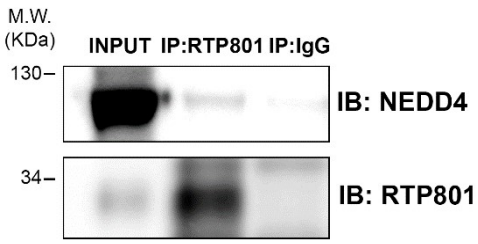

Figure 23. Endogenous RTP801 and NEDD4 interact in NPC12 cells. NGF-differentiated PC12 cells were treated with 1 μM epoxomicin during 2 hours. Then, cultures were exposed to DSP at 4 ºC for 2 hours prior harvesting. RTP801 was immunoprecipitated and the resulting samples were resolved in a WB. The membrane was incubated with anti-NEDD4 and anti-RTP801 antibodies. A representative image is shown of at least two independent assays. IP= immunoprecipitation; IB= immunoblot.

We next investigated whether NEDD4 and RTP801 interaction could be visualized in primary neurons by immunofluorescence colocalization studies. Ideally, we should have immunostained the cultures with specific antibodies to detect both endogenous RTP801 and NEDD4. However, after a thorough antibody screening for NEDD4, we concluded that the only one that was specific for NEDD4 and did not cross-react with NEDD4-2 was produced in the same host species than the primary RTP801 antibody. For this reason, cortical neurons were transfected with HA-tagged NEDD4. Forty-eight hours later, neurons were fixed and immunostained with a specific mouse antibody to detect HA-tag and visualize ectopic NEDD4 (in green) and with a rabbit antibody against RTP801 (in red). Interestingly, colocalization of both proteins (in orange) was observed in the soma and dendrites of neurons (Figure 24).

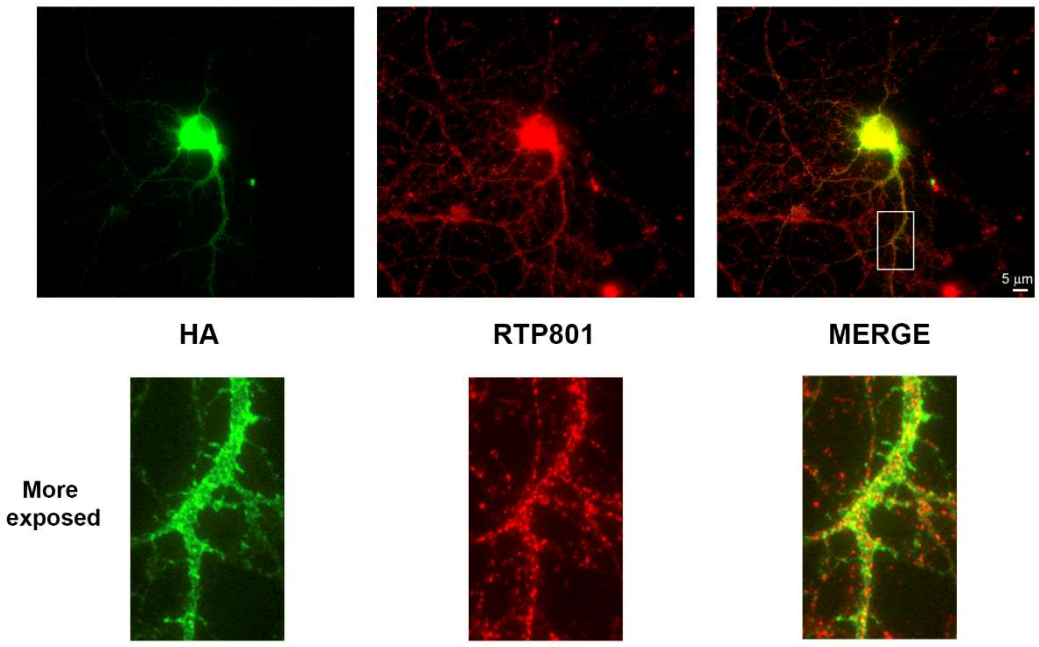

Figure 24. NEDD4 and RTP801 colocalize in neurons. DIV 19 primary rat cortical neurons were transfected with pCI-HA-NEDD4. Forty-eight hours post-transfection, neurons were fixed and stained with anti-RTP801 (in red) and anti-HA (in green) to visualize ectopic NEDD4. Scale bar, 5 μM.

2.3 NEDD4 regulates RTP801 protein levels in cellular models

Since we have observed that NEDD4 was able to polyubiquitinate RTP801 and that they interacted physically, we next wondered whether NEDD4 could regulate RTP801 steady-state protein levels in cells.

To answer this question we generated a NEDD4 inactive mutant with no E3 ligase activity by site-directed mutagenesis. The catalytic cysteine 867, responsible for the ubiquitin transfer[241,242], was mutated to serine (C867S) from pCI-HA-NEDD4 and pHAGE-NEDD4 vectors. The resulting constructs pCI-HA-NEDD4-C867S and pHAGE-NEDD4-C867S express an E3 ligase unable to charge and transfer ubiquitin to its substrates (Figure 25).

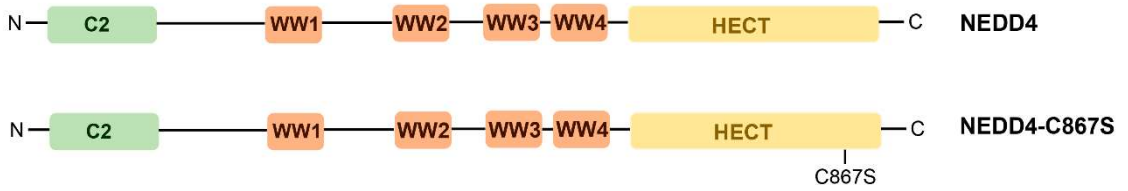

Figure 25. Schematic representation of the NEDD4 protein constructs. NEDD4 has a C2 domain, four WW domains and a C-terminal HECT domain with catalytic activity. In the NEDD4-C867S mutant, the catalytic cysteine 867 was mutated to serine by site-directed mutagenesis.

2.3.1 Ectopic WT NEDD4 decreases RTP801 protein levels

First, we assessed whether NEDD4 overexpression affects endogenous RTP801 protein levels in two different cell types.

NGF-differentiated PC12 cells were transfected with the empty vector pCI-HA, pCI-HA-NEDD4 to overexpress HA-tagged NEDD4 or pCI-HA-NEDD4-C867S to overexpress HA-tagged inactive mutant. Forty-eight hours later, cells were harvested and RTP801 protein levels analysed by WB. Interestingly, wild-type (WT) NEDD4 but not the inactive mutant NEDD4-C867S significantly decreased RTP801 protein levels by 25 % (Figure 26a). Considering that neuronal PC12 cells present a low efficiency of transfection, between 15-20%, the observed reduction in RTP801 protein levels is noteworthy.

We next wanted to confirm this result in primary neurons. Since post-mitotic neurons have even a lower liposome-mediated transfection efficiency[316] we used lentiviral infection techniques to over express NEDD4. Lentiviruses are capable to infect non-dividing cells and insert their genetic information to the host genome, ensuring a constant and stable expression over time[317].

Primary rat cortical neurons were infected with lentiviral particles packed with the constructs pHAGE as control, pHAGE-NEDD4 to overexpress WT NEDD4 or pHAGE-NEDD4-C867S to overexpress the inactive mutant. Four days later, cells were lysed and RTP801 levels

analysed by WB. Note that RTP801 was decreased in neurons transduced with NEDD4 WT but not in neurons transduced with the inactive mutant NEDD4-C867S (Figure 26b).

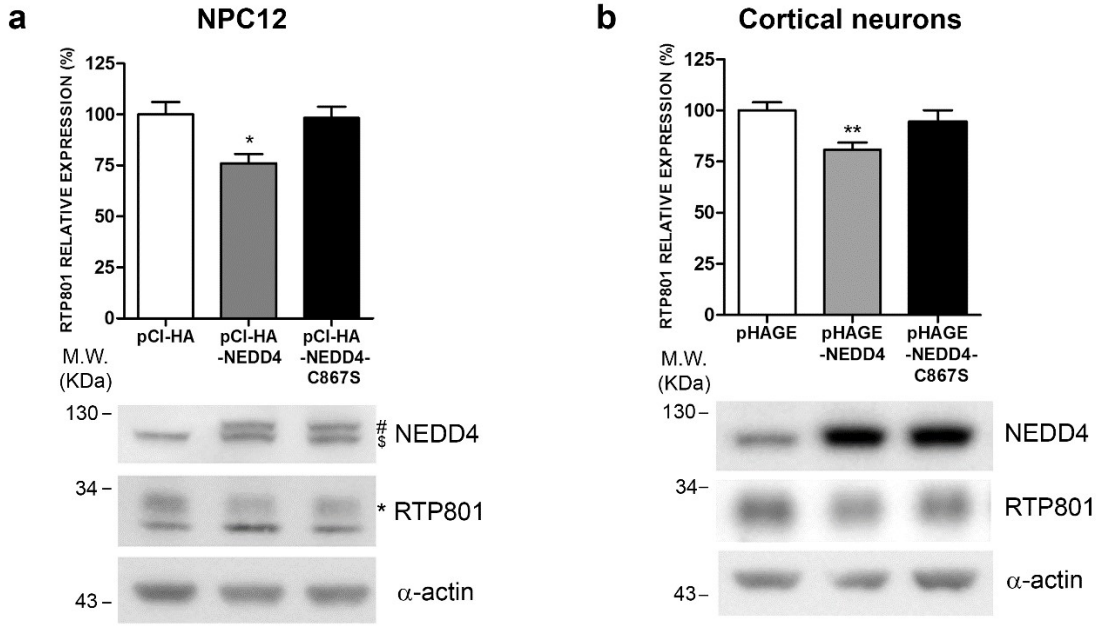

Figure 26. Ectopic NEDD4 decreases RTP801 protein levels in neuronal PC12 cells (a) and in cortical neurons (b). a) NGF-differentiated PC12 cells were transfected with pCI-HA, pCI-HA-NEDD4 or pCI-HA-NEDD4-C867S constructs. Forty-eight hours post-transfection, cultures were harvested and analysed by WB with anti-NEDD4, anti-RTP801 and anti-α-actin antibodies. Representative immunoblots are shown along with densitometric quantification from at least three independent experiments done in triplicate. ($ Endogenous NEDD4, # ectopic NEDD4, * specific band for RTP801). One-way ANOVA with Bonferroni multiple comparison test, *P<0.05 *versus* pCI-HA. **b)** DIV 8 rat primary cortical neurons were infected with lentiviruses containing the empty vector pHAGE, pHAGE-NEDD4 or pHAGE-NEDD4-C867S inactive mutant. Cell lysates were harvested 4 days later and analysed by WB with antibodies against RTP801, NEDD4 and α-actin as loading control. The graph represents RTP801 densitometries of at least three independent experiments done in triplicate. One-way ANOVA with Bonferroni multiple comparison test, **P<0.01 *versus* pHAGE.

To sum up, NEDD4 overexpression reduces RTP801 protein levels in neuronal PC12 cells and in cortical neurons.

2.3.2 NEDD4 does not regulate RTP801 at transcriptional level

To obtain further evidence that NEDD4 E3 ligase regulates RTP801 at a post-translational level, we assessed the mRNA levels of RTP801 in the presence of NEDD4. As in the previous experiment, cortical neurons were infected with lentiviral particles containing NEDD4, NEDD4-C867S or the empty vector pHAGE. Four days later, RNA was extracted and DDIT4 gene (gene encoding for RTP801 protein) mRNA levels were quantified by RT-qPCR. No differences were observed between NEDD4 overexpression, inactive mutant NEDD4-C867S overexpression and the control with the empty vector (Figure 27). Hence, NEDD4 does not regulate RTP801 transcriptionally.

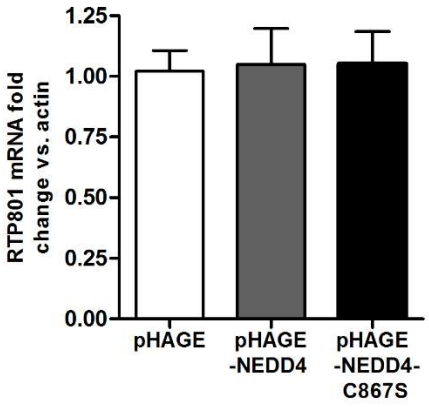

Figure 27. Ectopic NEDD4 does not affect RTP801 mRNA levels. DIV 8 cortical neurons were infected with lentiviruses containing the constructs pHAGE, pHAGE-NEDD4 or pHAGE-NEDD4-C867S. RNA was extracted 4 days later, and reverse transcription-qPCR was performed to quantify RTP801 transcripts. Results are displayed as RTP801 mRNA fold change respect to α-actin mRNA levels. The graph shows values (mean ± SEM) of three independent experiments done in triplicate.

2.3.3 NEDD4 knockdown increases RTP801 protein levels

To further corroborate the regulation of RTP801 by NEDD4 we investigated whether NEDD4 knockdown could also modulate RTP801 protein levels.

Cortical neurons were infected with commercial lentiviral particles containing three short hairpin RNA (shRNA) sequences designed to knockdown NEDD4 gene expression (ShNEDD4) or a scrambled shRNA sequence as control (ShCt). Six days later, neurons were lysed and RTP801 levels analysed by WB. NEDD4 knockdown was very efficient and RTP801 protein levels were significantly increased by 40% (Figure 28). This result confirms that RTP801 is regulated by NEDD4 E3 ligase.

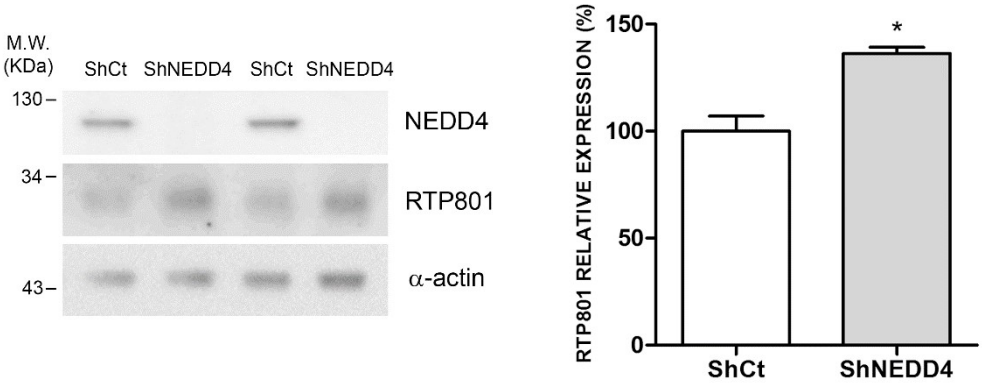

Figure 28. NEDD4 knockdown increases RTP801 protein levels. DIV 4 cortical neurons were infected with lentiviruses containing a scrambled ShRNA (ShCt) or a mix of three shRNA sequences against NEDD4 (ShNEDD4). Cell lysates were analysed 6 days later by WB. Membranes were incubated with NEDD4 and RTP801 antibodies, and with α-actin antibody as loading control. RTP801 densitometries of at least two independent experiments done in triplicate are represented in the graph along with a representative immunoblot. Student's t-test, *P<0.05 *versus* ShCt.

2.3.4 NEDD4 knockdown decreases phosphorylation of survival kinase Akt and is detrimental for neurons

In differentiated cells, such as neurons, RTP801 has a pro-apoptotic role[136,275], since it inactivates sequentially mTOR kinase and survival kinase Akt[136,137,292]. Therefore, a sustained RTP801 elevation can impair neuron function and eventually lead to neuron death.

Here, we examined whether RTP801 elevation induced by NEDD4 knockdown is accompanied by a toxic mTOR/Akt signaling pathway inhibition. For that, cell lysates from the previous experiment were analysed by WB for Akt phosphorylation at Ser473 (P-Akt S473) as a readout of mTORC2 complex activity and survival signal[194], and for α-spectrin caspase-cleaved fragment (spectrin breakdown product 120, SBDP120) as a readout of apoptotic cell death.

α-spectrin is a 280 KDa cytoskeletal protein localized in the intracellular side of the plasma membrane that is an accepted marker for apoptosis, since it is cleaved by caspases[318,319]. More concretely, α-spectrin is cleaved by caspase-3 generating a 120 KDa fragment that is specific for apoptosis. Moreover, α-spectrin can be cleaved by calpains generating a 145 KDa fragment. Both fragments (SBDP120 and SBDP145) can be easily detected in a WB with a α-spectrin antibody[319].

Interestingly, when NEDD4 expression was abrogated we observed a decrease of Akt phosphorylation at Ser473 and an increment of α-spectrin caspase-cleaved fragment SBDP120 (Figure 29), suggesting an mTORC2 complex inhibition and the appearance of neuronal death.

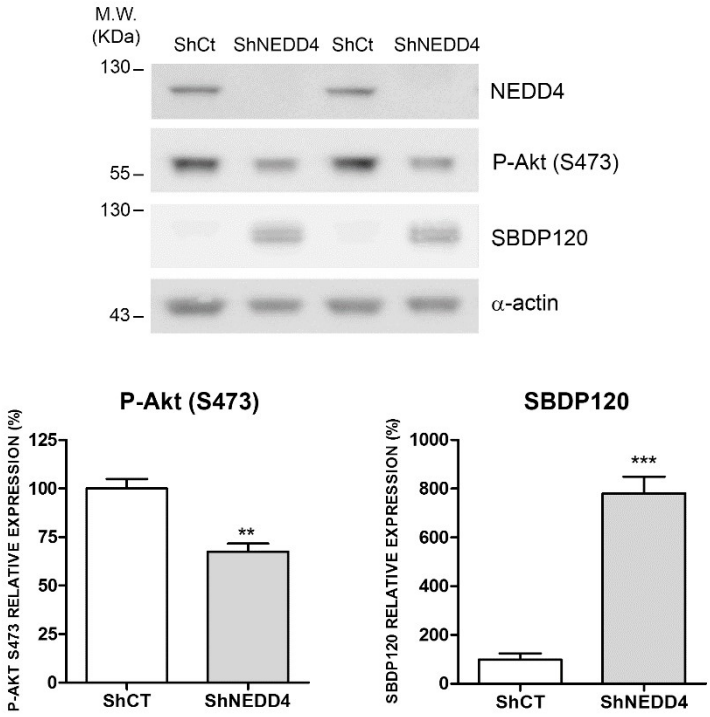

Figure 29. NEDD4 knockdown is detrimental for neurons. DIV 4 cortical neurons were infected with lentiviruses containing a scrambled ShRNA (ShCt) or a mix of three shRNA sequences against NEDD4 (ShNEDD4). Cell lysates were analysed 6 days later by WB. Membranes were incubated with antibodies against P-Akt (S473) and α-spectrin, and with antibody against α-actin as loading control. In the case of α-spectrin the caspase-cleaved fragment (spectrin breakdown product 120, SBDP120) is shown. Representative immunoblots are shown along with densitometries (mean ± SEM) of at least two independent experiments done in triplicate. Student's t-test, **P<0.01 and ***P<0.001 *versus* ShCt.

To sum up, NEDD4 depletion promotes an increase of RTP801 protein levels, which is accompanied by Akt pro-survival kinase inactivation and neuronal death.

2.4 RTP801 is accumulated in NEDD4$^{f/f}$;Emx1Cre conditional knockout mice

In order to further confirm RTP801 as a real NEDD4 substrate *in vivo*, we next assessed whether the lack of NEDD4 could affect RTP801 protein levels in an animal model. NEDD4 conventional knockout mice are not viable[251,253], so we used the NEDD4$^{f/f}$;Emx1Cre conditional knockout mice that abolishes the expression of NEDD4 in glutamatergic neurons and glia cells in the cerebral cortex[254,320].

Lysates from NEDD4$^{f/f}$;Emx1Cre mice dissected cortices and their WT littermates were resolved in a WB in order to study RTP801 protein levels. We observed that in the conditional knockout mice NEDD4 levels were decreased by 50% while RTP801 was significantly increased (Figure 30a).

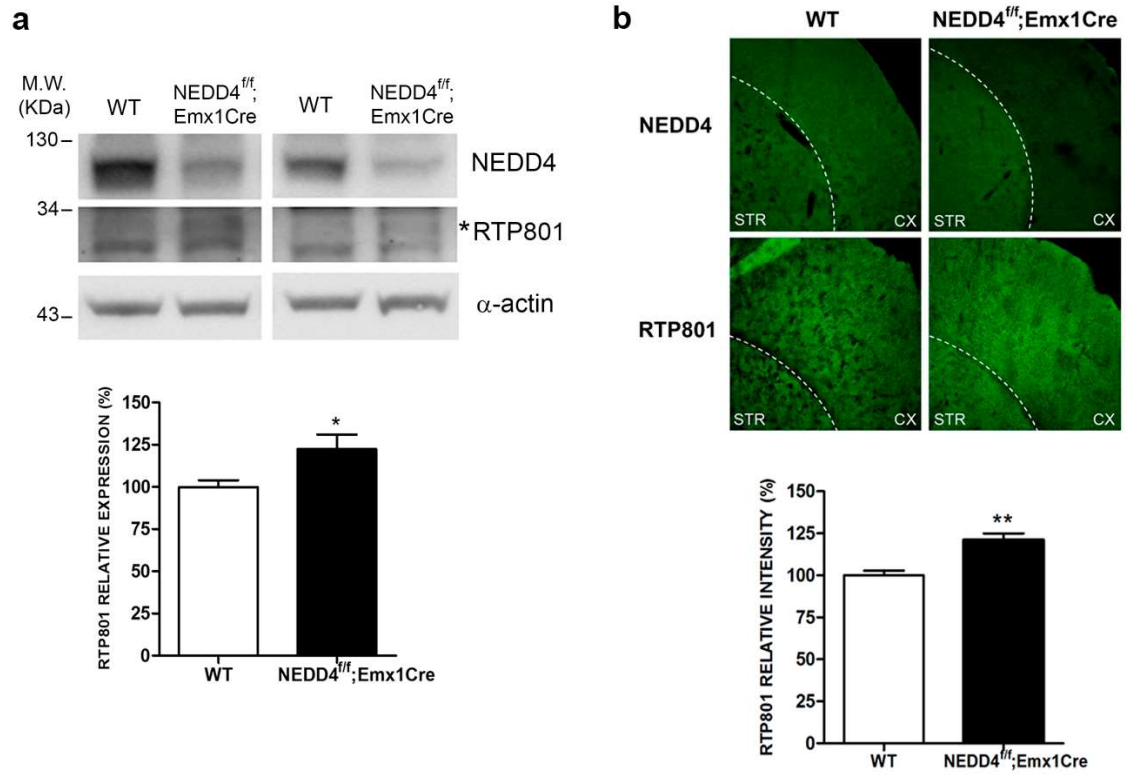

Figure 30. NEDD4$^{f/f}$;Emx1Cre conditional knockout mice have elevated RTP801 protein levels in the cortex. a) Cortical lysates of 6-week old mice were analysed by WB with anti-NEDD4 and anti-RTP801 antibodies, and then reprobed with anti-α-actin antibody as loading control. Representative immunoblots are shown along with RTP801 densitometries (mean ± SEM) of at least three independent gels. All samples were immunoblotted in the same membrane, but some irrelevant bands were deleted. Student's t-test, *P<0.05 *versus* WT. **b)** Brain sections (30 μm) of fixed 21-week old mice were immunostained for NEDD4 and RTP801. Representative confocal microscopy images acquired at 10x magnification showing RTP801 and NEDD4 immunostaining in the cortex (CX) and striatum (STR) are shown. RTP801 staining in the cortex was quantified using imageJ of at least 6 different sections from 4 different animals and the results are represented in the graph. Student's t-test, **P<0.01 *versus* WT.

To further confirm this result, coronal brain sections were immunostained against RTP801 and NEDD4. In NEDD4$^{f/f}$;Emx1Cre mice, the lack of NEDD4 staining was visible in the cortex in comparison to the striatum, confirming the expected phenotype. Then, by measuring the intensity of RTP801 staining with Image J software we observed that RTP801 levels in the cortex of conditional knockout mice were increased in comparison to WT mice littermates (Figure 30b). Hence, the loss of NEDD4 expression elevates RTP801 protein levels in the NEDD4$^{f/f}$;Emx1Cre conditional knockout mice.

3. NEDD4 PROTECTS FROM RTP801-INDUCED CELL DEATH

Evidence indicates that NEDD4 can have a neuroprotective role in front of some toxic insults. More precisely, NEDD4 E3 ligase was able to protect against α-synuclein toxicity in different PD animal models by polyubiquitinating it and targeting it to lysosomal degradation[271,272]. Interestingly, NEDD4 E3 ubiquitin ligase activity was shown to be necessary for its protective actions[272].

We know that RTP801 overexpression promotes cell death in differentiated cells, such as neuronal PC12 cells or sympathetic neurons[136,137,275]. Taking into account that NEDD4 decreases RTP801 protein levels, we next investigated whether NEDD4 is able to protect from ectopic RTP801 toxicity.

3.1 Ectopic WT NEDD4 partially prevents from RTP801-induced cell death

First, we investigated whether NEDD4 is able to protect against RTP801 overexpression and if so, if it is via its ubiquitin E3 ligase activity. For that, WT NEDD4, the inactive mutant NEDD4-C867S or the empty vector pCI-HA were overexpressed in NGF-differentiated PC12 cells along with pCMS-eGFP or pCMS-eGFP-RTP801 constructs. Twenty-four hours later, cell viability was evaluated by scoring the number of eGFP+ living cells under fluorescence microscopy.

RTP801 overexpression induced, as previously observed, around 50% of cell death, and WT NEDD4 partially prevented from RTP801-induced cell death. Otherwise, the inactive mutant NEDD4-C867S, that is not able to ubiquitinate any protein, did not confer protection in front of RTP801 (Figure 31). Note that cell viability was not altered in neuronal PC12 cells co-transfected with empty vector pCMS-eGFP and WT NEDD4 or empty vector pCMS-eGFP and NEDD4-C867S. The fact that inactive mutant NEDD4-C867S does not promote cell death by itself correlates with the no alteration in RTP801 protein levels previously observed (Figure 26a).

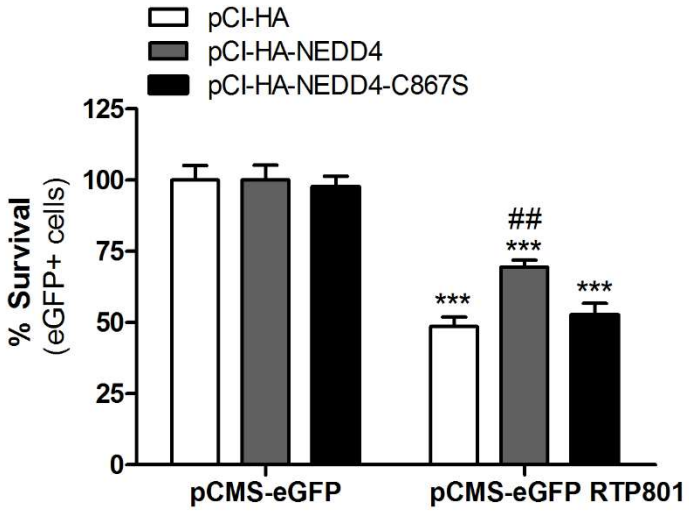

Figure 31. Ectopic WT NEDD4 protects from RTP801-induced cell death. NGF-differentiated PC12 cells were co-transfected with pCI-HA, pCI-HA-NEDD4 or pCI-HA-NEDD4-C867S constructs, together with either pCMS-eGFP or pCMS-eGFP-RTP801. Cells were fixed 24 hours later and cell survival (eGFP+ cells) scored under fluorescence microscopy. The graph represents mean ± SEM of at least three independent experiments in quadruplicates. One-way ANOVA with Bonferroni multiple comparison test, ***P<0.001 *versus* pCI-HA/pCMS-eGFP, ##P<0.01 *versus* pCI-HA/pCMS-eGFP-RTP801.

Thus, NEDD4 protection against RTP801 toxicity requires NEDD4 E3 ligase activity.

3.2 NEDD4 protection from RTP801 toxicity requires its ubiquitination

To confirm that NEDD4 E3 ligase confers protection by polyubiquitinating RTP801 we generated a non-ubiquitinable form of RTP801 by site-directed mutagenesis. RTP801-KR was generated replacing the six lysines (K) present in the amino acid sequence to arginine (R).

Before evaluating cell survival we performed an assay to verify that RTP801-KR was not polyubiquitinated in cells. HEK293 cells were co-transfected with eGFP, RTP801 or RTP801-KR, and twenty-four hours later RTP801 was immunoprecipitated in order to study its ubiquitination levels. Results showed that RTP801-KR polyubiquitination was mostly abrogated in comparison to WT RTP801 (Figure 32a). Moreover, there was a higher accumulation of RTP801-KR in whole cell lysates (inputs), indicating an impaired protein degradation of the mutant.

NGF-differentiated PC12 cells were co-transfected with pCI-HA or pCI-HA-NEDD4 along with pCMS-eGFP, pCMS-eGFP-RP801 or pCMS-eGFP-RTP801-KR constructs. Again, cell survival was measured twenty-four hours later by scoring the number of eGFP+ living cells. Non-ubiquitinable RTP801-KR mutant also promoted around 50% of cell death, but in this case ectopic NEDD4 did not exert protection in front its toxicity (Figure 32b). All these results confirm that NEDD4-mediated RTP801 ubiquitination is necessary for protection.

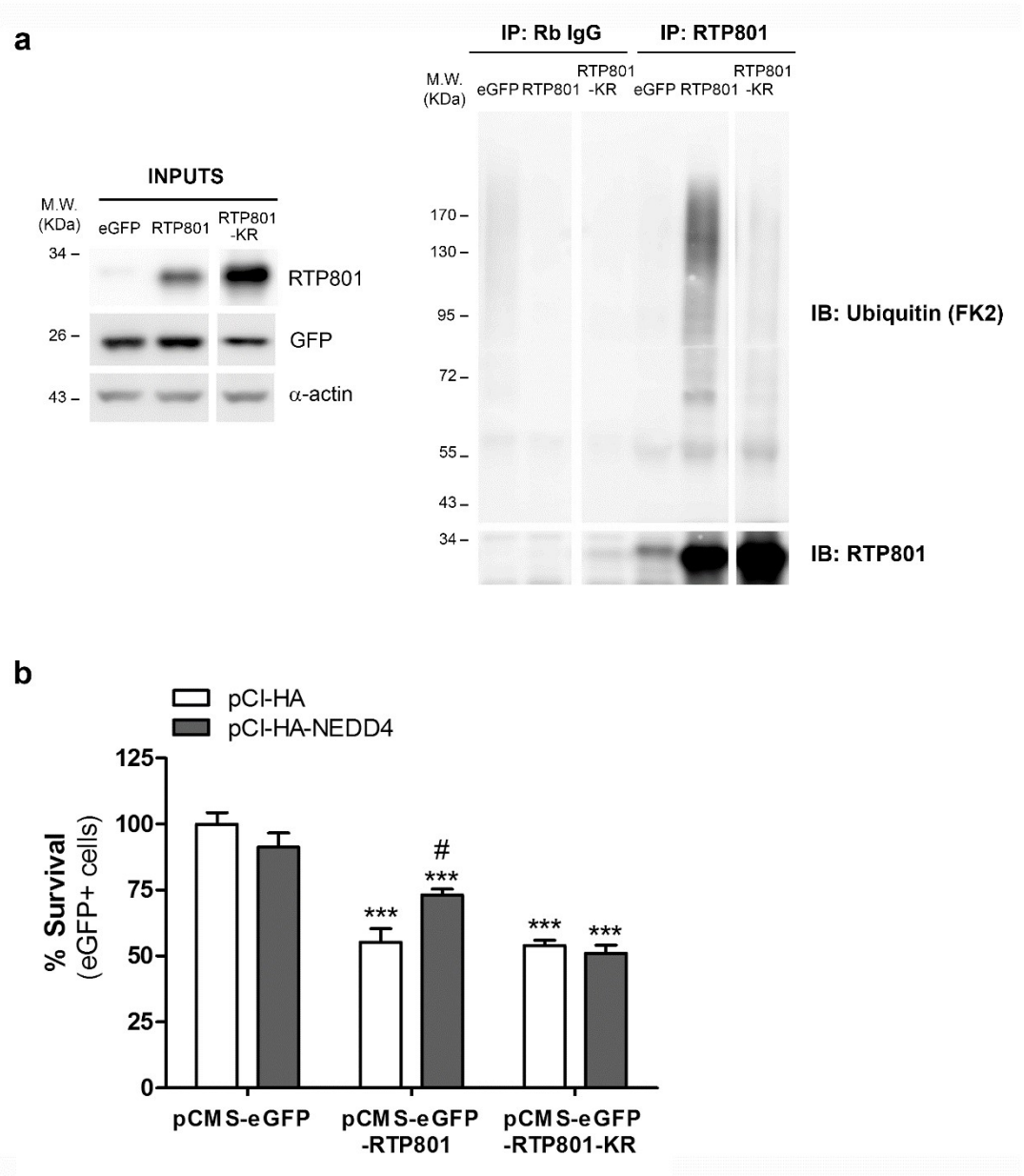

Figure 32. NEDD4 protection from RTP801-induced cell death requires its ubiquitination. a) Abrogation of RTP801-KR mutant polyubiquitination. HEK293 cells were transfected with pCMS-eGFP, pCMS-eGFP-RTP801 or pCMS-eGFP-RTP801-KR constructs. Twenty-four hours later, cells were harvested and RTP801 was immunoprecipitated to assess ubiquitination levels. Non-specific rabbit immunoglobulins (Rb IgG) were used as a negative control. Whole cell lysates (inputs) and RTP801 immunocomplexes were resolved in a WB. Membrane was probed for ubiquitin, RTP801, GFP to check transfection efficiency and α-actin as loading control. A representative image of two independent experiments is shown. All samples were immunoblotted in the same membrane, but some irrelevant bands were deleted. IP= immunoprecipitation; IB= immunoblot. **b) NEDD4 does not protect from RTP801-KR mutant toxicity.** NGF-differentiated PC12 cells were co-transfected with pCI-HA or pCI-HA-NEDD4 together with pCMS-eGFP, pCMS-eGFP-RTP801 or pCMS-eGFP-RTP801-KR. Twenty-four hours later, cells were fixed and eGFP+ surviving cells scored using fluorescence microscopy. The graph represents mean ± SEM of at least three independent experiments in quadruplicates. One-way ANOVA with Bonferroni multiple comparison test, ***P<0.001 *versus* pCI-HA/pCMS-eGFP and $^{\#}$P<0.05 *versus* pCI-HA/pCMS-eGFP-RTP801.

4. OXIDATIVE STRESS REGULATION OF NEDD4 AND RTP801

Then, we wondered whether NEDD4 is affected by cell stress situations in which RTP801 is induced, such as exposure to hypoxia-mimetic agent $CoCl_2$[321,322] or exposure to PD toxin 6-OHDA[136].

4.1 Hypoxia-mimetic agent $CoCl_2$ decreases NEDD4 and increases RTP801 protein levels

Cobalt chloride ($CoCl_2$) is widely used as a hypoxia-inducing agent since it mimics hypoxia response, including generation of reactive oxygen species (ROS) and upregulation of the hypoxia-inducible transcription factor-1 (HIF-1)[323]. In turn, HIF-1 transcription factor activates the RTP801-coding gene DDIT4[179,275].

Neuronal PC12 cells were exposed overnight to 200 µM $CoCl_2$ and cell lysates were resolved in a WB. As expected, RTP801 protein levels were highly incremented, while NEDD4 protein was significantly decreased (Figure 33).

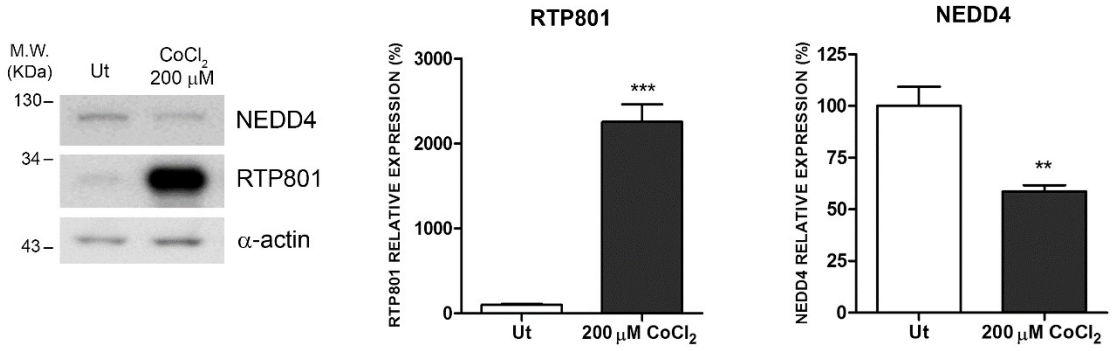

Figure 33. Exposure to hypoxia-mimetic agent $CoCl_2$ decreases NEDD4 and increases RTP801 protein levels in NPC12 cells. NGF-differentiated PC12 cells were treated or not with 200 µM $CoCl_2$ for 16 hours prior harvesting. Cell lysates were analysed by WB with antibodies against NEDD4, RTP801, and α-actin as loading control. Representative immunoblots are shown. Right panels show RTP801 and NEDD4 densitometries represented as mean ± SEM of at least three independent experiments done in triplicate. Student's t-test, **P<0.01 and ***P<0.001 *versus* Ut (Untreated).

4.2 PD toxin 6-OHDA decreases NEDD4 and increases RTP801 protein levels

Evidence demonstrated that RTP801 is induced in neuronal PC12 cells treated with 6-OHDA, both at gene and protein levels[136]. Here, we assessed NEDD4 levels in this cellular PD model. NGF-differentiated PC12 cells were exposed overnight to 100 µM 6-OHDA and the resulting samples analysed by WB. We observed a 50% decrease of NEDD4 protein levels and we confirmed the expected RTP801 increase (Figure 34a).

Then, we wondered whether 6-OHDA would affect similarly RTP801 and NEDD4 protein levels in neurons. PD toxin 6-OHDA induces death of cortical neurons in a concentration-dependent manner by means of autoxidation and ROS generation[129]. Therefore, rat primary cortical neurons were treated overnight with 50 µM 6-OHDA. Once again, RTP801 protein levels were highly increased, while NEDD4 protein levels were reduced to the half (Figure 34b).

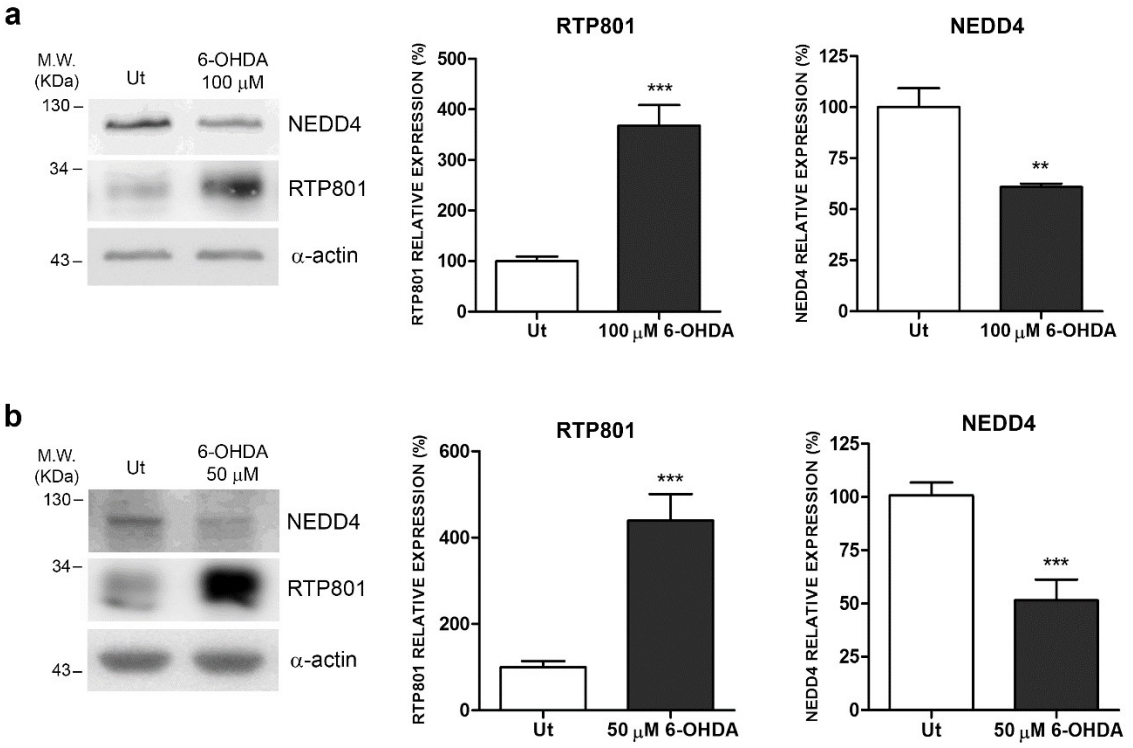

Figure 34. Exposure to PD toxin 6-OHDA decreases NEDD4 and increases RTP801 protein levels in NPC12 cells (a) and in cortical neurons (b). a) NGF-differentiated PC12 cells were treated or not with 100 μM 6-OHDA for 16 hours prior harvesting. Cell lysates were analysed by WB with antibodies against NEDD4, RTP801, and α-actin as loading control. Representative immunoblots are shown along with densitometries represented as mean ± SEM of at least three independent experiments done in triplicate. Student's t-test, **P<0.01 and ***P<0.001 *versus* Ut (Untreated). **b)** DIV 12 rat primary cortical neurons were treated or not with 50 μM 6-OHDA for 16 hours prior harvesting. Cell lysates were resolved in a WB. Membranes were incubated with antibodies against NEDD4, RTP801, and α-actin as loading control. Representative immunoblots are shown along with densitometries represented as mean ± SEM of at least three independent experiments done in triplicate. Student's t-test, ***P<0.001 *versus* Ut (Untreated).

These findings suggest that NEDD4 is sensitive to oxidative stress associated to PD toxin 6-OHDA and could contribute to the increase of RTP801.

4.3 PD toxin 6-OHDA increases RTP801 protein half-life

We next investigated RTP801 mRNA levels after exposure to the toxin. NGF-differentiated PC12 cells were treated with 100 μM 6-OHDA during 8 hours prior to RNA extraction. RTP801 transcripts were quantified by RT-qPCR. Results showed, as previously reported, a remarkable gene induction, since RTP801 mRNA levels increased almost four times in comparison to control cells (Figure 35a). This result correlates well with the previous observed elevation in RTP801 protein levels (Figure 34a).

Considering that NEDD4 regulates RTP801 in cells, we next explored whether 6-OHDA-induced NEDD4 reduction could be implicated in the observed RTP801 protein elevation. For this reason, we first studied whether 6-OHDA, apart from activating DDIT4 gene transcription, was also affecting its protein degradation by measuring RTP801 protein half-life.

NGF-differentiated PC12 cells were exposed to 6-OHDA overnight, and then new protein synthesis was inhibited during 10 and 60 minutes with cycloheximide (CHX) treatment. Cell lysates were resolved in a WB to calculate its protein half-life. Indeed, RTP801 protein half-life was significantly increased in cells exposed to 6-OHDA (Figure 35b), revealing that RTP801 protein degradation was impaired. At this point of the experiment NEDD4 levels were already reduced by the half. Hence, the loss of function of NEDD4 induced by 6-OHDA could contribute to the elevation of total RTP801 protein levels.

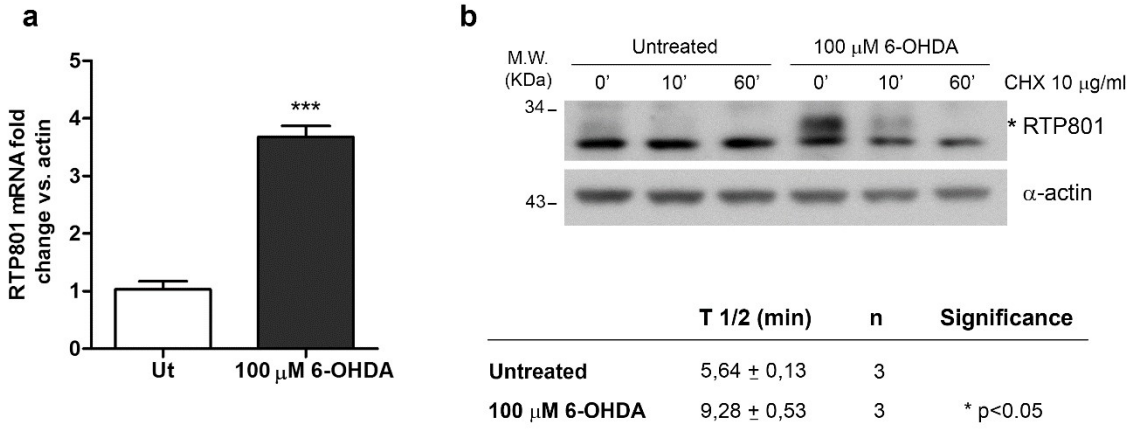

	T 1/2 (min)	n	Significance
Untreated	5,64 ± 0,13	3	
100 μM 6-OHDA	9,28 ± 0,53	3	* p<0.05

Figure 35. Exposure to PD toxin 6-OHDA induces DDIT4 gene and increases RTP801 protein half-life. a) 6-OHDA treatment increases RTP801 mRNA levels. NGF-differentiated PC12 cells were exposed to 100 μM 6-OHDA for 8 hours. Then, RNA was extracted and reverse transcription-qPCR was performed to determine RTP801 mRNA levels and α-actin mRNA levels as control. The graph shows values (mean ± SEM) of at least three independent experiments. Student's t-test, ***P<0.001 *versus* Ut (Untreated). **b) 6-OHDA treatment increases RTP801 protein half-life.** NGF-differentiated PC12 cells were exposed to 100 μM 6-OHDA for 16 hours. Then, cell cultures were treated with 10 μg/ml cycloheximide (CHX) during 10 or 60 minutes prior harvesting. Cell lysates were subjected to WB with antibodies against RTP801 and α-actin (* specific band for RTP801). RTP801 protein levels were quantified and half-life (T 1/2) was calculated applying a nonlinear regression with an exponential one-phase decay equation. Values represent the mean ± SEM of three different experiments. Student's t-test, *P<0.05 *versus* Ut (Untreated).

4.4 PD toxin 6-OHDA does not affect NEDD4 mRNA levels

We have previously showed that NEDD4 protein levels are decreased in neuronal PC12 cells and cortical neurons exposed to 6-OHDA (Figure 34a-b). Hence, we next investigated whether NEDD4 gene expression is also affected by 6-OHDA. NGF-differentiated PC12 cells were exposed to 100 μM 6-OHDA for 8 hours and RNA was extracted. By quantifying NEDD4 mRNA levels by RT-qPCR, we observed no differences between control cells and cells exposed to 6-OHDA (Figure 36). Therefore, these results suggest that 6-OHDA is regulating NEDD4 protein levels but not its gene expression.

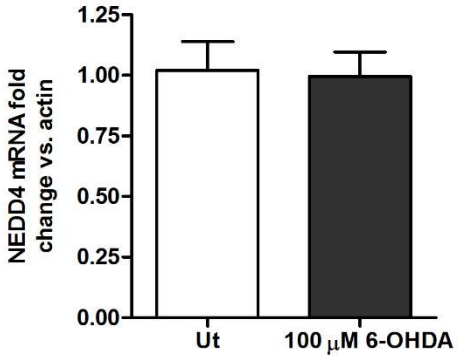

Figure 36. Exposure to PD toxin 6-OHDA does not affect NEDD4 mRNA levels. NGF-differentiated PC12 cells were exposed to 100 μM 6-OHDA for 8 hours. Then, RNA was extracted and reverse transcription-qPCR was performed to determine NEDD4 mRNA levels. Results are represented as NEDD4 mRNA fold change respect to α-actin mRNA levels. The graph shows values (mean ± SEM) of three independent experiments.

Such results raised the question of how NEDD4 protein levels are reduced after 6-OHDA exposure. Since this PD toxin promotes caspases and calpains activation[132,324,325] we hypothesized that NEDD4 could be cleaved by these proteases. To study this possibility cells were treated with the pan-caspase inhibitor Z-VAD-FMK or the calpain inhibitor ALLN respectively, prior to 6-OHDA exposure.

Neuronal PC12 cells were treated with 100 μM Z-VAD-FMK pan-caspase inhibitor one hour before 6-OHDA exposure. Sixteen hours later, cells were harvested and NEDD4 levels analysed by WB. Results confirmed the inhibitory function of the compound, since the increase of caspase-cleaved α-spectrin fragment SBDP120 induced by 6-OHDA was completely blocked by Z-VAD-FMK (Figure 37). Moreover, caspase inhibitor partially prevented NEDD4 reduction induced by 6-OHDA (Figure 37). Hence, 6-OHDA-induced NEDD4 protein reduction is due in part by caspases proteolysis.

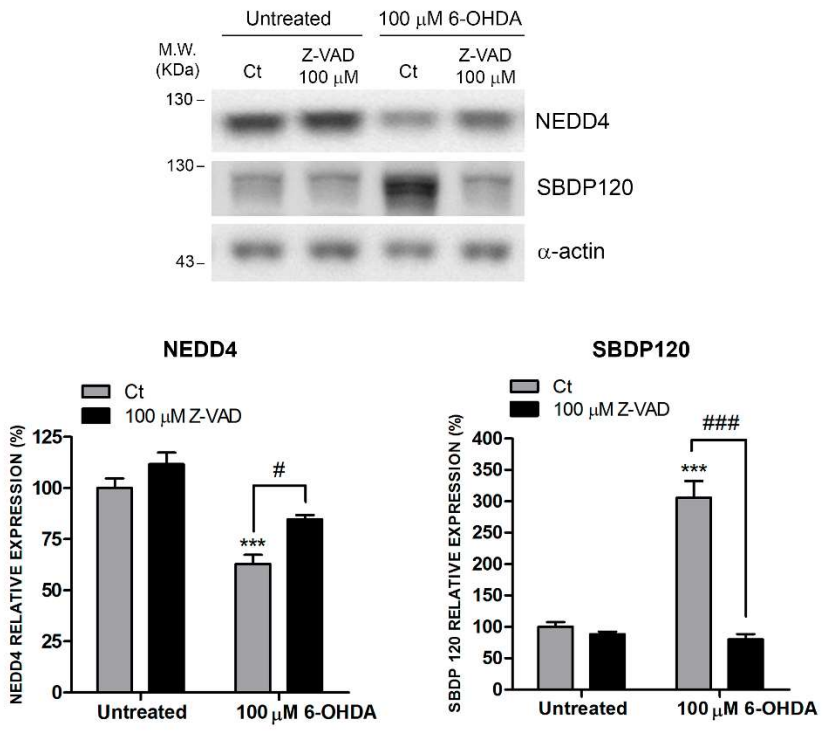

Figure 37. NEDD4 is cleaved by caspases after 6-OHDA exposure. Neuronal PC12 cells were treated with 100 μM Z-VAD-FMK pan-caspase inhibitor for 1 hour prior to 6-OHDA exposure. Sixteen hours later, cultures were harvested and analysed by WB. Membranes were incubated with antibodies against NEDD4, α-spectrin and α-actin as loading control. Graphs represent mean ± SEM of NEDD4 and caspase-cleaved α-spectrin fragment (SBDP120) densitometries of at least three independent experiments. One-way ANOVA with Bonferroni multiple comparison test, ***P<0.001 *versus* Untreated/Ct and $^{\#}$P<0.05, $^{\#\#\#}$P<0.001 *versus* 100 μM 6-OHDA/Ct.

Similarly, NPC12 cells were treated with 1 μM ALLN calpain inhibitor during one hour, prior to 16-hour 6-OHDA exposure. The resulting samples were analysed by WB. 6-OHDA treatment induced calpain activation as judged by the increment in the calpain-cleaved α-spectrin fragment SBDP145, a specific marker for calpain activation[318]. This elevation was completely blocked by calpain inhibitor ALLN (Figure 38). NEDD4 protein levels were also partially restored by calpain inhibitor, revealing that 6-OHDA-induced NEDD4 protein decrease is also due in part by calpain proteolysis.

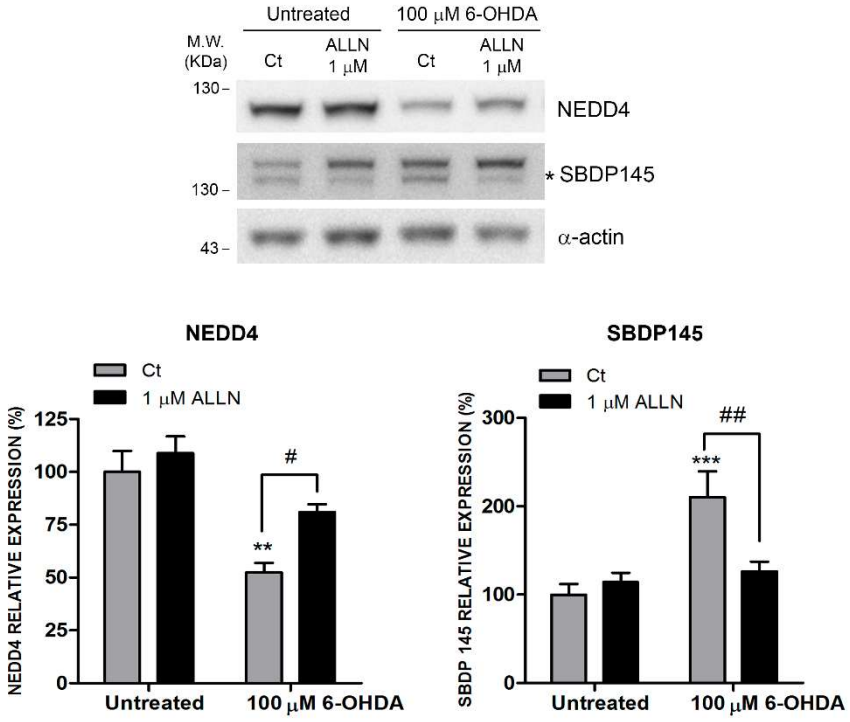

Figure 38. NEDD4 is cleaved by calpains after 6-OHDA exposure. Neuronal PC12 cells were treated with 1 μM ALLN calpain inhibitor for 1 hour prior to 6-OHDA exposure. Sixteen hours later, cultures were harvested and subjected to WB. Membranes were incubated with anti-NEDD4 and anti-α-spectrin antibodies and with anti-α-actin as loading control. Graphs represent mean ± SEM of NEDD4 and calpain-cleaved α-spectrin fragment (spectrin breakdown product 145 KDa, SBDP145) densitometric quantification of at least three independent experiments. One-way ANOVA with Newman-Keuls multiple comparison test, **P<0.01, ***P<0.001 *versus* Untreated/Ct and $^{\#}$P<0.05, $^{\#\#\#}$P<0.001 *versus* 100 μM 6-OHDA/Ct.

NEDD4 can also be released from cells within microvesicles called exosomes[229]. Exosomes are small extracellular vesicles (30-100 nm) derived from the endosomal system that play an important role in cell-to-cell communication[326]. Exosomal release is a process dependent on intracellular calcium changes[327–330]. Since 6-OHDA induces an increase of cytosolic calcium[331], we hypothesized that NEDD4 could be also released within exosomes, aggravating the loss of intracellular NEDD4.

Cortical neurons were exposed to 50 μM 6-OHDA overnight. Then, cells were lysed and extracellular microvesicles were isolated from their culture media, as well as from sister cultures not treated with the toxin as controls. By WB we observed the presence of NEDD4 in the exosomal enriched extracellular fraction from the control culture media (Figure 39). As we hypothesized, 6-OHDA-treated neurons showed elevated NEDD4 protein levels in the

exosomal-enriched fraction. Total lysates analysis confirmed the previous described NEDD4 decrease after 6-OHDA exposure. We also found evidence that 6-OHDA exposure increased the release of total extracellular vesicles, as judged by the elevation of exosomal markers TSG101 and flotillin-1 (Figure 39).

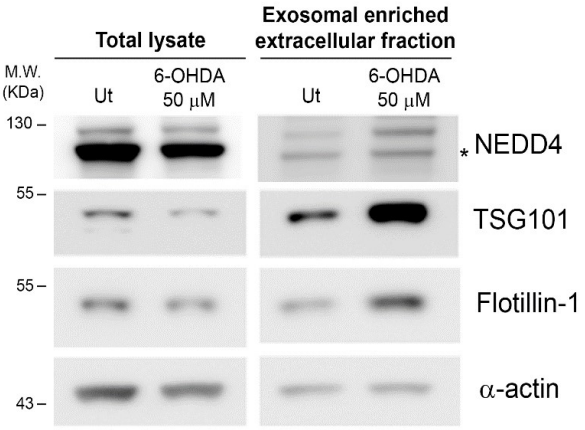

Figure 39. 6-OHDA exposure increases NEDD4 levels in extracellular microvesicles. DIV 14 rat primary cortical neurons were exposed to 50 μM 6-OHDA for 16 hours. Then, extracellular microvesicles were isolated from culture media and cells were lysed. Both fractions were resolved in a WB. Membrane was probed with anti-NEDD4 antibody, reprobed with anti-TSG01 and anti-flotillin-1 antibodies as extracellular microvesicles markers, and with anti-α-actin as loading control. All samples were immunoblotted in the same membrane, but some irrelevant bands were deleted. Representative immunoblots are shown of at least three independent experiments.

Taken together, these data suggest that 6-OHDA decreases NEDD4 protein levels by means of caspase and calpain cleavage and by promoting its exosomal release. Therefore, the loss of intracellular NEDD4 could contribute to RTP801 elevation following 6-OHDA PD toxin exposure.

5. NEDD4 IS PROTECTIVE AGAINST 6-OHDA TOXICITY BY REGULATING RTP801 PROTEIN LEVELS

It has been previously reported that RTP801 upregulation is essential for death evoked by PD toxin 6-OHDA[136,137,292]. Exposure to 100 μM 6-OHDA promoted around 50% of cell death in neuronal PC12 cells, while RTP801 knockdown with specific shRNA completely prevented from 6-OHDA-induced cell death[136]. Since 6-OHDA decreased NEDD4 protein levels, we next asked whether NEDD4 restitution could be protective against this toxin by regulating RTP801 protein levels.

5.1 Ectopic NEDD4 protects against 6-OHDA-induced cell death

NGF-differentiated PC12 cells were co-transfected with pCI-HA empty vector, pCI-HA-NEDD4 to overexpress WT NEDD4 or pCI-HA-NEDD4-C867S to overexpress NEDD4-C867S inactive mutant along with pCMS-eGFP construct. Thirty-two hours later, cell cultures were exposed to 100 μM 6-OHDA for sixteen hours. Then, cell survival was evaluated by scoring the number of eGFP+ living cells under fluorescence microscopy. PD toxin 6-OHDA induced around 50% of cell death, as previously described[136]. Interestingly, ectopic NEDD4 but not the mutant partially prevented from 6-OHDA-induced cell death (Figure 40a), revealing that NEDD4 E3 ligase activity is required for protection. Again, cell viability was not altered in neuronal PC12 cells transfected with WT NEDD4 or the mutant NEDD4-C867S.

To further extend these findings to neurons, we next assessed whether NEDD4 restitution was also protective against 6-OHDA toxicity in cortical neurons. Rat primary cortical neurons were infected with lentiviral particles containing the constructs pHAGE, pHAGE-NEDD4 or pHAGE-NEDD4-C867S. Three days later, neurons were exposed to 50 μM 6-OHDA for sixteen hours before cell fixation and Hoechst nuclear staining. Cell survival was evaluated by counting the number of non-pyknotic nuclei respect the total number of nuclei. Results showed that 6-OHDA induced around 30% of cell death and that WT NEDD4 but not the inactive mutant was able to partially abrogate 6-OHDA-induced cell death (Figure 40b).

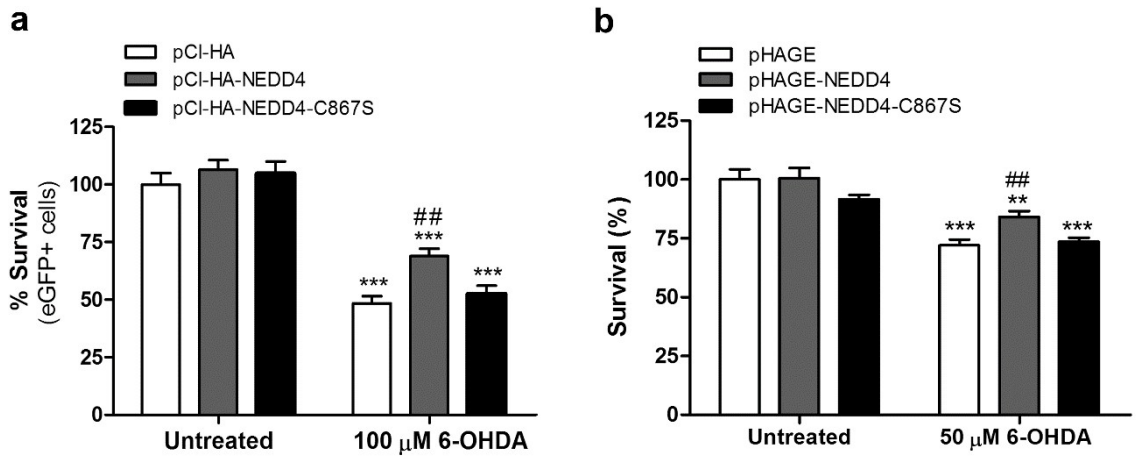

Figure 40. Ectopic NEDD4 partially protects from 6-OHDA-induced cell death in NPC12 cells (a) and in cortical neurons (b). a) NGF-differentiated PC12 cells were co-transfected with pCI-HA/pCMS-eGFP, pCI-HA-NEDD4/pCMS-eGFP or pCI-HA-NEDD4-C867S/pCMS-eGFP vectors with a 4:1 ratio. Thirty-two hours later, cell cultures were exposed to 100 μM 6-OHDA for 16 hours. Then, eGFP+ surviving cells were scored under fluorescence microscopy. The graph shows mean ± SEM of at least three independent experiments done in quadruplicate. One-way ANOVA with Bonferroni multiple comparison test, ***P<0.001 *versus* Untreated/pCI-HA and $^{\#\#}$P<0.01 *versus* 100 μM 6-OHDA /pCI-HA. **b)** DIV 7 rat primary cortical neurons were infected with lentiviruses containing the empty vector pHAGE, the vector pHAGE-NEDD4 to overexpress WT NEDD4 or the vector pHAGE-NEDD4-C867S to overexpress the inactive mutant. Three days later, cell cultures were exposed to 50 μM 6-OHDA for 16 hours prior cultures fixation and Hoechst staining. Then, surviving and pyknotic nuclei were scored under fluorescence microscopy. The graph shows mean ± SEM of at least three independent experiments done in triplicate. One-way ANOVA with Bonferroni multiple comparison test, **P<0.01, ***P<0.001 *versus* Untreated/pHAGE and $^{\#\#}$P<0.01 *versus* 50 μM 6-OHDA /pHAGE.

Thus, ectopic NEDD4 partially prevents from 6-OHDA-induced cell death in neuronal PC12 cells and in cortical neurons, being its E3 ligase activity required for protection.

5.2 Ectopic NEDD4 prevents from 6-OHDA-induced RTP801 elevation

To investigate whether ectopic NEDD4 protection against 6-OHDA toxicity was due to modulation of RTP801 protein levels, neuronal PC12 cells were equally transfected and exposed to 6-OHDA prior harvesting. WB analysis showed that WT NEDD4 not only reduced RTP801 protein levels in untreated cells (as previously shown in figure 26a), but also decreased RTP801 protein elevation in cells exposed to 6-OHDA. Otherwise, the inactive mutant NEDD4-C867S did not modify RTP801 protein levels in untreated cells or 6-OHDA-treated cells (Figure 41).

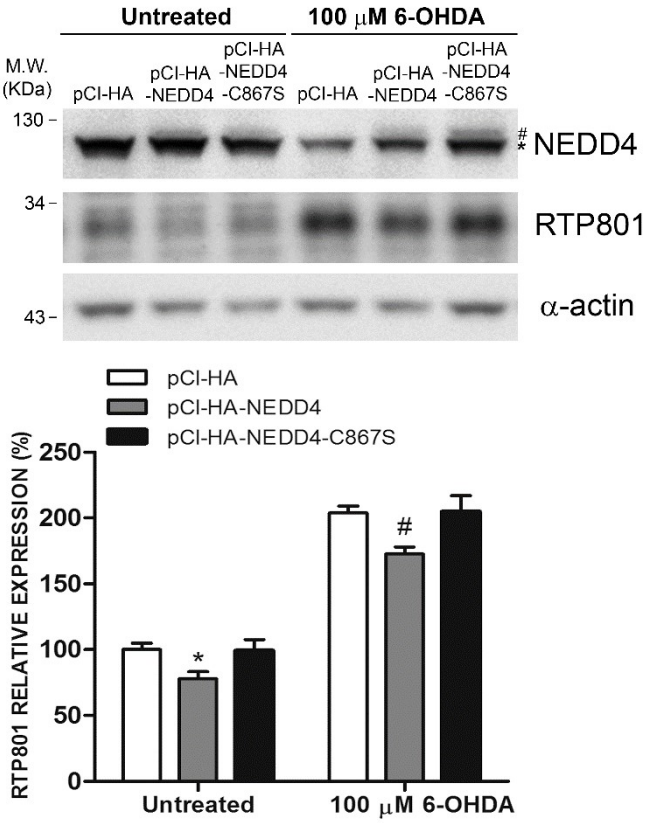

Figure 41. Ectopic NEDD4 reduces RTP801 elevation after 6-OHDA exposure. NGF-differentiated PC12 cells were transfected with pCI-HA, pCI-HA-NEDD4 or pCI-HA-NEDD4-C867S. Thirty-two hours later, cell cultures were exposed to 100 μM 6-OHDA for 16 hours and cell lysates were analysed by WB. Membranes were incubated with antibodies against NEDD4, RTP801 and α-actin as loading control (* endogenous NEDD4, # ectopic NEDD4). Representative immunoblots are shown along with RTP801 densitometric normalized quantification (mean ± SEM) from at least three independent experiments done in triplicate. One-way ANOVA with Bonferroni multiple comparison test, *P<0.05 *versus* Untreated/pCI-HA, #P<0.05 *versus* 100 μM 6-OHDA/pCI-HA.

Taken together, these results suggest that NEDD4 is protective against PD toxin 6-OHDA probably by mediating RTP801 ubiquitination and degradation.

6. RTP801 ELEVATION IS RESPONSIBLE FOR THE TOXICITY INDUCED BY NEDD4 KNOCKDOWN

Up to now, we showed that ectopic NEDD4 is protective in front of 6-OHDA toxin, probably by decreasing RTP801. On the contrary, NEDD4 knockdown induced cell death and elevated RTP801 protein levels. To determine whether NEDD4 loss of expression lethality is at least in part caused by RTP801 protein elevation, we next assessed toxicity in neurons where RTP801 and NEDD4 were knocked down.

Cortical neurons were infected with lentiviral particles containing a shRNA against RTP801 (ShRTP801) or a scrambled shRNA sequence as control (ShCt). Two days later, neurons were transduced with commercial lentiviral particles designed to knockdown NEDD4 (ShNEDD4) or the corresponding control shRNA (ShCt). All the combinations were studied; knockdown of both proteins (ShRTP801/ShNEDD4), knockdown of one protein or the other (ShCt/ShNEDD4 or ShRTP801/ShCt) and infection with both control shRNA (ShCt/ShCt). Four days later, neurons were harvested and subjected to WB. Membranes were probed for NEDD4 and RTP801 to validate efficient protein knockdown. Again, NEDD4 knockdown was very effective, while RTP801 knockdown (ShRTP801/ShCt) was more modest, but significantly reduced RTP801 protein levels respect to the control (ShCt/ShCt). As previously shown, NEDD4 knockdown (ShCt/ShNEDD4) increased RTP801 protein levels, while double knockdown (ShRTP801/ShNEDD4) prevented from this RTP801 elevation (Figure 42).

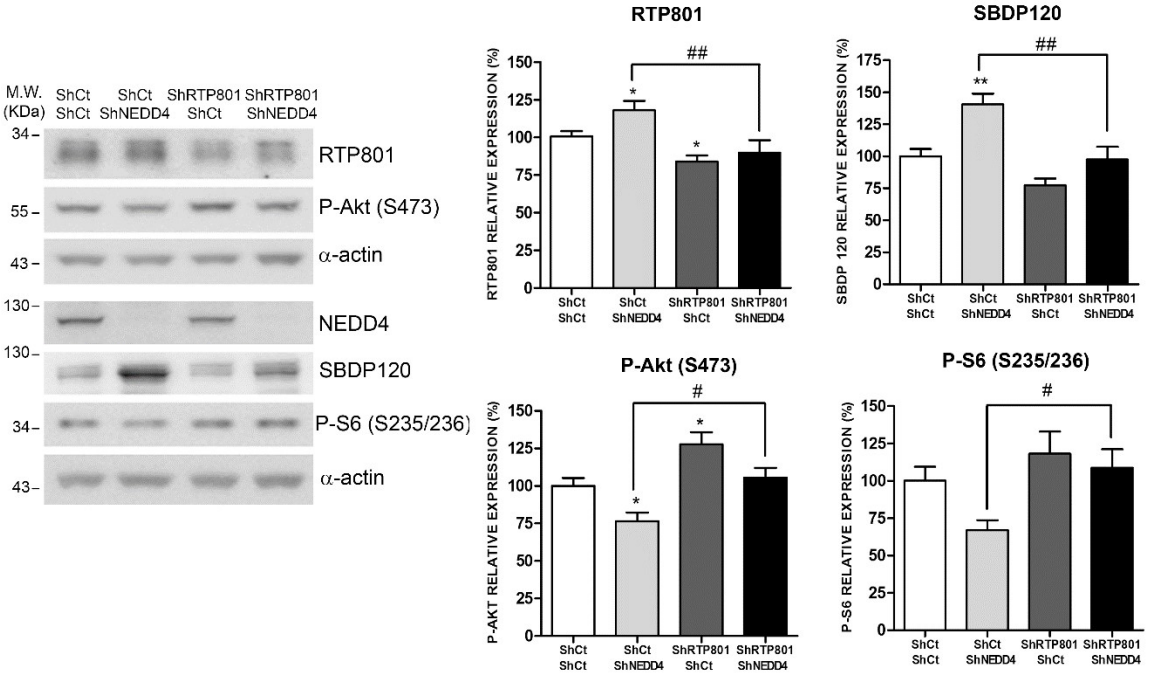

Figure 42. NEDD4 knockdown toxicity is dependent on RTP801 protein. DIV 5 primary rat cortical neurons were infected with lentiviruses containing a scrambled ShRNA (ShCt) or a shRNA against RTP801 (ShRTP801). Two days later, neurons were transduced with a mix of three shRNA sequences against NEDD4 (ShNEDD4) or the corresponding control shRNA (ShCt). Cell lysates were analysed 4 days later by WB. Membranes were incubated with antibodies against RTP801, NEDD4, P-Akt (S473), P-S6 (S235/236) and α-spectrin, and with antibody against α-actin as loading control. For α-spectrin, the caspase-cleaved fragment (spectrin breakdown product 120, SBDP120) is shown. Representative immunoblots are shown along with densitometries (mean ± SEM) of at least two independent experiments done in triplicate. One-way ANOVA with Newman-Keuls multiple comparison test, *P<0.05, **P<0.01 *versus* ShCt/ShCt and $^{\#}$P<0.05, $^{\#\#}$P<0.01 *versus* ShCt/ShNEDD4.

We also corroborated that NEDD4 knockdown is detrimental for neurons, as judged by the increase of α-spectrin caspase-cleaved fragment (SBDP120) and the decrease of Akt pro-survival kinase phosphorylation (P-Akt S473). The phosphorylation in this residue is a readout of mTORC2 complex activity[194]. Moreover, S6 protein phosphorylation levels (P-S6 S235/236), readout of mTORC1 complex activity[182], tended to decrease, although the difference was not significant. Interestingly, RTP801 knockdown reversed the toxic effects of abolishing NEDD4 expression, as SBDP120 protein levels and Akt and S6 phosphorylation levels were returned to control levels. In accordance with RTP801 as an mTOR pathway inhibitor, ShRTP801 promoted a significant increase of Akt phosphorylation and a tendency to increase of S6 phosphorylation levels (Figure 42).

These findings directly linked the toxic actions of knocking down NEDD4 to RTP801 protein levels. So, the repression of mTOR signaling pathway and the increase of caspase activity induced by NEDD4 knockdown are, at least in part, due to RTP801 protein elevation.

7. NEDD4 LEVELS ARE DIMINISHED IN NIGRAL NEURONS OF PD BRAINS

Evidence demonstrated that RTP801 is upregulated in nigral neurons in the SNpc of human PD patients[136,296]. Here, we next explored whether NEDD4 expression is also altered in neuromelanin-positive neurons of postmortem human sections from sporadic PD patients. SNpc sections from six cases of sporadic PD and six control non-PD cases (Table 10) were immunostained with a specific antibody for NEDD4.

PATIENT ID	DIAGNOSTICS	GENDER	AGE	TIME POSTMORTEM (hours)
CT1	Control	Male	64	10
CT2	Control	Male	83	13
CT3	Control	Female	56	14
CT4	Control	Female	86	4
CT5	Control	Male	78	6
CT6	Control	Male	76	11,5
SPD1	PD	Male	71	5
SPD2	PD	Male	77	12
SPD3	PD	Male	88	15
SPD4	PD	Female	83	4
SPD5	PD	Male	74	8
SPD6	PD	Male	81	5

Table 10. Human brain samples information. CT= control individuals, SPD= sporadic PD patients.

We scored the number of nigral neurons, visualized in brown, due to neuromelanin pigment (NM) that were positive for NEDD4 (in blue) versus total nigral neurons in each case. Indeed, we observed that the % of remaining nigral neurons positive for NEDD4 was lower in sporadic PD brains than in the control brains (Figure 43). As a negative control we incubated sections with the secondary antibody, omitting the primary antibody and no staining was appreciated.

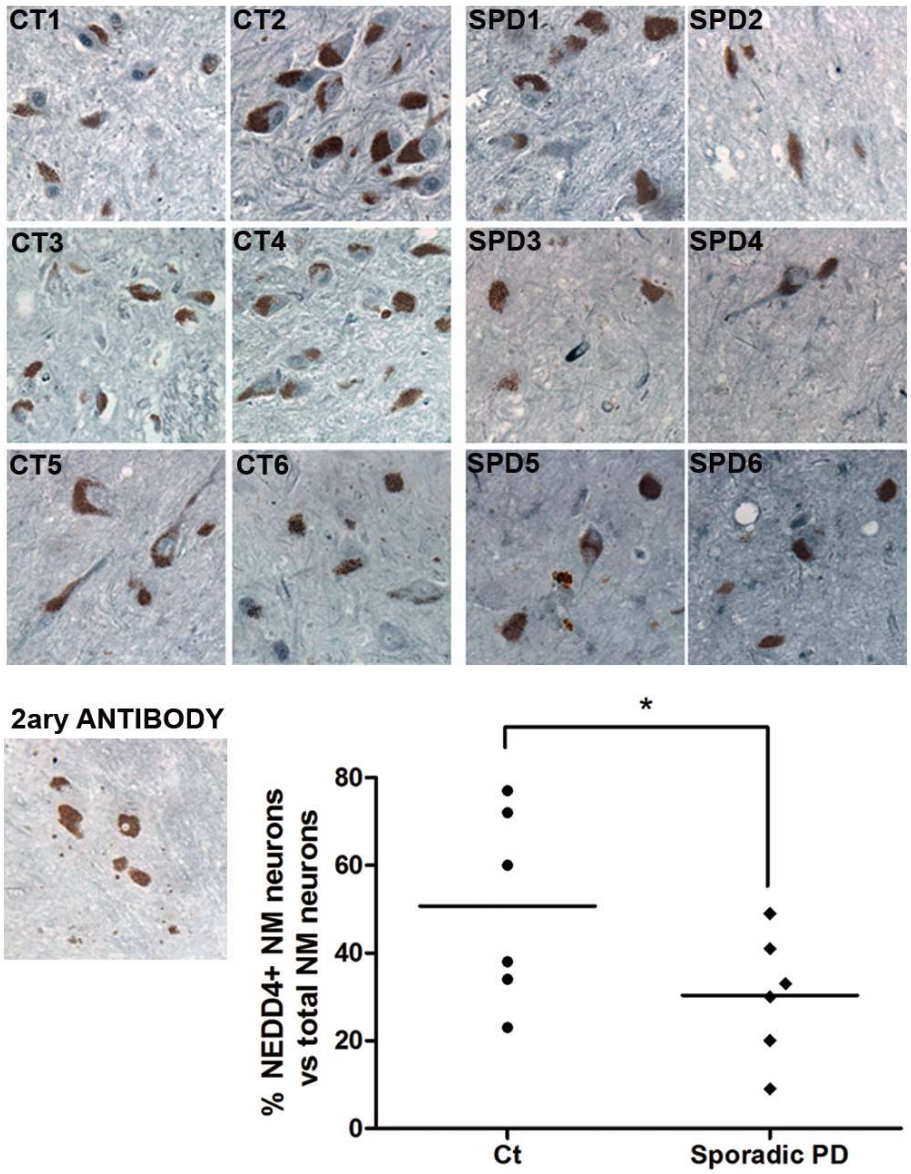

Figure 43. NEDD4 is decreased in pigmented nigral neurons from sporadic PD patients. SNpc human postmortem sections from control individuals (CT1-CT6) and sporadic PD patients (SPD1-SPD6) were immunostained for NEDD4 (grey-blue). Note the presence of neuromelanin (NM) granules (brown) within the somas of dopaminergic neurons. Neuromelanin-positive (NM+) neurons were scored positive for NEDD4 when detectable staining was observed. For each case, the percentage of NM+ and NEDD4+ neurons versus total NM+ neurons was represented in the graph. A control section was immunostained with no primary antibody as negative control. .Student's t-test, *P<0.05 *versus* Ct (Control).

These data point out that there is a NEDD4 deregulation in human PD nigral neurons. Therefore, the previous reported RTP801 elevation in PD brains could be related with this observed NEDD4 protein decrease.

8. NAB2, A NEDD4 ACTIVATOR, REGULATES RTP801 PROTEIN LEVELS

We next asked whether RTP801 protein levels could be sensitive to a situation where NEDD4 activity is enhanced chemically. We used a small molecule called NAB2 that is a NEDD4 signaling inducer. This compound is described to promote endocytosis and vesicular trafficking events dependent on NEDD4[273,274].

8.1 NAB2 decreases RTP801 protein levels without modifying NEDD4 levels

However, it is not well established how NAB2 activates NEDD4 pathway. It could be possible that NAB2 only enhances NEDD4 catalytic activity or that also increases its protein levels. So first, we assessed whether NAB2 exposure affected NEDD4 and RTP801 protein levels in cortical neurons.

Rat primary cortical neurons were exposed to 20 μM NAB2 or to DMSO as vehicle during forty-eight hours. WB analysis of cell lysates showed that NAB2 decreased to the half the levels of RTP801 protein (Figure 44). However, it did not affect NEDD4 protein levels, suggesting that this molecule is somehow enhancing its catalytic activity without modifying protein levels. Hence, NEDD4 activator NAB2 effectively reduces RTP801 protein levels without altering NEDD4 levels.

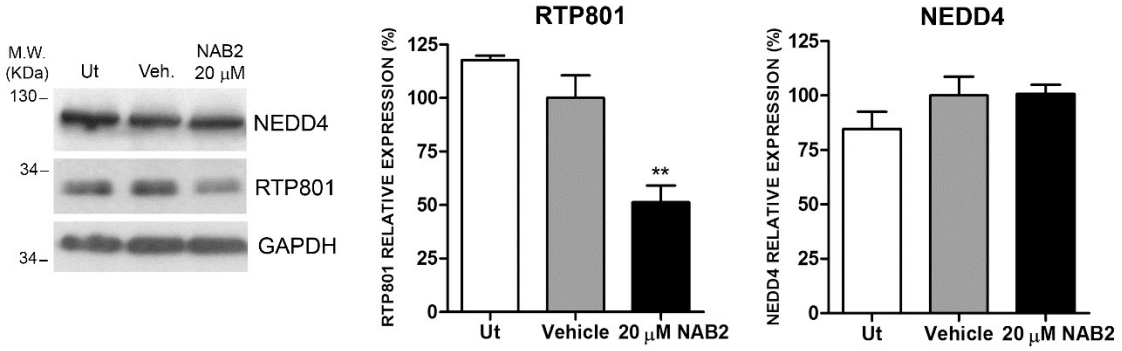

Figure 44. NAB2 exposure diminishes RTP801 protein levels without modifying NEDD4 protein levels. DIV12 rat primary cortical neurons were exposed to 20 μM NAB2 or DMSO as vehicle for 48 hours. Cell extracts were analysed by WB with anti-RTP801 and anti-NEDD4 antibodies and anti-GAPDH antibody as loading control. Representative immunoblots are shown along with graphs of RTP801 and NEDD4 densitometric quantification (mean ± SEM) of at least three independent experiments. One-way ANOVA with Bonferroni multiple comparison test, **P<0.01 *versus* Vehicle.

8.2 NAB2 enhances NEDD4 polyubiquitination

Most E3 ligases have the ability to catalyse their own ubiquitination, a feature that is widely used as a readout of its E3 ligase activity[332], including for NEDD4 family proteins[257,333,334]. So, in order to test whether NAB2 activates NEDD4 E3 ligase we evaluated its polyubiquitination levels.

As in the previous experiment, cortical neurons were exposed to 20 μM NAB2 or to DMSO as vehicle during forty-eight hours. Then, cells were harvested and NEDD4 was immunoprecipitated to evaluate its ubiquitination levels by WB. Results showed that NAB2 slightly increased NEDD4 polyubiquitinated smear (Figure 45), suggesting that it enhances its E3 ligase activity.

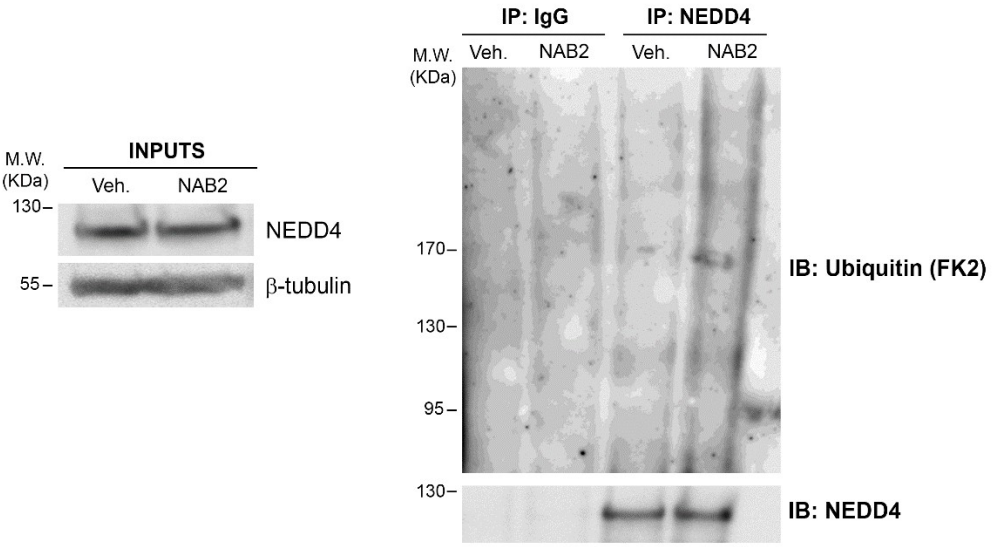

Figure 45. NAB2 treatment enhances NEDD4 polyubiquitination. DIV12 rat primary cortical neurons were exposed to 20 μM NAB2 or DMSO as vehicle for 48 hours. Then, cells were harvested and NEDD4 was immunoprecipitated to investigate its ubiquitination levels. Non-specific rabbit immunoglobulins (IgG) were used as a negative control. Whole cell lysates (inputs) and NEDD4 immunocomplexes were resolved in a WB. Membrane was probed for ubiquitin (FK2), NEDD4 and β-tubulin as loading control. A representative image of two independent experiments is shown. IP= immunoprecipitation; IB= immunoblot.

8.3 NAB2 prevents from 6-OHDA-induced RTP801 elevation

In our previous experiments we observed that ectopic NEDD4 reduced 6-OHDA-induced RTP801 elevation in neuronal PC12 cells (Figure 41). Given these findings, we next explored whether NAB2, by enhancing NEDD4 activity, is also able to mitigate RTP801 elevation promoted by PD toxin 6-OHDA in neurons.

Rat primary cortical neurons were pre-treated with 20 μM NAB2 or DMSO for thirty-two hours. Then, neurons were exposed or not to 50 μM 6-OHDA overnight prior harvesting. WB analysis of cell lysates showed that NAB2 significantly reduced RTP801 protein levels in 6-OHDA-treated neurons (Figure 46). Importantly, the decline of RTP801 induced by NAB2 was also confirmed in untreated control neurons. Again, NAB2 did not modify NEDD4 protein levels since neither blocked the loss of NEDD4 protein induced by 6-OHDA. Thus, NEDD4 signaling inducer NAB2 prevents from 6-OHDA-induced RTP801 protein elevation.

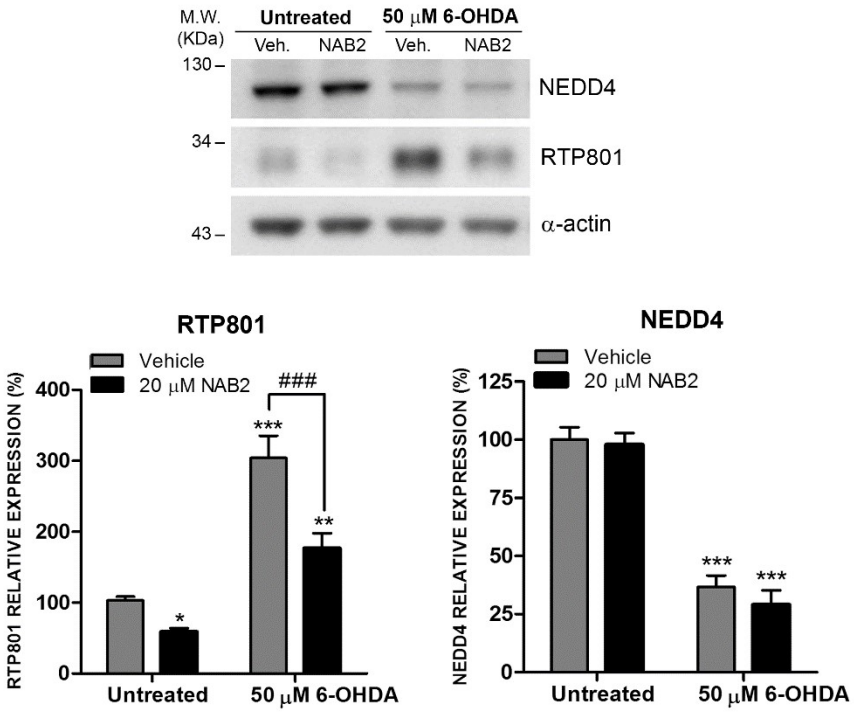

Figure 46. NAB2 exposure abrogates RTP801 elevation induced by 6-OHDA. DIV12 rat primary cortical neurons were treated with 20 μM NAB2. Thirty-two hours later, cultures were exposed to 50 μM 6-OHDA for 16 hours prior harvesting. Cell extracts were subjected to WB and membranes were probed for RTP801, NEDD4 and α-actin as loading control. RTP801 and NEDD4 densitometries are represented as mean ± SEM (graphs) of at least three independent experiments. One-way ANOVA with Bonferroni multiple comparison test,*P<0.05, **P<0.01 and ***P<0.001 *versus* Untreated/Vehicle and ###P<0.001 *versus* 50 μM 6-OHDA/Vehicle.

8.4 NAB2 does not regulate RTP801 transcriptionally

To obtain further evidence that NAB2 regulates RTP801 at post-translational level, probably by enhancing its NEDD4-mediated protein degradation, we next investigated RTP801 mRNA levels.

As in the previous experiment, cortical neurons were pre-treated with 20 μM NAB2 or DMSO (vehicle) before exposure to 6-OHDA. Then, RNA was extracted and RTP801 mRNA levels were quantified by RT-qPCR. No significant differences were observed between NAB2 and vehicle-treated neurons, neither in neurons exposed to 6-OHDA (Figure 47). Thus, NAB2 does not affect RTP801 gene transcription. Similarly to earlier experiment in neuronal PC12 cells (Figure 35a), PD toxin 6-OHDA significantly induced RTP801 gene transcription in cortical neurons (Figure 47).

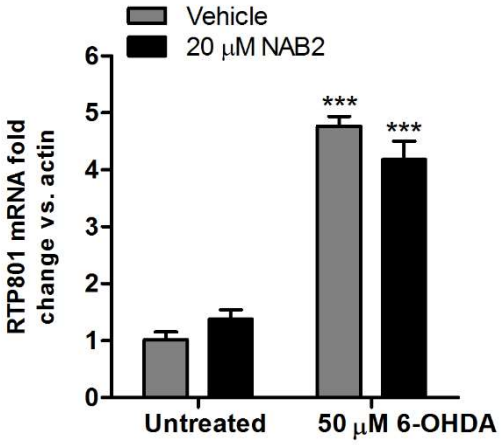

Figure 47. NAB2 exposure does not affect RTP801 mRNA levels. NGF-differentiated PC12 cells were treated with 20 μM NAB2 or DMSO as vehicle. Thirty-two hours later, cultures were exposed to 50 μM 6-OHDA for 8 hours. Then, RNA was extracted and reverse transcription-qPCR was performed to determine RTP801 mRNA levels and α-actin mRNA levels as control. The graph shows values (mean ± SEM) of at least three independent experiments. One-way ANOVA with Bonferroni multiple comparison test, ***P<0.001 *versus* Untreated/Vehicle.

In summary, NAB2 compound activates NEDD4 E3 ligase and promotes RTP801 protein degradation in control and 6-OHDA-treated neurons.

8.5 NAB2 is toxic for neurons and does not prevent from 6-OHDA-induced cell death

In previous experiments, we observed that ectopic NEDD4 was protective from 6-OHDA-induced cell death by decreasing RTP801 protein levels. Taking into account that NAB2 reduced RTP801 elevation after 6-OHDA exposure, we next explored whether NAB2 is also protective against this toxin.

For that purpose, cell viability was assessed in cortical neurons pretreated with NAB2 and then exposed to 6-OHDA toxin overnight. Neurons were fixed and stained with Hoechst to score the number of living nucleus. Results showed that NAB2 alone was toxic and that was not able to protect from 50 μM 6-OHDA exposure (Figure 48). We also tested milder 6-OHDA concentrations (25 μM) to avoid massive neuron death but again NAB2 did not protect from toxin-induced cell death (Figure 48).

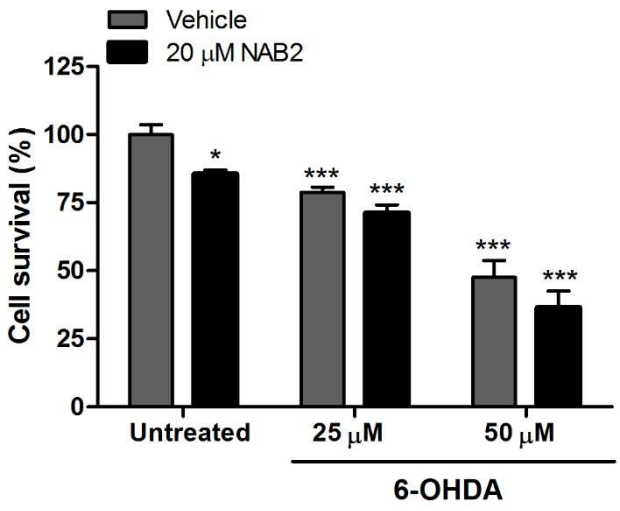

Figure 48. NAB2 does not protect from 6-OHDA-induced cell death. DIV12 rat primary cortical neurons were exposed to 20 μM NAB2. Thirty-two hours later, cultures were treated with 25 μM 6-OHDA or 50 μM 6-OHDA for 16 hours prior fixation and Hoechst nuclear staining. Cell survival was assessed by scoring the number of non-condensed nuclei. Values from at least three independent experiments in quadruplicate are represented in the graph as mean ± SEM. One-way ANOVA with Bonferroni multiple comparison test,*P<0.05, **P<0.01 and ***P<0.001 *versus* Untreated/Vehicle.

To further corroborate this NAB2 toxicity we evaluated cell lysates in the same conditions. Caspase-cleaved α-spectrin fragment (SBDP120) as readout of apoptotic death[319], and phosphorylation of mTOR signaling pathway proteins were analysed by WB. Specifically, we studied phosphorylation at Serine 473 residue of Akt (P-Akt S473) to evaluate mTORC2 activity[193,194], a complex implicated in cell survival, and phosphorylation at serines 235/236 of ribosomal protein S6 (P-S6 235/236) to evaluate mTORC1 activity[182,335]. Finally, phosphorylation at serine 2448 of mTOR (P-mTOR S2448) was also evaluated as a readout of kinase activity of both complexes[336–338].

Interestingly, NAB2 exposure promoted an increase of SBDP120 levels along with a decrease of Akt pro-survival kinase phosphorylation, confirming the toxicity of the compound. Moreover, phosphorylation of S6 and mTOR proteins also had a tendency to decrease, although the differences were not significant. As expected, exposure to 50 μM 6-OHDA induced SBDP120 and decreased phosphorylation of Akt, S6 and mTOR, but in any case there were significant differences between 6-OHDA exposed vehicle and NAB2 treated neurons (Figure 49). These findings go in line with the previous experiment, where no differences were observed in cell survival.

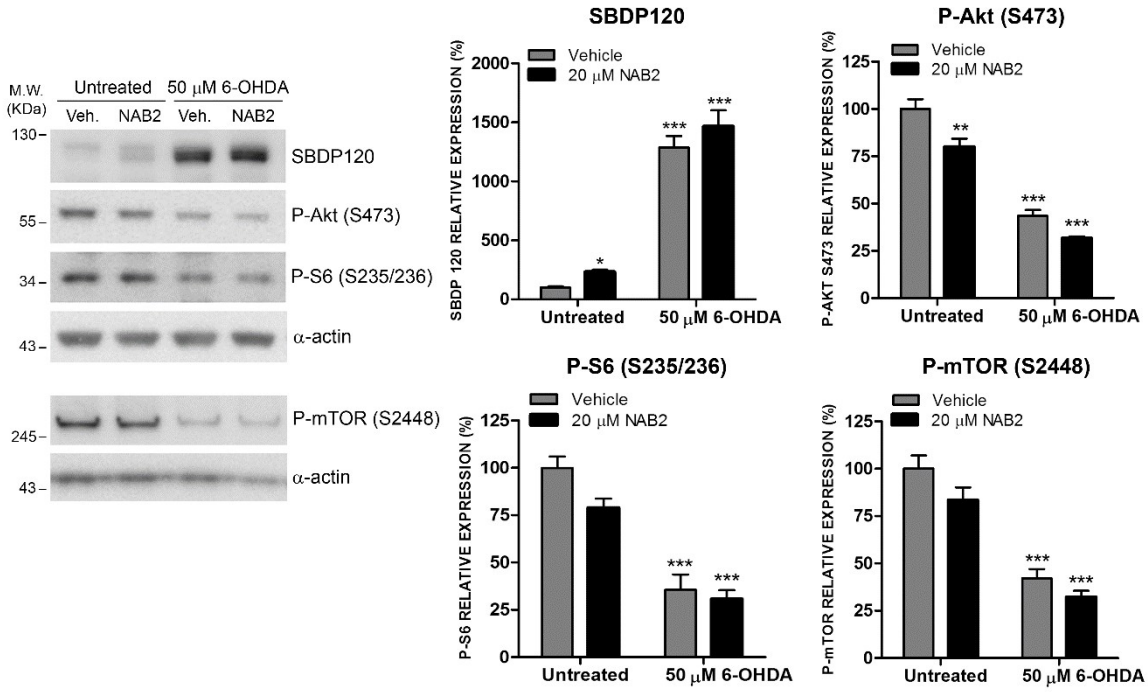

Figure 49. NAB2 is toxic for neurons. DIV12 rat primary cortical neurons were exposed to 20 μM NAB2. Thirty-two hours later, cultures were treated with 50 μM 6-OHDA for 16 hours prior harvesting. Cell extracts were resolved in a WB. Membranes were probed with antibodies against α-spectrin, P-Akt (S473), P-S6 (S235/236), p-mTOR (S2448) and α-actin as loading control. In the case of α-spectrin the caspase-cleaved fragment (spectrin breakdown product 120, SBDP120) is shown. Densitometries are represented as mean ± SEM (graphs) of at least three independent experiments in triplicate. One-way ANOVA with Bonferroni multiple comparison test,*P<0.05, **P<0.01 and ***P<0.001 *versus* Untreated/Vehicle.

To sum up, NAB2 decreases RTP801 protein levels, but this reduction is not accompanied with the expected increase in mTOR pathway activity, presumably because the compound

is otherwise repressing this signaling pathway. In 6-OHDA-treated neurons, NAB2 is not sufficient to confer protection, probably because the compound itself compromises cell survival.

9. PARKIN REGULATES NEDD4 PROTEIN LEVELS

In our group we have previously identified RTP801 as a substrate for parkin E3 ligase[296]. Interestingly, ectopic WT parkin is protective against RTP801 and 6-OHDA toxicity[296]. Here, we reported NEDD4 as another E3 ligase that regulates RTP801 protein levels. Moreover, ectopic WT NEDD4 has also been shown to partially prevent from RTP801 and 6-OHDA-induced cell death. So, we next considered the possibility that both E3 ligases together could have a larger protective effect against RTP801 toxicity.

9.1 Parkin overexpression decreases ectopic NEDD4 protein levels

To explore this hypothesis we co-transfected both E3 ligases in HEK293 cells. Concretely, cells were transfected with pCI-HA-NEDD4 construct or with pCI-HA-NEDD4 along with an increasing amount of pRK5-myc-Parkin (1 µg or 2 µg). Twenty-four hours later, cells were harvested and subjected to WB. Surprisingly, results showed that parkin overexpression decreased ectopic NEDD4 levels in a dose-dependent manner (Figure 50a), pointing out a putative crosstalk between both E3 ligases.

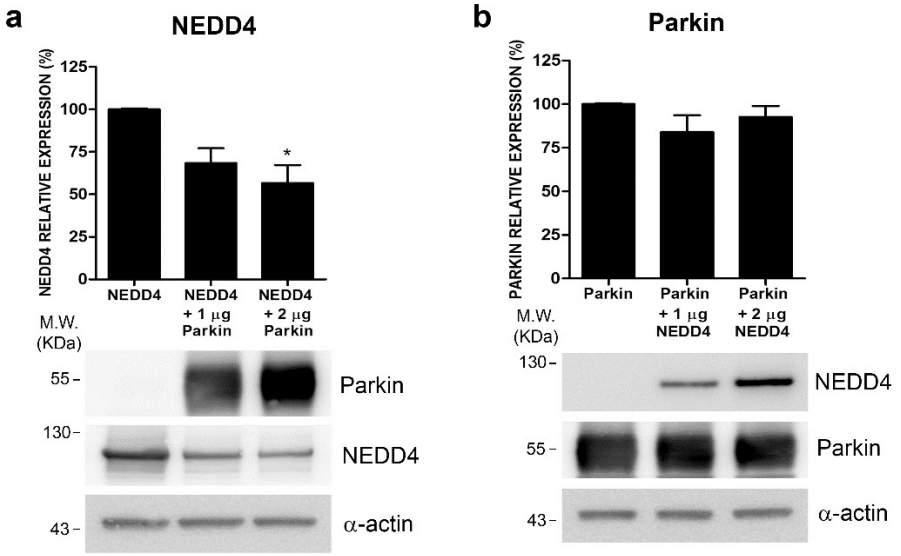

Figure 50. Parkin regulates overexpressed NEDD4 protein levels. a) Ectopic Parkin decreases overexpressed NEDD4 in HEK293 cells. HEK293 cells were co-transfected with pCI-HA-NEDD4 (NEDD4) and pRK5-myc-parkin (parkin) constructs as indicated. Twenty-four hours later, cells were harvested and the resulting lysates analysed by WB with antibodies against parkin, NEDD4 and α-actin as loading control. Representative immunoblots are shown along with densitometries (mean ± SEM) from at least three independent experiments. One-way ANOVA with Bonferroni multiple comparison test, *P<0.05, *versus* NEDD4. **b) Ectopic NEDD4 does not modify overexpressed parkin levels in HEK293 cells.** HEK293 cells were co-transfected with pRK5-myc-parkin (parkin) and pCI-HA-NEDD4 (NEDD4) as indicated. Twenty-four hours later, cultures were harvested and subjected to WB. Membranes were incubated with antibodies against NEDD4, parkin, and α-actin as loading control. Graph shows densitometric quantification (mean ± SEM) from at least three independent experiments.

Similarly, HEK293 cells were transfected only with pRK5-myc-Parkin construct or with pRK5-myc-Parkin along with 1 µg or 2 µg of pCI-HA-NEDD4. Twenty-four hours later, cell lysates were resolved in a WB. In this case, NEDD4 overexpression did not alter ectopic parkin levels (Figure 50b). These findings indicate that the regulation between the two proteins occur only in one direction, being NEDD4 downstream of parkin.

To further study whether this NEDD4 regulation by parkin is dependent on its E3 ligase activity we took advantage of two parkin mutant constructs: pRK5-myc-parkin-ΔUBL, a construct without the UBL domain that has been demonstrated to be active[339], and pRK5-myc-parkin-ΔR2, a construct that overexpress a truncated form of parkin that lacks the RING2 domain and therefore is inactive. HEK293 cells were co-transfected with pCI-HA-NEDD4 along with empty vector pRK5-myc, pRK5-myc-parkin, pRK5-myc-parkin-ΔUBL or pRK5-myc-parkin-ΔR2. Cell lysates were resolved in a WB to evaluate ectopic NEDD4 protein levels. Wild-type parkin and parkin-ΔUBL mutant reduced NEDD4 levels, although the differences were only significant for WT parkin. In contrast, the inactive parkin-ΔR2 mutant did not modify ectopic NEDD4 levels (Figure 51). Hence, ectopic NEDD4 reduction promoted by parkin overexpression requires its E3 ligase activity.

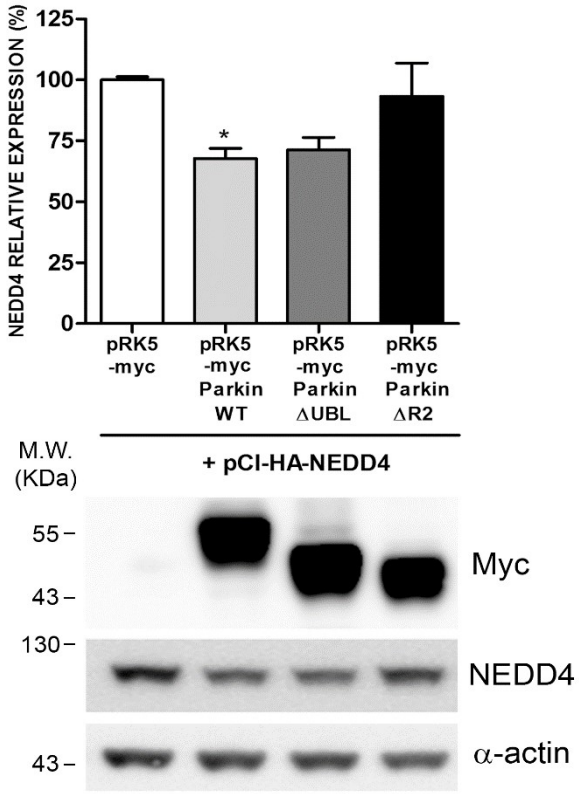

Figure 51. NEDD4 regulation by parkin requires its E3 ligase activity. HEK293 cells were co-transfected with pCI-HA-NEDD4 along with pRK5-myc, pRK5-myc-parkin, pRK5-myc-parkin-ΔUBL or pRK5-myc-parkin-ΔR2 as indicated. Thirty hours later, cells were harvested and analysed by WB with antibodies anti-myc, anti-NEDD4 and anti-α-actin as loading control. Representative immunoblots are shown along with densitometries (mean ± SEM) from at least three independent experiments. One-way ANOVA with Bonferroni multiple comparison test, *P<0.05, *versus* pCI-HA-NEDD4 + pRK5-myc.

9.2 Ectopic parkin does not modify endogenous NEDD4 protein levels

Such results raised the question of whether parkin also regulates endogenous NEDD4 protein levels. To test this possibility, HEK293 cells were transfected with pRK5-myc, pRK5-myc-parkin, pRK5-myc-parkin-ΔUBL or pRK5-myc-parkin-ΔR2. Thirty hours later, cells were harvested and analysed by WB. Neither WT parkin nor parkin mutants altered endogenous

NEDD4 protein levels (Figure 52). Consequently, endogenous NEDD4 is not regulated by parkin E3 ligase in HEK293 cells.

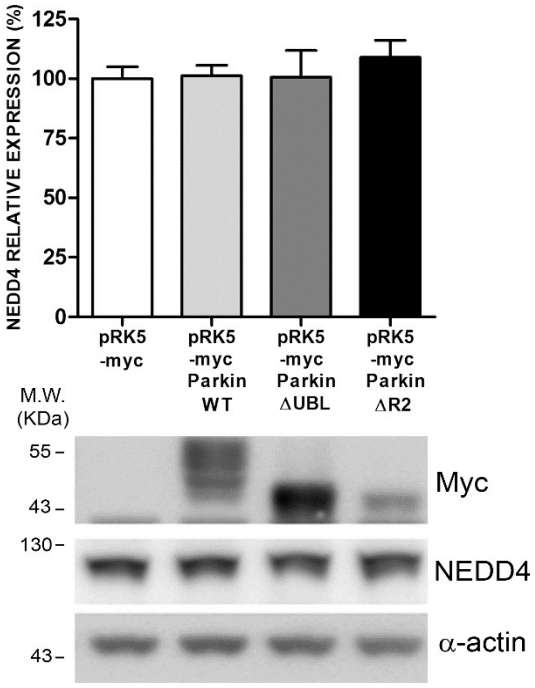

Figure 52. Parkin does not regulate endogenous NEDD4 protein levels. HEK293 cells were transfected with pRK5-myc, pRK5-myc-Parkin, pRK5-myc-Parkin-ΔUBL or pRK5-myc-Parkin-ΔR2 as indicated. Thirty hours later, cells were harvested and the resulting lysates resolved in a WB. Membranes were incubated with antibodies against myc, NEDD4 and α-actin as loading control. Representative immunoblots are shown along with densitometries (mean ± SEM) from at least three independent experiments.

9.3 NEDD4 is elevated in Parkin knockout mice and in AR-JP patients bearing parkin mutations

To further validate the regulatory function of parkin E3 ligase towards NEDD4, its protein levels were quantified in parkin knockout (PaKO) mice brain and in human fibroblasts derived from AR-JP (Autosomal Recessive Juvenile Parkinsonism) patients with parkin mutations.

Therefore, we tested whether loss of parkin affects NEDD4 protein levels in a mouse model that presents an exon 3 deletion in the parkin gene[340]. Whole-brain lysates of five PaKO and five wild-type littermates were resolved in a WB. Results showed that NEDD4 is significantly accumulated in PaKO mouse brains compared to control WT brains (Figure 53a), proving *in vivo* that the lack of parkin elevates NEDD4 protein levels.

We next tested NEDD4 levels in pure fibroblasts cultures established from skin punches collected from AR-JP patients bearing exon deletions in the parkin gene (*PARK2*) and from age-matched controls (Table 11). Fibroblasts were reseeded between five or six times before harvesting and WB analysis. We observed that NEDD4 levels were significantly higher in parkin mutant fibroblasts than in control fibroblasts (Figure 53b).

PATIENT ID	DIAGNOSTICS	PARK2 MUTATION	GENDER	AGE AT SKIN PUNCH BIOPSY	AGE OF ONSET
1	CONTROL	-	Male	66	-
2	CONTROL	-	Female	48	-
3	CONTROL	-	Female	47	-
4	CONTROL	-	Male	52	-
5	CONTROL	-	Female	63	-
6	CONTROL	-	Male	42	-
7	AR-JP	Homozygous *PARK2* ex3del*	Male	49	25
8	AR-JP	Homozygous *PARK2* ex2-4del*	Male	69	35
9	AR-JP	Compound homozygous *PARK2* 205-206 ex2del/ex6del*	Female	44	32
10	AR-JP	Homozygous*PARK2* ex5-6del*	Female	63	27
11	AR-JP	Compound homozygous *CRG* ex1del / *PARK2* ex6del*	Male	35	9
12	AR-JP	Compound homozygous *PARK2* ex2dup/ex6del*	Male	49	15

Table 11. Human fibroblasts donor information. AR-JP= Autosomal Recessive Juvenile Parkinsonism (* breakpoint not mapped).

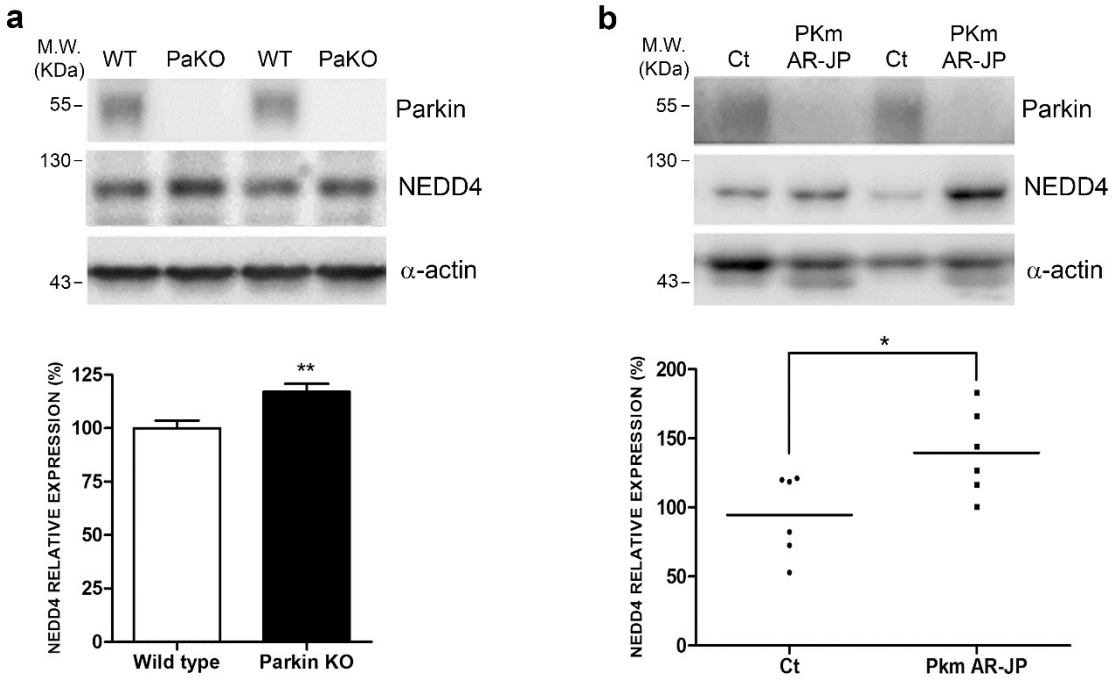

Figure 53. NEDD4 is increased in parkin knockout mouse brains (a) and in human fibroblasts from AR-JP patients with parkin mutations (b). a) Whole-brain lysates from five 8-month-old parkin KO mice and five WT littermates were resolved in a WB. Membranes were incubated with antibodies against NEDD4, parkin and α-actin as loading control. Representative immunoblots are shown along with densitometries (mean ± SEM) of at least three independent membranes. Student's t-test, **P<0.01 *versus* Wild type. **b)** Extracts from human primary fibroblasts obtained from six diagnosed AR-JP patients with parkin mutations (Pkm AR-JP) and six control individuals (Ct) were analysed by WB. Membranes were incubated with anti-NEDD4 and anti-parkin antibodies and reprobed with anti-α-actin antibody as loading control. The graph represents mean ± SEM of NEDD4 densitometries of at least three independent membranes. Student's t-test, *P<0.05 *versus* Ct.

Taken together, NEDD4 protein levels are elevated in animal and human samples lacking parkin.

10. RTP801 PROTEIN HOMEOSTASIS

RTP801 is a protein with a very short half-life[292,295] that has been reported to be ubiquitinated as a signal for protein degradation[296]. We next wanted to explore how ubiquitination affects to RTP801 protein homeostasis. Polyubiquitin chains are attached to lysine (K) residues in the amino acid sequence of the target protein. Since RTP801 has six lysines, these are the unique residues susceptible to ubiquitination.

10.1 RTP801 mutants generation

For that purpose, each lysine (K) of RTP801 was mutated to arginine (R), an amino acid that is structurally similar to lysine but cannot be ubiquitinated. The different RTP801 mutants were generated by site-directed mutagenesis of the pCMS-eGFP-RTP801 construct, a bicistronic vector that expresses eGFP and rat RTP801. A non-ubiquitinable mutant with all six lysines exchanged to arginines was also generated and it was named RTP801-KR. This vector was used in section 3.2 of this thesis and in the parkin study[296]. So, in total we generated seven RTP801 mutants: K126R, K152R, K185R, K215R, K216R, K217R and KR (Figure 54).

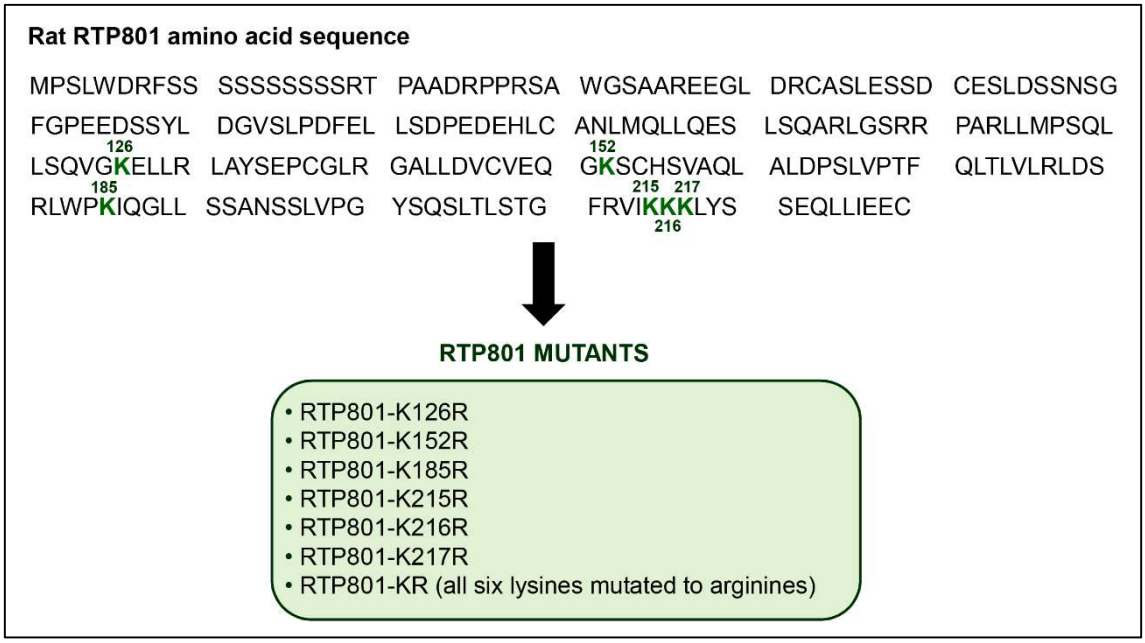

Figure 54. RTP801 amino acid sequence and nomenclature of RTP801 mutants. RTP801 protein sequence from Rattus Norvegicus (upper part) consists of 229 amino acids. Each of the lysines (K) (126, 152, 185, 215, 216 and 217) was mutated to arginine (R) to generate the different RTP801 mutants (lower part). A mutant with all the lysines mutated to arginine was also generated and it was named RTP801-KR.

The obtained RTP801 mutant constructs were first transfected in cells to check proper expression. HEK293 cells were transfected with the empty vector pMCS-eGFP, pCMS-eGFP-RTP801 and the different RTP801 mutant vectors. Twenty-four hours later, cultures were fixed and eGFP expression (visualized in green) was used as readout of RTP801 mutants expression and cell viability (Figure 55). Because HEK293 are proliferative cells, RTP801 overexpression did not promote cell death, as expected. None of the RTP801 mutants induced cell death (Figure 55), indicating that they are not toxic in proliferating cells.

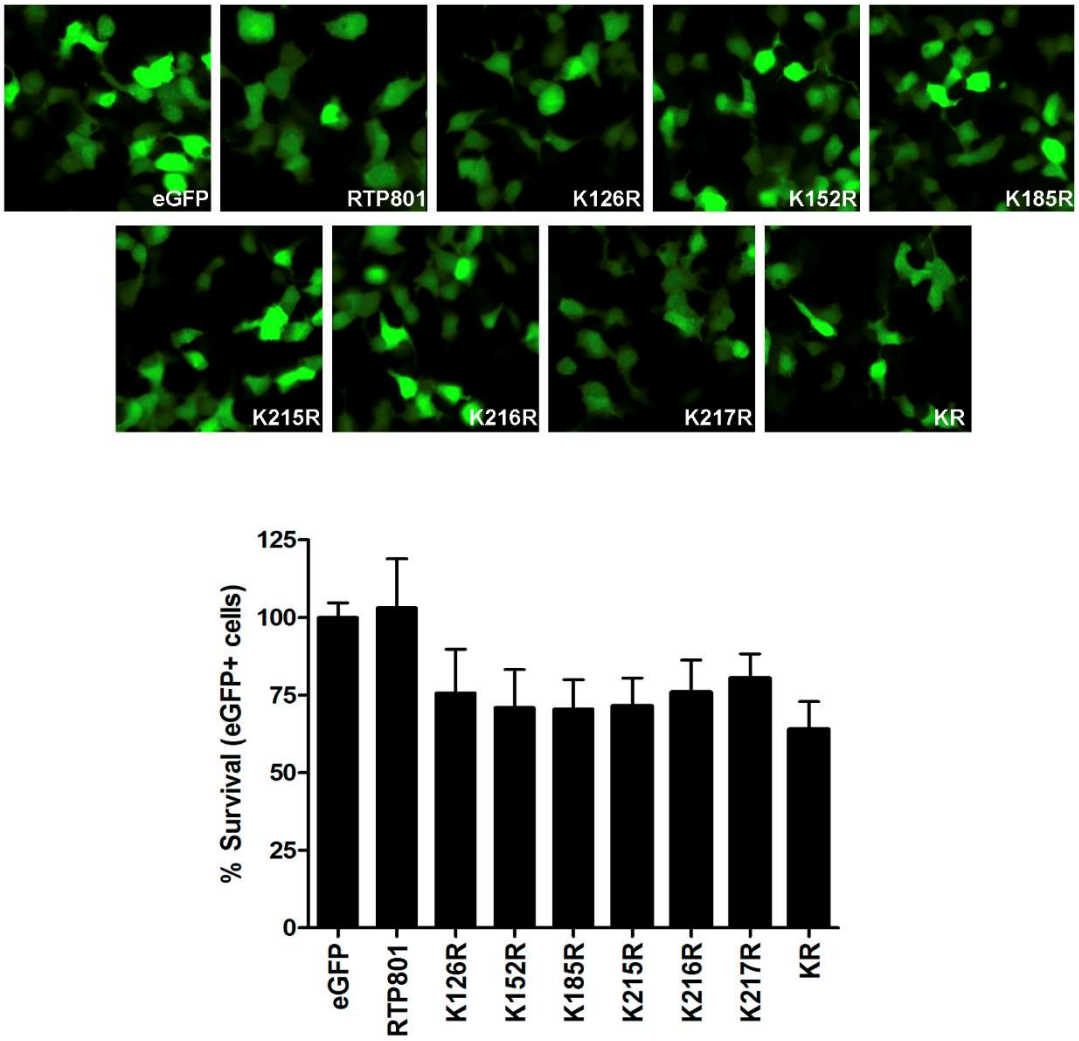

Figure 55. Either WT RTP801 or RTP801 mutants overexpression does not promote cell death in HEK293 cells. HEK293 cells were transfected with pCMS-eGFP empty vector, pCMS-eGFP-RTP801, pCMS-eGFP-RTP801-K126R, pCMS-eGFP-RTP801-K152R, pCMS-eGFP-RTP801-K185R, pCMS-eGFP-RTP801-K215R, pCMS-eGFP-RTP801-K216R, pCMS-eGFP-RTP801-K217R or pCMS-eGFP-RTP801-KR. Twenty-four hours later, cells were fixed and eGFP+ transfected cells were visualized under fluorescence microscopy. Representative images of the different RTP801 mutants transfection are shown (upper panel). eGFP+ surviving cells were scored to evaluate cell survival. Graph represents mean ± SEM of at least three independent experiments in triplicate (lower panel).

10.2 Ubiquitination is involved in RTP801 protein stability

Next, we assessed whether the different mutations affected RTP801 protein levels and therefore its stability. HEK293 cells were transfected with the empty vector pCMS-eGFP, with WT RTP801 and with all the other RTP801 mutants. Twenty-four hours later, cells were harvested and subjected to WB. Results indicate that RTP801 protein levels differ between some of the mutants. For instance, the KR mutant, the RTP801 form with no lysines, accumulated the most. This result was expected, since this mutant cannot be ubiquitinated and therefore, degraded. Otherwise, K185R and K215R mutants presented lower protein levels than WT RTP801 (Figure 56), suggesting that ubiquitination of these two residues affect protein stability.

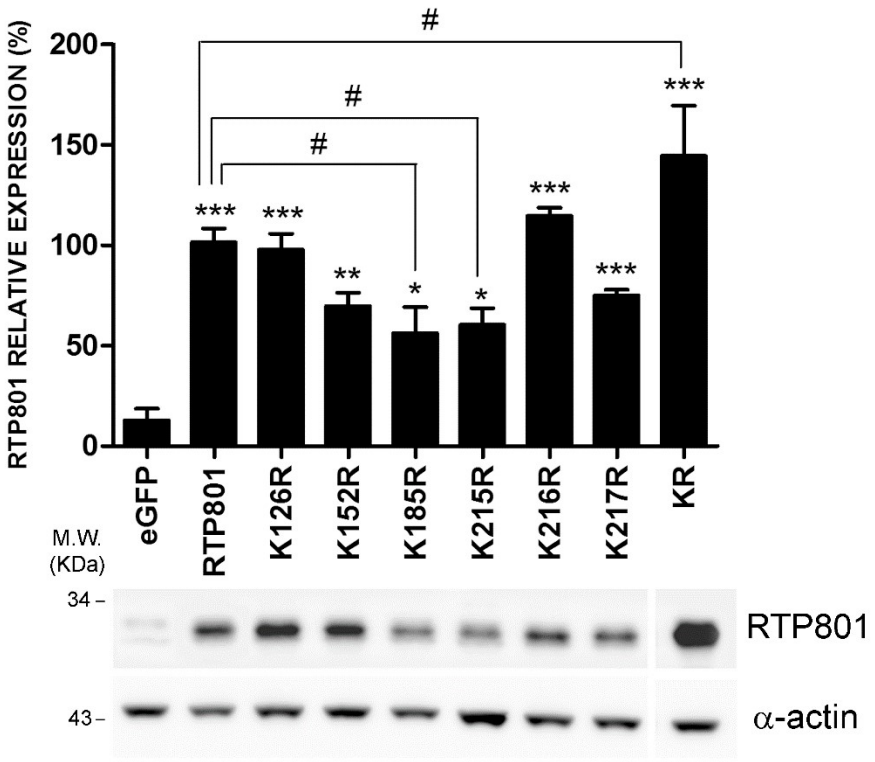

Figure 56. RTP801 mutants protein levels in HEK293 cells. HEK293 cells were transfected with pCMS-eGFP empty vector, pCMS-eGFP-RTP801, pCMS-eGFP-RTP801-K126R, pCMS-eGFP-RTP801-K152R, pCMS-eGFP-RTP801-K185R, pCMS-eGFP-RTP801-K215R, pCMS-eGFP-RTP801-K216R, pCMS-eGFP-RTP801-K217R or pCMS-eGFP-RTP801-KR. Twenty-four hours later, cells were harvested and RTP801 levels analysed by WB. Representative immunoblots are shown, along with densitometries (mean ± SEM) of at least three independent experiments. One-way ANOVA with Bonferroni multiple comparison test, *P<0.05, **P<0.01, ***P<0.001 *versus* eGFP and #P<0.05 *versus* RTP801.

10.3 Ubiquitination of RTP801 at lysine 185 is necessary for RTP801 function in NPC12 cells

Since the role of RTP801 depends on the cellular context, we next investigated the effects of RTP801 and its mutants in non-proliferative differentiated cells. NPC12 cells were transfected with empty vector, WT RTP801 or the different mutants. Twenty-four hours later, cultures were fixed and cell survival was evaluated by scoring the number of eGFP+ living cells under fluorescence microscopy. As previously reported, WT RTP801 induced around 50% of cell death[136]. The rest of the mutations also induced similar levels of cell death, including the mutant KR (Figure 57). This mutant accumulated more than WT RTP801 in HEK293 cells, but this protein elevation does not result in an increase of cell death. However, protein levels need to be confirmed in NPC12 cells since can vary between cell types. Interestingly, the mutant K185R abrogated almost completely the pro-apoptotic function of RTP801 (Figure 57), suggesting that ubiquitination at lysine 185 is critical for function. Indeed, this mutant presented lower protein levels than WT RTP801 in HEK293 cells (Figure 56).

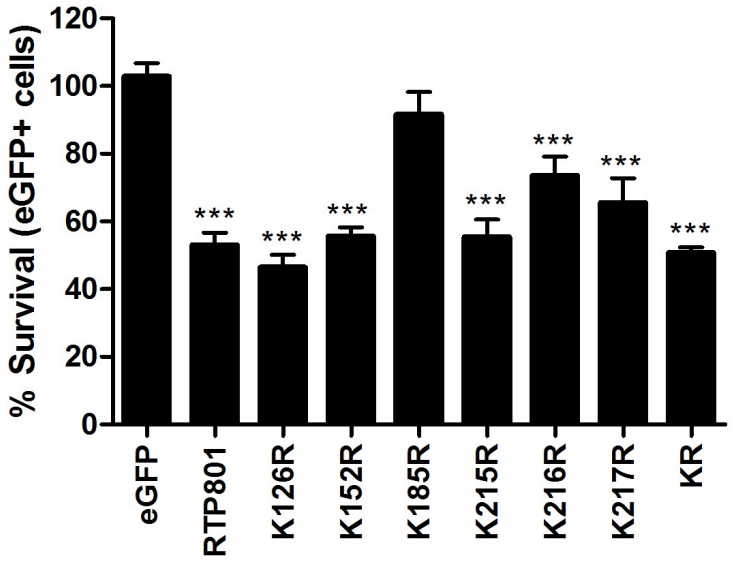

Figure 57. K185R mutation abrogates pro-apoptotic function of RTP801 in NPC12 cells. NGF-differentiated PC12 cells were transfected with pCMS-eGFP empty vector, pCMS-eGFP-RTP801, pCMS-eGFP-RTP801-K126R, pCMS-eGFP-RTP801-K152R, pCMS-eGFP-RTP801-K185R, pCMS-eGFP-RTP801-K215R, pCMS-eGFP-RTP801-K216R, pCMS-eGFP-RTP801-K217R or pCMS-eGFP-RTP801-KR. Twenty-four hours later, cells were fixed and eGFP+ surviving cells were scored under fluorescence microscopy. Graph represents mean ± SEM of at least three independent experiments in triplicate. One-way ANOVA with Bonferroni multiple comparison test, ***P<0.001 *versus* eGFP.

In order to investigate whether RTP801 mutants toxicity directly correlate with their protein levels, we studied protein accumulation in the same cell type, neuronal PC12 cells. For this experiment, we focused on K185R mutant, because is the only one that does not promote cell death, and on KR mutant, to corroborate its massive accumulation in NPC12 cells.

Neuronal PC12 cells were transfected with pMCS-eGFP empty vector, WT RTP801, K185R mutant or the non-ubiquitinable KR mutant during 20 hours. By WB, we observed that KR mutant protein levels were significantly higher than WT RTP801, while K185R protein levels were significantly lower (Figure 58). Therefore, protein levels correlated with cell death abrogation in the case of K185R mutant, but an increase of protein levels did not exacerbate cell death in the case of KR mutant.

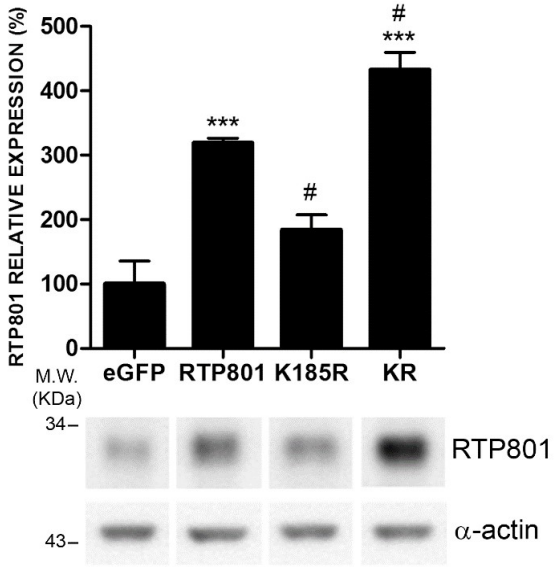

Figure 58. RTP801 mutants protein expression in NPC12 cells. NGF-differentiated PC12 cells were transfected with pCMS-eGFP empty vector, pCMS-eGFP-RTP801, pCMS-eGFP-RTP801-K185R or pCMS-eGFP-RTP801-KR. Twenty hours later, cells were harvested and subjected to WB. Membranes were incubated with antibodies against RTP801 and α-actin as loading control. All samples were immunoblotted in the same membrane, but some irrelevant bands were deleted. Graph represents mean ± SEM of at least three independent experiments. One-way ANOVA with Bonferroni multiple comparison test, ***P<0.001 *versus* eGFP and #P<0.05 *versus* RTP801.

Since RTP801 mediates cell death by inactivating sequentially mTOR and Akt kinases, we next explored the mTOR pathway status in NPC12 cells transfected with the RTP801 mutant K185R. Neuronal PC12 cells were transfected with pCMS-eGFP empty vector, WT RTP801, K185R mutant or KR mutant. Twenty hours post-transfection, cell cultures were harvested and subjected to WB. We tested Akt phosphorylation at Ser473 as readout of mTORC2 complex activity[193], and S6 ribosomal protein phosphorylation as readout of mTORC1 complex activity[335]. We also measured Akt phosphorylation at Thr308 to monitor the whole Akt activity, and mTOR phosphorylation at Ser2448 as readout of mTOR kinase activity[336–338].

We confirmed that WT RTP801 significantly decreased phosphorylation of mTOR, S6 and Akt at both residues, in comparison to control (eGFP transfected) cells (Figure 59). Similar results were obtained in cells transfected with the KR mutant. Interestingly, mutant K185R prevented from mTOR pathway repression, since it did not alter mTOR, S6 and pro-survival kinase Akt phosphorylation (Figure 59). These results go in line with the previous survival experiment where the K185R mutant did not induce cell death, while WT RTP801 and KR mutant were similarly toxic.

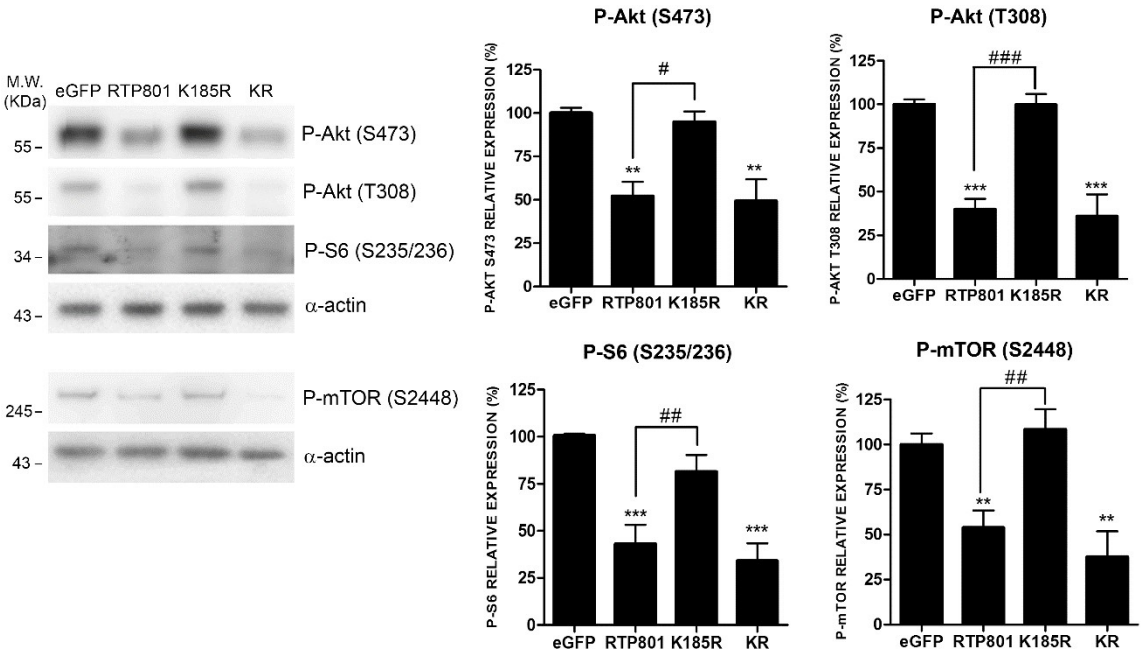

Figure 59. RTP801 mutant K185R does not inactivate mTOR signaling in NPC12 cells. NGF-differentiated PC12 cells were transfected with pCMS-eGFP empty vector, pCMS-eGFP-RTP801, pCMS-eGFP-RTP801-K185R or pCMS-eGFP-RTP801-KR. Twenty hours later, cells were harvested and resolved in a WB. Membranes were incubated with antibodies against P-Akt (S473), P-Akt (T308), P-S6 (S235/236), P-mTOR (S2448) and α-actin as loading control. Representative immunoblots are shown along with densitometries (mean ± SEM) of at least three independent experiments in duplicate. One-way ANOVA with Bonferroni multiple comparison test, **P<0.01, ***P<0.001 *versus* eGFP and $^{\#}$P<0.05, $^{\#\#}$P<0.01, $^{\#\#\#}$P<0.001 *versus* RTP801.

11. RTP801 PROTEOMIC ANALYSIS

RTP801 is a protein with no functional motifs or structural domains identified from its amino acid sequence analysis. Recently, one group was able to crystallize a segment and they found that RTP801 presents a unique topology[282]. Intriguingly, the only known function of RTP801 is its ability to repress mTOR[179,281], although the mechanism is not completely understood[180,282].

In this thesis, we have carried out proteomic analysis to identify new putative RTP801 interactors and proteins modulated by its overexpression. These studies were done in collaboration with Dr. Enrique Santamaría and the Navarrabiomed proteomics unit (Pamplona, Spain).

11.1 Putative RTP801 protein interactors

First, we performed a proteomic analysis to identify potential new RTP801 protein interactors and to better comprehend its regulatory mechanisms over mTOR. For that purpose, endogenous RTP801 was immunoprecipitated from untreated and 6-OHDA-treated cortical neurons. The resulting immunocomplexes were resolved in a polyacrylamide gel that was stained with SYPRO® Ruby to visualize protein bands (Figure 60). As negative controls, non-

specific rabbit immunoglobulins (IgG) were added to cell extracts or RTP801 antibody was added to lysis buffer alone (bands not shown in Figure 60). The numbered bands were cut for further analysis (Figure 60).

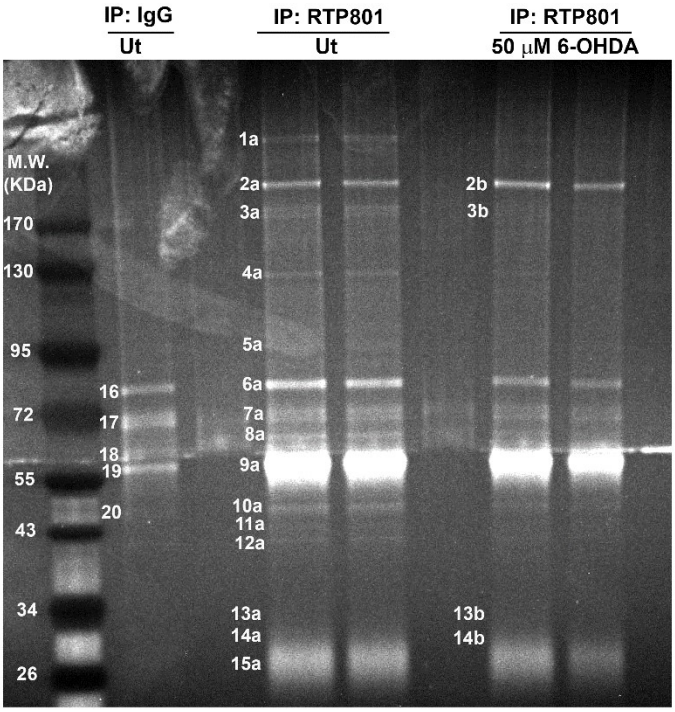

Figure 60. Polyacrylamide gel of RTP801 immunocomplexes. DIV 12 rat cortical neurons were exposed or not to 50 μM 6-OHDA. Sixteen hours later, cells were harvested, RTP801 was immunoprecipitated and the resulting immunocomplexes were resolved in a SDS-PAGE gel. As negative controls, non-specific rabbit immunoglobulins (IgG) were added to lysates or RTP801 antibody was added to lysis buffer. Gels were stained with SYPRO Ruby® and some bands were numbered and cut for further tryptic digestion and mass spectrometry analysis. A representative gel is shown of two independent experiments. Ut=untreated.

Excised bands were digested with trypsin and analysed by mass spectrometry to detect the peptides. Identified putative RTP801 partners are summarized in Table 12, containing protein name, accession number, molecular weight (M.W.), the obtained score and the number of identified peptides. It is also specified whether potential RTP801 partners were detected in one or two experiments (column n). Proteins detected both in negative controls and in RTP801 immunocomplexes were excluded as nonspecific. In the case of band number 13, apart from some potential interactors we also detected our bait protein, RTP801, confirming proper immunoprecipitation.

	Band	Accession Number	M.W. (KDa)	Protein Name	n	Score	Peptides (95%)
UNTREATED	1a	E9PSZ3	284,7	Spectrin alpha chain, non-erythrocytic 1	1	28	14
		G3V6S0	273,5	Protein Sptbn1, spectrin beta chain	1	16	8
		D3ZN76	253,3	Protein Sec16a	1	6	3
	2a	F1M779	191,6	**Clathrin heavy chain**	2	93	51
						78	41
		Q9JLA3	176,4	UDP-glucose:glycoprotein glucosyltransferase 1	1	4	2
		A0A0G2JYQ3	239,1	YLP motif-containing protein 1	1	26	13
	3a	F1LSE6	133,4	**Liprin-alpha-3**	2	41	22
						110	62
		D4A9D6	131,7	DEAH (Asp-Glu-Ala-His) box polypeptide 9	1	18	9
		Q3ZB99	131,3	Protein Tjp2	1	35	17
	4a	D4A962	96,0	Heterogeneous nuclear ribonucleoprotein U-like 1	1	6,2	3
		D3ZUY8	107,7	Adaptor protein complex AP-2, alpha 1 subunit	1	6,0	3
		P43244	94,4	Matrin-3	1	5,9	3
	5a	Q641Y8	82,5	ATP-dependent RNA helicase DDX1	1	23	11
		Q498R3	90,7	DnaJ homolog subfamily C member 10	1	8	3
		B5DFC3	86,2	Protein Sec23a	1	5	3
		F1M8L1	79,7	Kinesin-like protein	1	35	16
		A0A0G2JSM7	80,3	Adducin 1 (Alpha), isoform CRA_b	1	19	10
		D3ZKQ4	82,2	Protein Rabl6	1	14	7
	6a	D3ZN21	72,3	Protein RGD1309586	1	12	6
	7a	Q4AE70	70,3	Histone-arginine methyltransferase CARM1	1	12	6
	8a	Q5FVJ0	52,9	Protein RUFY3	1	20	11
		F1LM18	59,2	Polypyrimidine tract-binding protein 1	1	5	3
		Q6AYT3	55,2	tRNA-splicing ligase RtcB homolog	1	4	2
	10a	F1LPS8	33,7	Transcriptional activator protein Pur-alpha	1	9	5
	11a	F1LSL1	33,5	Transcription factor Pur-beta	2	7	3
						7	3
		Q1PBJ1	53,1	Lactadherin	1	12	6
		D4ABC7	34,2	Protein Uprt	1	10	5
		Q5PPL3	40,4	Sterol-4-alpha-carboxylate 3-dehydrogenase, decarboxylating	1	7	3
		P59215	40,1	Guanine nucleotide-binding protein G(o) subunit α	1	5	2
		M0R590	35,8	Glyceraldehyde-3-phosphate dehydrogenase	1	4	2
		D4AC85	41,1	Protein Qpct	1	4	1
	12a	P19945	34,2	60S acidic ribosomal protein P0	1	8	4
		P62138	37,5	Serine/threonine-protein phosphatase PP1-alpha catalytic subunit	1	6	3
	13a	Q6P9Y4	32,9	ADP/ATP translocase 1	1	13	9
		P62909	26,7	40S ribosomal protein S3	1	8	7
		B5DF24	31,7	Uridine-cytidine kinase	1	5	3
	14a	A0A0G2JV65	29	14-3-3 protein zeta/delta	1	19	10
		P68255	29	14-3-3 protein theta	1	12	9
		P61983	29	14-3-3 protein gamma	1	8	7
		P00762	29	Anionic trypsin-1	1	4	5
		P68511	29	14-3-3 protein eta	1	4	5

		P35213	29	14-3-3 protein beta/alpha	1	4	6
		D3ZTK0	25,8	Protein Ttc9b	1	4	2
	Band	**Accession Number**	**M.W. (KDa)**	**Protein Name**	**n**	**Score**	**Peptides (95%)**
6-OHDA	**2b**	F1M779	192	Clathrin heavy chain	1	101	52
	3b	F1LSE6	134	Liprin-alpha-3	1	45	22
	13b	Q6P9Y4	32,9	ADP/ATP translocase 1	1	7	4
		P62909	26,7	40S ribosomal protein S3	1	5	2
	14b	A0A0G2JV65	26	14-3-3 protein zeta/delta	1	12	6

Table 12. RTP801 putative protein interactors in cortical neurons. Identified putative RTP801 partners with their accession numbers (Uniprot database), molecular weight (M.W), number of times identified (n), score and the number of peptides detected. Proteins displayed in orange need to be further confirmed as specific, since from the corresponding band in controls any reliable identification could be determined. Proteins displayed in yellow has been identified in two independent experiments.

To obtain a general overview of the results we grouped RTP801 partners with similar functions. Some structural proteins were identified, such as α and β subunits of spectrin, that is a cytoskeletal protein that plays a role in the maintenance of the cell membrane structure[341]. Also, matrin-3, that is a nuclear matrix protein[342]. These findings can be indicative of RTP801 localization at the membrane and nucleus, two subcellular localizations that have been previously reported for RTP801[284].

The vast majority of the identified putative RTP801 partners were proteins related to RNA processing. There are some RNA helicases, enzymes that catalyze the unwinding of RNA, such as DEAH box polypeptide 9, ATP-dependent RNA helicase DDX1 and RGD1309586 protein. Also single-stranded DNA-binding proteins such as transcriptional activator protein Pur-alpha and the transcription factor Pur-beta, and some proteins related to splicing, such as tRNA-splicing ligase RtcB homolog and polypyrimidine tract-binding protein 1.

Moreover, proteins related to endoplasmic reticulum (ER) were also detected. For instance, UDP-glucose:glycoprotein glucosyltransferase 1 and DnaJ homolog subfamily C member 10 are involved in the correct folding of proteins[343,344], and Sec16a and Sec23a proteins play a role in the ER-Golgi trafficking[345,346]. This fact suggests the possibility that RTP801 could also localize in the ER. Nevertheless, further investigations are in process to confirm these binding partners.

Besides, we identified guanine nucleotide-binding protein G(o), a type of G protein, which are activated by G protein-coupled receptors (GPCRs). Interestingly, RTP801 translocates to the plasma membrane in response to GPCRs activation[284]. Hence, this interaction could be involved in the observed RTP801 localization change.

Remarkably, several isoforms of 14-3-3 proteins have been detected in RTP801 immunocomplexes, but need to be further confirmed as specific. These regulatory proteins can bind a broad range of partners to modulate several biological processes[347]. Importantly,

RTP801-14-3-3 interaction has been previously proposed to be involved in mTOR inhibition[180]. However, this hypothesis remains controversial[282]. Hence, it would be relevant to determine whether 14-3-3 proteins are specific RTP801 partners in neurons to clarify RT801 inhibition mechanism towards mTOR.

More interestingly, we identified several putative RTP801 interactors that play a relevant role in neuronal processes. These proteins are RUFY3, which is exclusively expressed in the brain and controls axon growth[348], protein phosphatase 1 (PP1), which regulates transcriptional events involved in long-term synaptic plasticity[349], glyceraldehyde-3-phosphate dehydrogenase (GAPDH), a protein that has been encountered in α-synuclein aggregates in PD[350] and Qpct, which has been identified as a potential druggable target for Huntington's disease[351]. These putative partners need to be further validated as RTP801 interactors, and also further studies are required to elucidate the physiological consequences of their interaction.

The most relevant proteins with the highest score and number of peptides in the analysis were liprin-α-3 and clathrin (heavy chain). Liprin-α-3 is expressed in the brain and is involved in synapse formation and maturation[352]. Clathrin is a protein that plays a major role in coated vesicles formation for intracellular trafficking and endocytosis[353]. Interestingly, AP-2 adaptor complex, a membrane protein involved in cargo internalization through clathrin-mediated endocytosis was also encountered in the proteomic analysis as a RTP801 interactor.

This putative RTP801-clathrin or RTP801-AP-2 interaction suggests that RTP801 could be internalized from the cell surface to endosomes through clathrin-coated vesicles. Moreover, clathrin-mediated endocytosis regulates synaptic vesicle recycling[354], a crucial process for neurons. Hence, RTP801 could also have an active role in synaptic dynamics.

In cortical neurons exposed to 6-OHDA, all the identified RTP801 interactors were also detected in untreated neurons. However, the intensity of bands 2b and 3b were markedly different from their equivalent bands in untreated neurons, suggesting variations in the abundance of detected proteins (Figure 60). In line with this, the intensity of the bands correlate well with the number of peptides identified. For instance, band number 2 showed higher intensity after 6-OHDA exposure and more clathrin peptides were identified in this condition. On the other hand, the intensity of band number 3 decreased after 6-OHDA treatment, while less liprin-α-3 peptides were detected (Table 13).

	Untreated	**6-OHDA**
Clathrin (band 2)	41	52
Liprin-α-3 (band 3)	62	22

Table 13. Number of peptides identified for clathrin and liprin-α-3 in untreated and 6-OHDA-treated neurons.

These differences in clathrin and liprin-α-3 abundance need to be further confirmed, but would represent valuable information to investigate RTP801-related changes induced by 6-OHDA exposure.

11.2 RTP801 and AP-2 co-immunoprecipitate in neurons

To further validate clathrin and AP-2 as RTP801 partners we performed co-immunoprecipitation assays. Endogenous RTP801 protein was immunoprecipitated from cortical neurons and the obtained immunocomplexes were subjected to WB. Intriguingly, we detected the presence of β-adaptin, a subunit of the AP-2 complex, but not the presence of clathrin (Figure 61, left panel). We also immunoprecipitated endogenous clathrin from cortical neurons. By WB, we detected β-adaptin (AP-2), that is a well-established clathrin partner[355], but we did not encounter RTP801 (Figure 61, right panel).

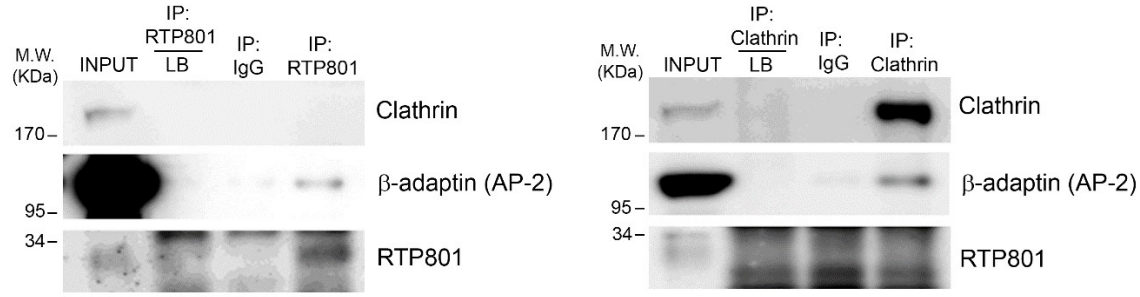

Figure 61. RTP801 and β-adaptin (AP-2) interact in neurons. RTP801 (left panel) and clathrin (right panel) were immunoprecipitated from DIV 13 rat primary cortical neurons. Non-specific rabbit immunoglobulins (IgG) and lysis buffer (LB) were used as negative controls. The resulting immunocomplexes were analysed by WB with antibodies against clathrin, β-adaptin (a subunit of the AP-2 complex) and RTP801. Representative immunoblots are shown of at least two independent experiments. IP=immunoprecipitation, LB= lysis buffer

So, we confirmed the RTP801-AP-2 interaction, but not the RTP801-clathrin interaction. However, RTP801 and clathrin are connected through AP-2, since both proteins are AP-2 partners. After validating this protein interaction, further studies will be required to explore the physiological consequences.

11.3 Proteome modulation by RTP801

To further explore RTP801 actions, we studied which proteins are upregulated or downregulated by RTP801 overexpression. Neuronal PC12 cells were transfected with RTP801 or pMCS-eGFP empty vector during 20 hours prior harvesting. The obtained proteins were precipitated from cell extracts and digested for further identification and quantification. A total of 1593 proteins were identified, of which 21 were differentially expressed between the two conditions. Proteins downregulated by RTP801 are displayed in green, while proteins upregulated by RTP801 are displayed in red (Table 14).

Unfortunately, any of the proteins modulated by RTP801 overexpression was identified previously as an RTP801 interactor. However, AP-3 complex and amphiphysin were upregulated by RTP801. These proteins, like RTP801 interactor AP-2, are related with clathrin-mediated endocytosis. Interestingly, AP-3, that is a clathrin adaptor protein like AP-2, has been implicated in biogenesis of synaptic vesicles and in the sorting of proteins from the Golgi to late endosomes or lysosomes[356,357]. Amphiphysin has been described to play a role in clathrin-mediated endocytosis of synaptic vesicles and to directly interact with AP-2 and clathrin[358–360]. So, the modulation of these clathrin-related proteins suggests a role for RTP801 in processes dependent on clathrin-coated vesicles dynamics. These events are particularly important at synaptic level.

Protein names	Accession number	Confidence score	Fold Change	P val
RNA polymerase II-associated protein 3	Q68FQ7	37	0,754	0,013
Transcription initiation factor IIA subunit 1	O08949	30	0,730	0,049
Glutaredoxin-1	Q9ESH6	23	0,720	0,013
Protein Gse1	F1M4A7	19	0,716	0,036
Uncharacterized protein	A0A0G2KB77	70	0,716	0,041
STE20-like serine/threonine-protein kinase	O08815	66	0,693	0,024
Protein Ranbp1	D4A2G9	117	0,690	0,032
Uncharacterized protein	M0R3V4	20	0,678	0,040
Histone H1.0	P43278	27	0,678	0,047
Protein Ppp1r13l	F1LW07	12	0,663	0,008
Protein Smarca2	A0A0G2JUS4	19	0,595	0,043
Histone H2A	D4AEC0	59	0,575	0,019
Protein LOC100362142	D3ZFY8	36	0,570	0,008
Protein Sdf2	D4A4H5	9	0,558	0,022
Importin subunit alpha	Q6P6T9	51	1,305	0,043
Inositol monophosphatase 1	F1M978	13	1,324	0,013
Amphiphysin	F1LPP0	34	1,326	0,029
Eukaryotic peptide chain release factor subunit 1	Q5U2Q7	10	1,450	0,014
AP-3 complex subunit beta	D4AE00	32	1,575	0,023
7-methylguanosine phosphate-specific 5'-nucleotidase	Q6AYP7	29	1,602	0,013
Coronin	G3V624	49	2,143	0,013

Table 14. Proteins modulated by RTP801 in NPC12 cells. NGF-differentiated PC12 cells were transfected with pCMS-eGFP empty vector or pMCS-eGFP-RTP801 for 20 hours. Then, cells were lysed and proteins were precipitated from cell extracts. The purified proteins were further digested with trypsin and the resulting peptides concentrated and analysed by nano-HPLC coupled to mass spectrometry using a label-free approach. A total of 1593 proteins were identified and quantified with the Progenesis QI software. The table shows the 21 proteins that were differentially expressed ($P<0.05$) in cells overexpressing RTP801 compared to controls (the experiment was performed in triplicate). Protein name, accession number (Uniprot database), the obtained confidence score, fold change and P value are displayed. Proteins that present a fold change lower than 0.77 (in green) are downregulated by RTP801 (more expressed in control cells), while proteins that present a fold change higher than 1.3 (in red) are upregulated by RTP801 (more expressed in cells overexpressing RTP801).

The majority of the proteins modulated by RTP801 were related to transcription or translation. In this group we found Histone H1.0, Histone H2A, Smarca2, RNA polymerase II-associated protein 3, transcription initiation factor IIA and eukaryotic peptide chain release factor 1. Many of the previous identified RTP801 interactors were also related to RNA processing (Table 3), so a role for RTP801 at transcriptional level should be considered.

Some proteins downregulated by RTP801 were related to apoptosis, which is a known RTP801 function in differentiated cells. This is the case of STE20-like serine/threonine-protein kinase and PPP1R13L protein (also known as iASPP). Interestingly, RTP801 overexpression downregulated iASPP, a protein that inhibits the apoptotic function of p53[361]. Another protein downregulated by RTP801 was Glutaredoxin-1, a protein reported protective in dopaminergic cells exposed to PD toxins[362]. Other differently expressed proteins were nucleus related proteins, such as importin and Ranbp1.

DISCUSSION

RTP801 is a pro-apoptotic protein induced in cellular and animal models of PD and in nigral neurons from sporadic PD patients. It triggers death by a sequential mechanism in which inactivates mTOR and the pro-survival kinase Akt[136,137]. So, RTP801 actions toward mTOR signaling pathway may play a significant role in neurodegeneration and would represent a potential therapeutic target.

One remarkable feature of RTP801 protein is its extremely short half-life (2-7 minutes)[292,295], suggesting that its synthesis and degradation are strictly and dynamically regulated. In our group we have already identified parkin as a RING E3 ligase that ubiquinates RTP801 targeting it to proteasomal degradation[296]. However, other E3 ligases may be contributing to RTP801 degradation and consequently be regulating its protein levels. Taking into account that there is a harmful RTP801 elevation in several PD models[136], it would be valuable to identify new E3 ligases regulating RTP801 and to study its possible implication in this neurodegenerative disease.

In this work, we show in neurons and in NGF-differentiated PC12 cells that there is a pool of RTP801 that is degraded via lysosomal pathway. We also demonstrate that RTP801 is a novel substrate for NEDD4 E3 ligase; both proteins interact physically in cells and NEDD4 enhances RTP801 polyubiquitination. We show that NEDD4 preferentially conjugates K63 ubiquitin chains to RTP801, a type of polyubiquitination associated with lysosomal degradation. Importantly, NEDD4 regulates RTP801 protein levels in cultured cells and in the conditional knockout mouse model. We also provide evidence that NEDD4 protects against RTP801 toxicity by polyubiquitinating it. Furthermore, NEDD4 levels are decreased in the 6-OHDA PD cellular model and its restoration protects against 6-OHDA-induced cell death by reducing RTP801 protein levels. Moreover, NEDD4 loss of function is toxic in cells due to RTP801 elevation and the subsequent mTOR/Akt inactivation. A role for NEDD4 in PD is supported by observation of diminished NEDD4 in nigral neurons from postmortem sporadic PD brains. In line with these findings, the NEDD4 signaling inducer NAB2 reduces RTP801 protein levels in control and in 6-OHDA-treated cortical neurons. However, NAB2 is not sufficient to confer protection against 6-OHDA toxicity, because the compound itself represses mTOR signaling pathway compromising cell survival.

Besides, a putative crosstalk between NEDD4 and parkin E3 ligases have been identified. Ectopic WT parkin overexpression significantly decreases overexpressed NEDD4, but it does not affect endogenous NEDD4 in cells. Furthermore, NEDD4 levels are increased in parkin knockout mouse brains and in human fibroblasts from AR-JP patients with parkin mutations.

We also provide evidence that ubiquitination is involved in RTP801 protein stability and function. Different RTP801 mutants have been obtained by mutating each lysine (K) to arginine (R), an amino acid that structurally resembles lysine but cannot be ubiquitinated. Moreover, a non-ubiquitinable mutant (RTP801-KR) has been generated by mutating the six

lysines present in RTP801 sequence. As expected, RTP801-KR mutant is massively accumulated in cells, although its toxicity does not differ from WT RTP801, suggesting that surpassed a determined threshold, increasing RTP801 levels does not exacerbate cell death. In contrast, RTP801-K185R mutant displays lower levels than WT RTP801 and abolishes the pro-apoptotic role of RTP801, pointing out that ubiquitination at lysine 185 is critical for its toxicity. Supporting these observations, WT RTP801 and RTP801-KR similarly repressed mTOR pathway, whereas RTP801-K185R prevented from mTOR signaling inactivation.

Finally, by performing proteomic analysis of RTP801 immunocomplexes, we have identified a subset of potential new RTP801 protein interactors in neurons. Among these potential partners, clathrin and liprin-α-3 were the ones displaying a highest score. Interestingly, AP-2 complex, a previously described clathrin partner involved in cargo internalization[355], has been also identified. These results suggest that RTP801 can be present in clathrin-coated vesicles.

To further explore RTP801 mechanism of action, another proteomic study allowed us to identify proteins significantly upregulated or downregulated by RTP801 overexpression. Interestingly, some of the identified RTP801-modulated proteins are related to clathrin-mediated endocytosis process, supporting previous results. The rest of RTP801-modulated proteins are related to various cellular functions, including apoptosis. These data have provided new valuable information about RTP801 protein actions that need to be further investigated.

1. RTP801 IS A NEW SUBSTRATE FOR NEDD4 E3 LIGASE

Here, we have confirmed that RTP801 protein is mostly degraded by the UPS in two different neuronal cell types. In agreement with that, proteins displaying short half-lives are considered more prone to be degraded by the proteasome[363]. However, our results reveal the existence of a pool of total RTP801 degraded through lysosomes. This lysosomal fraction is markedly higher in cortical neurons than in neuronal PC12 cells, pointing out that the amount of RTP801 degraded by each pathway can vary between cell types.

Lysosomes are responsible for the degradation of membrane proteins through endocytosis, as well as for the clearance of cytosolic proteins through autophagy[51,76]. Hence, the observed RTP801 lysosomal fraction can arise from membrane RTP801 endocytosis or from cytosolic RTP801 autophagy. Considering that RTP801 can be localized at the membrane[180,284], one can hypothesize that membrane-bound RTP801 is endocytosed and degraded via lysosomes, while cytosolic RTP801 is degraded via proteasome. However, the possibility of autophagy-mediated RTP801 degradation cannot be discarded. To further verify this issue, it would be interesting to test whether downregulation of ESCRT components, which mediate endosomal-lysosomal trafficking, alters RTP801 degradation.

Importantly, dysfunction of proteasome and lysosome systems has been described in PD[69,70,364–366]. Hence, both pathways could be contributing to the previously reported RTP801 elevation in PD pathogenesis[136].

We demonstrate that NEDD4 E3 ligase is able to ubiquitinate RTP801 in a cell-free system and to enhance RTP801 polyubiquitination in cells, pointing out RTP801 as a novel NEDD4 substrate. Moreover, NEDD4 preferentially attaches K63-polyubiquitin chains to RTP801, a type of chains that have lower affinity than K48-polyubiquitin chains for the 26S proteasome, and that are widely associated with lysosomal degradation[367]. Therefore, NEDD4 ubiquitinates RTP801 and targets it to lysosomal degradation (Figure 62).

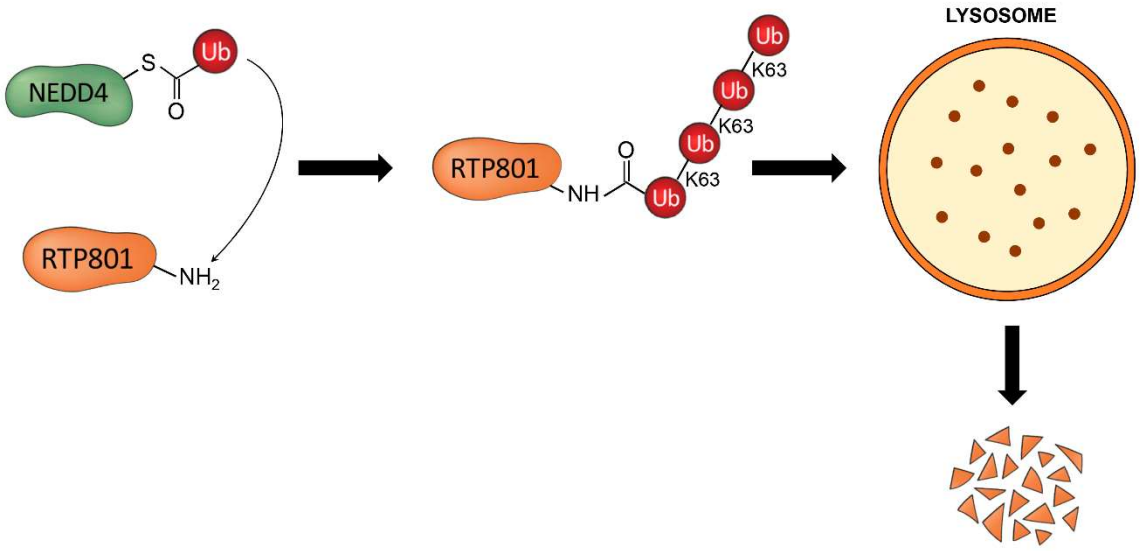

Figure 62. NEDD4 ubiquitinates RTP801 preferentially with K63-polyubiquitin chains as a signal for lysosomal degradation. Schematic representation of the final ubiquitination step by which NEDD4 E3 ligase conjugates ubiquitin to RTP801, the type of polyubiquitin chains formed and the subsequent degradation via lysosomes.

Again, whether NEDD4-polyubiquitinated RTP801 is delivered to lysosomes through membrane endocytosis or autophagy remains undetermined, since K63-polyubiquitin chains can function as a signal for both pathways[51,82]. However, the fact that NEDD4 can be localized at the membrane[228], like RTP801, suggests that NEDD4 targets RTP801 for endocytosis and subsequent lysosomal degradation. Supporting this notion, several of the previously identified NEDD4 substrates are membrane proteins targeted to the endosomal-lysosomal pathway[246,271,368]. In addition, NEDD4 membrane translocation has been reported to stabilize the active conformation of this E3 ligase[256].

Apart from NEDD4, only two E3 ligases have been described to ubiquitinate RTP801: CUL4A-DDB1-ROC1-β-TRCP E3 ligase complex[295] and parkin[296], since HUWE1 seemed to control RTP801 in a UPS independent manner, via a feedback loop controlled by mTORC1[369].

Nonetheless, CUL4A-DDB1-ROC1-β-TRCP E3 ligase complex has been questioned by others who claimed that RTP801 levels were not modified in cells treated with MLN4924 compound, an inhibitor of all cullin-RING E3 ligases[370]. Hence, RTP801 turnover might not be regulated by any of the cullin-RING ligases, which represent about half of all cellular E3 ubiquitin ligases.

On the other hand, parkin was reported to mediate RTP801 ubiquitination and subsequent proteasomal degradation[296]. Cellular and animal models along with human samples were used to demonstrate that RTP801 is a real parkin substrate, and that PD-associated parkin dysfunction contributes to RTP801 elevation[296].

So, RTP801 can be ubiquitinated by both parkin and NEDD4 E3 ligases, although they differ in the type of polyubiquitination and degradation. Parkin polyubiquitinates RTP801 with K48-ubiquitin chains, targeting it for proteasomal degradation while NEDD4 appears to polyubiquitinate RTP801 with K63-ubiquitin chains, targeting it to lysosomal degradation. One can speculate that each E3 ligase regulates different pools of RTP801; NEDD4 would most likely principally contribute to membrane RTP801 degradation, whereas parkin would mostly contribute to cytoplasmic RTP801 degradation. It is important to highlight that other unidentified E3 ligases could be also ubiquitinating RTP801 contributing to its post-translational regulation.

Some global ubiquitination studies have determined that human RTP801 is ubiquitinated at lysine 129 (K129)[371–373]. However, further investigations will be required to determine whether this is the specific lysine ubiquitinated by NEDD4, or even parkin.

Supporting the role of NEDD4 as an E3 ligase for RTP801, we show that both proteins physically interact in cells. Ectopic NEDD4 and RTP801 proteins co-immunoprecipitate in HEK293 cells, and endogenous proteins co-immunoprecipitate in NPC12 cells, but only in the presence of crosslinker DSP. This fact suggests that NEDD4 and RTP801 interact weakly and/or transiently. In agreement with this finding, E3-substrate binding has been reported to be transient[315]. Interestingly, the observation of both proteins colocalizing in the soma and dendrites of neurons support the idea of their interaction.

As previously mentioned, the WW domains of NEDD4 are normally responsible for substrate binding, via recognition of proline-rich motifs (PY), such as PPXY (X is any amino acid) and PPLP, or phospho-serine/threonine residues [p(S/T)][238,374,375]. RTP801 sequence does not have any defined proline-rich motif, but at the N-terminal part of the amino acid sequence it presents several serine and threonine residues susceptible for phosphorylation (see figure 15). Indeed, serine 19, threonine 23 and threonine 25 of human RTP801 have been identified as phosphorylation sites for GSK3β[295]. Hence, these residues could represent a binding site

for NEDD4 WW domains. An alternative way for RTP801 binding would be through action of NEDD4 adaptor proteins NDFIP1 and NDIFP2[258].

2. NEDD4 REGULATES RTP801 PROTEIN LEVELS IN CELLULAR AND ANIMAL MODELS

We demonstrate that NEDD4 regulates RTP801 protein steady-state levels in cells. Ectopic WT NEDD4 significantly reduces RTP801 protein levels in neuronal PC12 cells and in cortical neurons, without altering its transcription. On the other hand, NEDD4-C867S mutant does not modify RTP801 protein levels. The fact that RTP801 levels are not elevated by this inactive mutant suggests that is not acting as a dominant negative by disrupting endogenous NEDD4 activity in basal conditions.

Supporting this regulation, we show that knocking down NEDD4 in cortical neurons promotes an increase of RTP801, along with a phosphorylation decrease of Akt pro-survival kinase and an increase of caspase-cleaved α-spectrin fragment. Thus, NEDD4 depletion appears to be detrimental for neurons. Taking into account that RTP801 functions as an mTOR/Akt pathway repressor, a logic rationale would be that NEDD4 loss of function elevates the levels of its substrate RTP801, which in turn, represses pro-survival Akt signaling leading to neuron death.

This hypothesis was confirmed by a double knockdown experiment in which RTP801 elevation results indispensable for NEDD4 knockdown toxicity. In fact, knocking down RTP801 at the same time as NEDD4 prevented the loss of phospho-Akt and phospho-S6 and the appearance of caspase-cleaved α-spectrin fragments. Hence, NEDD4 activity over RTP801, which in turn is a negative regulator of Akt and mTOR, would be crucial to prevent neurodegeneration.

Besides, NEDD4 has been directly related to IGF-1R/PI3K/Akt pathway at different levels; NEDD4 polyubiquitinates phospho-Akt at the plasma membrane to modulate Akt subcellular localization[376]; it binds Grb10 to regulate ubiquitination and stability of IGF-1R[228,235] and it downregulates PTEN[248,249].

Importantly, we further corroborated that NEDD4 regulates RTP801 protein levels *in vivo*. Cortical lysates from NEDD4$^{f/f}$;Emx1Cre conditional knockout mice presented a 50% reduction of NEDD4 levels and a significant increase of RTP801 protein levels. This partial NEDD4 abrogation was expected, since its expression is abolished in cortex glutamatergic neurons and glia cells, but not in other cell types[254,320].

In contraposition to neurons, no significant changes are observed in Akt phosphorylation and caspase-cleaved α-spectrin fragment in mice (data not shown). These events suggest that the observed RTP801 elevation is not sufficient to induce neuronal death, probably due to

compensation effects of other redundant E3 ligases. Interestingly, parkin, a previously described E3 ligase for RTP801, was not altered in these mice (data not shown). However, other unexplored E3 ligases, such as NEDD4-2, the family member most closely related to NEDD4[223,225,262], could be compensating the lack of NEDD4. In addition, it should be emphasized that pro-apoptotic effect of RTP801 have only been observed in non-proliferating differentiated cells[136,275], so the potential RTP801 accumulation in cortical glial cells would not be toxic.

Little is known about NEDD4$^{f/f}$;Emx1Cre conditional mice phenotype, but the similar NEDD4$^{f/f}$;NEXCre mice presenting abolished NEDD4 expression in cortical and hippocampal glutamatergic neurons, showed smaller cerebrum and reduced dendrite branching of hippocampal neurons[254]. A molecular mechanism involving Rap2a and TNIK was proposed to explain this events[254]. Since RTP801 is also present at dendrites of hippocampal neurons[377], it would be interesting to investigate whether RTP801 levels are altered in neuron projections from this mice and whether it plays a role in the alterations reported.

3. NEDD4 IS DECREASED IN 6-OHDA-TREATED CELLS AND IN NIGRAL NEURONS FROM SPORADIC PD PATIENTS

PD toxin 6-OHDA is known to upregulate RTP801 in neuronal PC12 cells, both at gene and at protein level[136,296]. In this work we confirm these results and we show that 6-OHDA treatment increases RTP801 protein half-life, revealing an impairment in its protein degradation. So, RTP801 accumulation may be the result of two additive events: *DDIT4* gene induction and altered RTP801 protein degradation.

In neuronal PC12 cells, we show that PD toxin 6-OHDA reduces NEDD4 protein levels, without altering NEDD4 mRNA levels, an interesting finding that was yet not known. Moreover, these observations were extended to cortical neurons, where similar RTP801 and NEDD4 protein changes were induced by 6-OHDA. These findings suggest that NEDD4 is sensitive to 6-OHDA-associated oxidative stress and that its reduction could contribute to RTP801 elevation, by impairing its protein degradation rate.

Similarly to PD toxin 6-OHDA, the hypoxia-mimetic agent $CoCl_2$ significantly elevates RTP801 and reduces NEDD4 protein levels in neuronal PC12 cells. This RTP801 elevation was expected, since hypoxia has been described to induce DDIT4 transcription[179,275] and particularly $CoCl_2$ has been shown to upregulate RTP801[286,322]. However, the NEDD4 reduction induced by this hypoxia-mimetic compound was yet not described. These new data provides valuable knowledge about how NEDD4 is regulated in response to different cellular stressors.

Both compounds, PD toxin 6-OHDA and hypoxia-mimetic agent $CoCl_2$, have in common that generate ROS inducing oxidative stress. Also, they equivalently regulate NEDD4 and RTP801 protein levels in neuronal PC12 cells. Thus, our results suggest that oxidative stress promotes a significant NEDD4 decrease that could contribute to the observed RTP801 elevation.

Contrary to our findings, another group reported that oxidative stress elevated NEDD4 in cultured primary cortical neurons[245]. Neurotoxic agents H_2O_2, $ZnSO_4$ and camptothecin, all known to produce ROS, upregulated NEDD4 protein levels. In the case of H_2O_2 exposure, *NEDD4* gene was induced by FOXM1B transcription factor[245].

Hence, oxidative stress induced by different agents can have contrary effects in NEDD4 expression, suggesting that each compound can trigger activation of different pathways. Otherwise, the exposure time to the compounds was markedly different between both studies and could also influence results. While NEDD4 upregulation was showed after 4 hours, NEDD4 reduction by 6-OHDA and $COCl_2$ was measured after 16 hours of treatment. In view of NEDD4 potential neuroprotective role, one possibility would be that oxidative stress induces its expression at early time points as a protective mechanism to cope with stress and deal with RTP801 upregulation, while at later time points NEDD4 expression decays, contributing to RTP801 elevation and toxicity.

The fact that PD toxin 6-OHDA decreases NEDD4 protein levels without modifying its gene transcription prompted the question of which events alter its protein stability. It is well established that 6-OHDA neurotoxin induces caspases and calpains activation[132,324,325], and also that NEDD4 can be cleaved by caspases[378]. Consistent with this, our results show that 6-OHDA activates both type of proteases. Moreover, we show that not only caspases but also calpains participate into NEDD4 proteolysis in NPC12 cells. Still remains unexplored whether other processes could contribute to NEDD4 protein reduction.

In this direction, we demonstrate that 6-OHDA exposure increases NEDD4 protein levels in the exosomal-enriched extracellular fraction. Two exosomal markers, TSG101 and flotillin-1, are also elevated in this fraction after 6-OHDA treatment, suggesting that this toxin increases the release of total extracellular microvesicles. In agreement with that, 6-OHDA has been reported to trigger an increase of cytosolic calcium[331], an event described to enhance exosomal release in different cell types[327–330].

Consistent with the toxicity induced by the loss of NEDD4 in cultured neurons, we found in human PD brains that the percentage of NEDD4-stained nigral neurons from SN is lower in PD cases than in age-matched controls. This result correlates with the previously reported elevation of RTP801 in nigral neurons from sporadic PD cases[136].

Conversely, Tofaris et al. (2011) described that NEDD4 was strongly expressed in pigmented neurons containing LBs in the LC and SN from patients with LB pathologies[271]. This NEDD4 elevation was proposed to be a neuroprotective mechanism in response to accumulation of its toxic substrate α-synuclein[271]. According to literature, only 15% of the remaining nigral neurons contains LB[379]. The fact that we considered solely PD cases and all the remaining nigral neurons could explain the differences between these two works. Whether RTP801 levels are altered in the LC has not been yet explored.

Supporting a role for NEDD4 in neurodegeneration, Kwak et al. (2012) reported increased expression of NEDD4 in the forebrain of Parkinson's disease (PD), Alzheimer's disease (AD) and Huntington's disease (HD) patients[245]. However, this study is not comparable to ours, since the forebrain comprises other brain regions different from the SN.

Thus, NEDD4 is emerging as an important protein in PD pathogenesis, and in the process of neurodegeneration.

4. NEDD4 IS NEUROPROTECTIVE IN PD CELLULAR MODELS BY REGULATING RTP801 LEVELS

Previous studies demonstrated that RTP801 overexpression is sufficient to promote approximately 50% of death in NGF-differentiated PC12 cells and in cultured neurons[136,296]. Interestingly, we show that ectopic WT NEDD4, apart from decreasing endogenous RTP801 levels, partially prevents from RTP801 overexpression toxicity. As anticipated, NEDD4-C867S inactive mutant does not prevent from RTP801-induced cell death. This mutant neither aggravates cell death, supporting the perception that probably is not acting as a dominant negative.

Furthermore, RTP801 ubiquitination results necessary for NEDD4 protective actions, since it cannot prevent toxicity against RTP801-KR, a mutant with all six lysines exchanged to arginines. This mutant cannot be ubiquitinated and subsequently degraded via UPS or lysosomes. Consequently, it gets more accumulated than WT RTP801, although its toxicity is not higher. RTP801-KR mutant retains its ability to repress mTOR/Akt pathway, so it seems that surpassed a threshold, higher RTP801 levels do not exacerbate cell death. In addition, it should be considered that RTP801-KR polyubiquination smear was not completely abolished. The low signal observed could be attributed to endogenous RTP801 or even to non-canonical ubiquitination at other residues[380].

In cellular PD models, RTP801 was described to mediate death, since knocking down its expression was protective against 6-OHDA toxicity[136]. In this study, we demonstrate that ectopic NEDD4 prevents from 6-OHDA-induced RTP801 elevation, conferring protection against this neurotoxin in neuronal PC12 cells and cortical neurons. The direct correlation

between NEDD4 and RTP801 in mediating neuronal survival/death is clearly evident in the aforementioned double knockdown experiment.

Interestingly, a similar NEDD4 protective role has previously been reported against α-synuclein toxicity, a protein extensively associated with PD pathogenesis[271,272]. NEDD4 also preferentially ubiquitinated α-synuclein with K63-polyubiquitin chains targeting it to endosomal-lysosomal degradation[271]. In this case, NEDD4 protected against overexpressed WT α-synuclein in Drosophila, and against A53T mutant in rat dopaminergic neurons[272]. Controversially, NEDD4 has been described to underlie neurodegeneration by mediating HSF1 (heat shock transcription factor 1) degradation via UPS. HSF1 induces heat shock proteins, which represent a protective mechanism against misfolded proteins or aberrant accumulation of proteins[314].

Taken together, our results point out that NEDD4 neuroprotective effects are at least in part due to RTP801 degradation. Under oxidative stress induced by 6-OHDA exposure, RTP801 gets accumulated and mTOR/Akt kinases inactivated, leading to neuronal death. This toxicity can be partially reversed by NEDD4 overexpression, which enhances RTP801 degradation, leading to mTOR/Akt phosphorylation recovery (Figure 63).

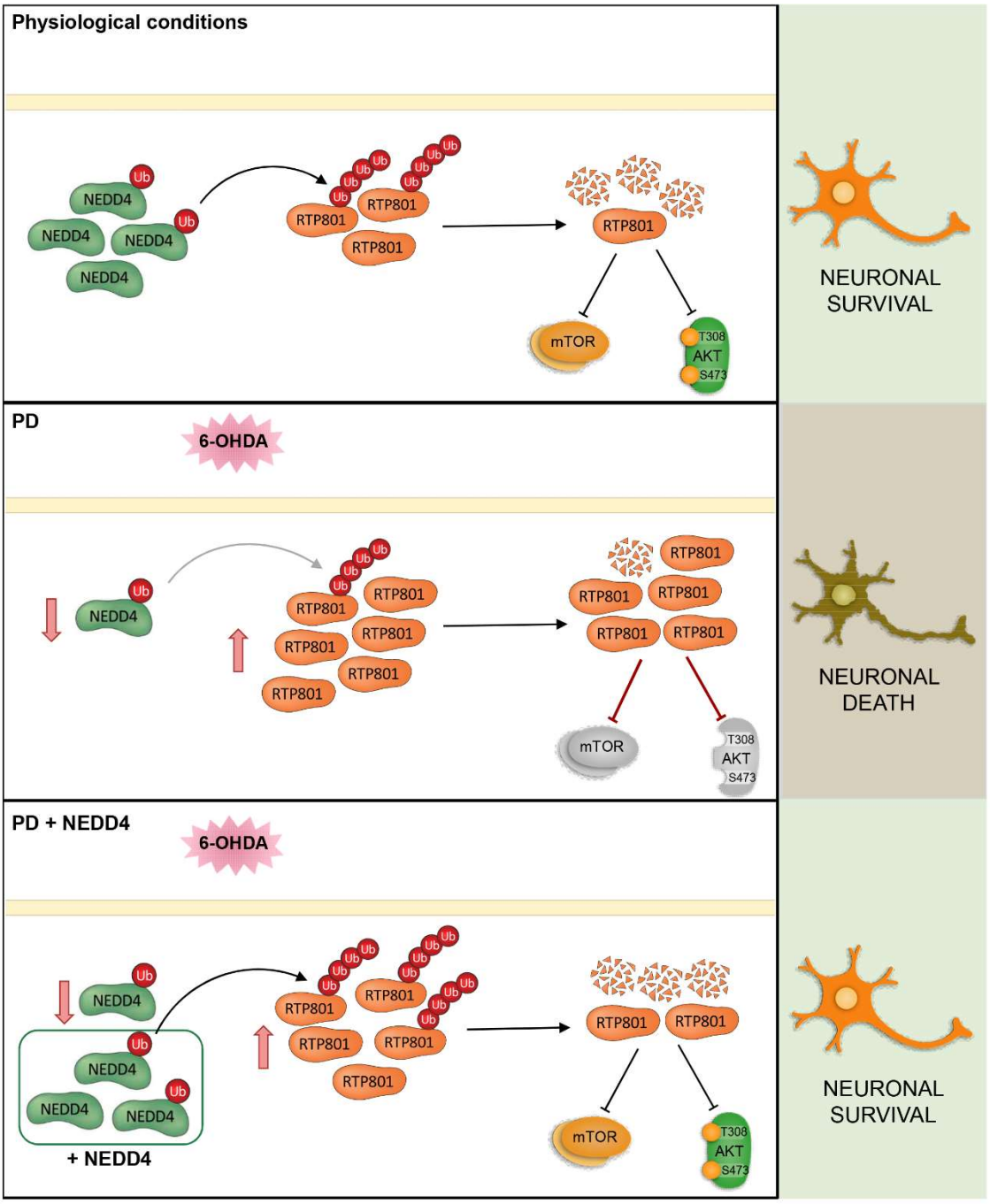

Figure 63. Schematic representation of the hypothesized NEDD4 regulation towards RTP801/mTOR/Akt in neuronal cells. In physiological conditions, RTP801 levels are low and NEDD4 normally contributes to its degradation. Hence, mTOR and Akt kinases are active promoting neuronal survival. In a PD context, when neurons are under 6-OHDA-induced stress, RTP801 is transcriptionally induced and NEDD4 protein levels are decreased. This NEDD4 reduction impairs RTP801 degradation rate contributing to its elevation. The resulting RTP801 accumulation is responsible for mTOR/Akt dephosphorylation and the subsequent neuronal death. This toxicity can be partially counteracted by ectopic NEDD4, which enhances RTP801 degradation rate decreasing its levels. Consequently, mTOR/Akt activity is partially recovered promoting neuronal survival.

5. THE NEDD4 SIGNALING INDUCER NAB2 REGULATES RTP801 PROTEIN LEVELS IN NEURONS

In neurons, we have further validated NEDD4 regulation towards RTP801 by using NAB2, a compound described to function as a NEDD4 signaling inducer. However the specific mechanism by which NAB2 activates NEDD4 remains unknown.

Here, we show that NAB2 does not modify NEDD4 protein levels, but it enhances NEDD4 polyubiquitination, suggesting that it induces NEDD4 catalytic activity instead of increasing its expression levels. One possibility would be that NAB2 interacts with NEDD4 releasing its autoinhibitory intramolecular interaction, thus promoting its active conformation[256].

Interestingly, Tardiff et al. (2013) reported that NAB2 was protective in various cell types against the toxic actions promoted by α-synuclein, a NEDD4 substrate[273]. Although α-synuclein toxicity is generally dependent on its levels[35,78], NAB2 reversed several α-synuclein-induced pathological phenotypes, such as defects in ER-to-Golgi and endosomal trafficking, without altering its protein levels[273,274].

Unlike α-synuclein, we show that NAB2 alters the expression of another NEDD4 substrate. NAB2 significantly reduces RTP801 protein levels in control and 6-OHDA-treated neurons without altering its transcription. Thus, this reduction in RTP801 protein levels could be attributed to an enhanced NEDD4-mediated RTP801 degradation. Most likely, NAB2 would enhance NEDD4-dependent endosomal trafficking events leading to an increased RTP801 endocytosis and lysosomal degradation.

Even though NAB2 reduces 6-OHDA-induced RTP801 elevation, this compound was not sufficient to confer protection against 6-OHDA toxicity in cortical neurons. Unexpectedly, NAB2 itself results toxic and inactivates mTOR/Akt pathway in control neurons. Thus, reduced RTP801 levels are not accompanied by an mTOR/Akt signaling induction, suggesting that NAB2 may affect this signaling pathway in another way compromising cell survival.

NAB2 toxic actions could be the consequence of alterations in other NEDD4 substrates and/or non-specific modifications affecting NEDD4-independent signaling pathways. These alterations may have higher influence in mTOR/Akt pathway and cell survival than the observed RTP801 reduction. More investigations are needed to establish the exact mechanism of action for NAB2 and thus understand its effects over NEDD4 activity and its substrates.

6. PUTATIVE CROSSTALK BETWEEN NEDD4 AND PARKIN E3 LIGASES

In this work, we have identified a putative crosstalk between parkin and NEDD4, two E3 ligases reported to ubiquitinate RTP801 targeting it for degradation[296]. We demonstrate that ectopic WT parkin, but not inactive parkin mutants, decrease overexpressed NEDD4 protein levels in a dose-dependent manner. Thus, parkin E3 ligase activity is required for NEDD4 downregulation. On the other hand, ectopic NEDD4 does no modify levels of overexpressed parkin, revealing that this putative regulation is occurring only in one direction, being parkin upstream of NEDD4.

We also show that overexpressed WT parkin does not affect endogenous NEDD4 levels, thus questioning the physiological relevance of this putative regulation. However, NEDD4 protein levels were found elevated in parkin knockout mouse brains and in human fibroblasts from AR-JP patients with parkin mutations, again supporting the notion that parkin could regulate NEDD4. To further corroborate this regulation it would be interesting to knockdown parkin with specific ShRNA and analyse NEDD4 protein levels. Moreover, it would be valuable to extend this study to other cell types different from HEK293 cells, particularly to neurons.

One could think that the observed NEDD4 elevation in animal and human samples is due to compensation effects, since lack of parkin could be restituted by elevation of other E3 ligases. Nevertheless, our previous results showing that parkin overexpression promotes a reduction of ectopic NEDD4 protein levels support the idea of a direct regulation between both E3 ligases. If that is the case, the most logical scenario would be that parkin ubiquitinates NEDD4 targeting it for degradation (Figure 64). This putative NEDD4 modulation by parkin would add a degree of complexity in RTP801 regulation.

In fact, E3 ligases degradation can be regulated by themselves or by the action of external ligases[332]. To date, parkin has not been described to target other ligases for degradation, but NEDD4 has been described to be targeted by $SCF^{\beta\text{-}TRCP}$ in a CKI-dependent manner[249]. Several other E3 ligases displayed this ability. For instance, NEDD4 and Itch E3 ligases have been reported to target Cbl (Casitas B-lineage lymphoma) to proteasomal degradation[381] and E6-AP (E6-associated protein) has been reported to ubiquitinate and target Ring1b ubiquitin-ligase to degradation[382].

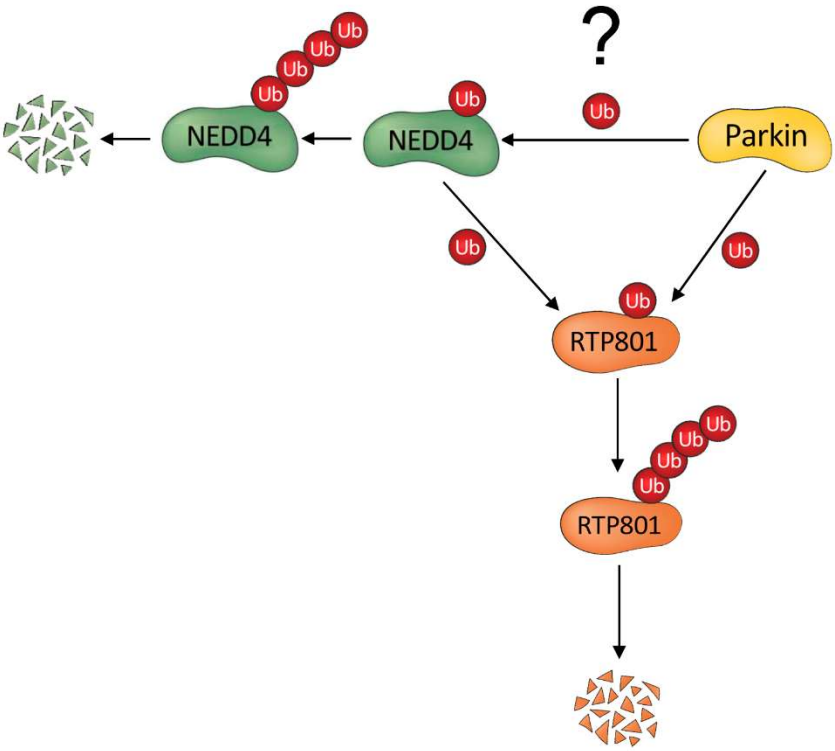

Figure 64. Putative crosstalk between parkin and NEDD4 E3 ligases. Parkin and NEDD4 have been identified as E3 ligases that ubiquitinate RTP801 targeting it to degradation. Some evidences point out that parkin could be also regulating NEDD4 protein levels, most likely by ubiquitin-mediated degradation.

7. RTP801 UBIQUITINATION AFFECTS ITS HOMEOSTASIS AND FUNCTION

A total of seven rat RTP801 mutants have been generated to study how ubiquitination affects RTP801 protein homeostasis; six mutants were obtained by mutating each lysine (K) of RTP801 amino acid sequence to arginine (R) and an extra non-ubiquitinable mutant was obtained by mutating all six lysines to arginines. These constructs were validated by transfection in HEK293 cells, obtaining similar efficiencies and no significant morphological changes in transfected cells.

According to bibliography, RTP801 overexpression is not toxic in non-differentiated proliferative cells[275]. In line with this, overexpression of WT RTP801 or its mutants in HEK293 cells does not promote cell death. In the same cell type, some of the mutants display significant differences in the levels of expression compared to WT RTP801. As anticipated, given that is a non-ubiquitinable mutant form, RTP801-KR is more accumulated than WT RTP801. On the other hand, RTP801-K185 and RTP801-K215R present reduced protein levels compared to WT RTP801.

This result is surprising, since if we think in ubiquitination as a degradative protein signal, we expected that all mutants accumulated equal or more than WT protein. We suspected that preventing ubiquitination of a specific lysine would provoke two possible outcomes: RTP801

protein elevation if the mutated lysine is usually ubiquitinated (with polyubiquitin chains that target protein for degradation) or no alteration in RTP801 protein levels if the mutated lysine is not commonly ubiquitinated or it is ubiquitinated with a non-proteolytic type of ubiquitination. Some types of ubiquitination are associated with protein trafficking, such as monoubiquitination[383], but localization changes within the cell seems unlikely to change protein levels in cell lysates.

One feasible explanation for the obtained results would be that ubiquitination at residues K185 or K215 somehow enhances RTP801 protein stability, and thus mutating them would decrease its protein levels. However, RTP801-KR mutant, which contains these two lysines mutations, shows higher stability than WT RTP801, revealing that non-ubiquitination of other lysines can counteract the effect that K185 or K215 exert in the protein.

Unlike in HEK293 cells, WT RTP801 and the vast majority of RTP801 mutants induce similar levels of cell death in neuronal PC12 cells. This RTP801 toxicity in differentiated non-proliferative cells was previously described by others[136,137,275]. Of note, RTP801-K185R is the unique mutant that completely abrogated RTP801 toxicity, suggesting that ubiquitination at lysine 185 is critical for its pro-apoptotic function. Again, RTP801-KR, which also contains this K185R mutation among others, does not abolish cell death, indicating that mutation at other lysines can compensate this protective effect.

These viability results are in agreement with the degree of mTOR/Akt pathway activity in neuronal PC12 cells. Both WT RTP801 and RTP801-KR similarly reduce phosphorylation of mTOR, Akt and S6 when compared to control cells, while RTP801-K185R does not alter phosphorylation of these proteins.

Interestingly, RTP801-K185R mutant also presents significant lower protein levels than WT RTP801 in NPC12 cells, as previously observed in HEK293 cells. So, it seems that RTP801 protein levels are directly associated with its pro-apoptotic function, being less toxic when its levels are reduced. Nonetheless, RTP801-KR mutant displays higher protein levels but similar toxicity compared to WT RTP801. These findings suggest that RTP801 toxic actions are proportional to its protein levels until a threshold is reached, where higher amounts of protein does not aggravate cell death.

The fact that RTP801-K185R is less accumulated suggests that is a more unstable protein than WT RTP801. A possible explanation for this observation would be that lysine 185 exchange to arginine destabilizes RTP801 protein structure, making it more insoluble or prone to aggregate. However, these two amino acids structurally resemble each other and this type of mutation is widely used in several studies[384–387], prompting us to think that this is not the most reasonable scenario. Another explanation would be that this mutant is degraded at a higher rate. To further evaluate this option it would be decisive to study its ubiquitination

levels and to measure its protein half-life. Furthermore, blocking its degradation in cells by using proteasome and lysosomal inhibitors would tell us whether this mutant becomes toxic when gets accumulated, and therefore, would confirm whether RTP801 toxicity is proportional to its protein levels.

Taken together, our results suggest that ubiquitination at lysine 185 of rat RTP801 is important for mTOR/Akt repression and subsequent cell death, most likely because this mutation (K185) decreases RTP801 protein stability, leading to lower protein accumulation. However, non-ubiquitination at all other lysine residues can counteract this loss of function, as judged by RTP801-KR accumulation and survival assays.

In agreement with that, a structural/functional study of RTP801 human protein revealed two segments required for function: RTP801$^{85\text{-}193}$ and RTP801$^{207\text{-}225\ 282}$. In RTP801 sequence alignment (Figure 15), lysine 185 of rat RTP801 corresponds to lysine 188 of human RTP801, an amino acid localized in one of these two segments required for function. So, a point mutation in these regions could affect RTP801 activity.

On the other hand, lysine 188 was not identified to form part of the suggested surface patch identified by sequence conservation studies based on crystal structure: ^{138}EPCG^{141} and ^{218}KKKLYSSE^{225}. Nevertheless, mutations of individual surface patch residues, such as lysine 219 mutation to alanine, only resulted in modest functional impairment[282]. This observation would correlate with the results obtained with RTP801-K216R mutant, being lysine 216 its equivalent residue in rat sequence, which maintained RTP801 pro-apoptotic function.

Although the stretch of lysines ^{218}KKK^{220} was reported important for RTP801 localization to mitochondria and membrane[284,285], mutation of each individual lysine seems to not impair RTP801 function. In addition, RTP801-KR, the mutant form with all lysines mutated, also retains the ability to repress mTOR pathway.

Unfortunately, these mutants have not provided information about which RTP801 lysine might be ubiquitinated by NEDD4 or parkin. The fact that any of the single lysine mutants is significantly more accumulated than WT RTP801 reveals that more than one lysine may be normally ubiquitinated with chains that target RTP801 for degradation. The generation of RTP801 mutants with all lysines mutated except one would be more useful to study this issue.

8. RTP801 PROTEOMIC ANALYSIS

RTP801 protein presents a unique topology with no functional motifs identified[282]. To date, the only known function of RTP801 is to repress mTOR signaling pathway, although the exact mechanism remains controversial[179,281]. Here, we have performed various proteomic analyses in neuronal cells that led us to identify new potential interactors and proteins modulated by RTP801 overexpression.

The obtained list of putative RTP801 interactors in cortical neurons displays a remarkable variety of proteins. Numerous proteins are related to RNA processing, but also some structural proteins and ER-related proteins have been detected. The fact that cytoplasmic, membrane and nuclear proteins have been identified, confirms previous observations that this protein can localize at all these sites[283,284].

Different 14-3-3 isoforms have been detected as putative RTP801 partners, although they need to be further confirmed as specific. In 6-OHDA-treated neurons, a 14-3-3 isoform has also been identified. Interestingly, this interaction was previously described and implicated in mTOR repression mechanism. It was proposed that RTP801 binds and sequesters 14-3-3, thus disrupting the inhibitory function of this protein towards TSC2[180]. Other studies confirmed this interaction by co-immunoprecipitation assays[388–390]. However, RTP801 and 14-3-3 interaction hypothesis was rejected by others, who were not able to detect binding of both proteins in a variety of experimental systems[282]. Hence, it would be important to confirm whether these proteins interact in neurons and to investigate its implication in mediating mTOR inhibition.

However, the most interesting partners from our point of view were the ones known to develop relevant functions in neurons. Within this group we find RUFY3, PP1, GAPDH, Qpct, liprin-α-3 and clathrin. Remarkably, liprin-α-3 and clathrin have been detected in two independent experiments with the highest scores, suggesting that could be relevant RTP801 interactors.

Liprin-α are scaffold proteins implicated in the regulation of synaptic formation and transmission[352]. Interestingly, they were originally identified as partners of receptor protein tyrosine phosphatase LAR (Leukocyte common antigen-related), which regulate axon guidance[391]. In particular, liprin-α-3 is one of the most abundant liprin isoforms in the hippocampus[392].

On the other hand, clathrin is a protein that plays a key role in the formation of coated vesicles. These clathrin-coated vesicles are responsible for protein transport between the trans-Golgi network, endosomes, lysosomes and the plasma membrane[393]. Clathrin molecules combine to form a spherical “clathrin lattice” structure that function as a

mechanical scaffold. However, adaptor proteins are needed to bind membrane components and select cargo[393].

Interestingly, AP-2 complex, one of these clathrin-adaptor proteins, has also been identified as a putative RTP801 partner. AP-2 participates in the formation of vesicles that are endocytosed from the plasma membrane to fuse with early endosomes[394,395]. The fact that we have identified clathrin and AP-2 as potential RTP801 interactors supports the notion that RTP801 can be endocytosed from the plasma membrane through clathrin-coated vesicles. In neurons, clathrin-mediated endocytosis is crucial for synaptic vesicle recycling in the presynaptic site[354].

Thus, RTP801 could be actively implicated in synaptic dynamics and in axon formation. In fact, RTP801 has been found enriched in synaptosomal fractions prepared from different brain regions[377].

In the case of 6-OHDA-treated neurons, all detected RTP801 interactors were also identified in untreated neurons. However, evidence suggests some differences in clathrin and liprin-α-3 protein abundance, as judged by band intensities and the number of peptides obtained. Exposure to 6-OHDA seems to increase clathrin and decrease liprin-α-3 abundance in RTP801 immunocomplexes. It would be important to confirm this differences by WB and to study whether these proteins have a role in RTP801-related actions in these conditions.

All these potential RTP801 partners need to be further validated with additional experiments. So far, only AP-2 complex has been corroborated as an RTP801 interactor by co-immunoprecipitation assay. Once confirmed, it would be interesting to address the functional consequences and the physiological relevance of their interaction with RTP801 in neuronal cells. These investigations might provide new insights into RTP801 biological functions in neurons.

Unfortunately, among the putative RTP801 partners we have not identified NEDD4 E3 ligase. This fact does not invalidate our previous reported NEDD4-RTP801 interaction, since it was shown to be a weak interaction that required the crosslinker DSP for being detected.

On the other hand, we have detected 21 proteins significantly modulated by RTP801 in NPC12 cells; 14 are downregulated while 7 are upregulated. Again, these proteins are related to diverse cellular functions. Although any of them was previously identified as a putative RTP801 interactor, we detected two upregulated proteins directly associated with clathrin-coated vesicles: amphiphysin and AP-.3 complex.

AP-3 complex is, like AP-2 complex, a clathrin-adaptor protein. Specifically, it has been implicated in cargo-selective protein transport from the Golgi to late endosomes or lysosomes[396]. Moreover, studies in neuronal cells have revealed a role for AP-3 in the

biogenesis of synaptic vesicles from endosomes[357,397,398]. Amphiphysin is a protein highly expressed in the brain that plays a major role in clathrin-mediated endocytosis of synaptic vesicles, particularly in the invagination and fission steps. Interestingly, this protein interacts with clathrin[359] and AP-2[360].

These findings confirm a link between RTP801 and clathrin-mediated processes and support the idea that RTP801 could play a role at synaptic level by regulating synaptic vesicles formation and recycling. This hypothesis needs to be further investigated. Indeed, the role of RTP801 at synaptic level is currently being studied in our group.

Of note, some of the modulated proteins by RTP801 are related to apoptosis, a known outcome of its overexpression in differentiated cells. Interestingly, RTP801 downregulates two proteins, iASPP and glutaredoxin-1, known to be protective against pro-apoptotic stimuli[361,362]. Hence, apart from repressing mTOR activity, RTP801 could regulate alternative signaling pathways that mediate toxicity in cells.

These proteomic studies have provided a large amount of valuable information regarding RTP801 potential interactors and proteome modulation. Moreover, they suggest novel functions for RTP801 that they have never been described so far. These preliminary data need to be confirmed by performing further experiments. In addition, future investigations will be important to determine which proteins are relevant in mediating RTP801 functions.

9. RTP801 AND NEDD4 AS POTENTIAL THERAPEUTIC TARGETS IN PARKINSON'S DISEASE

PD is characterized by the loss of SN dopaminergic neurons[5]. Unfortunately, current treatments ameliorate PD symptoms but do not prevent neuron death. Therefore, is crucial to study the molecular mechanisms underlying neurodegeneration to identify proteins involved in PD pathogenesis and design new therapeutic approaches able to halt or at least delay neuron death (reviewed in [42]).

Interestingly, RTP801 has emerged as an important protein in PD pathogenesis, since it can promote neuron death by repressing mTOR/Akt signaling pathway[136,137,292,296]. Hence, strategies able to block RTP801 toxic accumulation or modulate mTOR/Akt activity can become potential therapeutic targets (reviewed in [399]).

Indeed, some compounds that modulate RTP801/mTOR/Akt axis have been already reported protective in PD pathogenesis. FLZ (8-methyl-6-phenoxy-2-(tetrahydro-2H-pyran-4-ylamino)pyrido[2,3-d]pyrimidin-7(8H)-one), a synthetic compound derived from a Chinese herb, conferred protection in cellular and animal models of PD[400–402] by inhibiting RTP801 expression and maintaining Akt pro-survival kinase activity[402,403]. Rapamycin, an allosteric

inhibitor of mTOR, was also protective in cellular and animal PD models[88,292,404]. The neuroprotection conferred by rapamycin has been attributed to its ability to suppress certain mTOR activities. It only represses the translation of a subset of transcripts, including RTP801, leading to the maintenance of Akt survival signaling by preserving phosphorylation at threonine 308[292]. In addition, rapamycin protective effects have also been attributed to its ability to enhance autophagy and restore lysosomal levels[88].

Another valuable strategy would be to block RTP801 expression with small interfering RNAs (SiRNAs) or microRNAs (miRNAs). To date, these molecules have not been investigated as therapeutic agents for PD treatment, but a SiRNA against RTP801 is being evaluated in clinical trials for retinopathy treatment[405–408]. Moreover, taking into account that RTP801-K185R mutant does not promote cell death, it would be also useful to target this residue with small molecules to inhibit its ubiquitination. However, first it would be necessary to further explore why this mutant is not toxic, in order to understand its mechanism of action and properly design a therapeutic strategy.

Importantly, we have identified NEDD4 E3 ligase as a protein able to regulate RTP801 protein levels. Moreover, we have shown that NEDD4 is reduced in PD nigral neurons and that can protect against RTP801 toxicity. Hence, any compound able to induce NEDD4 expression or activity can also represent a potential PD therapeutic target.

In fact, NEDD4 has already been described protective in animal models against the toxicity induced by one of its substrates, α-synuclein[272]. In line with this, NAB2, a NEDD4 signaling inducer, is also neuroprotective against α-synuclein toxicity[273,274]. In this work, we have tested this compound in neurons, but it did not confer protection against PD toxin 6-OHDA, although it prevented RTP801 elevation. In our model, NAB2 itself resulted toxic, so maybe other experimental conditions or models must be tested to further explore its potential protective actions.

Considering NEDD4 regulation mechanisms, other strategies could be valuable to increase its stability. For instance, D4476, a CKI pharmacological inhibitor, significantly increased NEDD4 expression in 293T cells, by disrupting its phosphorylation and subsequent $SCF^{\beta\text{-}TRCP}$-mediated degradation[249]. Moreover, p34 stabilized NEDD4 in cancer cell lines by directly binding to its WW1 domain[409]. Hence, it would be interesting to study these NEDD4 stabilization mechanisms in neuronal cells.

In addition, compounds or strategies able to disrupt NEDD4 autoinhibitory state would enhance its E3 ligase activity (see figure 13). NDFIP adaptor proteins or c-Src-mediated phosphorylation are described to shift NEDD4 to an active conformation[257,258], and could be further explored as potential PD therapeutic targets.

CONCLUSIONS

1. RTP801 is degraded by the lysosomal pathway, along with the ubiquitin-proteasome system (UPS) in neuronal cells.

2. NEDD4 interacts with RTP801 and mediates its polyubiquitination and lysosomal degradation by preferentially conjugating K63-ubiquitin chains.

3. RTP801 protein levels are regulated by NEDD4 in cultured neuronal cells and in a mouse model.

4. NEDD4 loss of function is toxic to neurons due to RTP801 elevation and the subsequent mTOR/Akt signaling repression.

5. NEDD4 is protective against ectopic RTP801-induced toxicity or against 6-OHDA exposure.

6. PD toxin 6-OHDA decreases NEDD4 protein levels as a result of caspases and calpains-mediated proteolysis and increased release to the exosomal-enriched extracellular fraction.

7. NEDD4 is diminished in SNpc nigral neurons from human sporadic PD brains.

8. NAB2, a NEDD4 signaling inducer, reduces RTP801 protein levels but does not prevent from 6-OHDA-induced cell death in cortical neurons.

9. Parkin E3 ligase regulates ectopic NEDD4 in cells and endogenous NEDD4 in parkin knockout mouse brains and in human fibroblasts from AR-JP patients with parkin mutations.

10. RTP801 ubiquitination at lysine 185 affects protein stability and is necessary for function in neuronal PC12 cells

11. Proteomic studies have led to the identification of several putative RTP801 partners and proteins modulated by its overexpression.

BIBLIOGRAPHY

1 Parkinson J. *An essay on the shaking palsy*. Witthingham and Rowland, 181

2 Bartels AL, Leenders KL. Parkinson's disease: The syndrome, the pathogenesis and pathophysiology. *Cortex* 2009; **45**: 915–921.

3 Schneider SA, Obeso JA. Clinical and pathological features of Parkinson's disease. *Curr Top Behav Neurosci* 2015; **22**: 205–20.

4 Fahn S. Clinical aspects of Parkinson's disease. In: Nass R, Przedborski S (eds). *Parkinson's disease*. 2011, pp 3–7.

5 Dauer W, Przedborski S. Parkinson ' s Disease : Mechanisms and Models. 2003; **39**: 889–909.

6 Marsden CD. Neuromelanin and Parkinson's disease. *J Neural Transm Suppl* 1983; **19**: 121–41.

7 Halliday GM, Ophof A, Broe M, Jensen PH, Kettle E, Fedorow H *et al.* Alpha-synuclein redistributes to neuromelanin lipid in the substantia nigra early in Parkinson's disease. *Brain* 2005; **128**: 2654–64.

8 Bernheimer H, Birkmayer W, Hornykiewicz O, Jellinger K, Seitelberger F. Brain dopamine and the syndromes of Parkinson and Huntington. Clinical, morphological and neurochemical correlations. *J Neurol Sci* 1973; **20**: 415–55.

9 Fahn S. Description of Parkinson's disease as a clinical syndrome. *Ann N Y Acad Sci* 2003; **991**: 1–14.

10 Lang AE, Lozano AM. Parkinson's disease. First of two parts. *N Engl J Med* 1998; **339**: 1044–53.

11 Galvin JE, Lee VM, Schmidt ML, Tu PH, Iwatsubo T, Trojanowski JQ. Pathobiology of the Lewy body. *Adv Neurol* 1999; **80**: 313–24.

12 Forno LS. Neuropathology of Parkinson's disease. *J Neuropathol Exp Neurol* 1996; **55**: 259–72.

13 Shults CW. Lewy bodies. *Proc Natl Acad Sci U S A* 2006; **103**: 1661–8.

14 Srinivasan BS, Doostzadeh J, Absalan F, Mohandessi S, Jalili R, Bigdeli S *et al.* Whole genome survey of coding SNPs reveals a reproducible pathway determinant of Parkinson disease. *Hum Mutat* 2009; **30**: 228–38.

15 Sian-Hulsmann J, Monoranu C, Strobel S, Riederer P. Lewy Bodies: A Spectator or Salient Killer? *CNS Neurol Disord Drug Targets* 2015; **14**: 947–55.

16 Wichmann T, DeLong M. Systems level physiology of the basal ganglia, and pathophysiology of Parkinson's disease. In: Nass R, Przedborski S (eds). *Parkinson's disease*. 2011, pp 55–63.

17 Blandini F, Nappi G, Tassorelli C, Martignoni E. Functional changes of the basal ganglia circuitry in Parkinson's disease. *Prog Neurobiol* 2000; **62**: 63–88.

18 Gerfen CR, Engber TM, Mahan LC, Susel Z, Chase TN, Monsma FJ *et al.* D1 and D2 dopamine receptor-regulated gene expression of striatonigral and striatopallidal neurons. *Science* 1990; **250**: 1429–32.

19 Gerfen CR, Keefe KA, Gauda EB. D1 and D2 dopamine receptor function in the striatum: coactivation of D1- and D2-dopamine receptors on separate populations of neurons results in potentiated immediate early gene response in D1-containing neurons. *J Neurosci* 1995; **15**: 8167–76.

20 Fahn S, Przedborski S. Parkinsonism. In: Lippincott Williams and Wilkins (ed). *Merritt's Neurology*. 2000, pp 679–693.

21 Litvan I, Bhatia KP, Burn DJ, Goetz CG, Lang AE, McKeith I *et al.* Movement Disorders Society Scientific Issues Committee report: SIC Task Force appraisal of clinical diagnostic criteria for Parkinsonian disorders. *Mov Disord* 2003; **18**: 467–86.

22 Zesiewicz TA, Sullivan KL, Hauser RA. Nonmotor symptoms of Parkinson's disease. *Expert Rev Neurother* 2006; **6**: 1811–22.

23 Jankovic J. Parkinson's disease: clinical features and diagnosis. *J Neurol Neurosurg Psychiatry* 2008; **79**: 368–376.

24 Cummings JL. Depression and Parkinson's disease: a review. *Am J Psychiatry* 1992; **149**: 443–54.

25 Lees AJ, Blackburn NA, Campbell VL. The nighttime problems of Parkinson's disease. *Clin*

Neuropharmacol 1988; **11**: 512–9.

26 Löhle M, Storch A, Reichmann H. Beyond tremor and rigidity: non-motor features of Parkinson's disease. *J Neural Transm* 2009; **116**: 1483–92.

27 Steece-Collier K, Maries E, Kordower JH. Etiology of Parkinson's disease: Genetics and environment revisited. *Proc Natl Acad Sci U S A* 2002; **99**: 13972–13974.

28 Schapira AH, Jenner P. Etiology and pathogenesis of Parkinson's disease. *Mov Disord* 2011; **26**: 1049–1055.

29 Gubellini P, Kachidian P. Animal models of Parkinson's disease: An updated overview. *Rev Neurol (Paris)* 2015; **171**: 750–61.

30 Olanow CW, Tatton WG. Etiology and pathogenesis of Parkinson's disease. *Annu Rev Neurosci* 1999; **22**: 123–44.

31 Lesage S, Brice A. Parkinson's disease: From monogenic forms to genetic susceptibility factors. *Hum Mol Genet* 2009; **18**: 48–59.

32 Pankratz N, Foroud T. Genetics of Parkinson disease. *Genet Med* 2007; **9**: 801–11.

33 Tan JMM, Wong ESP, Lim K-L. Protein misfolding and aggregation in Parkinson's disease. *Antioxid Redox Signal* 2009; **11**: 2119–34.

34 Polymeropoulos MH, Lavedan C, Leroy E, Ide SE, Dehejia A, Dutra A *et al.* Mutation in the alpha-synuclein gene identified in families with Parkinson's disease. *Science* 1997; **276**: 2045–7.

35 Singleton AB, Farrer M, Johnson J, Singleton A, Hague S, Kachergus J *et al.* alpha-Synuclein locus triplication causes Parkinson's disease. *Science* 2003; **302**: 841.

36 Kitada T, Asakawa S, Hattori N, Matsumine H, Yamamura Y, Minoshima S *et al.* Mutations in the parkin gene cause autosomal recessive juvenile parkinsonism. *Nature* 1998; **392**: 605–8.

37 Valente EM, Abou-Sleiman PM, Caputo V, Muqit MMK, Harvey K, Gispert S *et al.* Hereditary early-onset Parkinson's disease caused by mutations in PINK1. *Science* 2004; **304**: 1158–60.

38 Bonifati V. Mutations in the DJ-1 Gene Associated with Autosomal Recessive Early-Onset Parkinsonism. *Science (80-)* 2002; **299**: 256–259.

39 Zimprich A, Biskup S, Leitner P, Lichtner P, Farrer M, Lincoln S *et al.* Mutations in LRRK2 cause autosomal-dominant parkinsonism with pleomorphic pathology. *Neuron* 2004; **44**: 601–7.

40 Paisán-Ruíz C, Jain S, Evans EW, Gilks WP, Simón J, van der Brug M *et al.* Cloning of the gene containing mutations that cause PARK8-linked Parkinson's disease. *Neuron* 2004; **44**: 595–600.

41 Ramirez A, Heimbach A, Gründemann J, Stiller B, Hampshire D, Cid LP *et al.* Hereditary parkinsonism with dementia is caused by mutations in ATP13A2, encoding a lysosomal type 5 P-type ATPase. *Nat Genet* 2006; **38**: 1184–1191.

42 Levy OA, Malagelada C, Greene LA. Cell death pathways in Parkinson's disease: proximal triggers, distal effectors, and final steps. *Apoptosis* 2009; **14**: 478–500.

43 Braak H, Del Tredici K, Rüb U, de Vos RAI, Jansen Steur ENH, Braak E. Staging of brain pathology related to sporadic Parkinson's disease. *Neurobiol Aging*; **24**: 197–211.

44 Spillantini MG, Schmidt ML, Lee VM, Trojanowski JQ, Jakes R, Goedert M. Alpha-synuclein in Lewy bodies. *Nature* 1997; **388**: 839–40.

45 Trojanowski JQ, Lee VMY. Parkinson's disease and related synucleinopathies are a new class of nervous system amyloidoses. *Neurotoxicology* 2002; **23**: 457–60.

46 Smith WW, Jiang H, Pei Z, Tanaka Y, Morita H, Sawa A *et al.* Endoplasmic reticulum stress and mitochondrial cell death pathways mediate A53T mutant alpha-synuclein-induced toxicity. *Hum Mol Genet* 2005; **14**: 3801–11.

47 Hsu LJ, Sagara Y, Arroyo A, Rockenstein E, Sisk A, Mallory M *et al.* alpha-synuclein promotes mitochondrial deficit and oxidative stress. *Am J Pathol* 2000; **157**: 401–10.

48 Tanaka Y, Engelender S, Igarashi S, Rao RK, Wanner T, Tanzi RE *et al.* Inducible expression of mutant alpha-synuclein decreases proteasome activity and increases sensitivity to mitochondria-dependent apoptosis. *Hum Mol Genet* 2001; **10**: 919–26.

49 Lopiano L, Fasano M, Giraudo S, Digilio G, Koenig SH, Torre E *et al.* Nuclear magnetic relaxation dispersion profiles of substantia nigra pars compacta in Parkinson's disease patients are consistent with protein aggregation. *Neurochem Int* 2000; **37**: 331–6.

50 Betarbet R, Sherer TB, Greenamyre JT. Ubiquitin-proteasome system and Parkinson's diseases. *Exp Neurol* 2005; **191 Suppl** : S17–27.

51 Tai H-C, Schuman EM. Ubiquitin, the proteasome and protein degradation in neuronal function and dysfunction. *Nat Rev Neurosci* 2008; **9**: 826–38.

52 Pickart CM. Ubiquitin in chains. *Trends Biochem Sci* 2000; **25**: 544–8.

53 Di Fiore PP, Polo S, Hofmann K. When ubiquitin meets ubiquitin receptors: a signalling connection. *Nat Rev Mol Cell Biol* 2003; **4**: 491–7.

54 Seirafi M, Kozlov G, Gehring K. Parkin structure and function. *FEBS J* 2015; **282**: 2076–88.

55 Komander D. The emerging complexity of protein ubiquitination. *Biochem Soc Trans* 2009; **37**: 937–53.

56 Pickart CM. Mechanisms underlying ubiquitination. *Annu Rev Biochem* 2001; **70**: 503–533.

57 Calistri A, Munegato D, Carli I, Parolin C, Palù G. The ubiquitin-conjugating system: multiple roles in viral replication and infection. *Cells* 2014; **3**: 386–417.

58 Glickman MH, Ciechanover A. The ubiquitin-proteasome proteolytic pathway: destruction for the sake of construction. *Physiol Rev* 2002; **82**: 373–428.

59 Thrower JS, Hoffman L, Rechsteiner M, Pickart CM. Recognition of the polyubiquitin proteolytic signal. *EMBO J* 2000; **19**: 94–102.

60 Ikeda F, Dikic I. Atypical ubiquitin chains: new molecular signals. 'Protein Modifications: Beyond the Usual Suspects' review series. *EMBO Rep* 2008; **9**: 536–42.

61 Pickart CM, Fushman D. Polyubiquitin chains: polymeric protein signals. *Curr Opin Chem Biol* 2004; **8**: 610–6.

62 Hamilton AM, Zito K. Breaking it down: the ubiquitin proteasome system in neuronal morphogenesis. *Neural Plast* 2013; **2013**: 196848.

63 Mukhopadhyay D, Riezman H. Proteasome-independent functions of ubiquitin in endocytosis and signaling. *Science* 2007; **315**: 201–5.

64 Spence J, Sadis S, Haas AL, Finley D. A ubiquitin mutant with specific defects in DNA repair and multiubiquitination. *Mol Cell Biol* 1995; **15**: 1265–73.

65 Voges D, Zwickl P, Baumeister W. The 26S proteasome: a molecular machine designed for controlled proteolysis. *Annu Rev Biochem* 1999; **68**: 1015–68.

66 Sherman MY, Goldberg AL. Cellular defenses against unfolded proteins: a cell biologist thinks about neurodegenerative diseases. *Neuron* 2001; **29**: 15–32.

67 Deveraux Q, Ustrell V, Pickart C, Rechsteiner M. A 26 S protease subunit that binds ubiquitin conjugates. *J Biol Chem* 1994; **269**: 7059–61.

68 Li X-J, Li S. Proteasomal dysfunction in aging and Huntington disease. *Neurobiol Dis* 2011; **43**: 4–8.

69 McNaught KS, Jenner P. Proteasomal function is impaired in substantia nigra in Parkinson's disease. *Neurosci Lett* 2001; **297**: 191–4.

70 McNaught KSP, Belizaire R, Isacson O, Jenner P, Olanow CW. Altered proteasomal function in sporadic Parkinson's disease. *Exp Neurol* 2003; **179**: 38–46.

71 Rideout HJ, Larsen KE, Sulzer D, Stefanis L. Proteasomal inhibition leads to formation of ubiquitin/alpha-synuclein-immunoreactive inclusions in PC12 cells. *J Neurochem* 2001; **78**: 899–908.

72 McNaught KSP, Mytilineou C, Jnobaptiste R, Yabut J, Shashidharan P, Jennert P *et al.* Impairment of the ubiquitin-proteasome system causes dopaminergic cell death and inclusion body formation in ventral mesencephalic cultures. *J Neurochem* 2002; **81**: 301–6.

73 Rideout HJ, Lang-Rollin ICJ, Savalle M, Stefanis L. Dopaminergic neurons in rat ventral midbrain

cultures undergo selective apoptosis and form inclusions, but do not up-regulate iHSP70, following proteasomal inhibition. *J Neurochem* 2005; **93**: 1304–13.

74 Dice JF. Chaperone-mediated autophagy. *Autophagy*; **3**: 295–9.

75 Luzio JP, Pryor PR, Bright NA. Lysosomes: fusion and function. *Nat Rev Mol Cell Biol* 2007; **8**: 622–32.

76 Perrett RM, Alexopoulou Z, Tofaris GK. The endosomal pathway in Parkinson's disease. *Mol Cell Neurosci* 2015; **66**: 21–8.

77 van Dijk KD, Persichetti E, Chiasserini D, Eusebi P, Beccari T, Calabresi P *et al.* Changes in endolysosomal enzyme activities in cerebrospinal fluid of patients with Parkinson's disease. *Mov Disord* 2013; **28**: 747–54.

78 Outeiro TF, Lindquist S. Yeast cells provide insight into alpha-synuclein biology and pathobiology. *Science* 2003; **302**: 1772–5.

79 Lynch-Day MA, Mao K, Wang K, Zhao M, Klionsky DJ. The role of autophagy in Parkinson's disease. *Cold Spring Harb Perspect Med* 2012; **2**: a009357.

80 Yue Z, Friedman L, Komatsu M, Tanaka K. The cellular pathways of neuronal autophagy and their implication in neurodegenerative diseases. *Biochim Biophys Acta* 2009; **1793**: 1496–507.

81 Xie Z, Klionsky DJ. Autophagosome formation: core machinery and adaptations. *Nat Cell Biol* 2007; **9**: 1102–9.

82 Tan JMM, Wong ESP, Kirkpatrick DS, Pletnikova O, Ko HS, Tay S-P *et al.* Lysine 63-linked ubiquitination promotes the formation and autophagic clearance of protein inclusions associated with neurodegenerative diseases. *Hum Mol Genet* 2008; **17**: 431–9.

83 Nixon RA, Wegiel J, Kumar A, Yu WH, Peterhoff C, Cataldo A *et al.* Extensive involvement of autophagy in Alzheimer disease: an immuno-electron microscopy study. *J Neuropathol Exp Neurol* 2005; **64**: 113–22.

84 Alvarez-Erviti L, Rodriguez-Oroz MC, Cooper JM, Caballero C, Ferrer I, Obeso JA *et al.* Chaperone-mediated autophagy markers in Parkinson disease brains. *Arch Neurol* 2010; **67**: 1464–72.

85 Banerjee R, Beal MF, Thomas B. Autophagy in neurodegenerative disorders: pathogenic roles and therapeutic implications. *Trends Neurosci* 2010; **33**: 541–9.

86 Spencer B, Potkar R, Trejo M, Rockenstein E, Patrick C, Gindi R *et al.* Beclin 1 gene transfer activates autophagy and ameliorates the neurodegenerative pathology in alpha-synuclein models of Parkinson's and Lewy body diseases. *J Neurosci* 2009; **29**: 13578–88.

87 Xiong N, Jia M, Chen C, Xiong J, Zhang Z, Huang J *et al.* Potential autophagy enhancers attenuate rotenone-induced toxicity in SH-SY5Y. *Neuroscience* 2011; **199**: 292–302.

88 Dehay B, Bové J, Rodríguez-Muela N, Perier C, Recasens A, Boya P *et al.* Pathogenic lysosomal depletion in Parkinson's disease. *J Neurosci* 2010; **30**: 12535–44.

89 Decressac M, Mattsson B, Weikop P, Lundblad M, Jakobsson J, Björklund A. TFEB-mediated autophagy rescues midbrain dopamine neurons from α-synuclein toxicity. *Proc Natl Acad Sci U S A* 2013; **110**: E1817–26.

90 Cuervo AM, Stefanis L, Fredenburg R, Lansbury PT, Sulzer D. Impaired degradation of mutant alpha-synuclein by chaperone-mediated autophagy. *Science* 2004; **305**: 1292–5.

91 Webb JL, Ravikumar B, Atkins J, Skepper JN, Rubinsztein DC. Alpha-Synuclein is degraded by both autophagy and the proteasome. *J Biol Chem* 2003; **278**: 25009–13.

92 Holtz WA, O'Malley KL. Parkinsonian mimetics induce aspects of unfolded protein response in death of dopaminergic neurons. *J Biol Chem* 2003; **278**: 19367–77.

93 Holtz WA, Turetzky JM, Jong Y-JI, O'Malley KL. Oxidative stress-triggered unfolded protein response is upstream of intrinsic cell death evoked by parkinsonian mimetics. *J Neurochem* 2006; **99**: 54–69.

94 Winklhofer KF, Haass C. Mitochondrial dysfunction in Parkinson's disease. *Biochim Biophys Acta* 2010; **1802**: 29–44.

95 Mann VM, Cooper JM, Daniel SE, Srai K, Jenner P, Marsden CD *et al.* Complex I, iron, and ferritin

in Parkinson's disease substantia nigra. *Ann Neurol* 1994; **36**: 876–81.

96 Silvestri L, Caputo V, Bellacchio E, Atorino L, Dallapiccola B, Valente EM *et al.* Mitochondrial import and enzymatic activity of PINK1 mutants associated to recessive parkinsonism. *Hum Mol Genet* 2005; **14**: 3477–92.

97 Darios F, Corti O, Lücking CB, Hampe C, Muriel M-P, Abbas N *et al.* Parkin prevents mitochondrial swelling and cytochrome c release in mitochondria-dependent cell death. *Hum Mol Genet* 2003; **12**: 517–26.

98 Langston JW, Ballard P, Tetrud JW, Irwin I. Chronic Parkinsonism in humans due to a product of meperidine-analog synthesis. *Science* 1983; **219**: 979–80.

99 Sian J, Dexter DT, Lees AJ, Daniel S, Agid Y, Javoy-Agid F *et al.* Alterations in glutathione levels in Parkinson's disease and other neurodegenerative disorders affecting basal ganglia. *Ann Neurol* 1994; **36**: 348–55.

100 Przedborski S, Jackson-Lewis V, Vila M, Wu DC, Teismann P, Tieu K *et al.* Free radical and nitric oxide toxicity in Parkinson's disease. *Adv Neurol* 2003; **91**: 83–94.

101 Muñoz P, Huenchuguala S, Paris I, Segura-Aguilar J. Dopamine oxidation and autophagy. *Parkinsons Dis* 2012; **2012**: 920953.

102 Jenner P. Oxidative mechanisms in nigral cell death in Parkinson's disease. *Mov Disord* 1998; **13 Suppl 1**: 24–34.

103 Kavya R, Saluja R, Singh S, Dikshit M. Nitric oxide synthase regulation and diversity: implications in Parkinson's disease. *Nitric Oxide* 2006; **15**: 280–94.

104 Tsang AHK, Chung KKK. Oxidative and nitrosative stress in Parkinson's disease. *Biochim Biophys Acta* 2009; **1792**: 643–50.

105 Jagmag SA, Tripathi N, Shukla SD, Maiti S, Khurana S. Evaluation of Models of Parkinson's Disease. *Front Neurosci* 2015; **9**: 503.

106 Ries V, Burke RE. Rodent toxin models of PD: an overview. In: Nass R, Przedborski S (eds). *Parkinson's disease*. 2008, pp 135–146.

107 Tranzer J., Thoenen H. Veränderungen der sympathischen Nervenendigungen der Katze nach Vorbehandlung mit 5- und 6-Hydroxy-Dopamin. *Naunyn Schmiedebergs Arch Exp Pathol Pharmakol* 1967; **257**: 73–75.

108 Luthman J, Fredriksson A, Sundström E, Jonsson G, Archer T. Selective lesion of central dopamine or noradrenaline neuron systems in the neonatal rat: motor behavior and monoamine alterations at adult stage. *Behav Brain Res* 1989; **33**: 267–77.

109 Napolitano A, Pezzella A, Prota G. New reaction pathways of dopamine under oxidative stress conditions: nonenzymatic iron-assisted conversion to norepinephrine and the neurotoxins 6-hydroxydopamine and 6, 7-dihydroxytetrahydroisoquinoline. *Chem Res Toxicol* 1999; **12**: 1090–7.

110 Curtius HC, Wolfensberger M, Steinmann B, Redweik U, Siegfried J. Mass fragmentography of dopamine and 6-hydroxydopamine. Application to the determination of dopamine in human brain biopsies from the caudate nucleus. *J Chromatogr* 1974; **99**: 529–40.

111 Andrew R, Watson DG, Best SA, Midgley JM, Wenlong H, Petty RK. The determination of hydroxydopamines and other trace amines in the urine of parkinsonian patients and normal controls. *Neurochem Res* 1993; **18**: 1175–7.

112 Karoum F, Chrapusta SJ, Egan MF, Wyatt RJ. Absence of 6-hydroxydopamine in the rat brain after treatment with stimulants and other dopaminergic agents: a mass fragmentographic study. *J Neurochem* 1993; **61**: 1369–75.

113 Heikkila R, Cohen G. Further studies on the generation of hydrogen peroxide by 6-hydroxydopamine. Potentiation by ascorbic acid. *Mol Pharmacol* 1972; **8**: 241–8.

114 Seitz G, Stegmann HB, Jäger HH, Schlude HM, Wolburg H, Roginsky VA *et al.* Neuroblastoma cells expressing the noradrenaline transporter are destroyed more selectively by 6-fluorodopamine than by 6-hydroxydopamine. *J Neurochem* 2000; **75**: 511–20.

115 Soto-Otero R, Méndez-Alvarez E, Hermida-Ameijeiras A, Muñoz-Patiño AM, Labandeira-Garcia JL. Autoxidation and neurotoxicity of 6-hydroxydopamine in the presence of some antioxidants: potential implication in relation to the pathogenesis of Parkinson's disease. *J Neurochem* 2000; **74**: 1605–12.

116 Cohen G, Heikkila RE. The generation of hydrogen peroxide, superoxide radical, and hydroxyl radical by 6-hydroxydopamine, dialuric acid, and related cytotoxic agents. *J Biol Chem* 1974; **249**: 2447–52.

117 Saner A, Thoenen H. Model experiments on the molecular mechanism of action of 6-hydroxydopamine. *Mol Pharmacol* 1971; **7**: 147–54.

118 Kostrzewa RM, Jacobowitz DM. Pharmacological actions of 6-hydroxydopamine. *Pharmacol Rev* 1974; **26**: 199–288.

119 Kumar R, Agarwal AK, Seth PK. Free radical-generated neurotoxicity of 6-hydroxydopamine. *J Neurochem* 1995; **64**: 1703–7.

120 Rodriguez-Pallares J, Parga JA, Muñoz A, Rey P, Guerra MJ, Labandeira-Garcia JL. Mechanism of 6-hydroxydopamine neurotoxicity: the role of NADPH oxidase and microglial activation in 6-hydroxydopamine-induced degeneration of dopaminergic neurons. *J Neurochem* 2007; **103**: 145–56.

121 Glinka YY, Youdim MB. Inhibition of mitochondrial complexes I and IV by 6-hydroxydopamine. *Eur J Pharmacol* 1995; **292**: 329–32.

122 Glinka Y, Tipton KF, Youdim MB. Nature of inhibition of mitochondrial respiratory complex I by 6-Hydroxydopamine. *J Neurochem* 1996; **66**: 2004–10.

123 Glinka Y, Gassen M, Youdim MB. Mechanism of 6-hydroxydopamine neurotoxicity. *J Neural Transm Suppl* 1997; **50**: 55–66.

124 Glinka Y, Tipton KF, Youdim MB. Mechanism of inhibition of mitochondrial respiratory complex I by 6-hydroxydopamine and its prevention by desferrioxamine. *Eur J Pharmacol* 1998; **351**: 121–9.

125 Blum D, Torch S, Nissou MF, Benabid AL, Verna JM. Extracellular toxicity of 6-hydroxydopamine on PC12 cells. *Neurosci Lett* 2000; **283**: 193–6.

126 Berretta N, Freestone PS, Guatteo E, de Castro D, Geracitano R, Bernardi G *et al.* Acute effects of 6-hydroxydopamine on dopaminergic neurons of the rat substantia nigra pars compacta in vitro. *Neurotoxicology* 2005; **26**: 869–81.

127 Hanrott K, Gudmunsen L, O'Neill MJ, Wonnacott S. 6-hydroxydopamine-induced apoptosis is mediated via extracellular auto-oxidation and caspase 3-dependent activation of protein kinase Cdelta. *J Biol Chem* 2006; **281**: 5373–82.

128 Clement M-V, Long LH, Ramalingam J, Halliwell B. The cytotoxicity of dopamine may be an artefact of cell culture. *J Neurochem* 2002; **81**: 414–21.

129 Offen D, Beart PM, Cheung NS, Pascoe CJ, Hochman A, Gorodin S *et al.* Transgenic mice expressing human Bcl-2 in their neurons are resistant to 6-hydroxydopamine and 1-methyl-4-phenyl-1,2,3,6- tetrahydropyridine neurotoxicity. *Proc Natl Acad Sci U S A* 1998; **95**: 5789–94.

130 Blum D, Torch S, Lambeng N, Nissou M, Benabid AL, Sadoul R *et al.* Molecular pathways involved in the neurotoxicity of 6-OHDA, dopamine and MPTP: contribution to the apoptotic theory in Parkinson's disease. *Prog Neurobiol* 2001; **65**: 135–72.

131 Ungerstedt U. 6-Hydroxy-dopamine induced degeneration of central monoamine neurons. *Eur J Pharmacol* 1968; **5**: 107–10.

132 Saito Y, Nishio K, Ogawa Y, Kinumi T, Yoshida Y, Masuo Y *et al.* Molecular mechanisms of 6-hydroxydopamine-induced cytotoxicity in PC12 cells: involvement of hydrogen peroxide-dependent and -independent action. *Free Radic Biol Med* 2007; **42**: 675–85.

133 Blum D, Wu Y, Nissou MF, Arnaud S, Alim-Louis-Benabid, Verna JM. p53 and Bax activation in 6-hydroxydopamine-induced apoptosis in PC12 cells. *Brain Res* 1997; **751**: 139–42.

134 Ryu EJ, Harding HP, Angelastro JM, Vitolo O V, Ron D, Greene LA. Endoplasmic reticulum stress and the unfolded protein response in cellular models of Parkinson's disease. *J Neurosci* 2002; **22**: 10690–8.

135 Ryu EJ, Angelastro JM, Greene LA. Analysis of gene expression changes in a cellular model of Parkinson disease. *Neurobiol Dis* 2005; **18**: 54–74.

136 Malagelada C, Ryu EJ, Biswas SC, Jackson-Lewis V, Greene LA. RTP801 is elevated in Parkinson brain substantia nigral neurons and mediates death in cellular models of Parkinson's disease by a mechanism involving mammalian target of rapamycin inactivation. *J Neurosci* 2006; **26**: 9996–

10005.

137 Malagelada C, Jin ZH, Greene LA. RTP801 is induced in Parkinson's disease and mediates neuron death by inhibiting Akt phosphorylation/activation. *J Neurosci* 2008; **28**: 14363–71.

138 Grau CM, Greene LA. Use of PC12 cells and rat superior cervical ganglion sympathetic neurons as models for neuroprotective assays relevant to Parkinson's disease. *Methods Mol Biol* 2012; **846**: 201–11.

139 Malagelada C, Greene LA. PC12 cells as a model for Parkinson's disease research. In: Nass R, Przedborski S (eds). *Parkinson's disease*. 2008, pp 375–383.

140 Wakabayashi K, Takahashi H. Neuropathology of autonomic nervous system in Parkinson's disease. *Eur Neurol* 1997; **38 Suppl 2**: 2–7.

141 Li S-T, Dendi R, Holmes C, Goldstein DS. Progressive loss of cardiac sympathetic innervation in Parkinson's disease. *Ann Neurol* 2002; **52**: 220–3.

142 Orimo S, Uchihara T, Nakamura A, Mori F, Kakita A, Wakabayashi K *et al.* Axonal alpha-synuclein aggregates herald centripetal degeneration of cardiac sympathetic nerve in Parkinson's disease. *Brain* 2008; **131**: 642–50.

143 Alberio T, Lopiano L, Fasano M. Cellular models to investigate biochemical pathways in Parkinson's disease. *FEBS J* 2012; **279**: 1146–55.

144 Hartmann A. Postmortem studies in Parkinson's disease. *Dialogues Clin Neurosci* 2004; **6**: 281–93.

145 Rohn TT, Catlin LW. Immunolocalization of influenza A virus and markers of inflammation in the human Parkinson's disease brain. *PLoS One* 2011; **6**: e20495.

146 Lindgren HS, Rylander D, Iderberg H, Andersson M, O'Sullivan SS, Williams DR *et al.* Putaminal upregulation of FosB/ΔFosB-like immunoreactivity in Parkinson's disease patients with dyskinesia. *J Parkinsons Dis* 2011; **1**: 347–57.

147 Gatt AP, Duncan OF, Attems J, Francis PT, Ballard CG, Bateman JM. Dementia in Parkinson's disease is associated with enhanced mitochondrial complex I deficiency. *Mov Disord* 2016; **31**: 352–9.

148 Murphy KE, Gysbers AM, Abbott SK, Tayebi N, Kim WS, Sidransky E *et al.* Reduced glucocerebrosidase is associated with increased α-synuclein in sporadic Parkinson's disease. *Brain* 2014; **137**: 834–48.

149 Nagatsu T, Sawada M. Biochemistry of postmortem brains in Parkinson's disease: historical overview and future prospects. *J Neural Transm Suppl* 2007; : 113–20.

150 Auburger G, Klinkenberg M, Drost J, Marcus K, Morales-Gordo B, Kunz WS *et al.* Primary skin fibroblasts as a model of Parkinson's disease. *Mol Neurobiol* 2012; **46**: 20–7.

151 Laplante M, Sabatini DM. mTOR signaling in growth control and disease. *Cell* 2012; **149**: 274–93.

152 Vézina C, Kudelski A, Sehgal SN. Rapamycin (AY-22,989), a new antifungal antibiotic. I. Taxonomy of the producing streptomycete and isolation of the active principle. *J Antibiot (Tokyo)* 1975; **28**: 721–6.

153 Sabatini DM, Barrow RK, Blackshaw S, Burnett PE, Lai MM, Field ME *et al.* Interaction of RAFT1 with gephyrin required for rapamycin-sensitive signaling. *Science* 1999; **284**: 1161–4.

154 Lipton JO, Sahin M. The Neurology of mTOR. *Neuron* 2014; **84**: 275–291.

155 Jacinto E, Loewith R, Schmidt A, Lin S, Rüegg MA, Hall A *et al.* Mammalian TOR complex 2 controls the actin cytoskeleton and is rapamycin insensitive. *Nat Cell Biol* 2004; **6**: 1122–8.

156 Sarbassov DD, Ali SM, Kim D-H, Guertin DA, Latek RR, Erdjument-Bromage H *et al.* Rictor, a novel binding partner of mTOR, defines a rapamycin-insensitive and raptor-independent pathway that regulates the cytoskeleton. *Curr Biol* 2004; **14**: 1296–302.

157 Brown EJ, Albers MW, Bum Shin T, ichikawa K, Keith CT, Lane WS *et al.* A mammalian protein targeted by G1-arresting rapamycin–receptor complex. *Nature* 1994; **369**: 756–758.

158 Sabatini DM, Erdjument-Bromage H, Lui M, Tempst P, Snyder SH. RAFT1: a mammalian protein that binds to FKBP12 in a rapamycin-dependent fashion and is homologous to yeast TORs. *Cell* 1994; **78**: 35–43.

159 Loewith R, Jacinto E, Wullschleger S, Lorberg A, Crespo JL, Bonenfant D *et al.* Two TOR complexes, only one of which is rapamycin sensitive, have distinct roles in cell growth control. *Mol Cell* 2002; **10**: 457–68.

160 Chen J, Zheng XF, Brown EJ, Schreiber SL. Identification of an 11-kDa FKBP12-rapamycin-binding domain within the 289-kDa FKBP12-rapamycin-associated protein and characterization of a critical serine residue. *Proc Natl Acad Sci U S A* 1995; **92**: 4947–51.

161 Kim D-H, Sarbassov DD, Ali SM, King JE, Latek RR, Erdjument-Bromage H *et al.* mTOR interacts with raptor to form a nutrient-sensitive complex that signals to the cell growth machinery. *Cell* 2002; **110**: 163–75.

162 Yip CK, Murata K, Walz T, Sabatini DM, Kang SA. Structure of the human mTOR complex I and its implications for rapamycin inhibition. *Mol Cell* 2010; **38**: 768–74.

163 Sarbassov DD, Ali SM, Sengupta S, Sheen J-H, Hsu PP, Bagley AF *et al.* Prolonged rapamycin treatment inhibits mTORC2 assembly and Akt/PKB. *Mol Cell* 2006; **22**: 159–68.

164 Zoncu R, Efeyan A, Sabatini DM. mTOR: from growth signal integration to cancer, diabetes and ageing. *Nat Rev Mol Cell Biol* 2011; **12**: 21–35.

165 Burgering BM, Coffer PJ. Protein kinase B (c-Akt) in phosphatidylinositol-3-OH kinase signal transduction. *Nature* 1995; **376**: 599–602.

166 Franke TF, Yang SI, Chan TO, Datta K, Kazlauskas A, Morrison DK *et al.* The protein kinase encoded by the Akt proto-oncogene is a target of the PDGF-activated phosphatidylinositol 3-kinase. *Cell* 1995; **81**: 727–36.

167 McKay MM, Morrison DK. Integrating signals from RTKs to ERK/MAPK. *Oncogene* 2007; **26**: 3113–21.

168 Inoki K, Li Y, Zhu T, Wu J, Guan K-L. TSC2 is phosphorylated and inhibited by Akt and suppresses mTOR signalling. *Nat Cell Biol* 2002; **4**: 648–57.

169 Ma L, Chen Z, Erdjument-Bromage H, Tempst P, Pandolfi PP. Phosphorylation and functional inactivation of TSC2 by Erk implications for tuberous sclerosis and cancer pathogenesis. *Cell* 2005; **121**: 179–93.

170 Manning BD, Tee AR, Logsdon MN, Blenis J, Cantley LC. Identification of the tuberous sclerosis complex-2 tumor suppressor gene product tuberin as a target of the phosphoinositide 3-kinase/Akt pathway. *Mol Cell* 2002; **10**: 151–62.

171 Potter CJ, Pedraza LG, Xu T. Akt regulates growth by directly phosphorylating Tsc2. *Nat Cell Biol* 2002; **4**: 658–65.

172 Roux PP, Ballif BA, Anjum R, Gygi SP, Blenis J. Tumor-promoting phorbol esters and activated Ras inactivate the tuberous sclerosis tumor suppressor complex via p90 ribosomal S6 kinase. *Proc Natl Acad Sci U S A* 2004; **101**: 13489–94.

173 Zhang Y, Gao X, Saucedo LJ, Ru B, Edgar BA, Pan D. Rheb is a direct target of the tuberous sclerosis tumour suppressor proteins. *Nat Cell Biol* 2003; **5**: 578–581.

174 Inoki K, Li Y, Xu T, Guan K-L. Rheb GTPase is a direct target of TSC2 GAP activity and regulates mTOR signaling. *Genes Dev* 2003; **17**: 1829–34.

175 Tee AR, Manning BD, Roux PP, Cantley LC, Blenis J. Tuberous sclerosis complex gene products, Tuberin and Hamartin, control mTOR signaling by acting as a GTPase-activating protein complex toward Rheb. *Curr Biol* 2003; **13**: 1259–68.

176 Garami A, Zwartkruis FJT, Nobukuni T, Joaquin M, Roccio M, Stocker H *et al.* Insulin activation of Rheb, a mediator of mTOR/S6K/4E-BP signaling, is inhibited by TSC1 and 2. *Mol Cell* 2003; **11**: 1457–66.

177 Wullschleger S, Loewith R, Hall MN. TOR signaling in growth and metabolism. *Cell* 2006; **124**: 471–84.

178 Inoki K, Zhu T, Guan K-L. TSC2 mediates cellular energy response to control cell growth and survival. *Cell* 2003; **115**: 577–90.

179 Brugarolas J, Lei K, Hurley RL, Manning BD, Reiling JH, Hafen E *et al.* Regulation of mTOR function in response to hypoxia by REDD1 and the TSC1/TSC2 tumor suppressor complex. *Genes Dev* 2004; **18**: 2893–904.

180 DeYoung MP, Horak P, Sofer A, Sgroi D, Ellisen LW. Hypoxia regulates TSC1/2 mTOR signaling and tumor suppression through REDD1-mediated 14 3 3 shuttling. *Genes Dev* 2008; **22**: 239–251.

181 Reiling JH, Hafen E. The hypoxia-induced paralogs Scylla and Charybdis inhibit growth by down-regulating S6K activity upstream of TSC in Drosophila. *Genes Dev* 2004; **18**: 2879–92.

182 Hay N, Sonenberg N. Upstream and downstream of mTOR. *Genes Dev* 2004; **18**: 1926–45.

183 Tee AR, Blenis J. mTOR, translational control and human disease. *Semin Cell Dev Biol* 2005; **16**: 29–37.

184 Ganley IG, Lam DH, Wang J, Ding X, Chen S, Jiang X. ULK1.ATG13.FIP200 complex mediates mTOR signaling and is essential for autophagy. *J Biol Chem* 2009; **284**: 12297–305.

185 Hosokawa N, Hara T, Kaizuka T, Kishi C, Takamura A, Miura Y *et al.* Nutrient-dependent mTORC1 Association with the ULK1-Atg13-FIP200 Complex Required for Autophagy. *Mol Biol Cell* 2009; **20**: 1981–1991.

186 Jung CH, Jun CB, Ro S-H, Kim Y-M, Otto NM, Cao J *et al.* ULK-Atg13-FIP200 complexes mediate mTOR signaling to the autophagy machinery. *Mol Biol Cell* 2009; **20**: 1992–2003.

187 Düvel K, Yecies JL, Menon S, Raman P, Lipovsky AI, Souza AL *et al.* Activation of a metabolic gene regulatory network downstream of mTOR complex 1. *Mol Cell* 2010; **39**: 171–83.

188 Hudson CC, Liu M, Chiang GG, Otterness DM, Loomis DC, Kaper F *et al.* Regulation of hypoxia-inducible factor 1alpha expression and function by the mammalian target of rapamycin. *Mol Cell Biol* 2002; **22**: 7004–14.

189 Laplante M, Sabatini DM. An emerging role of mTOR in lipid biosynthesis. *Curr Biol* 2009; **19**: R1046–52.

190 Iadevaia V, Liu R, Proud CG. mTORC1 signaling controls multiple steps in ribosome biogenesis. *Semin Cell Dev Biol* 2014; **36**: 113–20.

191 Gan X, Wang J, Su B, Wu D. Evidence for direct activation of mTORC2 kinase activity by phosphatidylinositol 3,4,5-trisphosphate. *J Biol Chem* 2011; **286**: 10998–1002.

192 Zinzalla V, Stracka D, Oppliger W, Hall MN. Activation of mTORC2 by association with the ribosome. *Cell* 2011; **144**: 757–68.

193 García-Martínez JM, Alessi DR. mTOR complex 2 (mTORC2) controls hydrophobic motif phosphorylation and activation of serum- and glucocorticoid-induced protein kinase 1 (SGK1). *Biochem J* 2008; **416**: 375–85.

194 Sarbassov DD, Guertin DA, Ali SM, Sabatini DM. Phosphorylation and regulation of Akt/PKB by the rictor-mTOR complex. *Science* 2005; **307**: 1098–101.

195 Manning BD, Cantley LC. AKT/PKB signaling: navigating downstream. *Cell* 2007; **129**: 1261–74.

196 Franke TF. PI3K/Akt: getting it right matters. *Oncogene* 2008; **27**: 6473–88.

197 Alessi DR, James SR, Downes CP, Holmes AB, Gaffney PR, Reese CB *et al.* Characterization of a 3-phosphoinositide-dependent protein kinase which phosphorylates and activates protein kinase Balpha. *Curr Biol* 1997; **7**: 261–9.

198 Sancak Y, Thoreen CC, Peterson TR, Lindquist RA, Kang SA, Spooner E *et al.* PRAS40 is an insulin-regulated inhibitor of the mTORC1 protein kinase. *Mol Cell* 2007; **25**: 903–15.

199 Thedieck K, Polak P, Kim ML, Molle KD, Cohen A, Jenö P *et al.* PRAS40 and PRR5-like protein are new mTOR interactors that regulate apoptosis. *PLoS One* 2007; **2**: e1217.

200 Vander Haar E, Lee S-I, Bandhakavi S, Griffin TJ, Kim D-H. Insulin signalling to mTOR mediated by the Akt/PKB substrate PRAS40. *Nat Cell Biol* 2007; **9**: 316–23.

201 Wang L, Harris TE, Roth RA, Lawrence JC. PRAS40 regulates mTORC1 kinase activity by functioning as a direct inhibitor of substrate binding. *J Biol Chem* 2007; **282**: 20036–44.

202 Dudek H, Datta SR, Franke TF, Birnbaum MJ, Yao R, Cooper GM *et al.* Regulation of neuronal survival by the serine-threonine protein kinase Akt. *Science* 1997; **275**: 661–5.

203 Crowder RJ, Freeman RS. Phosphatidylinositol 3-kinase and Akt protein kinase are necessary and sufficient for the survival of nerve growth factor-dependent sympathetic neurons. *J Neurosci* 1998;

18: 2933–43.

204 Brunet A, Datta SR, Greenberg ME. Transcription-dependent and -independent control of neuronal survival by the PI3K-Akt signaling pathway. *Curr Opin Neurobiol* 2001; **11**: 297–305.

205 Orike N, Middleton G, Borthwick E, Buchman V, Cowen T, Davies AM. Role of PI 3-kinase, Akt and Bcl-2-related proteins in sustaining the survival of neurotrophic factor-independent adult sympathetic neurons. *J Cell Biol* 2001; **154**: 995–1005.

206 Downward J. PI 3-kinase, Akt and cell survival. *Semin Cell Dev Biol* 2004; **15**: 177–82.

207 Duronio V. The life of a cell: apoptosis regulation by the PI3K/PKB pathway. *Biochem J* 2008; **415**: 333–44.

208 Datta SR, Dudek H, Tao X, Masters S, Fu H, Gotoh Y *et al.* Akt phosphorylation of BAD couples survival signals to the cell-intrinsic death machinery. *Cell* 1997; **91**: 231–41.

209 Gardai SJ, Hildeman DA, Frankel SK, Whitlock BB, Frasch SC, Borregaard N *et al.* Phosphorylation of Bax Ser184 by Akt regulates its activity and apoptosis in neutrophils. *J Biol Chem* 2004; **279**: 21085–95.

210 Zhang X, Tang N, Hadden TJ, Rishi AK. Akt, FoxO and regulation of apoptosis. *Biochim Biophys Acta* 2011; **1813**: 1978–86.

211 Dijkers PF, Birkenkamp KU, Lam EW-F, Thomas NSB, Lammers J-WJ, Koenderman L *et al.* FKHR-L1 can act as a critical effector of cell death induced by cytokine withdrawal: protein kinase B-enhanced cell survival through maintenance of mitochondrial integrity. *J Cell Biol* 2002; **156**: 531–42.

212 Kim AH, Khursigara G, Sun X, Franke TF, Chao M V. Akt phosphorylates and negatively regulates apoptosis signal-regulating kinase 1. *Mol Cell Biol* 2001; **21**: 893–901.

213 Greene LA, Levy O, Malagelada C. Akt as a victim, villain and potential hero in Parkinson's disease pathophysiology and treatment. *Cell Mol Neurobiol* 2011; **31**: 969–78.

214 Richter JD, Klann E. Making synaptic plasticity and memory last: mechanisms of translational regulation. *Genes Dev* 2009; **23**: 1–11.

215 Costa-Mattioli M, Sossin WS, Klann E, Sonenberg N. Translational Control of Long-Lasting Synaptic Plasticity and Memory. *Neuron* 2009; **61**: 10–26.

216 Buffington SA, Huang W, Costa-Mattioli M. Translational control in synaptic plasticity and cognitive dysfunction. *Annu Rev Neurosci* 2014; **37**: 17–38.

217 Cheng H-C, Kim SR, Oo TF, Kareva T, Yarygina O, Rzhetskaya M *et al.* Akt suppresses retrograde degeneration of dopaminergic axons by inhibition of macroautophagy. *J Neurosci* 2011; **31**: 2125–35.

218 Ries V, Henchcliffe C, Kareva T, Rzhetskaya M, Bland R, During MJ *et al.* Oncoprotein Akt/PKB induces trophic effects in murine models of Parkinson's disease. *Proc Natl Acad Sci U S A* 2006; **103**: 18757–62.

219 Xu Y, Liu C, Chen S, Ye Y, Guo M, Ren Q *et al.* Activation of AMPK and inactivation of Akt result in suppression of mTOR-mediated S6K1 and 4E-BP1 pathways leading to neuronal cell death in in vitro models of Parkinson's disease. *Cell Signal* 2014; **26**: 1680–9.

220 Zhou Q, Liu C, Liu W, Zhang H, Zhang R, Liu J *et al.* Rotenone induction of hydrogen peroxide inhibits mTOR-mediated S6K1 and 4E-BP1/eIF4E pathways, leading to neuronal apoptosis. *Toxicol Sci* 2015; **143**: 81–96.

221 Kumar S, Tomooka Y, Noda M. Identification of a set of genes with developmentally down-regulated expression in the mouse brain. *Biochem Biophys Res Commun* 1992; **185**: 1155–61.

222 Kumar S, Harvey KF, Kinoshita M, Copeland NG, Noda M, Jenkins NA. cDNA cloning, expression analysis, and mapping of the mouse Nedd4 gene. *Genomics* 1997; **40**: 435–43.

223 Scheffner M, Kumar S. Mammalian HECT ubiquitin-protein ligases: biological and pathophysiological aspects. *Biochim Biophys Acta* 2014; **1843**: 61–74.

224 Kamynina E, Tauxe C, Staub O. Distinct characteristics of two human Nedd4 proteins with respect to epithelial Na(+) channel regulation. *Am J Physiol Renal Physiol* 2001; **281**: F469–77.

225 Persaud A, Alberts P, Amsen EM, Xiong X, Wasmuth J, Saadon Z *et al.* Comparison of substrate specificity of the ubiquitin ligases Nedd4 and Nedd4-2 using proteome arrays. *Mol Syst Biol* 2009; **5**: 333.

226 Ingham RJ, Gish G, Pawson T. The Nedd4 family of E3 ubiquitin ligases: functional diversity within a common modular architecture. *Oncogene* 2004; **23**: 1972–84.

227 Anan T, Nagata Y, Koga H, Honda Y, Yabuki N, Miyamoto C *et al.* Human ubiquitin-protein ligase Nedd4: expression, subcellular localization and selective interaction with ubiquitin-conjugating enzymes. *Genes Cells* 1998; **3**: 751–63.

228 Vecchione A, Marchese A, Henry P, Rotin D, Morrione A. The Grb10/Nedd4 complex regulates ligand-induced ubiquitination and stability of the insulin-like growth factor I receptor. *Mol Cell Biol* 2003; **23**: 3363–72.

229 Putz U, Howitt J, Lackovic J, Foot N, Kumar S, Silke J *et al.* Nedd4 family-interacting protein 1 (Ndfip1) is required for the exosomal secretion of Nedd4 family proteins. *J Biol Chem* 2008; **283**: 32621–7.

230 Metzger MB, Hristova VA, Weissman AM. HECT and RING finger families of E3 ubiquitin ligases at a glance. *J Cell Sci* 2012; **125**: 531–537.

231 Boase NA, Kumar S. NEDD4: The founding member of a family of ubiquitin-protein ligases. *Gene* 2015; **557**: 113–22.

232 Wong BR, Parlati F, Qu K, Demo S, Pray T, Huang J *et al.* Drug discovery in the ubiquitin regulatory pathway. *Drug Discov Today* 2003; **8**: 746–54.

233 Fotia AB, Cook DI, Kumar S. The ubiquitin-protein ligases Nedd4 and Nedd4-2 show similar ubiquitin-conjugating enzyme specificities. 2006; **38**: 472–479.

234 Dunn R, Klos DA, Adler AS, Hicke L. The C2 domain of the Rsp5 ubiquitin ligase binds membrane phosphoinositides and directs ubiquitination of endosomal cargo. *J Cell Biol* 2004; **165**: 135–44.

235 Morrione A, Plant P, Valentinis B, Staub O, Kumar S, Rotin D *et al.* mGrb10 interacts with Nedd4. *J Biol Chem* 1999; **274**: 24094–9.

236 Plant PJ, Lafont F, Lecat S, Verkade P, Simons K, Rotin D. Apical membrane targeting of Nedd4 is mediated by an association of its C2 domain with annexin XIIIb. *J Cell Biol* 2000; **149**: 1473–84.

237 Bork P, Sudol M. The WW domain: a signalling site in dystrophin? *Trends Biochem Sci* 1994; **19**: 531–3.

238 Sudol M, Chen HI, Bougeret C, Einbond A, Bork P. Characterization of a novel protein-binding module--the WW domain. *FEBS Lett* 1995; **369**: 67–71.

239 Sudol M, Hunter T. NeW wrinkles for an old domain. *Cell* 2000; **103**: 1001–4.

240 Rotin D, Kumar S. Physiological functions of the HECT family of ubiquitin ligases. *Nat Rev Mol Cell Biol* 2009; **10**: 398–409.

241 Blot V, Perugi F, Gay B, Prévost M-C, Briant L, Tangy F *et al.* Nedd4.1-mediated ubiquitination and subsequent recruitment of Tsg101 ensure HTLV-1 Gag trafficking towards the multivesicular body pathway prior to virus budding. *J Cell Sci* 2004; **117**: 2357–67.

242 Maspero E, Valentini E, Mari S, Cecatiello V, Soffientini P, Pasqualato S *et al.* Structure of a ubiquitin-loaded HECT ligase reveals the molecular basis for catalytic priming. *Nat Struct Mol Biol* 2013; **20**: 696–701.

243 Dinudom A, Harvey KF, Komwatana P, Young JA, Kumar S, Cook DI. Nedd4 mediates control of an epithelial Na+ channel in salivary duct cells by cytosolic Na+. *Proc Natl Acad Sci U S A* 1998; **95**: 7169–73.

244 Monami G, Emiliozzi V, Morrione A. Grb10/Nedd4-mediated multiubiquitination of the insulin-like growth factor receptor regulates receptor internalization. *J Cell Physiol* 2008; **216**: 426–437.

245 Kwak Y-D, Wang B, Li JJ, Wang R, Deng Q, Diao S *et al.* Upregulation of the E3 ligase NEDD4-1 by Oxidative Stress Degrades IGF-1 Receptor Protein in Neurodegeneration. *J Neurosci* 2012; **32**: 10971–10981.

246 Persaud A, Alberts P, Hayes M, Guettler S, Clarke I, Sicheri F *et al.* Nedd4-1 binds and ubiquitylates activated FGFR1 to control its endocytosis and function. *EMBO J* 2011; **30**: 3259–73.

247 Huang Z, Choi B-K, Mujoo K, Fan X, Fa M, Mukherjee S *et al.* The E3 ubiquitin ligase NEDD4 negatively regulates HER3/ErbB3 level and signaling. *Oncogene* 2014; : 1–11.

248 Wang X, Trotman LC, Koppie T, Alimonti A, Chen Z, Gao Z *et al.* NEDD4-1 is a proto-oncogenic ubiquitin ligase for PTEN. *Cell* 2007; **128**: 129–39.

249 Liu J, Wan L, Liu P, Inuzuka H, Liu J, Wang Z *et al.* SCF(β-TRCP)-mediated degradation of NEDD4 inhibits tumorigenesis through modulating the PTEN/Akt signaling pathway. *Oncotarget* 2014; **5**: 1026–37.

250 Fouladkou F, Landry T, Kawabe H, Neeb A, Lu C, Brose N *et al.* The ubiquitin ligase Nedd4-1 is dispensable for the regulation of PTEN stability and localization. *Proc Natl Acad Sci U S A* 2008; **105**: 8585–90.

251 Cao XR, Lill NL, Boase N, Shi PP, Croucher DR, Shan H *et al.* Nedd4 controls animal growth by regulating IGF-1 signaling. *Sci Signal* 2008; **1**: ra5.

252 Liu Y, Oppenheim RW, Sugiura Y, Lin W. Abnormal development of the neuromuscular junction in Nedd4-deficient mice. *Dev Biol* 2009; **330**: 153–66.

253 Fouladkou F, Lu C, Jiang C, Zhou L, She Y, Walls JR *et al.* The ubiquitin ligase Nedd4-1 is required for heart development and is a suppressor of thrombospondin-1. *J Biol Chem* 2010; **285**: 6770–80.

254 Kawabe H, Neeb A, Dimova K, Young SM, Takeda M, Katsurabayashi S *et al.* Regulation of Rap2A by the ubiquitin ligase Nedd4-1 controls neurite development. *Neuron* 2010; **65**: 358–72.

255 Camera D, Boase NA, Kumar S, Pow D V, Poronnik P. Subtle gait abnormalities in Nedd4 heterozygous mice. *Behav Brain Res* 2014; **260**: 15–24.

256 Wang J, Peng Q, Lin Q, Childress C, Carey D, Yang W. Calcium activates Nedd4 E3 ubiquitin ligases by releasing the C2 domain-mediated auto-inhibition. *J Biol Chem* 2010; **285**: 12279–88.

257 Persaud A, Alberts P, Mari S, Tong J, Murchie R, Maspero E *et al.* Tyrosine phosphorylation of NEDD4 activates its ubiquitin ligase activity. *Sci Signal* 2014; **7**: ra95.

258 Mund T, Pelham HRB. Control of the activity of WW-HECT domain E3 ubiquitin ligases by NDFIP proteins. *EMBO Rep* 2009; **10**: 501–7.

259 Foot NJ, Dalton HE, Shearwin-Whyatt LM, Dorstyn L, Tan S-S, Yang B *et al.* Regulation of the divalent metal ion transporter DMT1 and iron homeostasis by a ubiquitin-dependent mechanism involving Ndfips and WWP2. *Blood* 2008; **112**: 4268–75.

260 Foot NJ, Leong YA, Dorstyn LE, Dalton HE, Ho K, Zhao L *et al.* Ndfip1-deficient mice have impaired DMT1 regulation and iron homeostasis. *Blood* 2011; **117**: 638–46.

261 DiAntonio A. Nedd4 branches out. *Neuron* 2010; **65**: 293–4.

262 Donovan P, Poronnik P. Nedd4 and Nedd4-2: ubiquitin ligases at work in the neuron. *Int J Biochem Cell Biol* 2013; **45**: 706–10.

263 Drinjakovic J, Jung H, Campbell DS, Strochlic L, Dwivedy A, Holt CE. E3 ligase Nedd4 promotes axon branching by downregulating PTEN. *Neuron* 2010; **65**: 341–57.

264 Christie KJ, Martinez JA, Zochodne DW. Disruption of E3 ligase NEDD4 in peripheral neurons interrupts axon outgrowth: Linkage to PTEN. *Mol Cell Neurosci* 2012; **50**: 179–92.

265 Hsia H-E, Kumar R, Luca R, Takeda M, Courchet J, Nakashima J *et al.* Ubiquitin E3 ligase Nedd4-1 acts as a downstream target of PI3K/PTEN-mTORC1 signaling to promote neurite growth. *Proc Natl Acad Sci U S A* 2014; **111**: 13205–10.

266 Hsia H-E, Kawabe H. Translational regulation of the expression of the ubiquitin E3 ligase Nedd4-1 by mTORC1-dependent signaling. *Commun Integr Biol*; **8**: e1017161.

267 Lin A, Hou Q, Jarzylo L, Amato S, Gilbert J, Shang F *et al.* Nedd4-mediated AMPA receptor ubiquitination regulates receptor turnover and trafficking. *J Neurochem* 2011; **119**: 27–39.

268 Scudder SL, Goo MS, Cartier AE, Molteni A, Schwarz LA, Wright R *et al.* Synaptic strength is bidirectionally controlled by opposing activity-dependent regulation of Nedd4-1 and USP8. *J Neurosci* 2014; **34**: 16637–49.

269 Rodrigues EM, Scudder SL, Goo MS, Patrick GN. Aβ-Induced Synaptic Alterations Require the E3 Ubiquitin Ligase Nedd4-1. *J Neurosci* 2016; **36**: 1590–5.

270 Camera D, Coleman HA, Parkington HC, Jenkins TA, Pow D V, Boase N *et al.* Learning, memory and long-term potentiation are altered in Nedd4 heterozygous mice. *Behav Brain Res* 2016; **303**: 176–81.

271 Tofaris GK, Kim HT, Hourez R, Jung J-W, Kim KP, Goldberg AL. Ubiquitin ligase Nedd4 promotes alpha-synuclein degradation by the endosomal-lysosomal pathway. *Proc Natl Acad Sci U S A* 2011; **108**: 17004–9.

272 Davies SE, Hallett PJ, Moens T, Smith G, Mangano E, Kim HT *et al.* Enhanced ubiquitin-dependent degradation by Nedd4 protects against α-synuclein accumulation and toxicity in animal models of Parkinson's disease. *Neurobiol Dis* 2014; **64**: 79–87.

273 Tardiff DF, Jui NT, Khurana V, Tambe MA, Thompson ML, Chung CY *et al.* Yeast reveal a 'druggable' Rsp5/Nedd4 network that ameliorates α-synuclein toxicity in neurons. *Science* 2013; **342**: 979–83.

274 Chung CY, Khurana V, Auluck PK, Tardiff DF, Mazzulli JR, Soldner F *et al.* Identification and rescue of α-synuclein toxicity in Parkinson patient-derived neurons. *Science* 2013; **342**: 983–7.

275 Shoshani T, Faerman A, Mett I, Zelin E, Tenne T, Gorodin S *et al.* Identification of a novel hypoxia-inducible factor 1-responsive gene, RTP801, involved in apoptosis. *Mol Cell Biol* 2002; **22**: 2283–93.

276 Ellisen LW, Ramsayer KD, Johannessen CM, Yang A, Beppu H, Minda K *et al.* REDD1, a developmentally regulated transcriptional target of p63 and p53, links p63 to regulation of reactive oxygen species. *Mol Cell* 2002; **10**: 995–1005.

277 Whitney ML, Jefferson LS, Kimball SR. ATF4 is necessary and sufficient for ER stress-induced upregulation of REDD1 expression. *Biochem Biophys Res Commun* 2009; **379**: 451–5.

278 Wang Z, Malone MH, Thomenius MJ, Zhong F, Xu F, Distelhorst CW. Dexamethasone-induced gene 2 (dig2) is a novel pro-survival stress gene induced rapidly by diverse apoptotic signals. *J Biol Chem* 2003; **278**: 27053–8.

279 Jin H-O, Seo S-K, Woo S-H, Kim E-S, Lee H-C, Yoo D-H *et al.* Activating transcription factor 4 and CCAAT/enhancer-binding protein-beta negatively regulate the mammalian target of rapamycin via Redd1 expression in response to oxidative and endoplasmic reticulum stress. *Free Radic Biol Med* 2009; **46**: 1158–67.

280 Sofer A, Lei K, Johannessen CM, Ellisen LW. Regulation of mTOR and cell growth in response to energy stress by REDD1. *Mol Cell Biol* 2005; **25**: 5834–45.

281 Corradetti MN, Inoki K, Guan K-L. The stress-inducted proteins RTP801 and RTP801L are negative regulators of the mammalian target of rapamycin pathway. *J Biol Chem* 2005; **280**: 9769–72.

282 Vega-Rubin-de-Celis S, Abdallah Z, Kinch L, Grishin N V, Brugarolas J, Zhang X. Structural analysis and functional implications of the negative mTORC1 regulator REDD1. *Biochemistry* 2010; **49**: 2491–501.

283 Lin L, Stringfield TM, Shi X, Chen Y. Arsenite induces a cell stress-response gene, RTP801, through reactive oxygen species and transcription factors Elk-1 and CCAAT/enhancer-binding protein. *Biochem J* 2005; **392**: 93–102.

284 Michel G, Matthes HWD, Hachet-Haas M, El Baghdadi K, de Mey J, Pepperkok R *et al.* Plasma membrane translocation of REDD1 governed by GPCRs contributes to mTORC1 activation. *J Cell Sci* 2014; **127**: 773–87.

285 Horak P, Crawford AR, Vadysirisack DD, Nash ZM, DeYoung MP, Sgroi D *et al.* Negative feedback control of HIF-1 through REDD1-regulated ROS suppresses tumorigenesis. *Proc Natl Acad Sci U S A* 2010; **107**: 4675–80.

286 del Olmo-Aguado S, Núñez-Álvarez C, Ji D, Manso AG, Osborne NN. RTP801 immunoreactivity in retinal ganglion cells and its down-regulation in cultured cells protect them from light and cobalt chloride. *Brain Res Bull* 2013; **98**: 132–44.

287 Canal M, Romaní-Aumedes J, Martín-Flores N, Pérez-Fernández V, Malagelada C. RTP801/REDD1: a stress coping regulator that turns into a troublemaker in neurodegenerative disorders. *Front Cell Neurosci* 2014; **8**: 313.

288 Dennis MD, Coleman CS, Berg A, Jefferson LS, Kimball SR. REDD1 enhances protein phosphatase 2A-mediated dephosphorylation of Akt to repress mTORC1 signaling. *Sci Signal* 2014; **7**: ra68.

289 Molitoris JK, McColl KS, Swerdlow S, Matsuyama M, Lam M, Finkel TH *et al.* Glucocorticoid elevation of dexamethasone-induced gene 2 (Dig2/RTP801/REDD1) protein mediates autophagy in lymphocytes. *J Biol Chem* 2011; **286**: 30181–9.

290 Dennis MD, McGhee NK, Jefferson LS, Kimball SR. Regulated in DNA damage and development 1 (REDD1) promotes cell survival during serum deprivation by sustaining repression of signaling through the mechanistic target of rapamycin in complex 1 (mTORC1). *Cell Signal* 2013; **25**: 2709–16.

291 Malagelada C, López-Toledano MA, Willett RT, Jin ZH, Shelanski ML, Greene LA. RTP801/REDD1 regulates the timing of cortical neurogenesis and neuron migration. *J Neurosci* 2011; **31**: 3186–96.

292 Malagelada C, Jin ZH, Jackson-Lewis V, Przedborski S, Greene LA. Rapamycin Protects against Neuron Death in In Vitro andIn Vivo Models of Parkinson's Disease. *J Neurosci* 2010; **30**: 1166–1175.

293 Choo AY, Blenis J. Not all substrates are treated equally: implications for mTOR, rapamycin-resistance and cancer therapy. *Cell Cycle* 2009; **8**: 567–72.

294 Choo AY, Yoon S-O, Kim SG, Roux PP, Blenis J. Rapamycin differentially inhibits S6Ks and 4E-BP1 to mediate cell-type-specific repression of mRNA translation. *Proc Natl Acad Sci U S A* 2008; **105**: 17414–9.

295 Katiyar S, Liu E, Knutzen CA, Lang ES, Lombardo CR, Sankar S *et al.* REDD1, an inhibitor of mTOR signalling, is regulated by the CUL4A-DDB1 ubiquitin ligase. *EMBO Rep* 2009; **10**: 866–72.

296 Romaní-Aumedes J, Canal M, Martín-Flores N, Sun X, Pérez-Fernández V, Wewering S *et al.* Parkin loss of function contributes to RTP801 elevation and neurodegeneration in Parkinson's disease. *Cell Death Dis* 2014; **5**: e1364.

297 Shimura H, Hattori N, Kubo S i, Mizuno Y, Asakawa S, Minoshima S *et al.* Familial Parkinson disease gene product, parkin, is a ubiquitin-protein ligase. *Nat Genet* 2000; **25**: 302–5.

298 Chung KKK, Thomas B, Li X, Pletnikova O, Troncoso JC, Marsh L *et al.* S-nitrosylation of parkin regulates ubiquitination and compromises parkin's protective function. *Science* 2004; **304**: 1328–31.

299 Winklhofer KF, Henn IH, Kay-Jackson PC, Heller U, Tatzelt J. Inactivation of parkin by oxidative stress and C-terminal truncations: a protective role of molecular chaperones. *J Biol Chem* 2003; **278**: 47199–208.

300 LaVoie MJ, Ostaszewski BL, Weihofen A, Schlossmacher MG, Selkoe DJ. Dopamine covalently modifies and functionally inactivates parkin. *Nat Med* 2005; **11**: 1214–21.

301 Graham FL, Smiley J, Russell WC, Nairn R. Characteristics of a Human Cell Line Transformed by DNA from Human Adenovirus Type 5. *J Gen Virol* 1977; **36**: 59–72.

302 Greene LA, Tischler AS. Establishment of a noradrenergic clonal line of rat adrenal pheochromocytoma cells which respond to nerve growth factor. *Proc Natl Acad Sci U S A* 1976; **73**: 2424–8.

303 Greene LA, Rein G. Release of (3H)norepinephrine from a clonal line of pheochromocytoma cells (PC12) by nicotinic cholinergic stimulation. *Brain Res* 1977; **138**: 521–8.

304 Shevchenko A, Tomas H, Havlis J, Olsen J V, Mann M. In-gel digestion for mass spectrometric characterization of proteins and proteomes. *Nat Protoc* 2006; **1**: 2856–60.

305 Shilov I V, Seymour SL, Patel AA, Loboda A, Tang WH, Keating SP *et al.* The Paragon Algorithm, a next generation search engine that uses sequence temperature values and feature probabilities to identify peptides from tandem mass spectra. *Mol Cell Proteomics* 2007; **6**: 1638–55.

306 Tang WH, Shilov I V, Seymour SL. Nonlinear fitting method for determining local false discovery rates from decoy database searches. *J Proteome Res* 2008; **7**: 3661–7.

307 Keller JN, Hanni KB, Markesbery WR. Impaired proteasome function in Alzheimer's disease. *J Neurochem* 2000; **75**: 436–9.

308 Jana NR, Zemskov EA, Wang Gh, Nukina N. Altered proteasomal function due to the expression of polyglutamine-expanded truncated N-terminal huntingtin induces apoptosis by caspase activation through mitochondrial cytochrome c release. *Hum Mol Genet* 2001; **10**: 1049–59.

309 Meng L, Mohan R, Kwok BH, Elofsson M, Sin N, Crews CM. Epoxomicin, a potent and selective proteasome inhibitor, exhibits in vivo antiinflammatory activity. *Proc Natl Acad Sci U S A* 1999; **96**:

10403–10408.

310 Goldberg AL. Development of proteasome inhibitors as research tools and cancer drugs. *J Cell Biol* 2012; **199**: 583–8.

311 Blok J, Mulder-Stapel a a, Ginsel L a, Daems WT. The effect of chloroquine on lysosomal function and cell-coat glycoprotein transport in the absorptive cells of cultured human small-intestinal tissue. *Cell Tissue Res* 1981; **218**: 227–51.

312 Xu C, Fan CD, Wang X. Regulation of Mdm2 protein stability and the p53 response by NEDD4-1 E3 ligase. *Oncogene* 2015; **34**: 281–9.

313 Chesarino NM, McMichael TM, Yount JS. E3 Ubiquitin Ligase NEDD4 Promotes Influenza Virus Infection by Decreasing Levels of the Antiviral Protein IFITM3. *PLOS Pathog* 2015; **11**: e1005095.

314 Kim E, Wang B, Sastry N, Masliah E, Nelson PT, Cai H *et al.* NEDD4-mediated HSF1 degradation underlies α-synucleinopathy. *Hum Mol Genet* 2016; **25**: 211–222.

315 Kim TY, Siesser PF, Rossman KL, Goldfarb D, Mackinnon K, Yan F *et al.* Substrate trapping proteomics reveals targets of the βTrCP2/FBXW11 ubiquitin ligase. *Mol Cell Biol* 2015; **35**: 167–81.

316 Karra D, Dahm R. Transfection techniques for neuronal cells. *J Neurosci* 2010; **30**: 6171–6177.

317 Tiscornia G, Singer O, Verma IM. Production and purification of lentiviral vectors. *Nat Protoc* 2006; **1**: 241–5.

318 Zhang Z, Larner SF, Liu MC, Zheng W, Hayes RL, Wang KKW. Multiple alphaII-spectrin breakdown products distinguish calpain and caspase dominated necrotic and apoptotic cell death pathways. *Apoptosis* 2009; **14**: 1289–1298.

319 Wang KKW. Calpain and caspase: Can you tell the difference? *Trends Neurosci* 2000; **23**: 20–26.

320 Gorski J a, Talley T, Qiu M, Puelles L, Rubenstein JLR, Jones KR. Cortical excitatory neurons and glia, but not GABAergic neurons, are produced in the Emx1-expressing lineage. *J Neurosci* 2002; **22**: 6309–6314.

321 Schwarzer R, Tondera D, Arnold W, Giese K, Klippel A, Kaufmann J. REDD1 integrates hypoxia-mediated survival signaling downstream of phosphatidylinositol 3-kinase. *Oncogene* 2005; **24**: 1138–49.

322 Zhong X, Lin R, Li Z, Mao J, Chen L. Effects of Salidroside on cobalt chloride-induced hypoxia damage and mTOR signaling repression in PC12 cells. *Biol Pharm Bull* 2014; **37**: 1199–1206.

323 Wang G, Hazra TK, Mitra S, Lee HM, Englander EW. Mitochondrial DNA damage and a hypoxic response are induced by CoCl(2) in rat neuronal PC12 cells. *Nucleic Acids Res* 2000; **28**: 2135–40.

324 Ochu EE, Rothwell NJ, Waters CM. Caspases mediate 6-hydroxydopamine-induced apoptosis but not necrosis in PC12 cells. *J Neurochem* 1998; **70**: 2637–40.

325 Grant RJ, Sellings LHL, Crocker SJ, Melloni E, Park DS, Clarke PBS. Effects of calpain inhibition on dopaminergic markers and motor function following intrastriatal 6-hydroxydopamine administration in rats. *Neuroscience* 2009; **158**: 558–69.

326 Urbanelli L, Magini A, Buratta S, Brozzi A, Sagini K, Polchi A *et al.* Signaling pathways in exosomes biogenesis, secretion and fate. *Genes (Basel)* 2013; **4**: 152–70.

327 Savina A, Furlán M, Vidal M, Colombo MI. Exosome release is regulated by a calcium-dependent mechanism in K562 cells. *J Biol Chem* 2003; **278**: 20083–90.

328 Fauré J, Lachenal G, Court M, Hirrlinger J, Chatellard-Causse C, Blot B *et al.* Exosomes are released by cultured cortical neurones. *Mol Cell Neurosci* 2006; **31**: 642–8.

329 Krämer-Albers E-M, Bretz N, Tenzer S, Winterstein C, Möbius W, Berger H *et al.* Oligodendrocytes secrete exosomes containing major myelin and stress-protective proteins: Trophic support for axons? - PubMed - NCBI. Proteomics. Clin. Appl. 2007; : Nov;1(11):1446–61.

330 Savina A, Fader CM, Damiani MT, Colombo MI. Rab11 promotes docking and fusion of multivesicular bodies in a calcium-dependent manner. *Traffic* 2005; **6**: 131–43.

331 Meng H, Li C, Feng L, Cheng B, Wu F, Wang X *et al.* Effects of Ginkgolide B on 6-OHDA-induced apoptosis and calcium over load in cultured PC12. *Int J Dev Neurosci* 2007; **25**: 509–14.

332 de Bie P, Ciechanover A. Ubiquitination of E3 ligases: self-regulation of the ubiquitin system via proteolytic and non-proteolytic mechanisms. *Cell Death Differ* 2011; **18**: 1393–402.

333 Gallagher E, Gao M, Liu Y-C, Karin M. Activation of the E3 ubiquitin ligase Itch through a phosphorylation-induced conformational change. *Proc Natl Acad Sci U S A* 2006; **103**: 1717–22.

334 Wiesner S, Ogunjimi AA, Wang H-R, Rotin D, Sicheri F, Wrana JL *et al.* Autoinhibition of the HECT-type ubiquitin ligase Smurf2 through its C2 domain. *Cell* 2007; **130**: 651–62.

335 Ruvinsky I, Meyuhas O. Ribosomal protein S6 phosphorylation: from protein synthesis to cell size. *Trends Biochem Sci* 2006; **31**: 342–348.

336 Navé BT, Ouwens M, Withers DJ, Alessi DR, Shepherd PR. Mammalian target of rapamycin is a direct target for protein kinase B: identification of a convergence point for opposing effects of insulin and amino-acid deficiency on protein translation. *Biochem J* 1999; **344 Pt 2**: 427–31.

337 Sekulić A, Hudson CC, Homme JL, Yin P, Otterness DM, Karnitz LM *et al.* A direct linkage between the phosphoinositide 3-kinase-AKT signaling pathway and the mammalian target of rapamycin in mitogen-stimulated and transformed cells. *Cancer Res* 2000; **60**: 3504–13.

338 Chiang GG, Abraham RT. Phosphorylation of mammalian target of rapamycin (mTOR) at Ser-2448 is mediated by p70S6 kinase. *J Biol Chem* 2005; **280**: 25485–90.

339 Chaugule VK, Burchell L, Barber KR, Sidhu A, Leslie SJ, Shaw GS *et al.* Autoregulation of Parkin activity through its ubiquitin-like domain. *EMBO J* 2011; **30**: 2853–67.

340 Stichel CC, Zhu X-R, Bader V, Linnartz B, Schmidt S, Lübbert H. Mono- and double-mutant mouse models of Parkinson's disease display severe mitochondrial damage. *Hum Mol Genet* 2007; **16**: 2377–93.

341 Zhang R, Zhang C, Zhao Q, Li D. Spectrin: structure, function and disease. *Sci China Life Sci* 2013; **56**: 1076–85.

342 Erazo A, Goff SP. Nuclear matrix protein Matrin 3 is a regulator of ZAP-mediated retroviral restriction. *Retrovirology* 2015; **12**: 57.

343 Daikoku S, Seko A, Son S-H, Suzuki K, Ito Y, Kanie O. The relationship between glycan structures and expression levels of an endoplasmic reticulum-resident glycoprotein, UDP-glucose: Glycoprotein glucosyltransferase 1. *Biochem Biophys Res Commun* 2015; **462**: 58–63.

344 Cunnea PM, Miranda-Vizuete A, Bertoli G, Simmen T, Damdimopoulos AE, Hermann S *et al.* ERdj5, an endoplasmic reticulum (ER)-resident protein containing DnaJ and thioredoxin domains, is expressed in secretory cells or following ER stress. *J Biol Chem* 2003; **278**: 1059–66.

345 Watson P, Townley AK, Koka P, Palmer KJ, Stephens DJ. Sec16 defines endoplasmic reticulum exit sites and is required for secretory cargo export in mammalian cells. *Traffic* 2006; **7**: 1678–87.

346 Ruohola H, Kabcenell AK, Ferro-Novick S. Reconstitution of protein transport from the endoplasmic reticulum to the Golgi complex in yeast: the acceptor Golgi compartment is defective in the sec23 mutant. *J Cell Biol* 1988; **107**: 1465–76.

347 Fu H, Subramanian RR, Masters SC. 14-3-3 Proteins: Structure, Function, and Regulation. *Annu Rev Pharmacol Toxicol* 2000; **40**: 617–647.

348 Wei Z, Sun M, Liu X, Zhang J, Jin Y. Rufy3, a protein specifically expressed in neurons, interacts with actin-bundling protein Fascin to control the growth of axons. *J Neurochem* 2014; **130**: 678–92.

349 Gräff J, Koshibu K, Jouvenceau A, Dutar P, Mansuy IM. Protein phosphatase 1-dependent transcriptional programs for long-term memory and plasticity. *Learn Mem* 2010; **17**: 355–63.

350 Leverenz JB, Umar I, Wang Q, Montine TJ, McMillan PJ, Tsuang DW *et al.* Proteomic identification of novel proteins in cortical lewy bodies. *Brain Pathol* 2007; **17**: 139–45.

351 Jimenez-Sanchez M, Lam W, Hannus M, Sönnichsen B, Imarisio S, Fleming A *et al.* siRNA screen identifies QPCT as a druggable target for Huntington's disease. *Nat Chem Biol* 2015; **11**: 347–54.

352 Spangler SA, Hoogenraad CC. Liprin-alpha proteins: scaffold molecules for synapse maturation. *Biochem Soc Trans* 2007; **35**: 1278–82.

353 McMahon HT, Boucrot E. Molecular mechanism and physiological functions of clathrin-mediated endocytosis. *Nat Rev Mol Cell Biol* 2011; **12**: 517–33.

354 Jung N, Haucke V. Clathrin-mediated endocytosis at synapses. *Traffic* 2007; **8**: 1129–36.

355 Owen DJ, Vallis Y, Pearse BM, McMahon HT, Evans PR. The structure and function of the beta 2-adaptin appendage domain. *EMBO J* 2000; **19**: 4216–27.

356 Gupta SN, Kloster MM, Rodionov DG, Bakke O. Re-routing of the invariant chain to the direct sorting pathway by introduction of an AP3-binding motif from LIMP II. *Eur J Cell Biol* 2006; **85**: 457–67.

357 Danglot L, Galli T. What is the function of neuronal AP-3? *Biol Cell* 2007; **99**: 349–61.

358 Wu Y, Matsui H, Tomizawa K. Amphiphysin I and regulation of synaptic vesicle endocytosis. *Acta Med Okayama* 2009; **63**: 305–23.

359 McMahon HT, Wigge P, Smith C. Clathrin interacts specifically with amphiphysin and is displaced by dynamin. *FEBS Lett* 1997; **413**: 319–22.

360 Olesen LE, Ford MGJ, Schmid EM, Vallis Y, Babu MM, Li PH *et al.* Solitary and repetitive binding motifs for the AP2 complex alpha-appendage in amphiphysin and other accessory proteins. *J Biol Chem* 2008; **283**: 5099–109.

361 Sullivan A, Lu X. ASPP: a new family of oncogenes and tumour suppressor genes. *Br J Cancer* 2007; **96**: 196–200.

362 Rodriguez-Rocha H, Garcia Garcia A, Zavala-Flores L, Li S, Madayiputhiya N, Franco R. Glutaredoxin 1 protects dopaminergic cells by increased protein glutathionylation in experimental Parkinson's disease. *Antioxid Redox Signal* 2012; **17**: 1676–93.

363 Fuertes G, Villarroya A, Knecht E. Role of proteasomes in the degradation of short-lived proteins in human fibroblasts under various growth conditions. *Int J Biochem Cell Biol* 2003; **35**: 651–64.

364 Cook C, Petrucelli L. A critical evaluation of the ubiquitin-proteasome system in Parkinson's disease. *Biochim Biophys Acta* 2009; **1792**: 664–75.

365 Zhang L, Sheng R, Qin Z. The lysosome and neurodegenerative diseases. *Acta Biochim Biophys Sin (Shanghai)* 2009; **41**: 437–445.

366 Bourdenx M, Dehay B. What lysosomes actually tell us about Parkinson's disease? *Ageing Res Rev* 2016. doi:10.1016/j.arr.2016.02.008.

367 Nathan JA, Kim HT, Ting L, Gygi SP, Goldberg AL. Why do cellular proteins linked to K63-polyubiquitin chains not associate with proteasomes? *EMBO J* 2013; **32**: 552–65.

368 Staub O, Abriel H, Plant P, Ishikawa T, Kanelis V, Saleki R *et al.* Regulation of the epithelial Na+ channel by Nedd4 and ubiquitination. *Kidney Int* 2000; **57**: 809–15.

369 Tan CY, Hagen T. mTORC1 Dependent Regulation of REDD1 Protein Stability. 2013; **8**: 1–8.

370 Zhao Y, Xiong X, Jia L, Sun Y. Targeting Cullin-RING ligases by MLN4924 induces autophagy via modulating the HIF1-REDD1-TSC1-mTORC1-DEPTOR axis. *Cell Death Dis* 2012; **3**: e386.

371 Xu G, Paige JS, Jaffrey SR. Global analysis of lysine ubiquitination by ubiquitin remnant immunoaffinity profiling. *Nat Biotechnol* 2010; **28**: 868–73.

372 Kim W, Bennett EJ, Huttlin EL, Guo A, Li J, Possemato A *et al.* Systematic and quantitative assessment of the ubiquitin-modified proteome. *Mol Cell* 2011; **44**: 325–40.

373 Lee KA, Hammerle LP, Andrews PS, Stokes MP, Mustelin T, Silva JC *et al.* Ubiquitin ligase substrate identification through quantitative proteomics at both the protein and peptide levels. *J Biol Chem* 2011; **286**: 41530–8.

374 Ingham RJ, Colwill K, Howard C, Dettwiler S, Lim CSH, Yu J *et al.* WW domains provide a platform for the assembly of multiprotein networks. *Mol Cell Biol* 2005; **25**: 7092–106.

375 Lu PJ, Zhou XZ, Shen M, Lu KP. Function of WW domains as phosphoserine- or phosphothreonine-binding modules. *Science* 1999; **283**: 1325–8.

376 Fan C-D, Lum MA, Xu C, Black JD, Wang X. Ubiquitin-dependent regulation of phospho-AKT dynamics by the ubiquitin E3 ligase, NEDD4-1, in the insulin-like growth factor-1 response. *J Biol Chem* 2013; **288**: 1674–84.

377 Romaní-Aumedes J. *Estudi de la regulació de la proteïna proapoptòtica RTP801 per l'E3 ubiquitina lligasa Parkina en la malaltia de Parkinson*. 2015.

378 Harvey KF, Harvey NL, Michael JM, Parasivam G, Waterhouse N, Alnemri ES *et al.* Caspase-mediated cleavage of the ubiquitin-protein ligase Nedd4 during apoptosis. *J Biol Chem* 1998; **273**: 13524–30.

379 Parkkinen L, O'Sullivan SS, Collins C, Petrie A, Holton JL, Revesz T *et al.* Disentangling the relationship between lewy bodies and nigral neuronal loss in Parkinson's disease. *J Parkinsons Dis* 2011; **1**: 277–86.

380 Kravtsova-Ivantsiv Y, Ciechanover A. Non-canonical ubiquitin-based signals for proteasomal degradation. *J Cell Sci* 2012; **125**: 539–48.

381 Magnifico A, Ettenberg S, Yang C, Mariano J, Tiwari S, Fang S *et al.* WW domain HECT E3s target Cbl RING finger E3s for proteasomal degradation. *J Biol Chem* 2003; **278**: 43169–77.

382 Zaaroor-Regev D, de Bie P, Scheffner M, Noy T, Shemer R, Heled M *et al.* Regulation of the polycomb protein Ring1B by self-ubiquitination or by E6-AP may have implications to the pathogenesis of Angelman syndrome. *Proc Natl Acad Sci U S A* 2010; **107**: 6788–93.

383 Hicke L. Protein regulation by monoubiquitin. *Nat Rev Mol Cell Biol* 2001; **2**: 195–201.

384 Mou C, Zhang Y, Zhang W, Ding Y, Chen L. Lysine residues 639 and 673 of mouse Ncoa3 are ubiquitination sites for the regulation of its stability. *Acta Biochim Biophys Sin (Shanghai)* 2014; **46**: 1066–71.

385 Rodriguez MS, Desterro JM, Lain S, Lane DP, Hay RT. Multiple C-terminal lysine residues target p53 for ubiquitin-proteasome-mediated degradation. *Mol Cell Biol* 2000; **20**: 8458–67.

386 Gerard B, Sanders MA, Visscher DW, Tait L, Shekhar MP V. Lysine 394 is a novel Rad6B-induced ubiquitination site on beta-catenin. *Biochim Biophys Acta* 2012; **1823**: 1686–96.

387 Batonnet S, Leibovitch MP, Tintignac L, Leibovitch SA. Critical role for lysine 133 in the nuclear ubiquitin-mediated degradation of MyoD. *J Biol Chem* 2004; **279**: 5413–20.

388 Favier FB, Costes F, Defour A, Bonnefoy R, Lefai E, Baugé S *et al.* Downregulation of Akt/mammalian target of rapamycin pathway in skeletal muscle is associated with increased REDD1 expression in response to chronic hypoxia. *Am J Physiol Regul Integr Comp Physiol* 2010; **298**: R1659–66.

389 Hernández G, Lal H, Fidalgo M, Guerrero A, Zalvide J, Force T *et al.* A novel cardioprotective p38-MAPK/mTOR pathway. *Exp Cell Res* 2011; **317**: 2938–49.

390 Pieri BLS, Souza DR, Luciano TF, Marques SO, Pauli JR, Silva ASR *et al.* Effects of physical exercise on the P38MAPK/REDD1/14-3-3 pathways in the myocardium of diet-induced obesity rats. *Horm Metab Res = Horm und Stoffwechselforsch = Horm métabolisme* 2014; **46**: 621–7.

391 Serra-Pagès C, Medley QG, Tang M, Hart A, Streuli M. Liprins, a family of LAR transmembrane protein-tyrosine phosphatase-interacting proteins. *J Biol Chem* 1998; **273**: 15611–20.

392 Spangler SA, Jaarsma D, De Graaff E, Wulf PS, Akhmanova A, Hoogenraad CC. Differential expression of liprin-α family proteins in the brain suggests functional diversification. *J Comp Neurol* 2011; **519**: 3040–60.

393 Ohno H. Physiological roles of clathrin adaptor AP complexes: lessons from mutant animals. *J Biochem* 2006; **139**: 943–8.

394 Collins BM, McCoy AJ, Kent HM, Evans PR, Owen DJ. Molecular architecture and functional model of the endocytic AP2 complex. *Cell* 2002; **109**: 523–35.

395 Owen DJ, Luzio JP. Structural insights into clathrin-mediated endocytosis. *Curr Opin Cell Biol* 2000; **12**: 467–74.

396 Cowles CR, Odorizzi G, Payne GS, Emr SD. The AP-3 Adaptor Complex Is Essential for Cargo-Selective Transport to the Yeast Vacuole. *Cell* 1997; **91**: 109–118.

397 Faúndez V, Horng JT, Kelly RB. A function for the AP3 coat complex in synaptic vesicle formation from endosomes. *Cell* 1998; **93**: 423–32.

398 Blumstein J, Faundez V, Nakatsu F, Saito T, Ohno H, Kelly RB. The neuronal form of adaptor protein-3 is required for synaptic vesicle formation from endosomes. *J Neurosci* 2001; **21**: 8034–42.

399 Tarazi FI, Sahli ZT, Wolny M, Mousa SA. Emerging therapies for Parkinson's disease: from bench to bedside. *Pharmacol Ther* 2014; **144**: 123–33.

400 Zhang D, Zhang J-J, Liu G-T. The novel squamosamide derivative (compound FLZ) attenuated 1-methyl, 4-phenyl-pyridinium ion (MPP+)-induced apoptosis and alternations of related signal transduction in SH-SY5Y cells. *Neuropharmacology* 2007; **52**: 423–9.

401 Zhang D, Zhang J-J, Liu G-T. The novel squamosamide derivative FLZ protects against 6-hydroxydopamine-induced apoptosis through inhibition of related signal transduction in SH-SY5Y cells. *Eur J Pharmacol* 2007; **561**: 1–6.

402 Bao X-Q, Kong X-C, Qian C, Zhang D. FLZ protects dopaminergic neuron through activating protein kinase B/mammalian target of rapamycin pathway and inhibiting RTP801 expression in Parkinson's disease models. *Neuroscience* 2012; **202**: 396–404.

403 Bao X-Q, Kong X-C, Kong L-B, Wu L-Y, Sun H, Zhang D. Squamosamide derivative FLZ protected dopaminergic neuron by activating Akt signaling pathway in 6-OHDA-induced in vivo and in vitro Parkinson's disease models. *Brain Res* 2014; **1547**: 49–57.

404 Tain LS, Mortiboys H, Tao RN, Ziviani E, Bandmann O, Whitworth AJ. Rapamycin activation of 4E-BP prevents parkinsonian dopaminergic neuron loss. *Nat Neurosci* 2009; **12**: 1129–35.

405 Lee DU, Huang W, Rittenhouse KD, Jessen B. Retina expression and cross-species validation of gene silencing by PF-655, a small interfering RNA against RTP801 for the treatment of ocular disease. *J Ocul Pharmacol Ther* 2012; **28**: 222–30.

406 Nguyen QD, Schachar RA, Nduaka CI, Sperling M, Basile AS, Klamerus KJ *et al.* Phase 1 dose-escalation study of a siRNA targeting the RTP801 gene in age-related macular degeneration patients. *Eye (Lond)* 2012; **26**: 1099–105.

407 Nguyen QD, Schachar RA, Nduaka CI, Sperling M, Basile AS, Klamerus KJ *et al*. Dose-ranging evaluation of intravitreal siRNA PF-04523655 for diabetic macular edema (the DEGAS study). *Invest Ophthalmol Vis Sci* 2012; **53**: 7666–74.

408 Rittenhouse KD, Johnson TR, Vicini P, Hirakawa B, Kalabat D, Yang AH *et al.* RTP801 gene expression is differentially upregulated in retinopathy and is silenced by PF-04523655, a 19-Mer siRNA directed against RTP801. *Invest Ophthalmol Vis Sci* 2014; **55**: 1232–40.

409 Hong S-W, Moon J-H, Kim J-S, Shin J-S, Jung K-A, Lee W-K *et al.* p34 is a novel regulator of the oncogenic behavior of NEDD4-1 and PTEN. *Cell Death Differ* 2014; **21**: 146–60.

410 Martín-Flores N, Romaní-Aumedes J, Rué L, Canal M, Sanders P, Straccia M *et al.* RTP801 Is Involved in Mutant Huntingtin-Induced Cell Death. *Mol Neurobiol* 2015. doi:10.1007/s12035-015-9166-6.

PUBLICATIONS

PUBLICATIONS DERIVED FROM THIS THESIS:

Canal M, Romaní-Aumedes J, Martín-Flores N, Pérez-Fernández V, Malagelada C. RTP801/REDD1: a stress coping regulator that turns into a troublemaker in neurodegenerative disorders. *Front Cell Neurosci* 2014; **8**: 313 [287]

Canal M, Martin-Flores N, Pérez-Sisqués L, Romaní-Aumedes J, Atlas B, Man H, Kawabe H, Alberch J, Malagelada C. Loss of NEDD4 contributes to RTP801 elevation and neuron toxicity: implications for Parkinson's disease (Submitted)

PUBLICATIONS IN WHICH I HAVE PARTICIPATED DURING THIS THESIS:

Romaní-Aumedes J, Canal M, Martín-Flores N, Sun X, Pérez-Fernández V, Wewering S *et al.* Parkin loss of function contributes to RTP801 elevation and neurodegeneration in Parkinson's disease. *Cell Death Dis* 2014; **5**: e1364 [296]

Martin-Flores N, Romani-Aumedes J, Rue L, Canal M, Sanders P, Straccia M et al. RTP801 is involved in mutant huntingtin-induced cell death. *Mol Neurobiol 2015*. Doi:10.1007/s12035-015-9166-6[410]

frontiers in
CELLULAR NEUROSCIENCE

MINI REVIEW ARTICLE
published: 02 October 2014
doi: 10.3389/fncel.2014.00313

RTP801/REDD1: a stress coping regulator that turns into a troublemaker in neurodegenerative disorders

Mercè Canal, Joan Romaní-Aumedes, Núria Martín-Flores, Víctor Pérez-Fernández and Cristina Malagelada*

Department of Pathological Anatomy, Pharmacology and Microbiology, Faculty of Medicine, University of Barcelona, Barcelona, Catalonia, Spain

Edited by:
Rosanna Parlato, Ulm University, Germany

Reviewed by:
Hermona Soreq, The Hebrew University of Jerusalem, Israel
Davide Pozzi, Humanitas Research Hospital, Italy

***Correspondence:**
Cristina Malagelada, Department of Pathological Anatomy, Pharmacology and Microbiology, Faculty of Medicine, University of Barcelona, Casanova 143, Barcelona, Catalonia 08036, Spain
e-mail: cristina.malagelada@ub.edu

Mechanistic target of Rapamycin (mTOR) pathway regulates essential processes directed to preserve cellular homeostasis, such as cell growth, proliferation, survival, protein synthesis and autophagy. Importantly, mTOR pathway deregulation has been related to many diseases. Indeed, it has become a hallmark in neurodegenerative disorders, since a fine-tuned regulation of mTOR activities is crucial for neuron function and survival. RTP801/REDD1/Dig2 has become one of the most puzzling regulators of mTOR. Although the mechanism is not completely understood, RTP801 inactivates mTOR and Akt via the tuberous sclerosis complex (TSC1/TSC2) in many cellular contexts. Intriguingly, RTP801 protects dividing cells from hypoxia or H_2O_2-induced apoptosis, while it sensitizes differentiated cells to stress. Based on experimental models of Parkinson's disease (PD), it has been proposed that at early stages of the disease, stress-induced RTP801 upregulation contributes to mTOR repression, in an attempt to maintain cell function and viability. However, if RTP801 elevation is sustained, it leads to neuron cell death by a sequential inhibition of mTOR and Akt. Here, we will review RTP801 deregulation of mTOR in a context of PD and other neurodegenerative disorders.

Keywords: RTP801, REDD1, mTOR, Akt, stress, neurodegeneration, neuron, Parkinson's disease

RTP801 OVERVIEW

RTP801 (also known as REDD1 or Dig2) is a protein encoded by the stress responsive gene DNA-damage-inducible transcript 4 (*DDIT4*). It was initially identified and cloned in 2002 by two different groups simultaneously.

Shoshani et al. (2002) screened for hypoxia-regulated genes in rat C6 glioma cells and they identified a highly up-regulated gene responsive to HIF-1, involved in the regulation of cellular reactive oxygen species (ROS). It was designated *RTP801* (Shoshani et al., 2002).

Concurrently, Ellisen et al. (2002) cloned a gene induced after DNA damage and during embryogenesis in a p53 and p63 dependent manner. This gene was involved in the regulation of ROS and was alternatively named *REDD1*, for regulated in development and DNA damage responses one (Ellisen et al., 2002).

Later in 2003, Wang et al. discovered Dig2 (for dexamethasone-induced gene 2), the mouse homolog of *RTP801/REDD1* in an oligonucleotide microarray analysis from dexamethasone-treated murine lymphoma T cells (Wang et al., 2003).

Further studies displayed *DDIT4* as a rapidly upregulated gene under multiple cellular stresses, such as heat shock (Wang et al., 2003), ionizing radiation (Ellisen et al., 2002), hypoxia (Shoshani et al., 2002; Brugarolas et al., 2004) and energy depletion (Sofer et al., 2005). Moreover other chemical molecules also upregulated *DDIT4* expression, such as dopaminergic neurotoxins 6-hydroxydopamine, MPTP/MPP+ and rotenone (Malagelada et al., 2006), endoplasmatic reticulum (ER) stress inducers tunicamycin and thapsigargin (Wang et al., 2003; Whitney et al., 2009), DNA damage agent etoposide (Wang et al., 2003) and arsenite (Lin et al., 2005b).

RTP801, as a 232 aminoacids protein, is ubiquitously expressed at low levels in numerous human adult tissues (Shoshani et al., 2002). RTP801 localizes in the cytoplasm, the nucleus (Ellisen et al., 2002; Lin et al., 2005b; Michel et al., 2014) and in the membranes (DeYoung et al., 2008; Michel et al., 2014). Besides, a small fraction of RTP801 was detected in the mitochondria in HEK293T cells (Horak et al., 2010) and in *RGC-5* retinal ganglion cell line (del Olmo-Aguado et al., 2013).

There is a related human transcript called RTP801L (RTP801-like) or REDD2 that displays ~50% sequence identity to RTP801 and has similar functions (Ellisen et al., 2002; Corradetti et al., 2005).

Besides humans, RTP801 is also present in other organisms such as rat, mouse and *Xenopus*. In *Drosophila* it has two related orthologs called Scylla and Charybdis (Reiling and Hafen, 2004).

No functional motifs or structural domains could be identified from RTP801 amino acid sequence analysis and, to date, the entire crystal structure has not been solved. Indeed, only one group crystallized a segment containing aminoacids 89–226 with a deletion of the hydrophobic region ^{200}FLPGF^{204} of the human RTP801 protein (Vega-Rubin-de-Celis et al., 2010). Their work has given new insights into RTP801 structure. They found

that RTP801 presents a unique topology characterized by a two-layered α/β sandwich with a psi-loop motif. Furthermore, a surface patch formed by highly conserved residues was found to be critical for its function. It is formed by two separated regions, ^{138}EPCG^{141} and ^{218}KKKLYSSE^{225}, that are contiguous in the three-dimensional structure (Vega-Rubin-de-Celis et al., 2010). Importantly, the stretch of three lysines ^{218}KKK^{220} is necessary for RTP801 to localize in both mitochondria (Horak et al., 2010) and plasma membrane (Michel et al., 2014).

The key function of RTP801 is its ability to inactivate mTOR (Brugarolas et al., 2004; Corradetti et al., 2005), a master regulator kinase that integrates extracellular signals with intracellular responses to nutrients, growth factors or stress. Indeed, mTOR regulation has a crucial role in development, cancer or in neural survival and plasticity (Hoeffer and Klann, 2010; Laplante and Sabatini, 2012).

RTP801 has a dual role depending on the cellular context, meaning that in proliferating non differentiated cells, RTP801 is anti-apoptotic, and in non-dividing differentiated cells like neurons, RTP801 is pro-apoptotic (Shoshani et al., 2002; Malagelada et al., 2006). This dual function could be nicely observed in a study of rat cortical neurogenesis, where RTP801 controlled neuroprogenitors proliferation and neuronal differentiation. In cortical neuroprogenitors RTP801 was elevated without being toxic. On the contrary, newborn and mature neurons showed lower levels of RTP801. Indeed, if RTP801 elevation was sustained in these differentiating neurons it became pro-apoptotic (Malagelada et al., 2011). How RTP801 can trigger these dual actions based on the cell context is not completely understood and requires further investigation.

In the last decade the role of mTOR in neural cells has become very relevant. Indeed, in the nervous system mTOR controls crucial processes such as protein translation, long-lasting synaptic plasticity and survival via Akt (Tang et al., 2002; Cammalleri et al., 2003; Malagelada et al., 2008). Evidence suggests that mTOR deregulation is involved in neurodegeneration, and therefore the role of RTP801 has emerged as an object of study. In this sense, it will be crucial to understand the fine balance between RTP801 as a stress-coping protein and RTP801 as a pro-apoptotic effector in neurological disorders. Understanding these complex mechanisms will help to design successful therapeutic strategies to halt or, at least, delay neurodegeneration.

HOW IS RTP801 UPREGULATED?

Previous studies suggest that RTP801 toxicity in neurons is proportional to its protein levels (Malagelada et al., 2010; Ota et al., 2014). RTP801 protein increase can be the end point of two different processes: (1) as a result of gene activation by cellular stress (Ryu et al., 2005; Malagelada et al., 2006); and (2) a defective RTP801 degradation (Romaní-Aumedes et al., 2014). Here we will describe the transcription factors responsible for *DDIT4* gene induction, the microRNAs (miRNAs) that regulate its translation and the post-translational events in charge of regulating RTP801 protein levels.

RTP801 TRANSCRIPTIONAL REGULATION

The variety of transcription factors able to induce *DDIT4* gene expression in response to different stressors illustrates the complexity of its regulation. In fact, one feature of the regulation of RTP801/*DDIT4* is its rapidity, crucial to activate the coping mechanisms of the cell in response to the hostile environment. For example, hypoxia upregulates RTP801 expression via HIF-1, since the *DDIT4* gene contains a HRE (hypoxia-response element) in the promoter (Shoshani et al., 2002; Brugarolas et al., 2004). Another hypoxia-mimetic agent, cobalt chloride ($CoCl_2$), needs co-activation of HIF-1 and Sp1 to induce RTP801 (Jin et al., 2007).

Deoxyribonucleic acid (DNA) damaging agents, including ionizing radiation and the DNA alkylating agent methyl methane sulfonate (MMS) also boosted RTP801 expression (Ellisen et al., 2002; Lin et al., 2005a). Ionizing radiation induced RTP801 in a p53-dependent manner in mouse embryonic fibroblasts (MEFs; Ellisen et al., 2002). DNA-damage-inducible transcript 4 transcription was also enhanced by MMS in human keratinocytes via Elk-1 and CCAAT/enhancer-binding protein (C/EBP) in a p53-independent manner (Lin et al., 2005a). Furthermore, RTP801 has also been identified as a transcription target of Elk-1 and C/EBP in response to arsenic-induced ROS (Lin et al., 2005b).

Endoplasmatic reticulum (ER) stress caused by tunicamycin or thapsigargin upregulated RTP801 via activating transcriptional factor 4 (ATF4; Jin et al., 2009; Whitney et al., 2009). ATF4 was also identified as a transcription factor for RTP801 in response to oxidative stress induced by hydrogen peroxide (Jin et al., 2009). Interestingly, ATF4 has a protective role in cellular models of Parkinson's disease (PD) by modulating the levels of the E3 ligase parkin (Sun et al., 2013).

Other transcription factors have been described for *DDIT4* gene regulation like the nuclear factor of activated T-cell c3 (NFAT c3; Zhou et al., 2012) or PLZF in spermatogonial progenitors (Hobbs et al., 2010).

It is noteworthy that all these stressors, via different transcription factors, elevate RTP801 with a common objective to inactivate mTOR. This common response to stressors corroborates the complexity of the integration of the stress signals to modulate mTOR effectively.

Many other stress responsive genes with pro-apoptotic functions are also upregulated in parallel with DDIT4. However, due to space limitations, they will not be reviewed in this text (reviewed in Fulda et al., 2010).

RTP801 TRANSLATIONAL REGULATION

MicroRNA are negative regulators of gene expression and can function as tumor suppressors or oncogenes. To date, at least three miRNAs have been described as regulators of RTP801/REDD1 expression in a context of tumorigenesis. MiR-495 regulates breast cancer stem cells proliferation and hypoxia resistance by regulating RTP801 expression (Hwang-Verslues et al., 2011). Another miRNA, the miR-221, stimulates hepatocarcinogenesis by down-regulating RTP801 expression (Pineau et al., 2010). Furthermore, Micro-RNA30c down-regulates REDD1 expression in human hematopoietic and osteoblast cells after gamma-irradiation (Li et al., 2012).

To our knowledge, no miRNA that modulates RTP801 expression in a context of neurodegeneration has been described. In a near future, miRNAs along with the long non-coding RNAs may have a relevant impact in the regulation of RTP801 levels and function.

RTP801 POST-TRANSLATIONAL REGULATION

Post-translational modifications like phosphorylation, acetylation, ubiquitination or myristoylation, have an important impact in protein stability, function and cellular localization. Indeed, cellular stresses can also affect turnover of many proteins, including RTP801.

Apart from its rapid gene induction under stress, RTP801 proteostasis will also determine its stability, and therefore, its regulatory function towards mTOR.

Related to that, RTP801 mRNA (Wang et al., 2003) and RTP801 protein (Kimball et al., 2008; Katiyar et al., 2009; Malagelada et al., 2010) half-lives are significantly short, revealing that RTP801 is an extremely unstable protein with a fine-tuned post-translational regulation.

One of the modifications that will lead to a rapid protein turnover is ubiquitination. In fact, RTP801 is poly-ubiquitinated and targeted for the ubiquitin-proteasome system (UPS; Katiyar et al., 2009; Romaní-Aumedes et al., 2014).

To date, only three E3 ring ligases have been identified to poly-ubiquitinate RTP801. The first one described was CUL4A-DDB1-ROC1-β-TRCP E3 ligase complex. The complex ubiquitinated RTP801 and targeted it for proteasomal degradation, in a GSK3β-phosphorylation-dependent manner (Katiyar et al., 2009).

The second E3 ubiquitin ligase for RTP801 was HUWE1/MULE that modulated RTP801 protein levels although this regulation seemed to be UPS-independent (Tan and Hagen, 2013).

So far, the role of both ligases in regulating RTP801 in neurodegenerative disorders has not been elucidated.

In our recent work, we found that parkin RING E3 ligase poly-ubiquitinates RTP801 to mediate its UPS degradation. Based on the results obtained in cellular and animal models and in samples from human parkin mutant carriers, we proposed that RTP801 elevation due to parkin loss-of-function in both parkin mutants and in idiopathic PD might contribute importantly to neurodegeneration (Romaní-Aumedes et al., 2014).

In a near future, other ligases will eventually be proved to ubiquitinate RTP801, due to its central role in regulating mTOR.

RTP801 INACTIVATES mTOR VIA TUBEROUS SCLEROSIS COMPLEX

Under stress conditions downregulation of mTOR activity caused by hypoxia, energy stress or exposure to dopaminergic neurotoxins required the expression of RTP801 and an intact TSC1/TSC2 tumor suppressor complex (Brugarolas et al., 2004; Sofer et al., 2005; Malagelada et al., 2006). Interestingly, despite the clear necessity of the intact TSC1/2 complex for RTP801 to downregulate mTOR, RTP801 does not seem to interact physically with either TSC1 or TSC2 (Vega-Rubin-de-Celis et al., 2010).

Tuberous sclerosis complex (TSC) is a heterodimer formed by two proteins, the tuberous sclerosis tumor suppressors TSC1 and TSC2. TSC2 has a catalytic function as a GTPase activating protein (GAP), and it acts toward the small GTPase Rheb, an upstream positive mTOR regulator (Inoki et al., 2003; Tee et al., 2003). TSC2 can be phosphorylated by several kinases in response to upstream signals, and they will modify its regulation towards mTORC1 (reviewed in Ma and Blenis, 2009). Akt can phosphorylate TSC2 in response to growth factors (Inoki et al., 2002). This event is thought to favor TSC2 binding to protein 14-3-3, instead to TSC1, leading to TSC2 inhibition, to finally activate mTORC1 (Cai et al., 2006).

Regarding the modulatory role of 14-3-3 towards TSC2, DeYoung et al. (2008) proposed a molecular mechanism by which RTP801 regulates TSC1/2-mTOR signaling involving 14-3-3. Other studies also reported interaction between RTP801 and 14-3-3 proteins by co-immunoprecipitation experiments (Favier et al., 2010; Hernández et al., 2011; Pieri et al., 2014).

However, this RTP801 direct binding to 14-3-3 has been questioned by others (Vega-Rubin-de-Celis et al., 2010). The supposed 14-3-3 binding motif in RTP801 (^{133}RLAYSEP^{139}) is not conserved within species and the crystallized RTP801 structure analysis does not reveal any established mode for 14-3-3 binding. Thus, the inhibitory mechanisms of RTP801 towards mTOR need to be further investigated.

RTP801 UPREGULATION IN NEURODEGENERATION

The etiology of PD and many other neurodegenerative disorders involves both environmental factors and genetic predisposition. Indeed, exposure to several environmental toxins such as pesticides and metals has been implicated in its pathogenesis (Migliore and Coppede, 2009; Cannon and Greenamyre, 2011; Baltazar et al., 2014).

Arsenic is a heavy metal that has been linked to neurotoxicity and carcinogenesis in humans by a mechanism involving ROS production (reviewed in Qian et al., 2003). Interestingly, arsenite induced RTP801 transcription (Lin et al., 2005b).

Moreover, extensively used dithiocarbamate pesticides Maneb (MB) and Mancozeb (MZ) induced DNA damage and elevated RTP801 mRNA and protein expression (Cheng et al., 2014). The toxicity mechanism of these pesticides has been linked to NF-κB activation, revealing a cross-talk between RTP801 and NF-κB (Cheng et al., 2014).

In line with this, RTP801 was also identified as an amyloid-β-peptide (Aβ) responsive gene. Amyloid-beta is a neurotoxic molecule and the main component of senile plaques in Alzheimer's disease (AD; Kim et al., 2003).

Dopaminergic neurotoxins also upregulated RTP801 in cellular and animal models. Specifically, RTP801 was upregulated at both transcriptional and protein level in neuronal PC12 cells treated with PD mimetic toxins 6-OHDA, MPP^+ and rotenone, and it was also induced in neurons of MPTP-treated mice and in Substantia Nigra pars compacta (SNpc) degenerating neurons of PD patients. Furthermore, RTP801 knockdown with short hairpin RNAs (shRNAs) protected the cultures from PD mimetic toxins (Malagelada et al., 2006).

Ubiquitin-proteasome system deregulation has been implicated in neurodegenerative disorders (Keller et al., 2000; Jana et al., 2001; McNaught et al., 2003). Accumulations of misfolded or aggregated proteins may hamper cellular functions and eventually lead to neuronal death (reviewed in Tanaka and Matsuda, 2014). RTP801 brief protein half-life suggests that UPS malfunction would affect RTP801 protein levels. Therefore it is logical to suggest that a proper RTP801 degradation might be crucial for neuron function and survival.

Thus, chronic and progressive RTP801 elevation could become a hallmark of neurodegenerative disorders due to a combination of stress-induced gene activation and UPS malfunction.

THE ROLE OF RTP801 IN NEURODEGENERATIVE DISORDERS

RTP801 behaves like many other stress-induced genes, where a small increase is beneficial but a chronic and sustained increase is detrimental for the neuron. Interestingly, since RTP801 is able to inactivate protein translation, via mTOR, and survival, via Akt (Malagelada et al., 2006, 2008, 2010), its pro-apoptotic role may be relevant to other neurodegenerative diseases.

In PD, RTP801 elevation was initially identified in cellular and animal models of the disease. These results were further confirmed in nigral neurons from both idiopathic PD and mutant parkin human brains, meaning that RTP801 may have a relevant role in the disease itself (Malagelada et al., 2006).

Since RTP801 elevation is necessary and sufficient to trigger neuronal death, it is logical to think that the upregulation in the SN from PD human brains might be detrimental for the nigral neurons. Interestingly RTP801 induces cell death through a mechanism involving TSC1/2 and mTOR repression (Malagelada et al., 2006). Indeed, RTP801 repression of mTOR led also to the suppression of the phosphorylation of the neuronal survival kinase Akt (Malagelada et al., 2008), reviewed in (Greene et al., 2011). This negative regulation of Akt was also observed in nigral neurons from PD human brains.

Based on these results, we proposed a mechanism to explain RTP801 contribution to neurodegeneration in PD, where low levels of RTP801 would help neurons to cope with stress, but if this inactivation were sustained in time, it would impair neuronal function and survival. At the latest stage, and when the critical threshold of mTOR/Akt inactivation is surpassed, neuronal death will occur (Malagelada et al., 2006, 2008; see **Figure 1**). This proposed mechanism is supported by the observation of elevated RTP801 and diminished Akt phosphorylation in nigral neurons of PD brains (Malagelada et al., 2006; Romaní-Aumedes et al., 2014).

To extend this working model, one possibility would be that at early stages of many neurodegenerative disorders, RTP801 induction by cellular stresses would contribute to mTOR depression in an attempt to preserve neuron function and viability. However, at more advanced disease stages, when RTP801 upregulation is prolonged in time, it can eventually promote neurodegeneration and neuronal death through mTOR and pro-survival kinase Akt inactivation, as it has been proposed in the PD studies.

In AD an elevation of both RTP801/REDD1 gene and protein was observed in lymphocytes from AD patients compared to age-matched controls. Damjanac et al. (2009) showed that Double-stranded RNA-dependent protein kinase (PKR), a cognitive decline biomarker with an impairing protein translation function, by phosphorylating p53, activated REDD1 gene transcription. It could be interesting to explore whether this mechanism can be observed also in hippocampal neurons or in AD murine models.

Recently, RT801 has been determined crucial for stress-mediated synaptic loss and depressive behavior. Chronic unpredictable stress increased RTP801 mRNA and protein levels in rat prefrontal cortex (PFC). This RTP801 upregulation was coincident with a reduced phosphorylation of mTORC1/2 signaling targets S6K, 4EBP1, and Akt. In agreement, RTP801 was elevated in postmortem PFC of patients with major depressive disorder compared to psychiatrically healthy controls. RTP801 knockout mice were resilient to the synaptic and behavior deficits caused by stress, while RTP801 overexpression in rat PFC was sufficient to promote neuronal atrophy and depressive behavior (Ota et al., 2014).

Further investigations are needed to elucidate the role of RTP801 in many other neurological disorders. It will be interesting to explore whether RTP801 levels are upregulated and whether they correlate with the degree of mTOR/Akt repression. Also, it will be important to determine whether RTP801 is promoting neuron death through the same mechanism proposed as in PD models.

RTP801 AS A POTENTIAL THERAPEUTIC TARGET IN NEUROLOGICAL DISORDERS

Neurodegenerative disorders are characterized by neuronal death of specific subpopulations, such as loss of SN dopaminergic neurons in PD (reviewed in Dauer and Przedborski, 2003). However, current PD therapies ameliorate symptoms but do not prevent neuronal death. Thus, it is essential to investigate the mechanisms that underlie neuronal death and identify targets involved in the pathophysiology (reviewed in Levy et al., 2009). Based on several studies, RTP801 could become one such potential therapeutic target (Brafman et al., 2004; Malagelada et al., 2010; Tarazi et al., 2014).

RTP801 promotes cell death by sequentially inactivating mTOR and Akt (Malagelada et al., 2006, 2008). Thus, compounds that can restrain RTP801 expression or modulate the mTOR/Akt pathway may become therapeutic and delay neurodegeneration and neuronal cell death in PD (reviewed in Tarazi et al., 2014).

One such compound is 8-methyl-6-phenoxy-2-(tetrahydropyran-4-ylamino)pyrido[2,3-d]pyrimidin-7-one (FLZ), a synthetic squamoside derivative from a Chinese herb that protected dopaminergic neurons from apoptosis triggered by MPP^+ and 6-OHDA (Zhang et al., 2007a,b). Interestingly, FLZ neuroprotective actions in PD involved activation of Akt/mTOR signaling pathway and inhibition of RTP801 expression (Bao et al., 2012, 2014).

Another promising compound is rapamycin, an allosteric inhibitor of some but not all mTOR activities. Rapamycin conferred neuroprotection in both cellular and animal models of PD (Tain et al., 2009; Dehay et al., 2010; Malagelada et al., 2010). The results obtained support the hypothesis in which rapamycin

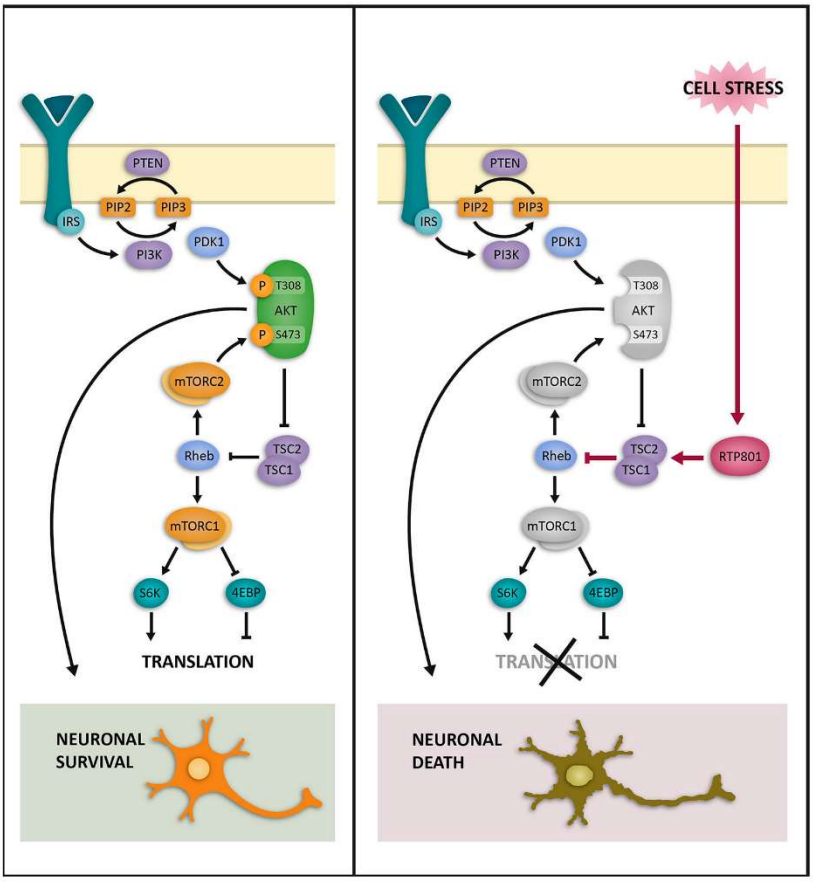

FIGURE 1 | Schematic representation of the hypothesized regulation of mTOR/Akt by RTP801 in neurons. In physiological conditions the gene and the protein levels of RTP801 are low; mTOR is active and promotes protein translation (mTORC1) and Akt phosphorylation at Ser473 residue (mTORC2). These signals mediate neuronal survival (left panel). However, when neurons are under stress, RTP801 is induced at gene and protein levels, and promotes mTORC1 and mTORC2 inhibition through TSC1-TSC2 complex and Rheb protein. These events result in protein translation inhibition and prevent Akt phosphorylation at residues Ser473 and, consequently, at Thr308. If this mTOR/Akt repression is sustained over time neuron function is impaired and leads to neuron death (right panel). *Illustration by Olivares-Boldú L.*

blocks RTP801 translation and, as a consequence, it mitigates mTOR repression leading to Akt phosphorylation maintenance at a site critical for its pro-survival activity (Malagelada et al., 2010). In contrast, Torin 1, an inhibitor of all mTOR actions since it blocks the ATP-binding site, was not protective and promoted Akt dephosphorylation and neuron death. So, rapamycin protection derives from its partial suppression of certain mTOR actions due to its allosteric properties (Malagelada et al., 2010).

Nonetheless, further investigations are required to evaluate the potential therapeutic role of these two agents in PD.

In animal and cellular models of cerebral ischemia, Ligustilide, a major active agent of Radix Angelicae Sinensis, the root of a chinese herb called Danngui, is neuroprotective by inhibiting RTP801 expression, in addition to promote Erythropoietin transcription via extracellular-signal-regulated kinases (ERK) signaling pathway (Wu et al., 2011).

The most advanced example of RTP801 as a therapeutic target is found in retinopathies. RTP801 has an important role in the pathogenesis of retinopathies, since the absence of RTP801 expression in a mouse model attenuated the development of the disease (Brafman et al., 2004). PF-04523655, a 19-ribonucleotide siRNA designated to inhibit RTP801 transcription is currently in clinical trials for retinopathy treatment (Lee et al., 2012; Nguyen et al., 2012a,b; Rittenhouse et al., 2014).

In summary, RTP801 is one clear example of a protein that is upregulated to cope with cellular stress although its sustained

progressive elevation leads to neuron degeneration and death. RTP801 progressive elevation and its inhibitory function towards pro-survival kinases mTOR and Akt could explain its role in several neurodegenerative diseases.

ACKNOWLEDGMENTS

Supported in part by grants from the Spanish Ministry of Science and Innovation (SAF2010-21058), the PEOPLE Programme—Marie Curie Actions, European Community (PIRG08-GA-2010-276957). Supported also by the crowdfunding campaign "SOS recerca en Parkinson" via Goteo.org, Portal d'Avall, S. L. and the app "Mememtum: early detection of neurological disorders". Illustrations were designed by Laura Olivares-Boldú.

REFERENCES

Baltazar, M. T., Dinis-Oliveira, R. J., de Lourdes Bastos, M., Tsatsakis, A. M., Duarte, J. A., and Carvalho, F. (2014). Pesticides exposure as etiological factors of Parkinson's disease and other neurodegenerative diseases-A mechanistic approach. *Toxicol. Lett.* 230, 85–103. doi: 10.1016/j.toxlet.2014.01.039

Bao, X. Q., Kong, X. C., Kong, L. B., Wu, L. Y., Sun, H., and Zhang, D. (2014). Squamosamide derivative FLZ protected dopaminergic neuron by activating Akt signaling pathway in 6-OHDA-induced in vivo and in vitro Parkinson's disease models. *Brain Res.* 1547, 49–57. doi: 10.1016/j.brainres.2013.12.026

Bao, X. Q., Kong, X. C., Qian, C., and Zhang, D. (2012). FLZ protects dopaminergic neuron through activating protein kinase B/mammalian target of rapamycin pathway and inhibiting RTP801 expression in Parkinson's disease models. *Neuroscience* 202, 396–404. doi: 10.1016/j.neuroscience.2011.11.036

Brafman, A., Mett, I., Shafir, M., Gottlieb, H., Damari, G., Gozlan-Kelner, S., et al. (2004). Inhibition of oxygen-induced retinopathy in RTP801-deficient mice. *Invest. Ophthalmol. Vis. Sci.* 45, 3796–3805. doi: 10.1167/iovs.04-0052

Brugarolas, J., Lei, K., Hurley, R. L., Manning, B. D., Reiling, J. H., Hafen, E., et al. (2004). Regulation of mTOR function in response to hypoxia by REDD1 and the TSC1/TSC2 tumor suppressor complex. *Genes Dev.* 18, 2893–2904. doi: 10.1101/gad.1256804

Cai, S. L., Tee, A. R., Short, J. D., Bergeron, J. M., Kim, J., Shen, J., et al. (2006). Activity of TSC2 is inhibited by AKT-mediated phosphorylation and membrane partitioning. *J. Cell. Biol.* 173, 279–289. doi: 10.1083/jcb.200507119

Cammalleri, M., Lütjens, R., Berton, F., King, A. R., Simpson, C., Francesconi, W., et al. (2003). Time-restricted role for dendritic activation of the mTOR-p70S6K pathway in the induction of late-phase long-term potentiation in the CA1. *Proc. Natl. Acad. Sci. U S A* 100, 14368–14373. doi: 10.1073/pnas.2336098100

Cannon, J. R., and Greenamyre, J. T. (2011). The role of environmental exposures in neurodegeneration and neurodegenerative diseases. *Toxicol. Sci.* 124, 225–250. doi: 10.1093/toxsci/kfr239

Cheng, S. Y., Oh, S., Velasco, M., Ta, C., Montalvo, J., and Calderone, A. (2014). RTP801 regulates maneb- and mancozeb-induced cytotoxicity via NF-kappaB. *J. Biochem. Mol. Toxicol.* 28, 302–311. doi: 10.1002/jbt.21566

Corradetti, M. N., Inoki, K., and Guan, K. L. (2005). The stress-inducted proteins RTP801 and RTP801L are negative regulators of the mammalian target of rapamycin pathway. *J. Biol. Chem.* 280, 9769–9772. doi: 10.1074/jbc.c400557200

Damjanac, M., Page, G., Ragot, S., Laborie, G., Gil, R., Hugon, J., et al. (2009). PKR, a cognitive decline biomarker, can regulate translation via two consecutive molecular targets p53 and Redd1 in lymphocytes of AD patients. *J. Cell. Mol. Med.* 13, 1823–1832. doi: 10.1111/j.1582-4934.2009.00688.x

Dauer, W., and Przedborski, S. (2003). Parkinson's disease: mechanisms and models. *Neuron* 39, 889–909. doi: 10.1016/S0896-6273(03)00568-3

Dehay, B., Bové, J., Rodríguez-Muela, N., Perier, C., Recasens, A., Boya, P., et al. (2010). Pathogenic lysosomal depletion in Parkinson's disease. *J. Neurosci.* 30, 12535–12544. doi: 10.1523/jneurosci.1920-10.2010

del Olmo-Aguado, S., Núñez-Árez, C., Ji, D., Manso, A. G., and Osborne, N. N. (2013). RTP801 immunoreactivity in retinal ganglion cells and its down-regulation in cultured cells protect them from light and cobalt chloride. *Brain Res. Bull.* 98, 132–144. doi: 10.1016/j.brainresbull.2013.08.002

DeYoung, M. P., Horak, P., Sofer, A., Sgroi, D., and Ellisen, L. W. (2008). Hypoxia regulates TSC1/2-mTOR signaling and tumor suppression through REDD1-mediated 14-3-3 shuttling. *Genes Dev.* 22, 239–251. doi: 10.1101/gad.1617608

Ellisen, L. W., Ramsayer, K. D., Johannessen, C. M., Yang, A., Beppu, H., Minda, K., et al. (2002). REDD1, a developmentally regulated transcriptional target of p63 and p53, links p63 to regulation of reactive oxygen species. *Mol. Cell* 10, 995–1005. doi: 10.1016/s1097-2765(02)00706-2

Favier, F. B., Costes, F., Defour, A., Bonnefoy, R., Lefai, E., Baugé, S., et al. (2010). Downregulation of Akt/mammalian target of rapamycin pathway in skeletal muscle is associated with increased REDD1 expression in response to chronic hypoxia. *Am. J. Physiol. Regul. Integr. Comp. Physiol.* 298, R1659–R1666. doi: 10.1152/ajpregu.00550.2009

Fulda, S., Gorman, A. M., Hori, O., and Samali, A. (2010). Cellular stress responses: cell survival and cell death. *Int. J. Cell Biol.* 2010:214074. doi: 10.1155/2010/214074

Greene, L. A., Levy, O., and Malagelada, C. (2011). Akt as a victim, villain and potential hero in Parkinson's disease pathophysiology and treatment. *Cell. Mol. Neurobiol.* 31, 969–978. doi: 10.1007/s10571-011-9671-8

Hernández, G., Lal, H., Fidalgo, M., Guerrero, A., Zalvide, J., Force, T., et al. (2011). A novel cardioprotective p38-MAPK/mTOR pathway. *Exp. Cell Res.* 317, 2938–2949. doi: 10.1016/j.yexcr.2011.09.011

Hobbs, R. M., Seandel, M., Falciatori, I., Rafii, S., and Pandolfi, P. P. (2010). Plzf regulates germline progenitor self-renewal by opposing mTORC1. *Cell* 142, 468–479. doi: 10.1016/j.cell.2010.06.041

Hoeffer, C. A., and Klann, E. (2010). mTOR signaling: at the crossroads of plasticity, memory and disease. *Trends Neurosci.* 33, 67–75. doi: 10.1016/j.tins.2009.11.003

Horak, P., Crawford, A. R., Vadysirisack, D. D., Nash, Z. M., DeYoung, M. P., Sgroi, D., et al. (2010). Negative feedback control of HIF-1 through REDD1-regulated ROS suppresses tumorigenesis. *Proc. Natl. Acad. Sci. U S A* 107, 4675–4680. doi: 10.1073/pnas.0907705107

Hwang-Verslues, W. W., Chang, P. H., Wei, P. C., Yang, C. Y., Huang, C. K., Kuo, W. H., et al. (2011). miR-495 is upregulated by E12/E47 in breast cancer stem cells and promotes oncogenesis and hypoxia resistance via downregulation of E-cadherin and REDD1. *Oncogene* 30, 2463–2474. doi: 10.1038/onc.2010.618

Inoki, K., Li, Y., Xu, T., and Guan, K. L. (2003). Rheb GTPase is a direct target of TSC2 GAP activity and regulates mTOR signaling. *Genes Dev.* 17, 1829–1834. doi: 10.1101/gad.1110003

Inoki, K., Li, Y., Zhu, T., Wu, J., and Guan, K. L. (2002). TSC2 is phosphorylated and inhibited by Akt and suppresses mTOR signalling. *Nat. Cell Biol.* 4, 648–657. doi: 10.1038/ncb839

Jana, N. R., Zemskov, E. A., Wang, G., and Nukina, N. (2001). Altered proteasomal function due to the expression of polyglutamine-expanded truncated N-terminal huntingtin induces apoptosis by caspase activation through mitochondrial cytochrome c release. *Hum. Mol. Genet.* 10, 1049–1059. doi: 10.1093/hmg/10.10.1049

Jin, H. O., An, S., Lee, H. C., Woo, S. H., Seo, S. K., Choe, T. B., et al. (2007). Hypoxic condition- and high cell density-induced expression of Redd1 is regulated by activation of hypoxia-inducible factor-1alpha and Sp1 through the phosphatidylinositol 3-kinase/Akt signaling pathway. *Cell. Signal.* 19, 1393–1403. doi: 10.1016/j.cellsig.2006.12.014

Jin, H. O., Seo, S. K., Woo, S. H., Kim, E. S., Lee, H. C., Yoo, D. H., et al. (2009). Activating transcription factor 4 and CCAAT/enhancer-binding protein-beta negatively regulate the mammalian target of rapamycin via Redd1 expression in response to oxidative and endoplasmic reticulum stress. *Free Radic. Biol. Med.* 46, 1158–1167. doi: 10.1016/j.freeradbiomed.2009.01.015

Katiyar, S., Liu, E., Knutzen, C. A., Lang, E. S., Lombardo, C. R., Sankar, S., et al. (2009). REDD1, an inhibitor of mTOR signalling, is regulated by the CUL4A-DDB1 ubiquitin ligase. *EMBO Rep.* 10, 866–872. doi: 10.1038/embor.2009.93

Keller, J. N., Hanni, K. B., and Markesbery, W. R. (2000). Impaired proteasome function in Alzheimer's disease. *J. Neurochem.* 75, 436–439. doi: 10.1046/j.1471-4159.2000.0750436.x

Kim, J. R., Lee, S. R., Chung, H. J., Kim, S., Baek, S. H., Kim, J. H., et al. (2003). Identification of amyloid beta-peptide responsive genes by cDNA microarray technology: involvement of RTP801 in amyloid beta-peptide toxicity. *Exp. Mol. Med.* 35, 403–411. doi: 10.1038/emm.2003.53

Kimball, S. R., Do, A. N., Kutzler, L., Cavener, D. R., and Jefferson, L. S. (2008). Rapid turnover of the mTOR complex 1 (mTORC1) repressor REDD1 and activation of mTORC1 signaling following inhibition of protein synthesis. *J. Biol. Chem.* 283, 3465–3475. doi: 10.1074/jbc.m706643200

Laplante, M., and Sabatini, D. M. (2012). mTOR signaling in growth control and disease. *Cell* 149, 274–293. doi: 10.1016/j.cell.2012.03.017

Lee, D. U., Huang, W., Rittenhouse, K. D., and Jessen, B. (2012). Retina expression and cross-species validation of gene silencing by PF-655, a small interfering RNA against RTP801 for the treatment of ocular disease. *J. Ocul. Pharmacol. Ther.* 28, 222–230. doi: 10.1089/jop.2011.0116

Levy, O. A., Malagelada, C., and Greene, L. A. (2009). Cell death pathways in Parkinson's disease: proximal triggers, distal effectors and final steps. *Apoptosis* 14, 478–500. doi: 10.1007/s10495-008-0309-3

Li, X. H., Ha, C. T., Fu, D., and Xiao, M. (2012). Micro-RNA30c negatively regulates REDD1 expression in human hematopoietic and osteoblast cells after gamma-irradiation. *PLoS One* 7:e48700. doi: 10.1371/journal.pone.0048700

Lin, L., Qian, Y., Shi, X., and Chen, Y. (2005a). Induction of a cell stress response gene RTP801 by DNA damaging agent methyl methanesulfonate through CCAAT/enhancer binding protein. *Biochemistry* 44, 3909–3914. doi: 10.1021/bi047574r

Lin, L., Stringfield, T. M., Shi, X., and Chen, Y. (2005b). Arsenite induces a cell stress-response gene, RTP801, through reactive oxygen species and transcription factors Elk-1 and CCAAT/enhancer-binding protein. *Biochem. J.* 392(Pt. 1), 93–102. doi: 10.1042/bj20050553

Ma, X. M., and Blenis, J. (2009). Molecular mechanisms of mTOR-mediated translational control. *Nat. Rev. Mol. Cell Biol.* 10, 307–318. doi: 10.1038/nrm2672

Malagelada, C., Jin, Z. H., and Greene, L. A. (2008). RTP801 is induced in Parkinson's disease and mediates neuron death by inhibiting Akt phosphorylation/activation. *J. Neurosci.* 28, 14363–14371. doi: 10.1523/jneurosci.3928-08.2008

Malagelada, C., Jin, Z. H., Jackson-Lewis, V., Przedborski, S., and Greene, L. A. (2010). Rapamycin protects against neuron death in in vitro and in vivo models of Parkinson's disease. *J. Neurosci.* 30, 1166–1175. doi: 10.1523/jneurosci.3944-09.2010

Malagelada, C., López-Toledano, M. A., Willett, R. T., Jin, Z. H., Shelanski, M. L., and Greene, L. A. (2011). RTP801/REDD1 regulates the timing of cortical neurogenesis and neuron migration. *J. Neurosci.* 31, 3186–3196. doi: 10.1523/jneurosci.4011-10.2011

Malagelada, C., Ryu, E. J., Biswas, S. C., Jackson-Lewis, V., and Greene, L. A. (2006). RTP801 is elevated in Parkinson brain substantia nigral neurons and mediates death in cellular models of Parkinson's disease by a mechanism involving mammalian target of rapamycin inactivation. *J. Neurosci.* 26, 9996–10005. doi: 10.1523/jneurosci.3292-06.2006

McNaught, K. S., Belizaire, R., Isacson, O., Jenner, P., and Olanow, C. W. (2003). Altered proteasomal function in sporadic Parkinson's disease. *Exp. Neurol.* 179, 38–46. doi: 10.1006/exnr.2002.8050

Michel, G., Matthes, H. W., Hachet-Haas, M., El Baghdadi, K., de Mey, J., Pepperkok, R., et al. (2014). Plasma membrane translocation of REDD1 governed by GPCRs contributes to mTORC1 activation. *J. Cell Sci.* 127(Pt. 4), 773–787. doi: 10.1242/jcs.136432

Migliore, L., and Coppede, F. (2009). Genetics, environmental factors and the emerging role of epigenetics in neurodegenerative diseases. *Mutat. Res.* 667, 82–97. doi: 10.1016/j.mrfmmm.2008.10.011

Nguyen, Q. D., Schachar, R. A., Nduaka, C. I., Sperling, M., Basile, A. S., Klamerus, K. J., et al. (2012a). Dose-ranging evaluation of intravitreal siRNA PF-04523655 for diabetic macular edema (the DEGAS study). *Invest. Ophthalmol. Vis. Sci.* 53, 7666–7674. doi: 10.1167/iovs.12-9961

Nguyen, Q. D., Schachar, R. A., Nduaka, C. I., Sperling, M., Basile, A. S., Klamerus, K. J., et al. (2012b). Phase 1 dose-escalation study of a siRNA targeting the RTP801 gene in age-related macular degeneration patients. *Eye (Lond)* 26, 1099–1105. doi: 10.1038/eye.2012.106

Ota, K. T., Liu, R. J., Voleti, B., Maldonado-Aviles, J. G., Duric, V., Iwata, M., et al. (2014). REDD1 is essential for stress-induced synaptic loss and depressive behavior. *Nat. Med.* 20, 531–535. doi: 10.1038/nm.3513

Pieri, B. L., Souza, D. R., Luciano, T. F., Marques, S. O., Pauli, J. R., Silva, A. S., et al. (2014). Effects of physical exercise on the P38MAPK/REDD1/14-3-3 pathways in the Myocardium of Diet-Induced obesity rats. *Horm. Metab. Res.* 46, 621–627. doi: 10.1055/s-0034-1371824

Pineau, P., Volinia, S., McJunkin, K., Marchio, A., Battiston, C., Terris, B., et al. (2010). miR-221 overexpression contributes to liver tumorigenesis. *Proc. Natl. Acad. Sci. U S A* 107, 264–269. doi: 10.1073/pnas.0907904107

Qian, Y., Castranova, V., and Shi, X. (2003). New perspectives in arsenic-induced cell signal transduction. *J. Inorg. Biochem.* 96, 271–278. doi: 10.1016/s0162-0134(03)00235-6

Reiling, J. H., and Hafen, E. (2004). The hypoxia-induced paralogs Scylla and Charybdis inhibit growth by down-regulating S6K activity upstream of TSC in Drosophila. *Genes Dev.* 18, 2879–2892. doi: 10.1101/gad.322704

Rittenhouse, K. D., Johnson, T. R., Vicini, P., Hirakawa, B., Kalabat, D., Yang, A. H., et al. (2014). RTP801 gene expression is differentially upregulated in retinopathy and is silenced by PF-04523655, a 19-Mer siRNA directed against RTP801. *Invest. Ophthalmol. Vis. Sci.* 55, 1232–1240. doi: 10.1167/iovs.13-13449

Romaní-Aumedes, J., Canal, M., Martín-Flores, N., Sun, X., Pérez-Fernández, V., Wewering, S., et al. (2014). Parkin loss of function contributes to RTP801 elevation and neurodegeneration in Parkinson's disease. *Cell Death Dis.* 5:e1364. doi: 10.1038/cddis.2014.333

Ryu, E. J., Angelastro, J. M., and Greene, L. A. (2005). Analysis of gene expression changes in a cellular model of Parkinson disease. *Neurobiol. Dis.* 18, 54–74. doi: 10.1016/j.nbd.2004.08.016

Shoshani, T., Faerman, A., Mett, I., Zelin, E., Tenne, T., Gorodin, S., et al. (2002). Identification of a novel hypoxia-inducible factor 1-responsive gene, RTP801, involved in apoptosis. *Mol. Cell. Biol.* 22, 2283–2293. doi: 10.1128/mcb.22.7.2283-2293.2002

Sofer, A., Lei, K., Johannessen, C. M., and Ellisen, L. W. (2005). Regulation of mTOR and cell growth in response to energy stress by REDD1. *Mol. Cell. Biol.* 25, 5834–5845. doi: 10.1128/mcb.25.14.5834-5845.2005

Sun, X., Liu, J., Crary, J. F., Malagelada, C., Sulzer, D., Greene, L. A., et al. (2013). ATF4 protects against neuronal death in cellular PD models by maintaining levels of parkin. *J. Neurosci.* 33, 2398–2407. doi: 10.1523/jneurosci.2292-12.2013

Tain, L. S., Mortiboys, H., Tao, R. N., Ziviani, E., Bandmann, O., and Whitworth, A. J. (2009). Rapamycin activation of 4E-BP prevents parkinsonian dopaminergic neuron loss. *Nat. Neurosci.* 12, 1129–1135. doi: 10.1038/nn.2372

Tan, C. Y., and Hagen, T. (2013). mTORC1 dependent regulation of REDD1 protein stability. *PLoS One* 8:e63970. doi: 10.1371/journal.pone.0063970

Tanaka, K., and Matsuda, N. (2014). Proteostasis and neurodegeneration: the roles of proteasomal degradation and autophagy. *Biochim. Biophys. Acta* 1843, 197–204. doi: 10.1016/j.bbamcr.2013.03.012

Tang, S. J., Reis, G., Kang, H., Gingras, A. C., Sonenberg, N., and Schuman, E. M. (2002). A rapamycin-sensitive signaling pathway contributes to long-term synaptic plasticity in the hippocampus. *Proc. Natl. Acad. Sci. U S A* 99, 467–472. doi: 10.1073/pnas.012605299

Tarazi, F. I., Sahli, Z. T., Wolny, M., and Mousa, S. A. (2014). Emerging therapies for Parkinson's disease: from bench to bedside. *Pharmacol. Ther.* doi: 10.1016/j.pharmthera.2014.05.010. [Epub ahead of print].

Tee, A. R., Manning, B. D., Roux, P. P., Cantley, L. C., and Blenis, J. (2003). Tuberous sclerosis complex gene products, Tuberin and Hamartin, control mTOR signaling by acting as a GTPase-activating protein complex toward Rheb. *Curr. Biol.* 13, 1259–1268. doi: 10.1016/s0960-9822(03)00506-2

Vega-Rubin-de-Celis, S., Abdallah, Z., Kinch, L., Grishin, N. V., Brugarolas, J., and Zhang, X. (2010). Structural analysis and functional implications of the negative mTORC1 regulator REDD1. *Biochemistry* 49, 2491–2501. doi: 10.1021/bi902135e

Wang, Z., Malone, M. H., Thomenius, M. J., Zhong, F., Xu, F., and Distelhorst, C. W. (2003). Dexamethasone-induced gene 2 (dig2) is a novel pro-survival stress gene induced rapidly by diverse apoptotic signals. *J. Biol. Chem.* 278, 27053–27058. doi: 10.1074/jbc.m303723200

Whitney, M. L., Jefferson, L. S., and Kimball, S. R. (2009). ATF4 is necessary and sufficient for ER stress-induced upregulation of REDD1 expression. *Biochem. Biophys. Res. Commun.* 379, 451–455. doi: 10.1016/j.bbrc.2008.12.079

Wu, X. M., Qian, Z. M., Zhu, L., Du, F., Yung, W. H., Gong, Q., et al. (2011). Neuroprotective effect of ligustilide against ischaemia-reperfusion injury via up-regulation of erythropoietin and down-regulation of RTP801. *Br. J. Pharmacol.* 164, 332–343. doi: 10.1111/j.1476-5381.2011.01337.x

Zhang, D., Zhang, J. J., and Liu, G. T. (2007a). The novel squamosamide derivative FLZ protects against 6-hydroxydopamine-induced apoptosis through inhibition of related signal transduction in SH-SY5Y cells. *Eur. J. Pharmacol.* 561, 1–6. doi: 10.1016/j.ejphar.2006.11.015

Zhang, D., Zhang, J. J., and Liu, G. T. (2007b). The novel squamosamide derivative (compound FLZ) attenuated 1-methyl, 4-phenyl-pyridinium ion (MPP+)-induced apoptosis and alternations of related signal transduction in SH-SY5Y cells. *Neuropharmacology* 52, 423–429. doi: 10.1016/j.neuropharm.2006.08.020

Zhou, Y., Wang, Q., Guo, Z., Weiss, H. L., and Evers, B. M. (2012). Nuclear factor of activated T-cell c3 inhibition of mammalian target of rapamycin signaling through induction of regulated in development and DNA damage response 1 in human intestinal cells. *Mol. Biol. Cell* 23, 2963–2972. doi: 10.1091/mbc.e12-01-0037

Conflict of Interest Statement: The authors declare that the research was conducted in the absence of any commercial or financial relationships that could be construed as a potential conflict of interest.

Received: 26 July 2014; accepted: 17 September 2014; published online: 02 October 2014.

Citation: Canal M, Romaní-Aumedes J, Martín-Flores N, Pérez-Fernández V and Malagelada C (2014) RTP801/REDD1: a stress coping regulator that turns into a troublemaker in neurodegenerative disorders. Front. Cell. Neurosci. ***8****:313. doi: 10.3389/fncel.2014.00313*

This article was submitted to the journal Frontiers in Cellular Neuroscience.